Design and Performance of a Pilot Submerged Membrane Electro-Bioreactor (SMEBR) for Wastewater Treatment

Shadi Hasan

A Thesis

In the Department

of

Building, Civil, and Environmental Engineering

Presented in Partial Fulfillment of the Requirements

For the Degree of

Doctor of Philosophy (Civil Engineering) at

Concordia University

Montreal, Quebec, Canada

November 2011

CONCORDIA UNIVERSITY

SCHOOL OF GRADUATE STUDIES

This is to certify that the thesis prepared

By: **Shadi Hasan**

Entitled: **Design and Performance of a Pilot Submerged Membrane Electro-Bioreactor (SMEBR) for Wastewater Treatment**

and submitted in partial fulfillment of the requirements for the degree of

DOCTOR OF PHILOSOPHY (Civil Engineering)

complies with the regulations of the University and meets the accepted standards with respect to originality and quality.

Signed by the final examining committee:

_____ Chair
Dr. R. Wuthrich

_____ External Examiner
Dr. H. Zhou

_____ External to Program
Dr. S. Hashtrudi-Zad

_____ Examiner
Dr. F. Haghighat

_____ Examiner
Dr. C. Mulligan

_____ Thesis Co-Supervisor
Dr. M. Elektorowicz

_____ Thesis Co-Supervisor
Dr. J. Oleszkiewicz

Approved by _____
Dr. M. Elektorowicz, Graduate Program Director

December 12, 2011

_____
Dr. Robin A.L. Drew, Dean
Faculty of Engineering & Computer Science

Abstract

Design and Performance of a Pilot Submerged Membrane Electro-Bioreactor (SMEBR) for Wastewater Treatment

Shadi Hasan, Ph.D.

Concordia University, 2011

The quality of wastewater treatment plants effluents in Canada, and more specifically in Quebec is of a huge concern. Hence, several technologies have been widely used in order to protect water resources from the discharge of many undesirable components. The main objective of this study was to design/scale-up, install, and operate a new hybrid, compact wastewater treatment system (Submerged Membrane Electro-Bioreactor; SMEBR) that would yield an excellent quality effluent, reduce membrane fouling, and improve sludge properties. SMEBR combined three phenomena; membrane filtration, electrokinetics, and biological treatment. Three Phases were performed in this study. In Phase 1 (4 Stages), SMEBR laboratory scale system treating synthetic wastewater operated under different operating conditions to screen out and determine the operating ranges of the technological design parameters. These included the determination of the membrane critical flux and variation of aeration intensity (Stage 1), variation of current density (Stage 2), variation of the electrical zone volume with respect to the total volume of the effective liquid in SMEBR (Stage 3), and variation of hydraulic retention time (HRT) (Stage 4). Phase 2 focused on the scaled-up pilot SMEBR treating raw municipal wastewater. It was divided into 3 Stages where in Stage 1 the pilot SMEBR was designed (Stage 1a), installed (Stage 1b), and operated (Stage 2) in the municipal wastewater treatment plant in the City of l'Assomption (Quebec, Canada) for 7 weeks. A comparative study to the conventioanl MBR was also performed in

Stage 2. Stage 3 investigated the relationship between the transmembrane pressure (TMP) and the sludge properties in SMEBR and MBR as well as the interaction among the sludge properties. In Phase 3, the scale-up process was verified using raw wastewater under steady state conditions; and conducted in conjunction to the pilot facility in Phase 2. The design scale-up protocol was also provided for full scale applications. At steady state operation, the removal efficiencies of COD, ammonia (as NH_3^+-N) and phosphorous (as PO_4^{3-}-P) in SMEBR were 92%, 99% and 99%, respectively. Furthermore, the monitored transmembrane pressure (TMP) had not shown any significant increase which could lead to the conclusion that the membrane fouling was marginal. In SMEBR system, sludge filterability and dewaterability were significantly enhanced by 78% when the mean particle size diameter of the sludge flocs decreased from 69 to 17.5 μm. Specific cake resistance was minimized to $0.15x10^{14}$ m/kg (82% reduction). Moreover, SMEBR enhanced sludge settleability by 30% while the sludge volume index (SVI) had decreased from 170 to 119 mL/g. SMEBR significantly improved sludge flocculation while zeta potential had changed from -26.2 to -14.2 mV. Electrodes were found to last for five months before replacement. SMEBR was a "self-purification" system as some of the generated aluminum and major metals were retained and adsorbed on the surface of the electrodes, and small amounts would leave with the effluent or present in the wasted sludge. SMEBR without any additional unit was able to remove undesirable metals from wastewater. High removal rates of Pb (100%), Ni (98.1%), Cu (100%), and Cd (94.6%) were reported. SMEBR energy requirements were less than 1 kWh/m^3 with a total energy cost of CAD $\$0.052/m^3$. It could be concluded that SMEBR showed superiority in performance over MBR and can be successfully applied to small and large scale wastewater treatment plants.

Acknowledgments

I would like to express my deep respects and profound gratitude to my supervisor, Dr. Maria Elektorowicz for her creative guidance, numerous valuable suggestions, and, most importantly, her herculean patience throughout this work.

I am extremely grateful to my co-supervisor, Dr. Jan Oleszkiewicz, for showing me the right direction and pushing me forwards. His inspiring discussion and valuable comments during the different stages of my work are gratefully acknowledged.

Indebtedness and appreciation are due to my committee members, Dr. Catherine Mulligan, Dr. Fariborz Haghighat, Dr. Shahin Hashtrudi Zad and Dr. Hondge Zhou for their valuable comments, suggestions and supports.

The financial support from the Natural Sciences and Engineering Research Council of Canada Strategic Grant Program (NSERC SGP-350666-07) and Le Fonds Québécois de la Recherche sur la Nature et les Technologies (FQRNT-B2) are acknowledged.

I am also grateful to the City of l'Assomption, City of Saint-Hyacinth, Claro Environmental Technologies and Equipment Inc., AC Plastiques, and Microza Asahi Kasei Chemicals Corporation (Japan) for their collaboration.

Special thanks to Mr. Joseph Harib and the rest of the Building, Civil, and Environmental Engineering department staff for their remarkable help.

Finally, I am sincerely grateful to my family in particular my parents who deserve big thanks for their great support and constant encouragement.

Dedication

To my parents and my beloved fiancée Yousra

Glossary

Parameter	Definition	Unit
TMP	Transmembrane pressure	kPa
PSD	Mean particle size diameter	μm
EPS	Extracellular polymeric substances	mg/L
EPS_p	Proteins	mg/L
EPS_c	Carbohydrates	mg/L
σ_{sludge}	Sludge conductivity	μS/cm
σ_{in}	Raw wastewater conductivity	μS/cm
T	Temperature	^oC
ZP	Zeta potential	mV
SV	Sludge viscosity	mPa.s
MLSS	Mixed liquor suspended solids	mg/L
MLVSS	Mixed liquor volatile suspended solids	mg/L
MLFSS	Mixed liquor fixed suspended solids	mg/L
HRT	Hydraulic retention time	h
SRT	Solids retention time	d
F/M	Food to microorganisms ratio	1/d
TN	Total nitrogen	mg/L
COD	Chemical oxygen demand	mg/L
J	Permeate flux	$L/m^2.h$
R_t	Total resistance	1/m
R_m	Intrinsic membrane resistance	1/m

R_f	Fouling resistance	1/m
R_c	Cake resistance	1/m
μ	Viscosity of the permeate	Pa.s
CFV	Cross flow velocity	m/s
α	Specific cake resistance	m/kg
τ	Shear stress	Pa
D	Shear rate	1/s
SVI	Sludge volume index	mL/g
MFI	Membrane fouling index	L/s^2
Q_{in}	Raw wastewater flow rate	L/d
r_p	Pearson's product momentum correlation coefficient	
J_c	Critical flux	$L/m^2.h$
DO	Dissolved oxygen	mg/L
OUR	Oxygen uptake rate	mg O_2/L.h
ORP	Oxidation-reduction potentional	mV
V	Applied voltage	V
v	Particle velocity	m/s
ε_r	Media dielectric constant	
ε_o	Permittivity of free space	
L_{Al}	Aluminum loss	kg
W_i	Aluminum electrode initial weight	kg
W_f	Aluminum electrode final weight	kg

t_d	Duration of experiment	d
t_e	Electrode lifetime	d
M_w	Molecular weight	g/mol
F_a	Faraday's constant	C/mol
I	Applied current	A
bCOD	Biodegradable COD	g/m^3
nbCOD	Non biodegradable COD	g/m^3
sCODe	Effluent soluble COD	g/m^3
nbVSS	Non biodegradable VSS	g/m^3
bpCOD	Biodegradable particulate COD	g/m^3
pCOD	Particulate COD	g/m^3
sBOD	Soluble BOD	g/m^3
sCOD	Soluble COD	g/m^3
iTSS	Inert TSS	g/m^3
Y	Yield coefficient	g VSS/g bCOD
S_o	Influent BOD or, bsCOD concentration	g/m^3
S	Concentration of growth limiting substrate	g/m^3
K_s	Half-saturation constant	g $bCOD/m^3$
k_d	Endogenous decay coefficient	1/d
μ_m	Maximum specific growth rate	g VSS/g VSS.d
K_n	Half-saturation constant (nitrification)	g NH_4-N/m^3
k_{dn}	Endogenous decay coefficient (nitrification)	1/d

$\mu_{n,m}$	Max. specific growth rate for nitrifying bacteria	g VSS/g VSS.d
Y_n	Yield coefficient (nitrification)	g VSS/g NH_4-N
f_d	Fraction of cell mass remaining as cell debris	g/g
K_o	Half-saturation constant for DO	g/m^3
k_T	Reaction rate constant at temperature T	1/d
k_{20}	Reaction rate constant at 20 ^oC	1/d
Θ	Temperature activity coefficient	Unitless
$P_{x,TSS}$	Net waste activated sludge produced each day, measured in terms of total suspended solids	kg/d
$P_{x,VSS}$	Amount of VSS produced and wasted daily	kg/d
$(P_{x,TSS})$	Mass of TSS in the aeration tank	kg
X	Mixed liquor suspended solids (MLSS)	g/m^3
$P_{x,bio}$	Biomass as VSS wasted per day	kg/d
NO_x	Concentration of NH_4-N in the influent flow that is nitrified	g/m^3
TSS_o	Influent wastewater TSS concentration	g/m^3
VSS_o	Influent wastewater VSS concentration	g/m^3
N_e	Effluent ammonia concentration	g/m^3
TKN	Influent TKN concentration	g/m^3
NO_x	Nitrogen oxidized	g/m^3

L_{org}	BOD volumetric organic loading	$kg/m^3.d$
Q_w	Sludge wastage per day	m^3/d
V	Volume	m^3
V_{TR}	Treated volume	m^3
V^*	Volume between electrodes	m^3
CD	Current density	A/m^2
U	Cell applied voltage	V
t	Net exposure time to intermittent electrical mode	h
E	Specific energy consumption	kWh/m^3
R_0	Oxygen demand for BOD oxidation	kg/h
SOTR	standard oxygen transfer rate	kg/h
α^*	Aeration factor	Unitless
β	The value relating oxygen saturation in waste water compared to clean water	Unitless
F	Diffuser fouling factor	Unitless
$C_{s,T,H}$	Oxygen saturation concentration corrected for altitude and temperature	g/m^3
C_L	Operating dissolved oxygen concentration	g/m^3
$C_{s,20}$	Oxygen saturation concentration for pure water at 20°C	g/m^3
ρ_A	Air density	kg/m^3
OTE	Oxygen transfer efficiency	
$Q_{A,b}$	air flow rate through the fine bubble diffusers	m^3/h

	(biological)	
K	Permeability	LMH/bar
$Q_{A,m}$	Aeration rate per unit membrane	m^3/h
$Q_{Permeate}$	Permeate flow rate	m^3/h
$P_{A,1}$	Inlet air pressure to membrane module	kPa
$P_{A,2}$	Blower outlet pressure	kPa
A_m	Membrane area	m^2
SAD_m	Membrane aeration demand per unit membrane area	$Nm^3/m^2.h$
SAD_p	Membrane aeration demand per unit permeate flow	Unitless
λ	Ratio of specific heat capacity at constant pressure to constant volume	Unitless
ζ	Blower efficiency	%
A_s	Anode surface area	m^2
ζ^*	Inorganic or chemical solids produced per day due to electrokinetics	kg Al/m^3

Table of Contents

List of Figures

List of Tables

Chapter 1: Introduction and Research Objectives

1.1 Problem statement

Three trillion liters of wastewater are annually discharged to Canadian surface waters (CCME, 2006). These effluents contain several types of contaminants which have impacts on human health and environment. Quebec, like any other province or country, is concerned about the quality of its water resources. Thus, it followed that the quality of effluent from wastewater treatment plants is a primary concern. A significant proportion of Quebec municipalities, however, do not incorporate advanced treatment facilities for municipal wastewater. Their effluents pose a risk of introducing a significant amount of nutrients (nitrogen and phosphorous), pathogens, endocrine disruptors, metal, and other undesirable compounds into receptors such as lakes and rivers. There has been an increasing need for advanced treatment at all municipalities, including the smallest ones which often discharge to fragile aquatic eco-system. The technologies used today required optimization and simplification when applied to smaller users. Contemporary wastewater treatment facilities occupy a huge land area due to the necessity to construct various operation units as each unit is dedicated to the removal of a distinct wastewater pollutant. A WWTP contains equipment to screen sewage incoming from collectors, many tanks for primary (physical-chemical) treatment, tanks for secondary (biological) treatment, sedimentation tanks after biological treatment, special facilities for phosphorous removal, facilities for ammonia removal, and disinfection. Furthermore, additional facilities are built to deal with the waste generated in each operation unit. Due to a high volume and the complexity of such waste, the costs of managing a basic WWTP might reach 60% of the total operation costs of the entire plant. On top of that, more advanced treatments of wastewater would dramatically increase capital and

operational costs. Advanced treatments were needed, but they required important investments and small municipalities could not afford such expenses. Consequently, a new approach which would eliminate many of the operational units (eg. primary clarifier and sludge thickening); and treat wastewater with high quality effluent at low cost was vital.

A recently developed technology called Submerged Membrane Electro-Bioreactor (SMEBR) appeared to fulfill these requirements (Elektorowicz et al., 2009). SMEBR combined three operational processes; biological treatment, membrane filtration, and electrokinetics (Fig. 1.1). SMEBR design balanced these processes in one operational unit (Bani-Melhem and Elektorowicz, 2010).

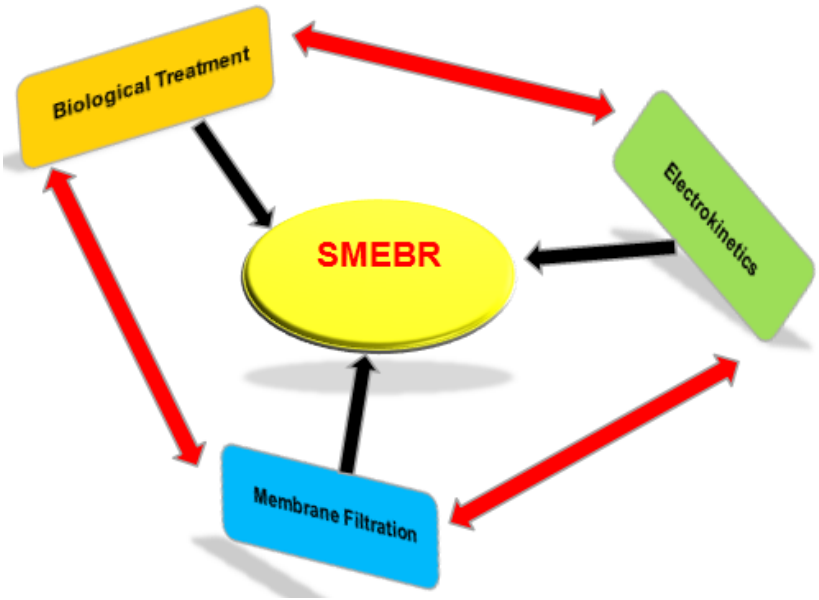

Fig. 1.1: Interaction between SMEBR processes.

Previous research in laboratory scale, performed by the same research team, has already shown biological transformation of organics and ammonia (Bani-Melhem and Elektorowicz, 2010), electrocoagulation, phosphorous removal (Wei et al., 2009), changing morphology of flocs (Ibeid et al., 2010a, 2010b) and transformation of many MLSS properties

(Ibeid et al., 2010a, 2010b) leading finally to significant lowering of membrane fouling (Wei et al., 2010). However, SMEBR has been never performed in full scale applications. That is why, it was necessary to conduct a pilot test in order to come up with a scientific approach to design SMEBR system for full scale applications. This research permitted to determine the most significant technological parameters in order to design a successfully working SMEBR unit in full scale. The proposed design had the capacity of adaptation to all kinds of wastewaters: e.g. low and high COD, nutrient content, and organic contaminants' contents due to full control of three basic processes biological, electrochemical, and membrane filtration. It also saved the real-estate because of designing multiple processes within one operation unit. This project had received NSERC-SGP-350666-07 award and FQRNT (B2) scholarship.

1.2 Research objectives

The main objective of this research was to investigate a novel submerged membrane electro-bioreactor (SMEBR); and to provide a background for its scale-up, confirmed by designing and testing the pilot SMEBR facility. A comparative study to the conventional membrane bioreactor (MBR) was also performed by testing a pilot MBR operated under same conditions. Detailed objectives were:

1. To determine the SMEBR operating ranges of the technological design parameters and investigate their impacts on water quality, sludge characteristics and membrane fouling through laboratory scale experiments. These included:
    - Determination of critical flux and variation of aeration intensities.
    - Effect of current densities and generation of inorganic sludge.

- Impact of hydraulic retention time (HRT).
- Impact of variation of electrical zone volume with respect to the total volume of effective liquid in SMEBR.

2. To design, install and operate SMEBR pilot facility in the municipal wastewater treatment plant and continuously treating raw municipal wastewater:
    - To verify the performance and applicability of SMEBR pilot system for wastewater treatment. Testing MBR pilot system was used for comparative purposes.
    - To investigate the relationship between the transmembrane pressure (TMP) and the sludge properties as well as the interaction among the sludge properties.
    - To determine the membrane and the electrodes lifetime.
    - To determine the fate of aluminum, phosphorus and metals throughout SMEBR system.
    - To model SMEBR system and provide design scale-up protocol.
    - To perform cost analysis and determine power requirements.

1.3 Organization of the thesis

This PhD thesis consisted of 8 chapters. Chapter 1 discussed introduction, problem statement and research objectives. Chapter 2 explained the literature review conducted in the field of study and the necessity of this research. Chapter 3 explained the methodology followed to achieve the research objectives. Chapter 4 illustrated the results obtained from the laboratory scale experiments treating synthetic wastewater in Phase 1. The technological design parameters were screened out so as to conduct successful laboratory and pilot scale SMEBRs

treating raw wastewater under steady state conditions in Phases 2 and 3. The results of Phases 2 and 3 were discussed in detail in Chapters 5 and 6. Chapter 7 summarized the conclusions drawn from this study. Finally, Chapter 8 explored the research contributions, and recommendations for future work.

Chapter 2: Literature Review

SMEBR operates based on the interaction between biological process, membrane filtration and electrokinetics. Therefore, an overview of each element of SMEBR system is provided in the literature review.

2.1 Biological process in wastewater treatment: activated sludge process

Biological processes can be defined as an engineered system, designed to accumulate microorganisms which oxidize organic (chemical oxygen demand, COD) and mineral (NH_3, Fe^{2+}, etc.) pollutants that are electron donors and reduced oxygen (O_2), nitrates (NO_3), sulphates (SO_4) or carbon dioxide (CO_2) that are electron acceptors (Rittmann, 1987). Activated sludge processes (ASP) refer to biological treatment processes that use a suspended growth of organisms to remove biological oxygen demand (BOD) and suspended solids. Activated sludge processes have many features, for instance, the formation of floc particles, ranging from 50-200 μm. These floc particles contain bacteria that are held together by extracellular polymeric substances (EPS) (Flemming and Wingender, 2001), and are usually removed by gravity settling. The supernatant is clarified, and purified wastewater is discharged to the receiver. The produced sludge underflow is split into waste activated sludge and return activated sludge which is returned to the aeration tank as seed to continue biodegradation of fresh wastewater. The activated sludge flocs contain a wide range of species of bacteria and protozoa which are responsible for the conversion of organic material and nutrients into water, carbon dioxide, and new cells. Several factors such as temperature, return rates, amount of oxygen available, amount of organic available, pH, waste rates, aeration time, and wastewater toxicity affect the performance of an activated sludge treatment system.

Depending on the type of organism and boundary conditions, different types of conversions take place. Aerobic oxidation is one type and occurs in the presence of oxygen which acts as the electron acceptor and organic compounds act as electron donors. Two other reactions are nitrification and denitrification. In nitrification, ammonia is converted to nitrite and nitrate (nitrification), which is further converted to nitrogen gas (denitrification). These reactions are considered as part of the life cycle of the respective bacteria and require a carbon source, an electron donor and an electron acceptor, which together yield an end product. Among the above mentioned processes, aerobic oxidation is relatively easy to accomplish since it only requires organic compounds and a solids retention time (SRT) of a few days. The first treatment plants that were built were designed mainly to perform this type of reaction, which required only aeration and mixing. In the past two decades also nutrient removal was incorporated in almost all biological treatment systems (Van de Graaf et al., 1996). For nutrient removal, certain operating conditions should be created in which the desired bacteria could grow in sufficient numbers. Nitrifying bacteria for example require a solids retention time of 10 to 20 d to properly perform nitrification (Metcalf and Eddy, 2003). Dytczak et al. (2008) investigated the impact of activated sludge operational regime on the nitrifying community and its nitrification rates. Two reactors operated under: a) alternating anoxic/aerobic conditions, b) aerobic conditions. They have concluded that 79.5% of the rapid nitrifiers (*Nitrosomonas and Nitrobacter*) were dominants in the alternating reactor when compared to 78.2% of the slower nitrifiers (*Nitrosospira and Nitrospira*) in the aerobic reactor. Sears et al. (2003) studied nitrification in pure oxygen activated sludge systems so as to determine the minimum SRT required to accomplish nitrification. They observed that when denitrification was not included, an SRT of 12 d was required to maintain nitrification at a

temperature of 24^{o}C and pH of 5.5, whereas an SRT of 5.6 d was required at pH up to 6.4 and a temperature of 24^{o}C when denitrification was included. Hwang and Oleszkiewicz (2007) investigated the impact of temperature on nitrification process. They compared two cases where a sharp decrease in temperature took place in the first case while a gradual decrease in temperature was applied in the second case. Their conclusion was that the sudden temperature decrease had significant impact on nitrification, through which the generated temperature correction factor of 1.072 could be applied to gradual temperature change situations.

2.2 Membrane bioreactors for wastewater treatment

2.2.1 Description and configurations of MBRs

Membrane bioreactors (MBR) combine the biological degradation of waste compounds by activated sludge with a direct solid/liquid separation by membrane filtration. Micro and ultrafiltration membranes (with pore size ranging from 0.05 to 0.4 μm) are commonly used in many wastewater applications. Membrane systems permit a complete physical retention of suspended solids within the bioreactor.

Different configurations of membrane systems take place, however, the most applicable ones are characterized to be either internal (submerged) or external membrane (side stream) units as shown in Fig. 2.1. In submerged systems, the membrane separation unit is immersed in the bioreactor vessel where permeation occurs under a vacuum, to the inside of the membrane. Commonly used membrane configurations are hollow fiber and plate and frame modules. Some of the advantages of submerged MBR are small footprint, feed-forward control of O_2 demand, low liquid pumping costs (28% of total costs) (Gender et al., 2000), low energy consumption (Côté et al., 1997), and lower operating cost. While some of the

disadvantages of submerged MBR are susceptible to membrane fouling and high aeration cost.

On the other hand, in external configuration, the membrane unit is placed outside the vessel where permeation takes place inside out and sludge is recirculated at a high flow through a tubular or spiral-wound membrane. Therefore, the power requirement is much higher than in submerged systems. The energy cost for the side stream membranes is increased from 2 to 10 kWh/m^3 of the water produced, depending on the internal diameter of the tubes used (Côté et al., 1997). Some of the advantages of side stream MBR are small footprint, complete solids removal from effluent, effluent disinfection, high loading rate capability, combined COD, solids and nutrient removal in a single unit, low sludge production, rapid start up, and sludge bulking was not a problem. Some of the disadvantages of side stream MBR are aeration limitations membrane fouling, membrane costs, high operating costs, high pumping cost (60-80% of total costs) (Gender et al., 2000), high cleaning requirement, and process complexity.

Unlike the side stream membranes, the energy consumption rates for submerged membranes are 0.2 to 0.4 kWh/m^3 of which more than 80% were for aeration (Chua et al., 2002). In submerged systems, the pressure across the membrane is applied by suction through the membrane or by pressurizing the bioreactor.

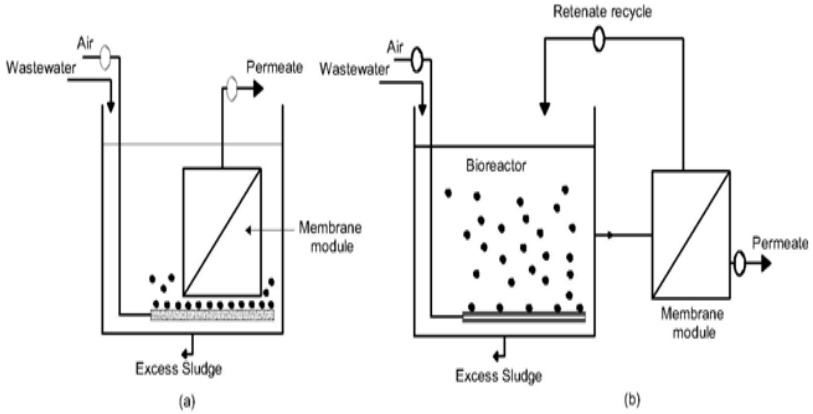

Fig. 2.1: Membrane configurations: (a) Submerged MBR (b) Side stream MBR (after Sombatsompop, 2007).

2.2.2 Membrane filtration process

2.2.2-1 Types of processes

The concept of membrane filtration is the separation of a mixture through a thin film. The membrane acts as a barrier between two phases through which the transport of matter is caused by a chemical potential difference between those two phases (Mulder, 1996). In pressure-driven membrane filtration systems, the driving force is a pressure difference across the membrane. The advantages of the membrane techniques include continuous separation, low energy consumption, easy combination with other existing technique, easy up-scaling, and no additives used. The membrane filtration is divided into four narrower ranges based on particle size (Fig. 2.2) such as microfiltration (MF), ultrafiltration (UF), nanofiltration (NF), and reverse osmosis (RO). MF is used to remove particulate and suspended material ranging in size from 0.1 to 10 μm (Cheryan, 1998), while UF is used to separate large macromolecules such as proteins and starches and all types of microorganism, such as bacteria and virus ranging in size from 0.01 to 0.1 μm (Aptel and Buckley, 1996). NF

membranes, on the other hand, remove small particles and viruses with a pore size ranging from 0.001 to 0.01 μm (Taylor and Jacobs, 1996) whereas RO membranes are capable of separating even the smallest solute molecules or particles with diameter of as small as 0.0001 μm (Taylor and Jacobs, 1996).

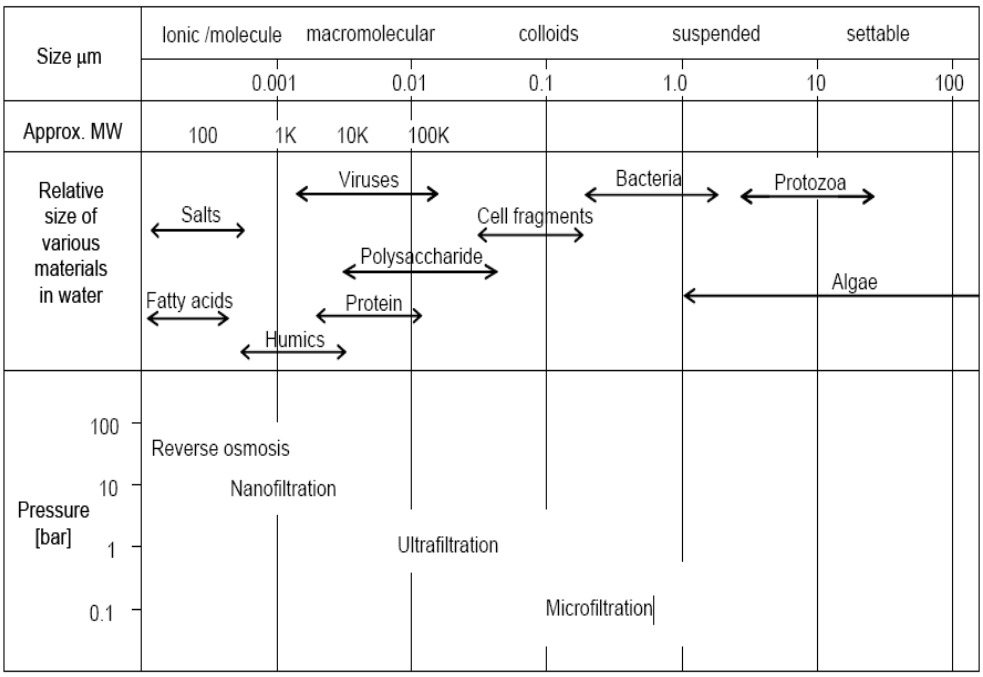

Fig. 2.2: Membrane process characteristics (after Mallevialle, 1996).

2.2.2-2 Membrane materials and membrane types

Membranes are produced from a variety of materials such as inorganic membranes (sintered metals and ceramics) and organic membranes (polymers, e.g, polyethylene, polypropylene, and polyvinylidene fluoride). The inorganic membranes have better chemical, mechanical and thermal stabilities; however, they are only used in certain applications e.g, solvent resistant and thermal stability due to their high costs (Baker, 2004). The organic membranes are widely used in water and wastewater applications because they are more flexible and can be put into a compact module with very high surface area. They are made from cellulose and all synthetic

polymers since they have good chemical, mechanical and thermal stability tendencies (Cheryan, 1998; Aptel and Buckley, 1996).

Membranes are manufactured in so many types to be applied in different applications and under different conditions. For instance, membranes can be plate and frame, hollow fibers, or tubular units (Kristine, 2005).

Plate and frame consist of two flat sheets of membrane material, usually an organic polymer, stretched across a thin frame. The driving force needed for filtration is provided by placing the space between the membrane sheets under vacuum. Several plates are arranged in a cassette which is immersed in the mixed liquor and the separation process takes place from the outside to the inside.

Hollow fibers consist of long strands, or fibers, of hollow extruded membrane mostly made of organic polymers. The fibers are mounted on a supporting structure which serves as a manifold for the permeate transport and as an air delivery system, and thus prevents the cake formation and enhances the lifetime of the membrane. Similar to the plate and frame membranes, they are arranged from the outside to the inside.

Tubular membranes are hollow tubes with the membrane placed on the surface of the tube. A very high porous supporting structure is below the membrane surface. Tubular membranes are made of inorganic materials like ceramic. Unlike the previous two types, the driving force is not based on the vacuum since the materials are separated at high velocity under pressure causing a transverse force to drive the water through the membrane while rejecting the large particles. These types of membranes can be arranged either way from the inside to the outside or vice versa.

2.2.3 Membrane operation parameters

The key elements in any membrane process are the transmembrane pressure (TMP), permeate flux (J), critical flux (J_c), resistance (R), permeability (K), and specific aeration demand (SAD). TMP is defined as the existing pressure difference between the membrane pressure at the sludge side and the pressure at the permeate side; and is considered as the driving force behind the filtration process. Critical flux is defined as the flux below which membrane fouling would not take place (Field et al., 1995). Equation 2.1 is used to calculate the permeate flux, which is defined as the quantity of materials passing through a unit area of the membrane per unit time. Flux is a system design parameter that has a direct correlation with membrane fouling rate. A clean membrane would have a relatively low TMP, whereas a fouled membrane would have a relatively high TMP, depending on the severity of fouling (Günder, 2001). Permeability is calculated as permeate flux per unit of TMP.

$$J = \frac{TMP}{\mu R_t} \qquad (2.1)$$

Where,

- J: permeate flux, $L/m^2.s$
- TMP: transmembrane pressure, Pa
- μ: viscosity of the permeate, Pa.s
- R_t: total resistance, 1/m: $R_t = R_m + R_c + R_f$
- R_m: intrinsic membrane resistance, 1/m
- R_c: cake resistance from by the cake layer, 1/m
- R_f: fouling resistance caused by solute adsorption into the membrane pore and gel formation, 1/m

The above mentioned resistances are measured through a series of filtration experiments in order to compare pure water filtration, sludge filtration, and pure water filtration after cake removal. However, those resistances are biomass characteristics, temperature and membrane material dependent. Specific aeration demand (SAD) is the air flow necessary for the physical cleaning of the membrane; and is expressed as air flow per permeate volume unit (SAD_p), or per membrane unit area (SAD_m). The SAD is a very essential key parameter in submerged MBR as aeration is required for membrane scouring, and therefore reducing fouling. In most of the currently operating large scale MBR, the SAD_p vary between 10 and 50 or even higher. Depending on the manufacturers and the operational methodologies, SAD_m could vary between 0.28 and 0.75 $m^3/m^2.h$. Biomass aeration is provided through fine bubble diffusers to increase oxygen transfer between the gas and the liquid phase. However the ideal aeration mode for preventing membrane fouling is supplied through coarse bubbles air diffusers.

2.2.4 Advantages of MBRs over conventional treatment methods

The operational advantages of membrane bioreactors over the conventional processes were well-reported (Manem and Sanderson, 1996; Cicek et al., 1998; Rosenberger et al., 2002). These include small footprint and reactor requirements, high effluent quality, good disinfection capability, higher volumetric loading and less sludge production (Stephenson et al., 2000). As a result of membrane separation, SRT is independent of HRT. Membrane separation in bioreactors is most attractive for situations where long SRTs are necessary to achieve the removal of pollutants. Early MBRs were operated with a long SRT (as high as 100 d) with mixed liquor suspended solids (MLSS) reaching 30 g/L and F/M ratio of 0.05 kg COD/kg MLSS.d. Visvanathan et al. (2000) concluded that MBR systems were operated in

long SRT (5-50 d) with high MLSS in the reactor and low F/M ratio. The recent trend focused on the operation of MBR at short SRT (around 10 to 20 d) with F/M ratios around 0.2 kg COD/kg MLSS.d. This approach would result in more manageable and sustainable MLSS in the reactor (10 - 15 g/L). Typical hydraulic retention times (HRT) varied between 3 to 10 h. It was reported that the organic removal in MBR was often greater than 95% even with relatively short HRT (Holler and Trösch, 2001; Soriano et al., 2003).

Nitrification in MBRs is more efficient than the conventional activated sludge process, due to longer retention time of the nitrifying bacteria (long SRT, low F/M ratio) and smaller floc sizes. The smaller the floc size, the greater the mass transport of nutrients and oxygen into the floc (Gender et al., 2000). In addition, at short SRT and HRT, the presence of membranes prevented the washout of nitrifiers (Soriano et al., 2003) and promoted the development of slow growth rate bacteria and produced little sludge (Muller et al. 1995; Trouve et al. 1994).

The need of on-site expertise was also reduced since membrane filtration in MBRs allowed for extensive automation and presented possibilities for remote controlled monitoring and operation. There were economic benefits behind the use of membrane filtration systems in terms of using smaller reactors to treat equivalent flows of wastewater. In addition, studies demonstrated that 20 membranes could be incorporated into existing treatment plants for enhanced effluent quality (Ahn et al., 1999).

Nevertheless, membrane fouling has been a critical issue and a huge obstacle limiting the wide applications of MBRs for wastewater treatment.

2.2.5 Disadvantages of MBRs: membrane fouling

2.2.5-1 Mechanisms of membrane fouling

Membrane fouling refers to the deposition or adsorption of feed water components or other impurities such as colloids, microorganisms, solutes and cell debris produced in the bioreactor on the internal and external structures of membrane surface. The accumulation of those materials causes an increase in the overall resistance to filtration process, thus increasing the energy demand. It also leads to a decline in the permeate flux, increase in TMP, and therefore deterioration of the membrane. Fouling is associated with several factors such as sludge properties, feed water characteristics, operating conditions and membrane characteristics through which sludge properties are directly related to membrane fouling while operating conditions have indirect impact on membrane fouling though changing the sludge characteristics (Meng et al., 2009). Fouling in MBR is also classified into three categories; biofouling, organic fouling, and inorganic fouling.

Biofouling refers to the deposition, growth and metabolism of the sludge flocs on the membrane surface and therefore a biocake (gel) layer is formed on the surface of the membrane. Extracellular polymeric substances (EPS) secreted by the microorganisms (Liu and Fang, 2002; Tsuneda et al., 2003) and soluble microbial products (SMP) were found to be major contributors to biofouling as they play vital role in the formation of the biological flocs and the gel layer on the membrane surface resulting in reducing the efficient pore diameter (Liao et al. 2004; Sombatsompop et al. 2007). EPS play an important role in the bacteria attachment and biofilm formation through which EPS provide a gel matrix; influencing the permeate flow towards the membrane and thus stabilizing the biofilm (e.g. on membrane surface). It was reported that EPS prevent any water loss from the cell to the surrounding

environment and hence causing higher deposition on the membrane surface (Laspidou and Rittmann, 2002). EPS is presented in two forms: 1) bound EPS: sheaths, capsular polymers, condensed gel, loosely bound polymers, attached organic material, and 2) soluble EPS: soluble macromolecules, colloids and slimes (Nielsen and Jahn, 1999). The impact of SMP in MBR on membrane fouling associated with the formation of the biofilm on the membrane surface was investigated (Rosenberger et al., 2005). Other studies concluded that SMP was the major foulant contributing to membrane fouling in MBR (Cabassud et al., 2004; Ng and Hermanowicz 2005).

EPS are high molecular compounds of carbohydrates, proteins, nucleic acids, and humic substances (Tsuneda et al., 2003; Guibaud et al., 2008). Organic fouling refers to the deposition of the biopolymeric substances (proteins and carbohydrates) on the membrane surface. These biopolymers are very small in size and thus would deposit more readily on the membrane surface than microbial flocs or colloids (larger when compared to biopolymers).

Inorganic fouling, on the other hand, is caused by concentration polarization where a large amount of matter has accumulated on the membrane surface due to size exclusion from pores. Several ions such as Ca^{2+}, Mg^{2+}, Al^{3+}, PO_4^{3-}, OH^- and others are present in MBR. In literature, it was reported that biopolymeric substances contain a large number of negatively charged functional groups (Liu et al., 2001; Sheng et al., 2005; Bhaskar and Bhosle, 2006) which would enhance the bioflocculation. Consequently, different complexes would be generated and formed a dense gel layer on the membrane surface.

2.2.5-2 Factors affecting membrane fouling

As shown in Fig. 2.3, many factors play major roles in membrane fouling. Operating conditions, sludge properties, and membrane characteristics had significant impacts on membrane fouling (Kwannate, 2007). Following is a brief overview of each factor.

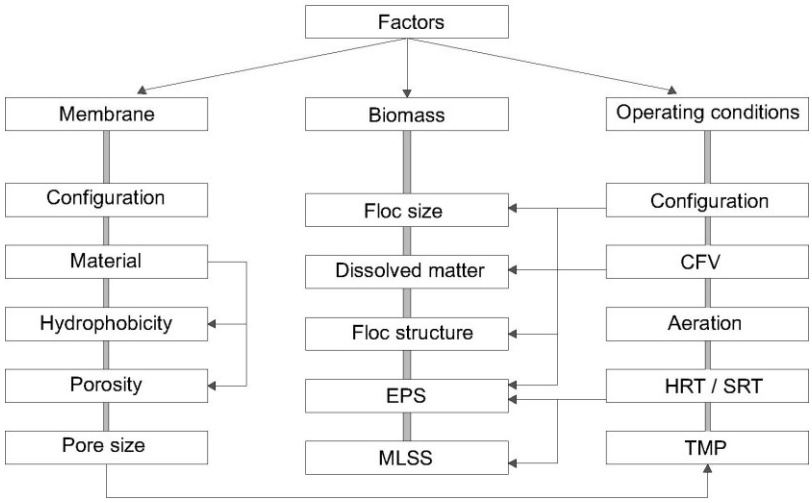

Fig. 2.3: Factors influencing membrane fouling in MBR process

(after Chang et al., 2002).

<u>Operating conditions</u>

Organic loading is a key parameter for the design and operation of membrane bioreactors. Hydraulic retention time (HRT) is associated with organic loading, but directly related to the tank volume and operational costs. Several studies have investigated the influence of such parameters on the performance of the filtration processes (Yamamoto et al., 1991; Harada et al., 1994; Seo et al., 1997; Rosenberger et al., 2002). The decrease in HRT caused an increase in the organic loading and mixed liquor suspended solids (MLSS) concentration, and

therefore, increasing the chances of membrane fouling. This was attributed to the formation of the cake layer on the membrane surface and hence an increase in TMP (Visvanathan et al., 1997).

Sludge retention time or sludge age (SRT) defines the excess sludge production and it is the time biomass stay in the system, thus affecting the performance of the biological process by changing the sludge compositions (Bouhabia et al., 2001). Changing the SRT has several impacts on the biological process. For example, increasing SRT might increase the MLSS concentration, which would enhance the biodegradation of different pollutants and produce less sludge (Manem et al., 1996). However, under these operating conditions, some negative effects might take place such as high viscosity of the sludge suspension resulting in membrane fouling (Ueda et al., 1996). Consequently, the efficiency of air sparging, and oxygen transfer rate to the microorganisms are reduced; resulting in a higher energy demand as well as increasing the risks of membrane fouling. Accordingly, and for economic reasons, most full-scale facilities are designed for MLSS range of 8-12 g/L and SRT range of 10-20 d (Asano et al., 2006; Judd, 2011).

In membrane bioreactors, like in all aerobic wastewater processes, both the biomass characteristics and the design of the aeration system were affecting the oxygen transfer (Mueller et al. 2002). Yet, 80% of the total energy cost in a submerged MBR could be due to aeration (Gunder et al., 2000; Owen et al., 1995); and accurate management of aeration appeared to be essential. An optimum value for aeration was determined through a series of experiments. Several studies have observed an optimum aeration rate beyond which any further increase had no effect on membrane fouling suppression (Ueda et al., 1997; Wicaksana et al., 2006; Espinosa et al., 2003). Hwang et al. (2002) suggested a range from 2

to 4 L/min at 5.6 g/L of sludge, and 50 kPa of pressure. Within this range, the flux was increased from 10 to 13 L/m^2.h. It was obvious that the strong aeration improved the filtration efficiency. Aeration and cross flow velocity (CFV) plays an important role in preventing or reducing membrane fouling. Liu et al. (2000) suggested that the CFV and aeration intensity were significantly related. It was reported that the critical cross flow velocity (at which TMP would increase below this value) was found to be 0.3 m/s. TMP sharply increased due to rapid deposition of suspended solids on the membrane surface and a corresponding increase of membrane resistance at CFV lower than 0.3 m/s. On the other hand, aeration rate would affect the biological and physical characteristics of the sludge. For instance, aeration intensities affected the shape and size of particles by breaking-up sludge flocs (Abbassi et al. 1999). Fan and Zhou (2007) investigated the interrelated impact of aeration intensity and mixed liquor fractions (MLSS, colloids and dissolved solutes) on membrane fouling. They concluded that their impact on membrane fouling was strongly related to aeration intensity where the aeration-induced turbulence should be considered when assessing the mixed liquor fouling potential for wastewater MBR processes. Their results revealed that initial increase in aeration intensity resulted in the dramatic drop in the overall fouling rates.

Sludge characteristics

Activated sludge is a very complex suspension and contained components from feed water and metabolites produced during the biological processes. Examples of sludge characteristics are: EPS, SMP, MLSS, floc size, dewaterability, settelability, and viscosity. EPS is an insoluble macromolecule polymerized by microorganisms, whereas SMP is produced by cell metabolism or self-digestion, and considered to be soluble and large molecules (Tarnacki et al., 2005). EPS and SMP could form many colloidal substances which would deposit on the

membrane surface and thus increasing the risk of fouling. EPS also have the ability to remove heavy metals and organic pollutants since they have a large number of negatively charged functional groups (Liu et al., 2001; Sheng et al., 2005; Bhaskar and Bhosle, 2006). EPS could also form multiple complexes with many heavy metals and as a result have a significant impact on geochemical behavior, bioavailability and toxicity of heavy metal ions (Selck et al., 1999).

Sludge concentration (MLSS) has a remarkable influence on membrane fouling. This was attributed to the fact that any changes in the biomass concentration would affect sludge viscosity and dynamic layer thickness, and thus would affect the sludge circulation. Consequently, changes in the hydrodynamic and the shear stress at the filtration cake surface would occur (Stephenson et al., 2000). Chang and Kim (2005) investigated the effect of biosolids concentration (3700, 2900, 250 and 90 mg/L) on filtration characteristics in wastewater treatment system. It was reported that the cake resistance had decreased with MLSS concentration. It was also found that the specific cake resistance (α) also increased as the MLSS concentration was decreased. However, the opposite behavior of cake resistance and specific cake resistance lead to the fact that specific cake resistance could not be used to estimate the cake fouling, particularly in low MLSS concentration.

Particle size distribution represents the average sludge particle size of the sludge suspension, which is evaluated based on number distribution of the sludge flocs. Fouling and the increase of resistance are relatively sensitive to the deposition of particles when particles of similar size as that of the membrane pores were filtrated through the membranes. Colloids play a major role in membrane fouling as they are released from EPS matrix into the bulk solution (Itonaga et al., 2004). Moreover, the reduction of particle size in the sludge

suspension would result in greater resistance and therefore lower permeate flux (Bai and Leow, 2002). Larger particles depositing on the membrane surface did not increase the TMP. Soluble fractions in the bulk solution enhanced the build up of a deposit on the membrane surface since the caused very strong physical and physico-chemical interactions with the membrane material (Wisniewski et. al., 2000).

Rheology is the science of flow and deformation of a matter. In wastewater, it refers to the relationship between shear stress and shear rate. Viscosity is measured by viscometers. Sludge rheological properties were related to solid concentration and sludge nature (particle size, surface charge, degree of hydration, and cohesion of flocs of agglomerated particles in suspension) (Lotito et al., 1997; Monteiro, 1997). Günder (2001) and Nagaoga et al. (1996) suggested that the existence of EPS and filamentous microorganisms increased sludge viscosity. The viscous characteristic of sewage sludge was non-Newtonian and has usually been modeled in the literature using the pseudoplastic rheological model (Lotito et al., 1997). Non-Newtonian viscosity is explained using Equation 2.2.

$$\mu = \tau / D \qquad (2.2)$$

Where, μ: viscosity (Pa.s), τ: shear stress (Pa) and D: shear rate (1/s)

In membrane bioreactors, it was recognized that aeration was a key parameter for the management and prevention of membrane fouling. Efficient aeration generated shear stress which released deposits from the membrane or washed away the suspended solids from the membrane. However, too much aeration was not recommended as well since it might enhance the breakage of the flocs and thus increase fouling (Gui et al., 2002).

Sludge dewaterability is characterized by the filterability test. It provides a quantitative measure of how the sludge repels water (i.e. rate of water released from sludge). Activated sludge filterability was commonly linked with activated sludge properties as SMP concentrations (Rosenberger et al., 2002), SRT, total suspended solids (TSS) or fractionations as particulate, colloid and soluble parts (Itonaga et al., 2004). SMP and colloidal particles were considered as major foulants, especially their role in pore blocking mechanism (Drews et al., 2008). For sewage sludge these rheological properties were not only important for the design of pumping and transporting facilities, but presumably also for sedimentation and dewatering. For example, the system would behave like a solid below a certain value of shear stress, while the viscosity of the sludge would vary above this value. The variability of viscosity was a shear velocity dependent and resulted from the structure changes proceeding in the sludge during the flow (Wolny et al., 2008).

The relationship between sludge filterability and the size of the microbial flocs was also investigated as the floc size affected the total particle surface area and the porosity formed from these particles, as a result had significant impact on the sludge dewaterability (Radaideh et al., 2010). Previous studies concluded that as the floc size decreased, the cake moisture content increased and the rate of filtration decreased. It was previously reported that flocs ranging in size from 0.001 and 0.1 mm have the ultimate impact as they blind the sludge cake during filtration (Karr and Keinath, 1978; Novak et al., 1988). Radaideh et al. (2010) investigated the dewaterability of sludge digested in extended aeration plants using conventional sand drying beds. Samples from wastewater treatment plans, one using aerobic/anoxic stabilization in extended aeration plants and other using anaerobic stabilization were collected and analyzed for sludge dewaterability. They have concluded that the

unconventional digestion of sludge in extended aeration plants with aeration periods and anoxic periods did not deteriorate the particle size distribution as the anaerobic digestion. It could be summarized that the sludge dewaterability is still a main issue and innovative technologies should be developed so as to increase the sludge filtration rate and reduce energy demand.

For activated sludge properties, sludge flocculation and settling were very essential. Sludge volume index (SVI), which is defined as the volume in millilitres occupied by 1 g of a suspension after 30 min of settling in a 1 L cylinder, characterized these properties. The lower the SVI, the denser the settled sludge, and therefore better sludge settleability. An activated sludge with a SVI below 120 mL/g was considered satisfactory, and that over 150 mL/g was considered bulking (Jenken et al., 1993). Cicek et al. (1999) reported that the activated sludge had a SVI of 80 mL/g whereas the MBR sludge observed no settling. Sun et al. (2007) studied the relationship between sludge settleability and membrane fouling in submerged MBR. They observed a decrease in the sludge settleability when the SVI had increased due to the propagation of the filamentous bacteria. As a result, the rate of TMP had increased and the stable filtration period was shortened.

Membrane characteristics/ Interaction between membrane and foulants

The affinity of a foulant to the membrane had a significant influence on the permeate quality as well as on fouling. Due to their small sizes, colloids and macromolecular organic matter had more interactions to membrane than any other materials. The interaction could be affected by several factors such as charge, hydrophobicity, membrane morphology, pH, divalent ions (Ca^{2+}, and Mg^{2+}), and ionic strength.

If colloids and organics have opposite hydrophobicity as the membrane surface, they would be repelled by the membrane (Hong and Elimelech, 1997). Many membranes were manufactured to be hydrophilic (Mulder, 1996). However, the hydrophobicity of the membrane was modified by the adsorption of colloids and organics causing the membrane to have the same hydrophobicity as the colloids and organics present in the solution (Hong and Elimelech, 1997). Besides, if the membrane and colloids or macromolecular organics had the same charge, then and due to electrostatic forces, repulsion took place between the membrane and the organics, and as a result, less fouling (Nystrom et al., 1995; Schafer et al., 2004). Most of the colloids and organics were negatively charged, hence, MF/UF membranes in water or wastewater were manufactured to be negatively charged.

Furthermore, ionic strength impact was not direct. Filtration of low ionic strength feed water minimized the adsorption of colloids and organics to the membrane surface. Nevertheless, in the filtration of proteins, screening of the charges was reduced at low ionic strength. Consequently, proteins molecules repelled each other at the membrane surface where they existed in large quantities (Kuzmenko et al., 2005). The presence of divalent ions enhanced membrane fouling. The charge of colloids and organics might increase (less negative) due to the binding between Ca^{2+} ions and the negative charged functional groups (Schafer et al., 2004; Lee et al., 2005). On the other hand, the charge of the membrane might also increase (less negative) due to the binding between Ca^{2+} ions and the negative charged membrane surface which would increase the risks of fouling (Hong and Elimelech, 1997; Schafer et al., 2004). Pore sizing, pore opening, and surface roughness affected membrane fouling. In general, membranes with narrow pores distribution could reduce membrane fouling (Mulder, 1996).

Membrane fouling index (MFI) is a parameter to determine the fouling potential, and was used as a tool for assessing the adequacy of pretreatment. This index was based on the cake filtration mechanism, which followed the relationship between filtration time and volume in dead-end flow and at a constant TMP. MFI was found to increase significantly with increasing applied pressure due to cake compression (Boerlage et al., 2003). The MFI was determined from the gradient of the general cake filtration as shown in Equation 2.4 for constant pressure in a plot of t/V versus V (Boerlage et al., 2003).

$$\frac{t}{V} = \frac{\mu R_m}{(TMP)A} + \frac{\mu \alpha C_b}{2(TMP)A^2} V \qquad (2.4)$$

Where V: filtrate volume, t: filtration time, TMP: transmembrane pressure, μ: solution viscosity, α: specific resistance of the cake deposited and C_b: the concentration of particles in feed water.

2.2.5-3 Fouling control

Fouling with respect to the mechanism of cleaning is classified as removable, irremovable and irreversible (Ferrero, 2011). Removable and irremovable types of membrane fouling were mainly attributed to the formation of the cake layer. Removable fouling could be removed via physical cleaning through aeration bubbles with relaxation periods or backwashing while chemical cleaning was necessary to remove irremovable fouling.

It was reported that irreversible fouling, which was attributed to pore blocking by attached foulants, could not be removed by either physical or chemical cleaning methods (Meng et al., 2009). Several strategies were proposed to control membrane fouling and were applied in full scale operations. These included pretreatment of the feed water through adding

acid to reduce scaling problems caused by the formation of calcium carbonates (Choi et al. 2009; Lee and Kim 2009), reducing the permeate flux, increasing aeration to scour the membrane and wash away any particles which might deposit on the membrane surface, changing the MLSS characteristics by the addition of adsorbent agents and chemical coagulants and flocculants (Le-Clech et al. 2006), and applying physical and chemical cleaning approaches (Judd, 2006).

Intensive researche has been done for the past years investigating the mechanisms as well as the factors affecting membrane fouling. Wang et al. (2011) investigated the fouling behaviors of polyacrylonitrile (PAN) and polyvinylidene fluoride (PVDF) membranes in a pilot-scale membrane bioreactor. They have concluded that the removable fouling was dominant for both membranes while irremovable fouling of the PVDF membrane was more significant than that of the PAN membrane. Gel filtration chromatography analysis indicated that the surface foulants of the PVDF membrane consisted of larger molecular weight molecules than those of the PAN membrane. Soluble microbial by-product-like substances were found to be the major foulants in both membranes. Hydrophobic humic-like substances played a more important role in forming irremovable fouling of the PAN membrane whereas protein-like substances were the main contributor to the irremovable fouling of the PVDF membrane.

Dizge et al. (2011) investigated the impact of organic cationic polyelectrolyte (CPE) addition on filterability and membrane fouling in submerged MBR. They have used cellulose acetate, polyethersulfone, mixed ester, polycarbonate (CA, PES, ME, PC) membranes. The results indicated that the cake resistance was the most significant fouling mechanism for all membranes, yet the addition of polyelectrolyte had decreased the cake

resistance. Additionally, the addition of such coagulant had significant impact on sustainable filtration time.

Pendashteh et al. (2011) characterized the fouling layer in MBR treating hypersaline oily wastewater. Different flocculants (aluminium sulfate, Chitosan, ferric chloride, polyaluminium chloride) were added and their impacts on membrane fouling were investigated. The results indicated that the deposition on the membrane surface consisted of organic and inorganic substances composed of extracellular polymeric substances (EPS), hydrocarbon components and inorganic matters. The analyses using energy dispersive X-ray (EDX) and inductively coupled plasma (ICP) indicated that the Mg, Al, Ca, Na, K and Fe were the major metal elements in the fouling cake. They concluded that the effect of organic flocculant in fouling mitigation was more than inorganic chemicals but the overall effects were insignificant.

Zhang et al. (2010) discussed the impact of organic loading on membrane fouling in submerged MBR. Two identical laboratory scale submerged MBRs were operated for 162 d with SRT of 30, whereas the influent organic loading was kept constant in one MBR, and varied in another. At steady state conditions, they observed less membrane fouling for variable feed strength where their observations were attributed to the fact that the contents of polysaccharides in the supernatant and particle size of the bioflocs were responsible for the observed differences in the fouling tendencies of the two MBRs.

2.2.6 MBR energy requirements and operational cost

There has been an immense growth in the MBR industry, which as a result increased the number of the manufacturers. Consequently, the cost of the MBR had reduced, yet the energy

demand and the power requirements in MBR still needs further optimization. The primary energy requirements were related to aeration including membrane scouring and aeration for biological community (Fig. 2.4).

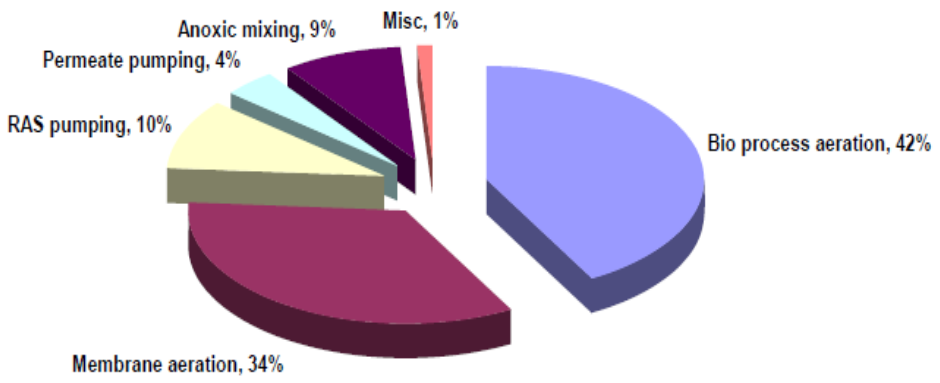

Fig. 2.4: Energy requirements in MBR (after Hribljan, 2007).

The advantages of MBR over the conventional activated sludge processes were widely reported, however, the energy requirements were 1.5 to 3 times higher than the conventional process, which would hinder the wide applications of MBR in wastewater treatment. In 2008, it was reported that the energy requirements for MBR was about 0.6-1.1 kWh/m^3, which was still higher than the energy requirements reported in conventional activated sludge treatment processes (0.38-0.48 kWh/m^3) (Evans and Laughton, 1994). Lesjean (2009) also reported that the energy requirements in MBR were also higher when compared to activated sludge process with tertiary disinfection. Additional studies were carried out and different conclusions were obtained with respect to the energy requirements in MBR. Visvanathan et al. (1997) and Krause and Cornel (2006) reported that the energy requirements of an immersed MBR could be as below as 0.14 and 0.7-0.8 kWh/m^3, respectively whereas 4 kWh/m^3 was reported by Jefferson et al. (1998). Zhan et al. (2003)

concluded that the total energy consumption by MBR could in some cases reach values between 6 and 8 kWh/m^3. The total energy consumptions of MBR, having immersed Kubota flat sheet membranes, reported by Gil et al. (2010) were 6.06 and 4.88 kWh/m^3 for tested fluxes of 19 and 25 LMH respectively.

It could be concluded that the energy requirements of MBR are still high and additional energy requirements would be involved when designing a full wastewater treatment plant. These would include the energy requirements of primary treatment, coagulation-flocculation tanks, and sludge processing. Therefore, a new technology would be necessary to reduce the energy requirements (operating and energy costs) of a complete wastewater treatment which includes all required operational units.

2.2.7 COD and nutrients removal in wastewater treatment

Nitrogen and phosphorus were key nutrients that result in water eutrophication and their removal was considered as one of the major problems in wastewater treatment. Many advantages were related to phosphorus denitrifying such as decreasing in greenhouse gas emission, saving of organics, and less sludge production. Several studies investigated different treatment methods such as biological processes, membrane bioreactors, and electrocoagulation to overcome this problem, yet did not accomplish the desired goals, particularly the removal of phosphorus.

For example, Kermani et al. (2009) evaluated the nutrients removal from synthetic wastewater by a laboratory scale moving bed biofilm process which was applied in series with anaerobic, anoxic and aerobic units in four separate reactors that were operated continuously at different loading rates of phosphorus and nitrogen and different hydraulic

retention times. Under optimum conditions, the average total nitrogen and phosphorus removal efficiencies were 80.9% and 95.8%, respectively. Cho et al. (2009) investigated the contribution of microfiltration to phosphorus removal in the sequencing anoxic/anaerobic membrane bioreactor and concluded that the microfiltration significantly contributed to phosphorus removal by retaining the particulate phosphorus inside the system.

Liu et al. (2010) conducted laboratory scale experiments to compare the removal efficiency of nitrogen, phosphorus and COD in simulated domestic wastewater using two sequencing batch membrane bioreactors operated in anaerobic-aerobic (AO) and anaerobic-aerobic-anoxic (AOA) mode. Results reported 94.1%, 78.9% and 58.6% for ammonium nitrogen, total nitrogen (TN) and total phosphorus (TP) removal rates, respectively in AO MBR system, and 96.9%, 81.9% and 78.3%, respectively in AOA MBR system.

MinGu and George (2010) compared a membrane bioreactor (MBR) system with a conventional anaerobic-anoxic-aerobic (A^2/O) system using synthetic wastewater (SWW) and municipal wastewater (MWW). They concluded that MBR exhibited better overall system performance than the A^2/O system, in terms of phosphorus removal. Nitrogen removal efficiencies were close in the two systems at 73 to 74% in both runs, while phosphorus removal efficiencies were 96 and 74% (SWW run) and 80 and 75% (MWW run), for the MBR and A^2/O, respectively.

Zhang and Huang (2011) proposed an enhanced biological phosphorus removal process coupled with membrane bioreactor. Different sludge retention times (20, 30, 40, and 50 d) were tested, and the results showed that the average phosphorus removal has decreased with SRT, the total phosphorus removal over 85% could be still achieved if the SRT was maintained under 40 d.

It could be concluded that nutrients removal is still a huge problem and further research including new technologies are required to obtain high quality effluents, especially with respect to COD and nutrients removal.

2.3 Electrokinetics/Electrocoagulation (EC)

2.3.1 Description and applications of EC

Electrocoagulation is electrochemical technology to treat water and wastewater by using an electrochemical cell where a DC voltage is applied to the electrodes, usually made of iron or aluminum. During electrocoagulation, hydroxide flocs within the wastewater were formed by electrodissolution of anodes. It had proven its success in the treatment of urban wastewater (Pouet and Grasmick, 1995), restaurant wastewater (Chen et al., 2000), oil-water emulsion wastewater (Ibanez et al., 1995; Chen et al., 2000), the removal of heavy metals (Panayotiva et al., 1996; Balasubramamian and Madhavan, 2001; Diaz et al., 2003; Adhoum et al., 2004; Kumar et al., 2004; Gao et al., 2005; Abdel-Ghani and El-Chaghaby, 2007), the removal of organic compounds (Laridi et al., 2005; Lin et al., 2005; Can et al., 2006; Soltanali and Shams Haghani, 2008), colloidal abrasive particles (Den and Huang, 2006), phosphate (Bektas et al., 2004; Akpor et al., 2008) and viruses (Zhu et al., 2005), suspensions of ultra-fine particles (Matteson et al., 1995), nitrate (Koparal and Ogutveren, 2002), arsenic (Parga et al., 2005), and chemical mechanical polishing wastewater (Lai and Lin, 2003).

2.3.2 Generation of coagulants

In electrocoagulation, water is treated using graphite or stainless steel as cathodes in conjunction with a metal anode (e.g., Al, Fe, Zn, Ni, etc.). Anode material selection is dependent on the wastewater composition. When current is applied, it passes through a metal

electrode, oxidising the metal (M) to its cation (M^{n+}). When the DC field is applied; *in situ* Al^{3+} metal ions (coagulation agent) are generated due to the electrooxidation of the sacrificial aluminum anode (Chen, 2004). The oxidation of water prodcues hydrogen (H^{+}) and oxygen gas at the anode whereas hydrogen gas and hydrogen oxide (OH^{-}), due to the water reduction, are generated at the cathode (Abuzaid et al., 1998). Oxidation also produces hydroxyle radical (OH^{o}) which normally behaves as a strong oxidizing agent and reacts with many organic pollutants (Apaydin et al., 2009) forming dehydrogenated or hydroxylated derivatives. The electrolytic dissolution (electrooxidation) of the aluminum anode produces cationic monomeric species such as Al^{3+} and $Al(OH)_2^{+}$ at acidic conditions. At suitable pH values, they are first transformed to $Al(OH)_3$ and finally polymerized to $Al_n(OH)_{3n}$ according to the following reactions (Mollah et al., 2004):

$$Al_{(s)} \rightarrow Al_{(aq)}^{3+} + 3e^{-} \quad (2.5)$$

$$Al_{(aq)}^{3+} + 3H_2O \rightarrow Al(OH)_3 + 3H_{(aq)}^{+} \quad (2.6)$$

$$nAl(OH)_3 \rightarrow Al_n(OH)_{3n} \quad (2.7)$$

Other compounds such as $Al(OH)^{2+}$, $Al_2(OH)_2^{4+}$ and $Al(OH)_4^{-}$ can be formed in the system depending on the pH of the aqueous media (eqs 2.8 to 2.11).

$$Al^{3+} + H_2O \rightarrow Al(OH)^{2+} + H^{+} \quad (2.8)$$

$$Al(OH)^{2+} + H_2O \rightarrow Al(OH)_2^{+} + H^{+} \quad (2.9)$$

$$Al(OH)_2^{+} + H_2O \rightarrow Al(OH)_3 + H^{+} \quad (2.10)$$

$$Al(OH)_3 + H_2O \rightarrow Al(OH)_4^{-} + H^{+} \quad (2.11)$$

Uncharged aluminum hydroxide $Al(OH)_3$ has low solubility in water with $K_{sp} = 3x10^{-34}$ at 25°C (Holt et al., 2005), and would precipitate at a certain pH value. Hydrolysis of

aluminum results in many monomeric and polymeric substances. In practice, monomeric forms and hydroxide precipitate were likely to be important. Aluminum speciation and the generated monomeric substances were shown in Fig. 2.5. It could be observed that minimum solubility occurs around neutral pH values, whereas the anionic form $Al(OH)_4^-$ (aluminate) is the dominant dissolved species above neutral pH. Up to pH of 4.5, the trivalent ion Al^{3+} is the predominant species, while aluminate ion; $Al(OH)_4^-$ becomes the predominant species at pH values higher than 8. Intermediate species such as $Al(OH)^{2+}$ and $Al(OH)_2^+$ have less contribution at pH between 4 and 6.5.

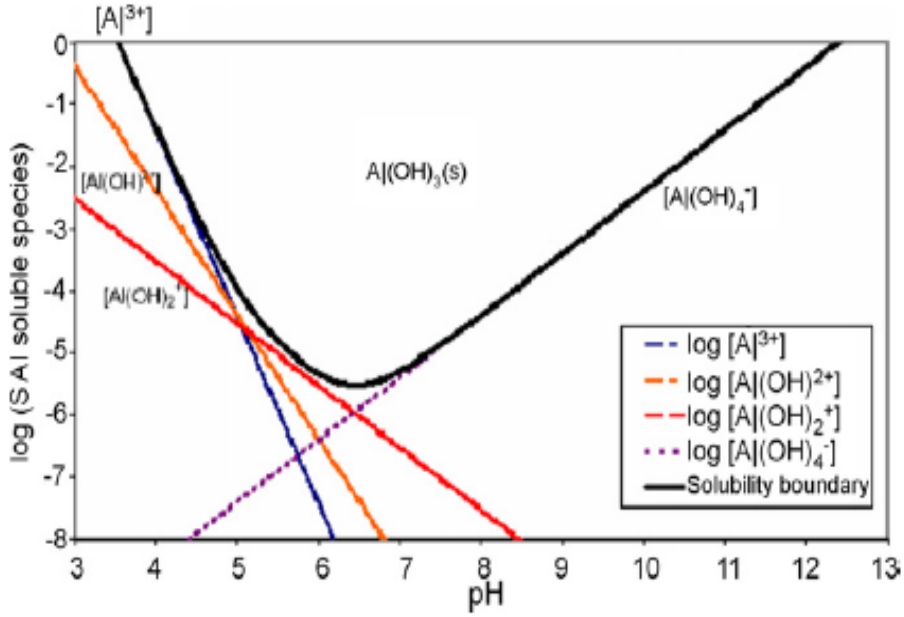

Fig. 2.5: Solubility diagram of aluminum hydroxide considering monomeric species (after Holt et al., 2005).

Once the highly charged metal cations are released in the solution, it destabilizes any colloidal particles by forming complexes of polyvalent polyhydroxide. These compounds have high adsorption properties, which result in forming aggregates with pollutants. The

production of hydrogen gas enhances mixing and flocculation process. Several ways could be predicted for species interaction in the solution. Examples were:

1. Electrophoresis through which charged particles move to the opposite electrode and aggregation due to charge neutralisation (Holt et al., 1999).

2. Electroosmosis which refers to the motion of polar liquid through a membrane or other porous structure (Holt et al., 1999).

3. The cation or hydroxyl ion (OH^-) forms a precipitate with the contaminant (Holt et al., 1999).

4. The cation reacts with OH^- to form a hydroxide which has the ability to form bonds with contaminants (bridge coagulation) (Holt et al., 1999).

5. Sweep coagulation where hydroxides form larger lattice-like structures through water (Holt et al., 1999).

6. Contaminants are oxidized to less toxic compounds (Holt et al., 1999).

7. Removal by electroflotation and adhesion to bubbles (Holt et al., 1999).

2.3.3 Electrocoagulation and colloids interaction and behavior

Colloids are solids that could not be dissolved completely or could not be settled due to their Brownian motion which prevents them from settling at the bottom of the reactor. As a result, they caused high water turbidity. Unlike in a solution, where the particles (ions or molecules) were mixed on a molecular level, a colloid is a solution of 1-1000 nm "aggregates" of particles. Colloids could be hydrophilic or hydrophobic. The hydrophobic colloids were responsible for water coloration and basically they had an organic origin with an $R\text{-}NH_2$ or R-

OH part. They created hydrogen links with water molecules. The hydrophilic colloids were from mineral origins. They had concentrated negative charges on their surfaces which made them hard to aggregate (Chen, 2004).

To understand the behavior of colloids in suspensions or solution; an overview of zeta potential, Stern layer, diffuse layer, and double layer is essential. Colloids have a like electrical charge which produces a repulsion force between particles. If the charge was high, the particles would remain discrete and in suspension. Thus, reducing electrical charge would help those colloids to aggregate and settle out of suspension (Elimelech et al., 1995).

Positive ions (counter-ions) in the solution were attracted by the negative colloids forming an attached layer around the surface of the colloid known as Stern layer. However, additional positive ions were attracted by the negative colloid, yet were repelled by the Stern layer and some other positive ions which were trying to reach the colloid. This dynamic equilibrium resulted in the formation of a diffuse layer of counter-ions. Those counter-ions had a high concentration near the surface, yet the concentration decreased with time until it reached equilibrium with the concentration of the counter-ions in the solution. Similarly, there was a lack of negative ions (co-ions) near the surface because of the repulsive force caused by the negative colloid, but their concentration increased with time until equilibrium was achieved. The diffuse layer could be described as a charged environment surrounding the colloid. The attached counter-ions in the stern layer and the charged atmosphere in the diffuse layer were what we referred to as the double layer. The thickness of this layer depends upon the type and concentration of ions in solution. The potential between the surface of the colloid and any point in the mass of the suspending liquid was referred to as the surface potential (Hunter, 1981; Elimelech et al., 1995). The magnitude of the surface potential (voltage

difference between the colloid and any point in the liquid solution measured in millivolts) indicated the strength of the electrical force between particles. It dropped linearly in the Stern layer and then dropped exponentially in the diffuse layer approaching zero at the boundary of the double layer as shown in Fig. 2.6.

Zeta potential is defined as the potential at the plane of shear between the surface and solution where relative motion occurs between them (Hunter, 1981). Zeta potential was quantified by tracking the colloidal particles through a microscope or Zeta Meter as they migrated in a voltage field. Zeta potential was used to indicate the degree of flocculation. If the magnitude of zeta potential was high, colloids would stabilize and would resist aggregation. When the potential was low, attraction exceeded repulsion and the dispersion would break and flocculate. So, colloids with high magnitude of zeta potential (negative or positive) were electrically stabilized while colloids with low magnitude of zeta potentials tended to coagulate or flocculate (Greenwood, 2003) as shown in Table 2.1.

Table 2.1: Colloids stability based on zeta potential (ASTM, 1985)

Zeta potential [mV]	**Colloid stability**
0 to ±5	Rapid coagulation or flocculation
±10 to ±30	Incipient instability
±30 to ±40	Moderate stability
±40 to ±60	Good stability
> ±61	Excellent stability

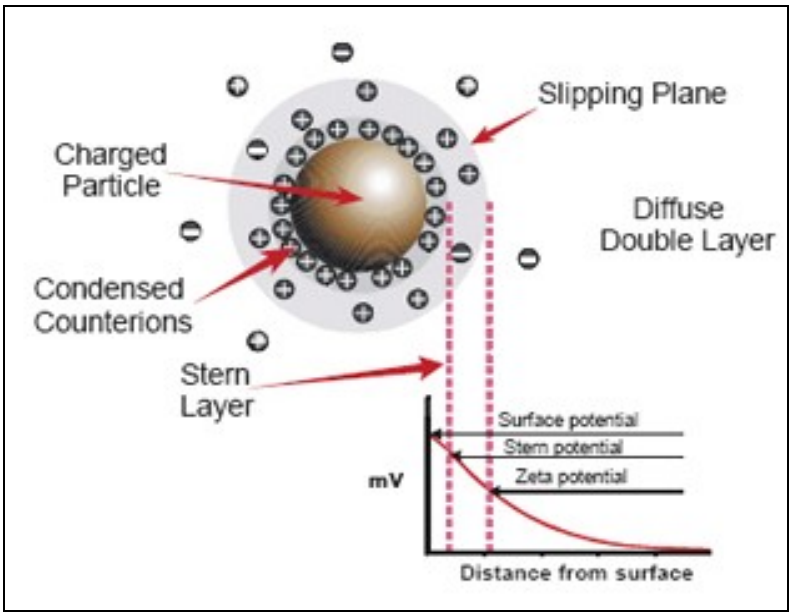

Fig. 2.6: Distribution of ions around a negative charged particle (adapted from Malvern Instruments Ltd., 2005).

2.3.4 Factors affecting electrocoagulation process

Many factors affect the performance of electrocoagulation. For instance, the contact time (exposure time) is considered as a major factor. Low exposure times might decrease the removal efficiency of electrocoagulation whereas high exposure times beyond the optimum value might increase the sludge production yet no additional removal efficiency is observed. Another important factor is the current density, which refers to the applied current per an effective surface area of the anode. This current determines how much aluminum or iron ions are released to the solution. The larger the current density is, the smaller the electrocoagulation unit. However, large current density is not favorable since it increases the chance of wasting energy in heating up the water. In addition, it causes a significant decrease in the removal efficiency. Therefore, an optimum current density has to be determined.

Suggested values were within the range of 10-150 A/m^2 unless there were measures taken for a periodical cleaning of the surface of electrodes (Chen, 2004).

The conductivity of water or wastewater is of a crucial concern. Sodium chloride (NaCl) was sometimes added to increase the conductivity of the water or wastewater to be treated. The advantage of adding NaCl was to enhance its ionic contribution in carrying the electric charge through which chloride ions showed a great ability to reduce the adverse effect of other anions such as HCO_3^-, SO_4^{2-}. NaCl had also decreased the power consumption due to the increase in conductivity. The pollutants removal efficiencies were found to be the best near neutral pH using aluminum electrode (Chen, 2004).

Reviewing the literature, a number of deficiencies to the electrocoagulation process could be addressed. Firstly, literature did not provide many details on the approach to electrocoagulation reactor design and operation. Reported ones varied from laboratory to pilot and industrial scales both as stand-alone reactors through to fully integrated units within a wastewater purification system. Accordingly, there was no dominant reactor design in use nowadays. Secondly, literature did not provide enough and satisfactory data on batch electrocoagulation reactors. Thirdly, little guidance was available for a prior reactor design or performance prediction. It could be noted that most of the reactors were of the continuous type which they had a continuous feed of wastewater and operating under (pseudo) steady-state conditions rather than batch systems. The advantage of the continuous reactors was that their coagulant requirements were essentially fixed which considered as a major advantage in terms of both design and operation. Batch reactors suffered from such an advantage since they operated with a fixed wastewater volume per treatment cycle (Holt et al., 2004).

2.3.5 Design parameters/limitations

As mentioned above, there was a lack of information regarding the design of electrocoagulation reactor due to the fact that not enough information on the approach to electrocoagulation reactor designs and operation. Hence, it was very difficult to compare the performance of electrocoagualtion reactors. The following section highlighted the essential physical and chemical design issues.

Electrocoagulation process could be found in accordance to many units including microfiltration, dissolved air flotation (DAF), sand filtration and electroflotation. Consequently, such combination had significant impacts on the performance of the electrocoagulation process. Physical factors such as reactor geometry and current density played key roles in the design of an electrocoagulation process. Bubble path, flotation effectiveness, floc formation, fluid flow regime and mixing/settling characteristics were physical properties which could be affected by the geometry of the reactor. Current density determined the rate of the electrochemical metal dosing to the solution. From the literature, it was reported that the recommended current density in the range of 10-150 A/m^2. High current densities were desirable for separation processes involving flotation cells or large settling tanks. Alternatively, small current densities were appropriate for electrocoagulators that were combined with conventional sand and coal filters (Chen, 2004).

The control of an electrocoagulation reactor, operation mode, and the chemical interactions of the system had impacts on the process performance. The rate of the cations released into the solution was related to the material of the anode. It was therefore affecting the performance of the electrocoagulation system. Several studies were conducted on the type of the anode material. Hulser et al. (1996) observed that electrocoagulation was strongly

enhanced at aluminum surfaces in comparison to steel. Zhu et al. (2005) had used iron anodes and porous cylindrical stainless steel cathodes for electrocoagulation and applied it as a pretreatment unit before the microfiltration facility for virus removal.

Passivation refers to the spontaneous formation of a hard non-reactive surface film that inhibits further corrosion. The passivation of the electrodes has been a major issue in the operation of electrocoagulation reactors. The longer the electrodes function, the better the type of the electrode material. It was reported that passivation was more observed in aluminum electrodes (Nikolaev et al., 1982; Novikova et al., 1982). However, using iron electrodes lead to deposition of calcium carbonate and magnesium hydroxide at the cathode and an oxide layer at the anode. To minimize the passivation of the electrodes, researchers suggested changing the polarity of the electrode, applying periodic mechanical cleaning, and using some inhibiting agents. The solution pH played a vital role in the speciation of metal ions. The pH influenced the state of other species in solution and the solubility of products formed. Hence, it contributed to the removal efficiency and the efficiency of the electrocoagulation process. An optimum value is in the range of 6 to 8. Since the SMEBR system is a novel development, no publications were found on scale up such a system.

2.4 Conclusions drawn from literature review

As illustrated in the forgoing sections, several technologies have been used for wastewater treatment such as biological processes (Rittmann, 1987), membrane filtration (MBR) (Stephenson et al., 2000), and electrocoagulation (EC-used in conjunction with other treatment process as water quality enhancer) (Inan et al., 2004). Nevertheless, each process had drawbacks when they operated separately. For instance, the membrane in MBR experienced reversible and irreversible fouling during filtration which resulted in a decrease

in the membrane performance (Bourgeous et al., 2001). As a result, the membrane required physical and chemical cleaning, hence increasing the cost of maintenance. Electrocoagulation proved its efficiency in wastewater treatment compared to chemical coagulation (Chen et al., 2000). It had better removal rates of metals, colloids, solid particles, and soluble inorganic pollutants, less sludge production, and more importantly the prevention of undesired ions to be transferred into the treated wastewater. Yet, the disadvantage of this process was that it had not been tested at the pilot or full scale and the process had high capital and operation and maintenance costs (Golder Associates Inc., 2009) when they operated at high current density.

It could be summarized that nutrients removal (in particular phosphorus removal), membrane fouling, and sludge processing are still of a huge concern, and other novel treatment methods should be implemented. For instance, previous efforts tried to combine several operational units for better treatment efficiency. Trivedi (2004) discussed the development and the evaluation of a flat plate microfiltration membrane bioreactor (MBR) technology designed for highly effective nitrogen and phosphorous removal using combined biological and chemical processes. Mavrov et al. (2006) have combined electrocoagulation (EC) with submerged microfiltration flat sheet ceramic membranes (mean pore size of 0.3 μm) in a bench scale for the removal of selenium from industrial wastewater.

Chen et al. (2007) have designed a bioreactor followed with an electro-reactor to investigate the influence of the electric field on membrane flux. In addition, Cui et al. (2009) investigated the combined membrane bioreactor with electrocoagulation process in a laboratory scale to enhance phosphorus removal from synthetic domestic wastewater. Wei et al. (2009) have studied the nutrient removal in an electrically enhanced membrane bioreactor

through which the membrane was separated in another reactor after the electrocoagulation took place in a separate unit, whereas Wei et al. (2010) reported low membrane fouling.

It could be observed that the interaction between biological process, membrane filtration, and electrokinetics in one operational unit (shown earlier in Fig. 1.1) had never been investigated until Elektorowicz et al. (2009) were the first to do so in the submerged membrane electro-bioreactor (SMEBR). Later, Bani-Melhem and Elektorowicz et al. (2010) conducted several experiments in a laboratory scale under constant transmembrane pressure (TMP). Ibeid et al. (2010a, 2010b) investigated the changing in the flocs morphology in a laboratory scale SMEBR system.

This study focused on the necessity of applying a novel technology in wastewater treatment so as to obtain an excellent water quality, to overcome any problems encountered with membrane fouling, to enhance sludge properties for better sludge processing, and to minimize the unit footprint at low cost. The applicability of the new hybrid SMEBR system was investigated. Several laboratory scale experiments were carried out in order to facilitate the design and the scale-up of SMEBR to pilot scale, which had been never applied before in this field. The following Chapter explained the methodology used to accomplish all research objectives.

Chapter 3: Methodology

3.1 SMEBR system

SMEBR stands for "Submerged Membrane Electro-Bioreactor", which is a compact hybrid unit that combines biological, membrane processes and electrokinetic phenomena. SMEBR consisted of a cylindrical reactor. Two cylindrical electrodes were placed inside the SMEBR. 40% perforated aluminum was used as anode, while supporting stainless steel covered by a very fine mesh was used as cathode. The distance between electrodes was less than 10 cm. Electrodes were connected to a DC power supply. The electrical mode or exposure time (5 min ON: 10 min OFF) was controlled using a timer (Ibeid et al., 2010a).

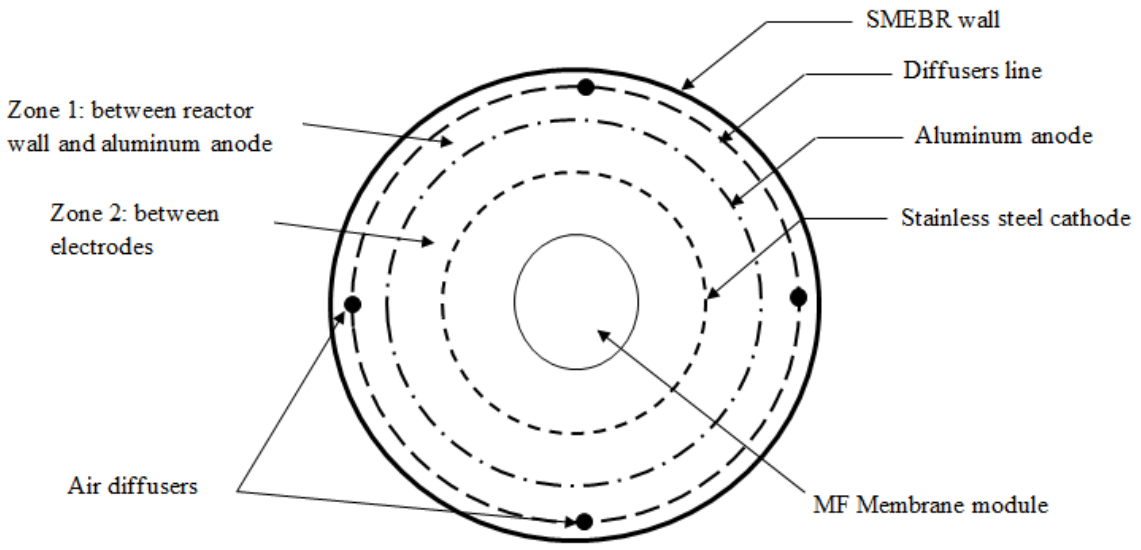

Fig. 3.1: Plan view-bottom of SMEBR.

Compressed air was supplied to SMEBR through 4 fine bubble air diffusers centered at the bottom of SMEBR. Pressure regulator and air flow meter were used to adjust the air pressure and flow rate, respectively. Microza hollow fiber microfiltration (MF)

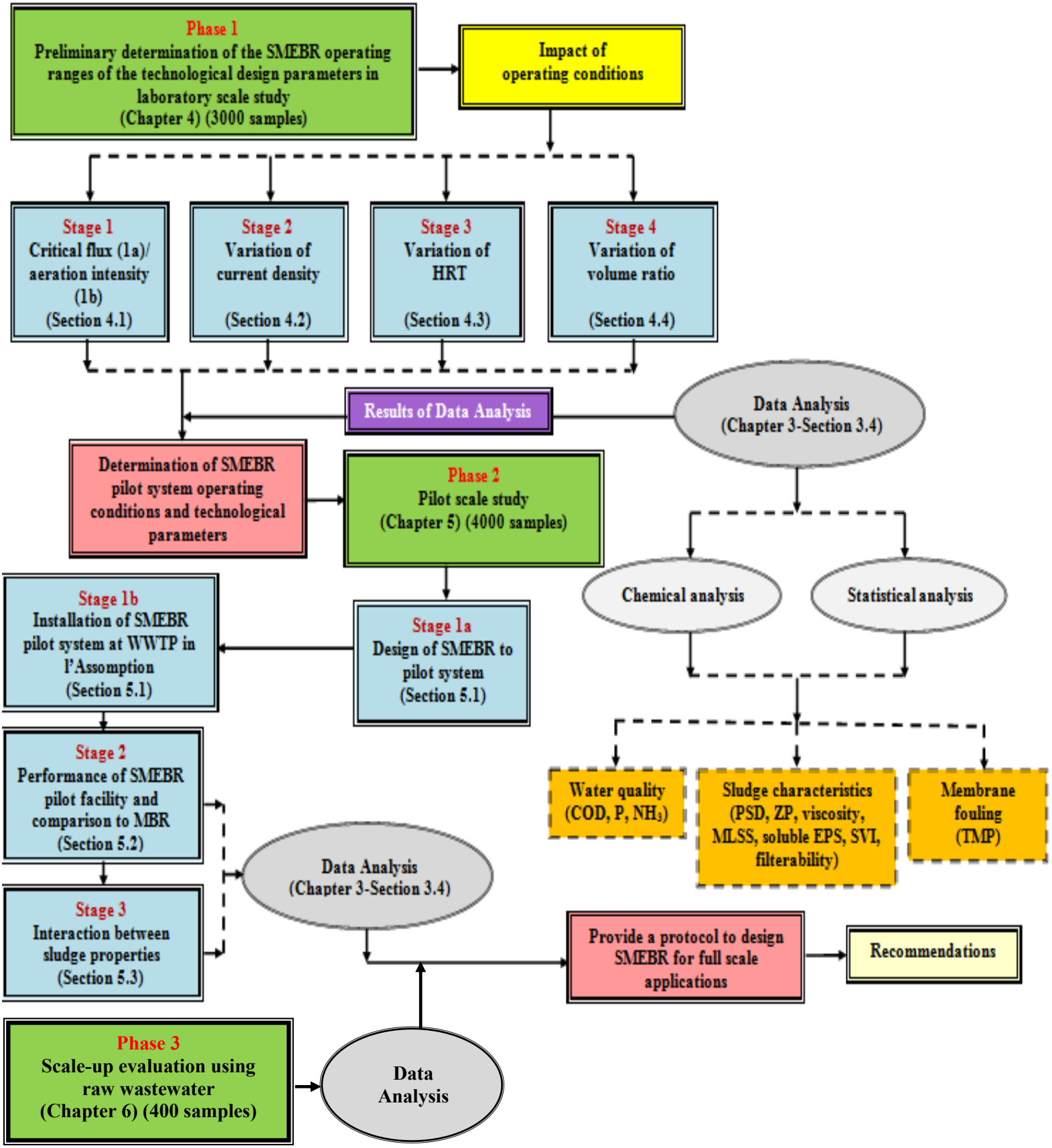

Fig. 3.2: Overall work plan/methodology.

membrane was placed at the center of SMEBR and scoured through a separate aerator provided from Microza. Consequently, the arrangement inside the SMEBR (Elektorowicz et al., 2009) was shown in Fig. 3.1.

To achieve the aforementioned objectives listed in Chapter 1, the proposed methodology shown in Fig. 3.2 was followed. Studies were divided into three Phases: 1) preliminary determination of the technological design parameters in laboratory scale study (4 Stages) treating synthetic wastewater prepared in the laboratory, 2) pilot scale study (3 Stages) treating raw municipal wastewater pumped directly from the influent channel at the wastewater treatment plant in the City of l'Assomption (Quebec), and 3) process scale-up evaluation where the laboratory scale SMEBR system treating raw wastewater and the SMEBR pilot system in Phase 2 operated simultaneously. Detailed description of Phase 1, Phase 2 and Phase 3 including operating conditions, duration of experimentation, and experimental set-ups are provided in Sections 3.2, 3.3, and 3.4, respectively.

3.2 Phase 1: Preliminary determination of the SMEBR operating ranges of technological design parameters in laboratory scale study using synthetic wastewater

The objective of the laboratory scale study was to evaluate the SMEBR by investigating the effects of operating conditions, such as, current density, volume of electrical zone with respect to the effective volume ratio, HRT, and critical flux/ aeration intensity on membrane performance, removal efficiency, and sludge properties. Synthetic wastewater used in this study was prepared in the laboratory. The compositions of synthetic wastewater in mg/L were: glucose (310), peptone (252), yeast extract (300), $(NH_4)_2SO_4$ (200), KH_2PO_4 (37), $MgSO_4 \cdot 7H_2O$ (40), $MnSO_4 \cdot H_2O$ (4.5), $FeCl_3 \cdot 6H_2O$ (0.4), $CaCl_2 \cdot 2H_2O$ (4), KCl (25), and $NaHCO_3$ (25) (Bani-Melhem and Elektorowicz, 2010).

Several factors contributed to membrane fouling including sludge properties (Fig. 2.7). According to the literature review summarized in Chapter 2, laboratory scale experiments were conducted under suitable ranges of operating conditions and sludge characteristics which were suggested for the conventional membrane bioreactors (HRT, SRT, MLSS, and aeration intensity), and electrocoagulation (current density, exposure time).

3.2.1 Stage 1: Objective: Critical flux and aeration intensity

Stage 1a: Objective: Determination of critical flux of MF Membrane

At a fixed MLSS of 7000 mg/L with controlled HRT of 9 h, the critical flux of Microza hollow fiber microfiltration membrane module was measured at different aeration intensities for SMBER and MBR. For comparative purposes, two bioreactors (MBR and SMEBR) with an effective volume of 15 L each were operated in parallel. The time period for this Phase was one day.

Stage 1b: Objective: Effect of aeration intensity

At a fixed MLSS of 5600 mg/L with controlled HRT of 9 h, the effect of aeration intensity was investigated on fouling behavior, and sludge characteristics. Five aeration intensities of 418, 552, 691, 815 and 1143 L/h were applied to adjust the amount of oxygen required for the microorganisms, and to provide adequate mixing throughout SMEBR without breaking down the flocs formation. Experiments of a 5-hour unit step were conducted. SMEBR with an effective volume of 15 L was operated in this phase. The time period for this Phase was two days.

3.2.2 Stage 2: Objective: Impact of applied current density in SMEBR

At a fixed sludge retention time of 20 d with controlled HRT of 9 h and organic loading of 1.3 kg COD/m^3.d, SMEBR was operated at four current densities: 5, 10, 15, and 27 A/m^2. These values were selected according to previous studies (Ibeid et al., 2010b; Bani-Melhem and Elektorowicz, 2010; Bani-Melhem and Elektorowicz, 2011) and to make sure that SMEBR operated under adequate current density which did not inhibit the biological process. The first run was conducted at 27 A/m^2 for 14 days. The second run was conducted at 15 A/m^2 for 14 days. The third run was conducted at 10 A/m^2 for 14 days. Finally, the fourth run was conducted at 5 A/m^2 for 14 days. Two bioreactors (MBR and SMEBR) with an effective volume of 15 L each were operated in parallel for comparative purposes. In SMEBR, two cylindrical electrodes were used: 40% perforated aluminum was used as an anode, while supporting stainless steel covered by a very fine mesh was used as a cathode. The distance between electrodes was less than 10 cm. Electrodes were connected to the DC power supply. The electrical mode (5 min ON: 10 min OFF) was controlled using a timer. The time period for this Phase was forty five days.

3.2.3 Stage 3: Objective: Effect of hydraulic retention time (HRT)

At a fixed current density (15 A/m^2, adequate current density obtained from Stage 2) and SRT (20 d) but varying organic loading, SMEBR was operated for three different HRTs, 6, 9, and 15 h. The selected range of HRT was based on previous studies carried out using MBR (Yamamoto et al., 1991; Harada et al., 1994; Seo et al., 1997; Rosenberger et al., 2002). The first run was carried out at 9 h of HRT with a permeated flux of 16.7 L/m^2.h for 8 days. After that, the second run was commenced for 6 h of HRT for 8 days, while the permeate flux was increased to 25 L/m^2.h. Finally, the third run was operated at HRT 15 h for 8 days with a

permeate flux of 10 L/m^2.h. SMEBR with an effective volume of 15 L was operated in this phase under different flow rates. The time period for this Phase was one month.

3.2.4 Stage 4: <u>Objective:</u> Impact of volume ratio (V^*/V)

At a fixed current density (15 A/m^2, adequate current density obtained from Stage 2) and SRT (20 d) but varying HRT, SMEBR was operated at different volume to volume ratios, i.e. the volume percentage of the electrical zone was varied by increasing the diameter of the SMEBR, and thus increasing the outer zone of the reactor. The volume of the electrical zone (between electrodes) (V^*) was fixed throughout all runs, yet the volume of the effective liquid (V) was changing. The first run was performed when the electrical zone occupies 47% of the total volume of SMEBR with HRT of 9 h for 8 days. The second run was performed when the electrical zone occupies 24% of the total volume of SMEBR with HRT of 18 h for 8 days. Effective volumes of SMEBR were 15 and 30 L, respectively. The time period for this Phase was three weeks.

3.2.5 Experimental set-up of Phase 1

Laboratory scale experiments were carried out at ambient conditions through which synthetic wastewater was used. MF hollow fiber Microza membranes were used and submerged in the bioreactors. The membrane had an effective membrane area of 0.1 m^2. Membrane characteristics were shown in Table 3.1. Each bioreactor was fed with synthetic wastewater and pumped into the bioreactors by means of peristaltic pumps (MasterFlex pump, Cole-Parmer). Effluents were pumped out from the bioreactors by suction pumps (MasterFlex pump, Cole-Parmer). The membrane cleaning process was temporarily required when the membrane was clogged, which was indicated by the increase in the transmembrane pressure

(TMP) up to ~70 kPa. The TMP value was measured using a digital gauge pressure. Compressed air was supplied through several air diffusers placed at the bottom of the bioreactor. Average dissolved oxygen was monitored using a DO meter in order to keep it above 2 mg/L. Analyses were performed immediately to avoid any changes in the sludge characteristics. Schematic diagrams of the SMEBR and MBR experimental set-ups were shown in Figs 3.3 and 3.4. Activated sludge mixed liquor used in Phase 1 was brought from the municipal wastewater treatment in Saint-Hyacinth, Quebec, Canada.

Table 3.1: Laboratory scale MF membrane module characteristics (Asahi Kasei Chemicals Corporation (Japan))

Item	Membrane characteristics
Membrane material and configuration	Hollow fiber PVDF
Normal pore size	0.1 µm
Membrane surface area	0.1 m^2
Module diameter	0.042 m
Module length	0.32 m
Manufacturer	Asahi Kasei Chemicals Corporation (Japan)

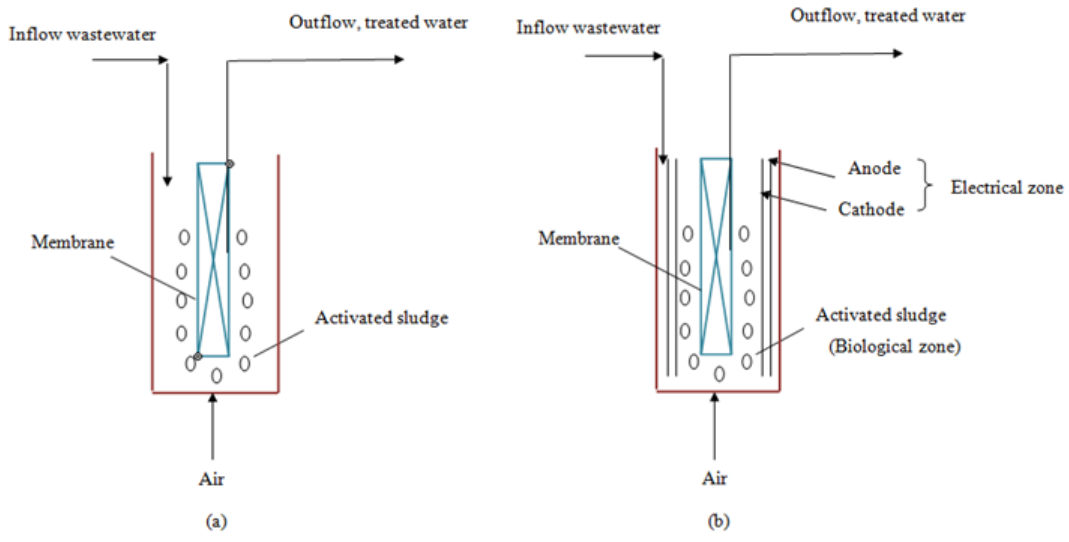

Fig. 3.3: Cross-section of the (a) MBR and (b) SMEBR.

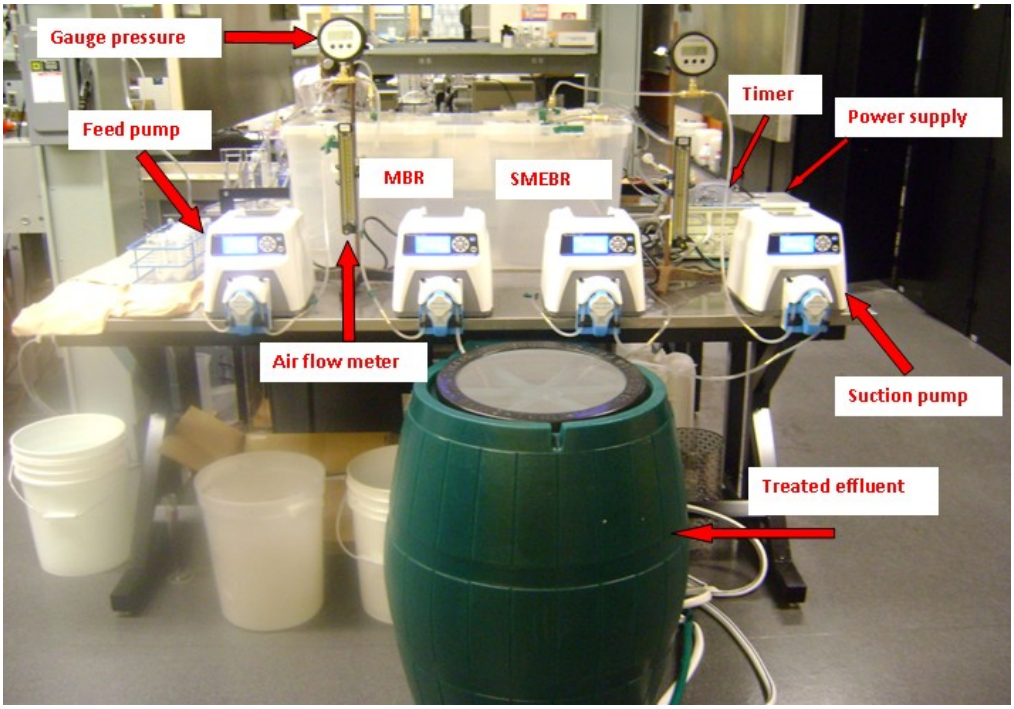

Fig. 3.4: Laboratory scale SMEBR and MBR systems.

3.3 Phase 2: Pilot scale design and investigation study

3.3.1 Stage 1: Objective: Design and installation of MBR and SMEBR pilot facilities treating raw wastewater

Stage 1a: Objective: Design pilot scale SMEBR system

Based on results obtained from the chemical and the statistical data analysis in Phase 1, the technological operational parameters such as current density/exposure time, aeration intensity, HRT, SRT, and reactor geometry were determined for the operation of SMEBR pilot facility in Phase 2. Since SMEBR is a novel technology, no scale-up protocol was found in literature, and thus the preliminary design scale-up approach shown in Fig. 3.5 was followed based on the operating flow rate of the influent wastewater, membrane critical flux (Stage 1 - Phase 1), and dimensional geometry. For example, the volume of the electrical zone (i.e. between

electrodes) was maintained within the desired range based on the results obtained from Stage 4 in Phase 1. Similarly, the operating current density was selected according to Stage 2 in Phase 1. Operational HRT was also adjusted within the results from Stage 3 in Phase 1, and consequently the volume of SMEBR was determined taking into consideration the height of the membrane module to be completely submerged in the reactor. Activated sludge mixed liquor used in Phase 2 was brought from the municipal wastewater treatment in Saint-Hyacinth, Quebec, Canada.

Stage 1b: Objective: Installation of pilot SMEBR system

For comparative purposes, a conventional MBR pilot test was also conducted provided that the same operating conditions and the same wastewater were maintained. SMEBR and MBR pilot facilities were located in the WWTP in the City of l'Assomption (Quebec), and consisted of a PVC cylindrical reactor (235 L), two cylindrical electrodes connected to a low DC power supply (in SMEBR), and a hollow fiber microfiltration membrane (MUNC-600A, Microza, Asahi Kasei Chem. Corp., Japan) (Fig. 3.6). The characteristics of the membrane were shown in Table 3.2. Compressed air was supplied through fine bubble air diffusers centered at the bottom of the reactor.

3.3.2 Stage 2: Objective: Operation and performance of SMEBR and MBR pilot systems

SMEBR and MBR were continuously supplied with de-gritted and screened raw municipal wastewater redirected from the influent channel at a flow rate of 550 L/d. SRT and HRT were 10 d and 11 h, respectively. SMEBR operated under constant current density of 12 A/m^2. The influent COD, ammonia, and phosphorous varied in the wastewater, ranging between 160-700 mg/L, 30-70 mg NH_3^+-N/L, and 2-10 mg PO_4^{3-}-P /L, respectively. Each test of SMEBR and MBR was conducted for 7 weeks (Hasan et al., 2011; Elektorowicz et al., 2011).

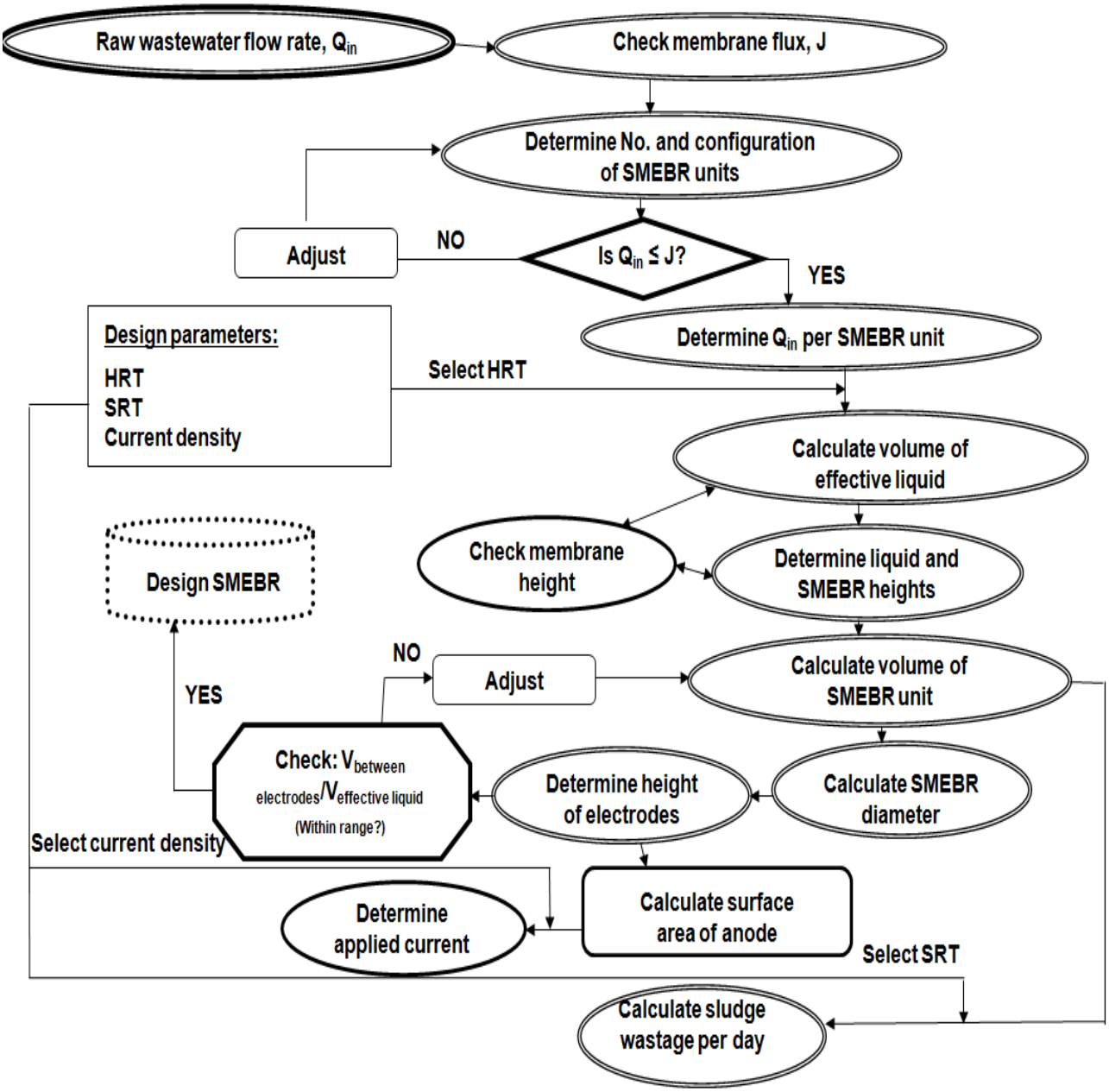

Fig. 3.5: SMEBR experimental design protocol to pilot scale (Preliminary design scale-up approach).

Table 3.2: Pilot scale membrane module characteristics (Asahi Kasei Chemicals Corporation-Japan)

Item	Membrane characteristics
Membrane material	PVDF
Normal pore size	0.1 µm
Membrane surface area	12.5 m^2
Module diameter	0.167 m
Module length	1.131 m
Membrane configuration	Hollow fiber
Filtration mode	Suction filtration by submerged membrane
Maximum TMP	300 kPa
Maximum operating Temperature	40^oC
pH range	1-10
Designed flux	0.2 – 0.7 $m^3/m^2.d$
Manufacturer	Asahi Kasei Chemicals Corporation (Japan)

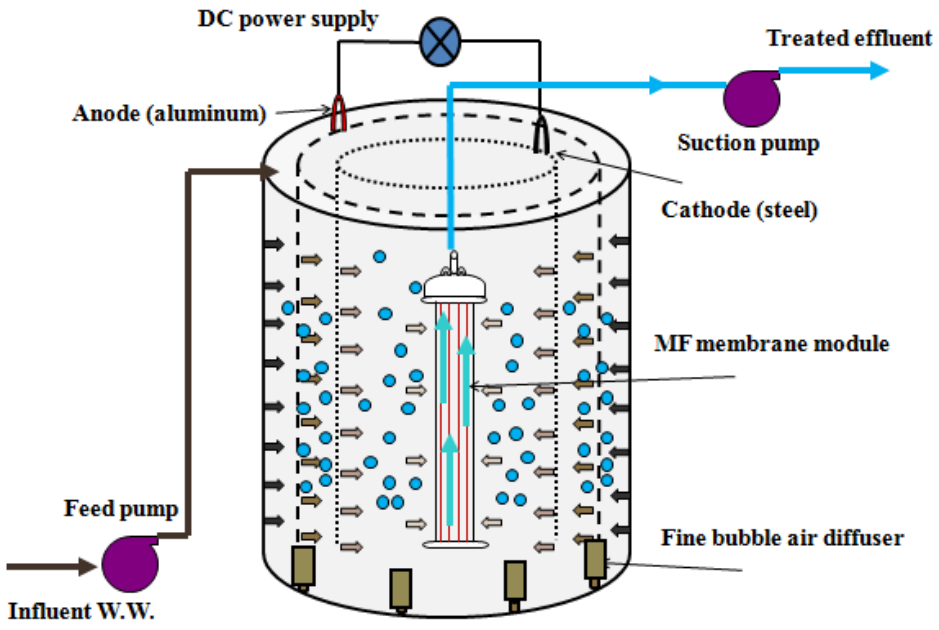

Fig. 3.6: Schematic diagram of pilot SMEBR.

3.3.3 Stage 3: Objective: Interaction between sludge properties in SMEBR and MBR

Statistical analysis was conducted to identify the major factors affecting membrane fouling. The data used for the statistical analyses were generated from the above described pilot facilities where the tests were subject to daily and seasonal variations. Statistical analyses were carried out using Microsoft Excel built-in statistical functions. Pearson's product momentum correlation coefficient, r_p (eq. 3.1), was used for linear estimations of the strength and direction of linear correlations between two parameters.

$$r_p = \frac{\Sigma(x - x_{avg})(y - y_{avg})}{\sqrt{\Sigma(x - x_{avg})^2 (y - y_{avg})^2}} \qquad (3.1)$$

Where, r_p is the Pearson's product momentum correlation coefficient, (x, y) is a sample of paired data, $x_{avg.}$ and $y_{avg.}$ are mean values.

Generally, the value of r_p oscillated between -1 and +1, as r_p = -1 or r_p = +1 represented a perfect correlation, and 0 showed no correlation (Jin et al., 2004). If $-0.4 < r_p < +0.4$, the correlation was assumed weak and ignored. The positive r_p showed a direct proportionality, while the negative r_p showed an inverse proportionality. In this study, correlations were considered statistically significant at a 95% confidence level where the p-value was less than 0.05. Multiple regression was used to generate statistical models which represented the TMP (dependent variable) as a function of sludge properties (independent variables) in SMEBR and MBR. The statistical approach gave an indication for future investigations to better understand interactive processes in both reactors.

3.4 Phase 3: Scale-up verification: laboratory scale study treating raw wastewater under steady state conditions

The objective of Phase 3 was to verify the process scale-up in SMEBR system. A laboratory scale SMEBR experiment was carried out in parallel to the SMEBR pilot system. The pre-screened technological design parameters of the SMEBR system in Phase 1 were verified under steady state conditions in both laboratory and pilot scale systems. These included 11 h, 10 d, and 12 A/m^2 of HRT, SRT and current density, respectively. Intermittent exposure mode of 5 min ON: 10 min OFF was controlled using a timer. Both reactors were fed with the same raw wastewater (see characteristics in Stage 2 - Phase 2). The time period for this Phase was forty five days.

3.5 Analytical methods for laboratory and pilot tests

Fresh activated sludge samples were collected from different locations in SMEBR and MBR four times per week and tested for MLSS, PSD, EPS, and zeta potential immediately. Samples were tested twice and an average value was recorded. Analytical techniques used in this study for MLSS, MLVSS, and MLFSS followed Standard Methods (APHA et al., 1998). COD, phosphorus, ammonia, total nitrogen, nitrates, and aluminum concentrations were measured using Hach TNT vials. Colloids (COD_c) were measured by extracting the soluble COD (COD_s) from the sludge supernatant. Samples were first centrifuged at 4000 rpm for 20 min then 250 mg/L aluminum sulphate was added to separate the colloids from the soluble substances (Rojas et al., 2005). The mean particle size diameter was determined by injecting fresh samples directly into the Horiba Laser Scattering Particle Size Distribution Analyzer (LA-950). The sludge viscosity was measured by a falling ball viscometer (Gilmont instrument, Model GV-2100). In this study, proteins (EPS_p) and carbohydrates (EPS_c), were

considered as main components of EPS and were analyzed by phenol/sulfuric-acid method (Dubois, 1956) and folin method (Lowry, 1951), respectively. Zeta potential was measured directly in the sludge supernatant samples using the Zeta Meter Analyzer (Zeta Meter 3.0+, USA). Sludge volume index (SVI) was measured using one liter graduated cylinder, where sludge was left behind to settle for 45 minutes.

Dissolved oxygen (DO), pH, conductivity, and temperature (T) were measured using DO Meter (YSI, Model 52, USA). The OUR test essentially consists of adding an aerated sample of mixed liquor to the test chamber, placing the dissolved oxygen (DO) probe into the chamber and monitoring the decline in dissolved oxygen over time. The slope represents the OUR and has the units of mg O_2/L.h. Oxidation-reduction potential (ORP) was analyzed using ORP tester manufactured by Eutech instruments. The sludge samples from each reactor were filtrated using a filtration set and the membrane fouling index (MFI) was calculated from the ratio of filtration time to filtrate volume (t/V) as a function of the total filtrate volume. The specific cake resistance (α) was calculated from the slope of the t/V curve as shown earlier (eq. 2.4).

When transmembrane pressure (TMP) was increased up to 70 kPa (Laboratory modules) or 100 kPa (Pilot module), a cleaning procedure was performed on the membranes. All suction lines and electrical connections were disconnected from the membrane modules, and then the membranes were taken out from the reactors in order to remove the cake layers. Membrane modules were washed carefully with tap water. After that the membranes were immersed in a chemical cleaning tank (%0.05 NaOCl solution) for 8 h. The chemical cleaning process was repeated if the desired membrane efficiency was not achieved.

Statistical analysis such as multiple regression (presented earlier in eq. 3.1) and the one-way ANalysis Of VAriance (one-way ANOVA) analysis were applied in this study. ANOVA was a powerful and common statistical procedure used in many fields such as social sciences, engineering, economics, etc. It was used to determine the major factors which have significant influences on membrane fouling. Correlations were considered statistically significant when their P-values were less than 0.05.

The handheld NITON XRF analyzer was used to identify the elements present in the deposition observed on the surface of the electrodes, and in the dry sludge produced during the treatment. Pearson's Crystal Data software was also used to predict the different chemical compounds and complexes which could be formed in SMEBR system. An Atomic Absorption Spectrometer (Perkin Elmer, Analyst 100) was used to analyze major metals.

Chapter 4: Results and Discussions of Laboratory Scale Experiments - Phase 1

4.1 Stage 1a: Objective: Determination of critical flux at different aeration intensities

The concept of critical flux was introduced by Field et al. (1995) and defined as the flux below which fouling would not take place. Operating under the critical flux might not lead to irreversible fouling (Howell, 1995). Nevertheless, some researchers observed fouling even if the membrane bioreactors operated below the critical flux, yet the rate of fouling is much smaller and more sustainable (Le-Clech et al., 2003). Membrane fouling which could be attributed to several and complex mechanisms was related to critical flux (Fane, 2002). Critical flux could be affected by many factors, but most importantly: membrane materials and configurations, operating parameters, and sludge properties (Fane, 2002). It was noticed that critical flux had an inverse proportion to the mixed liquor suspended solid (MLSS) concentration from 0 to 10000 mg/L (Madaeni et al., 1999). Manem and Sanderson (1996) reported that MLSS could not be used to predict filterability. Colloidal particles played a key role in membrane fouling. EPS mainly in soluble forms were also major participants to fouling (Chang et al., 2002).

Experiments were conducted to determine the critical flux of the MF hollow fiber membrane module from Microza. Experiments were carried out under different aeration intensities to examine the influence of aeration on critical flux. MBR and SMEBR with an effective volume of 15 L each were operated in parallel for this study. At the start of the each experimental run, the initial membrane resistance was measured using tap water. Tables 4.1 and 4.2 and Fig. 4.1 showed the initial membrane resistances of MBR and SMEBR. A little difference in the initial resistances could be observed as 7.44×10^{11} and 8.84×10^{11} 1/m were reported in MBR and SMEBR, respectively. This could be attributed to the addition of the

electrodes to SMEBR which increased the membrane resistance. Critical flux was measured using the stepwise flux method suggested by Ognier et al. (2002). Before conducting the experiments, the membrane modules were cleaned by air scouring without permeation. The flux was increased by an increment of 8.3 $L/m^2.h$. Each step lasted for 10 minutes with continuous permeation. The critical flux was determined by averaging two values of the permeate flux (as shown in Appendix A – Figs A-1 to A-10). These points were: the maximum flux which TMP increased linearly with the flux and the minimum flux where the linear relationship was not valid anymore.

Five intensities including aeration tank and membrane were tested in these experiments (418, 552, 691, 815 and 1143 L/h). It could be reported that the critical flux increased with the aeration intensity (Liu et al., 2003) as shown in Fig. 4.2. This behavior was observed in MBR and SMEBR. It could be said that higher aeration intensities enhanced the scrubbing of small particles which could be accumulated on the surfaces of the membrane and hence lower TMP and less fouling. Table 4.3 listed the critical flux of MBR and SMEBR at each aeration intensity. It could be also noticed that the critical flux values for SMEBR was a bit higher than those in MBR. This could be explained by the reactor configuration (i.e. addition of electrode in SMEBR) where the membrane module was surrounded by two cylindrical electrodes and those electrodes worked as air intensifiers around the membrane module through which the air flow was directed vertically towards the membrane, and therefore more particles were washed away from the membrane surfaces. It could be also speculated that an open circuit was generated in SMEBR, due to the presence of electrodes, and thus gas bubbles were created and enhanced the removal of particles away from the surface of the membrane.

Table 4.1: Initial membrane resistance for MBR

Q, L/d	Flux, $m^3/m^2.h$	TMP, kPa	R_m, 1/m
20	0.0083	1.3	$5.61x10^{11}$
40	0.0167	4.2	$9.06x10^{11}$
60	0.0250	5.1	$7.33x10^{11}$
80	0.0333	7.2	$7.76x10^{11}$
100	0.0417	8.6	$7.42x10^{11}$
			Avg. R_m = $7.44x10^{11}$

Table 4.2: Initial membrane resistance for SMEBR

Q, L/d	Flux, $m^3/m^2.h$	TMP, kPa	R_m, 1/m
20	0.0083	1.9	$8.19x10^{11}$
40	0.0167	4.7	$1.01x10^{12}$
60	0.0250	6.7	$9.63x10^{11}$
80	0.0333	7.6	$8.19x10^{11}$
100	0.0417	9.3	$8.02x10^{11}$
			Avg. R_m = $8.84x10^{11}$

Note: Viscosity of the water at 20°C is $1.0x10^{-6}$ kPa.s

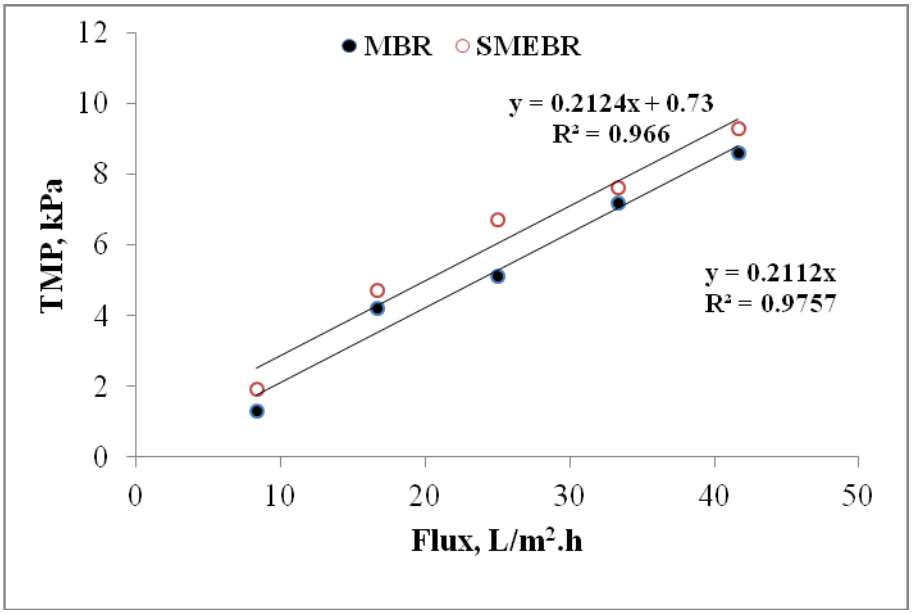

Fig. 4.1: Variation of TMP with filtration flux for MBR and SMEBR.

Table 4.3: Critical flux vs. aeration intensity for MBR and SMEBR

	MBR	**SMEBR**
Aeration intensity, L/h	**Critical flux, L/m^2.h**	**Critical flux, L/m^2.h**
418	29.2	31.3
552	31.3	32.5
691	32.1	33.8
815	33.3	34.6
1143	35.0	35.8

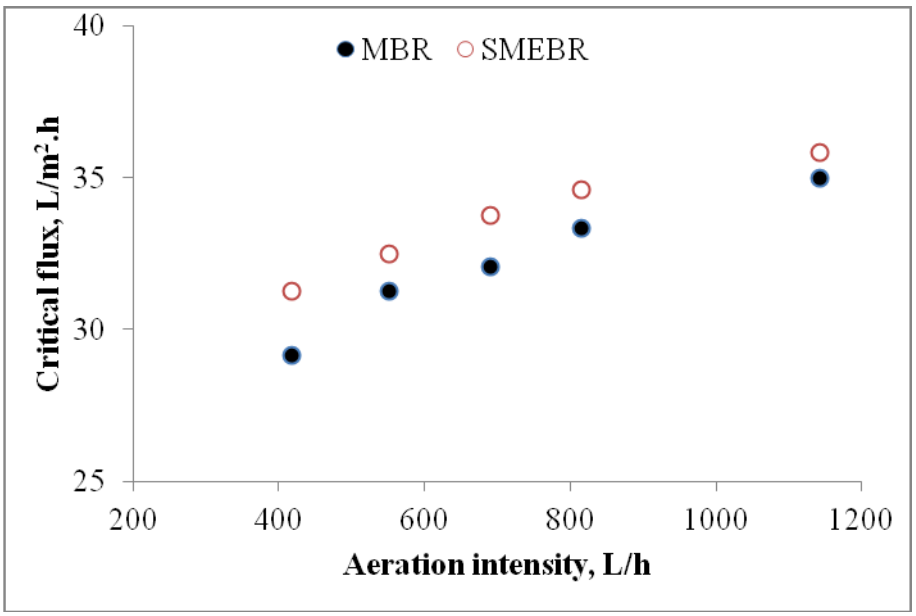

Fig. 4.2: Critical flux vs. aeration intensity for MBR and SMEBR.

4.2 Stage 1b: <u>Objective:</u> Variation of aeration intensity on sludge characteristics

The increase in aeration rate in membrane bioreactors minimized fouling and enhanced the permeate flux. Aeration in submerged membrane bioreactors created shear stress which resulted in not only providing oxygen to the biomass, but also in keeping the solids in suspension and scouring the membrane surface. It was reported that more than 80% of the energy consumption was for aeration (Churchouse, 2002). In addition, aeration had significant influence on sludge characteristics. Several studies investigated the influence of aeration intensities on membrane permeability and biomass characteristics. Others investigated the impacts of aeration intensity on the formation of membrane foulants. Results showed that low or high aeration intensity had negative impacts on membrane permeability (Meng et al., 2007).

Experiments of 5-hour unit step were conducted. SMEBR having an effective volume of 15 L with the MLSS concentration of 5600 mg/L were used. Hydraulic retention

time (HRT) was set at 9 h. Samples from sludge supernatant were taken, centrifuged using IEC HN-SII centrifuge, and then analyzed for viscosity, zeta potential, and soluble extracellular polymeric substances (soluble EPS) in terms of carbohydrates (EPS_c) and proteins (EPS_p). Samples from sludge suspension were taken and analyzed for mean particle size diameter (PSD), and filterability. The effect of aeration intensity was investigated on fouling behavior, and sludge characteristics. Different intensities were applied: 418, 552, 691, 815 and 1143 L/h. An optimum value was determined which satisfied providing desired amount of air at minimum energy consumption due to aeration. Initial sludge properties (average values of three repetitions per sludge property) are shown in Table 4.4. Statistical analysis using one-way ANOVA was used to determine the major properties which have been significantly influenced by the variation of aeration intensity.

Table 4.4: Initial sludge properties in Stage 1b

MLSS, mg/L	5600 ± 46.3
PSD, µm	45.71 ± 0.9
EPS_c, mg/L	3.14 ± 0.3
EPS_p, mg/L	12.47 ± 0.6
SVI, mL/g	143.1 ± 4.1
Viscosity, mPa.s	1.63 ± 0.07
Zeta potential, mV	-31.9 ± 1.1
Filtration time (50 mL), sec	620 ± 2.5

4.2.1 Relationship between aeration intensity and mean particle size diameter (PSD)

Fig. 4.3 showed the variation of mean particle size diameter (PSD) with aeration. It could be observed that the particle or floc size reduced as the aeration intensity increased. For instance, flocs had initial size of 45.71 µm which slightly decreased to 45.6 µm when the entire reactor was under 418 L/h. An increase in aeration rate to 552 L/h caused a slight decrease in floc size and went down to 45.4 µm. As aeration increases to 691 L/h, floc size reduced to 44.1 µm.

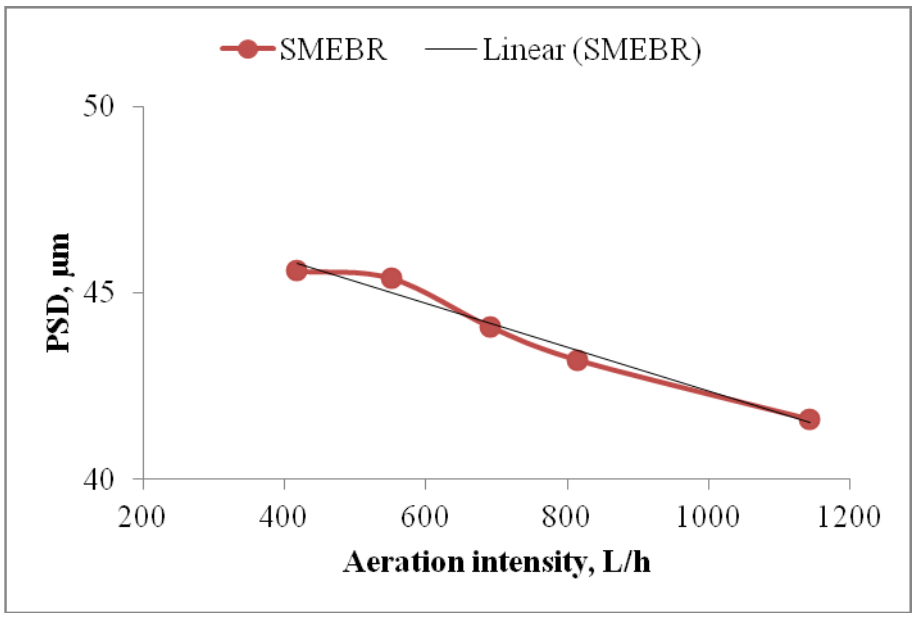

Fig. 4.3: Mean particle size diameter variation at different aeration intensities.

Vigorous aeration of 815 and 1143 L/h showed a reduction in floc size of 43.2 and 41.6 µm, respectively. Consequently, as the aeration rate increased, flocs started to break down. This might be due to erosion strength or to certain rupture in the network of polysaccharide fibrils which would work as cell supports (Meng et al., 2007; Parker et al., 1972). From the above results, it could be summarized that an aeration intensity of 552 L/h achieved better results than the rest of the higher aeration intensities. Statistical analysis

performed reached the same conclusion which stated that particle size had been significantly influenced by the aeration intensity (P = 0.00097).

4.2.2 Relationship between aeration intensity and soluble extracellular polymeric substances (soluble EPS)

Soluble extracellular polymeric substances could be characterized by the sum of many components mainly carbohydrates or polysaccharides (EPS_c) and proteins (EPS_p). Several studies concluded that these components played a vital role in the decline of the permeate flux (Ye et al., 2005; Nagaoka and Kudo, 2002). Figs 4.4 and 4.5 showed the variation of soluble EPS with aeration. It was clear that the concentration of proteins was higher than the concentration of carbohydrates, and therefore being one of the major foulants (Bouhabila et al., 2001). It could be deduced that as the aeration intensity increased, more EPS were released to the sludge suspension, and thus more fouling. From the above results, it could be summarized that an aeration intensity of 552 L/h achieved better results than the rest of the higher aeration intensities. Statistical analysis performed pointed to the same conclusion which stated that soluble EPS had been significantly influenced by the aeration intensity (P = 0.00073 for carbohydrates and P = 0.00079 for protein). The role of EPS in fouling and flocs formation in pilot SMEBR is explained in detail in Chapter 5 - Section 5.2.

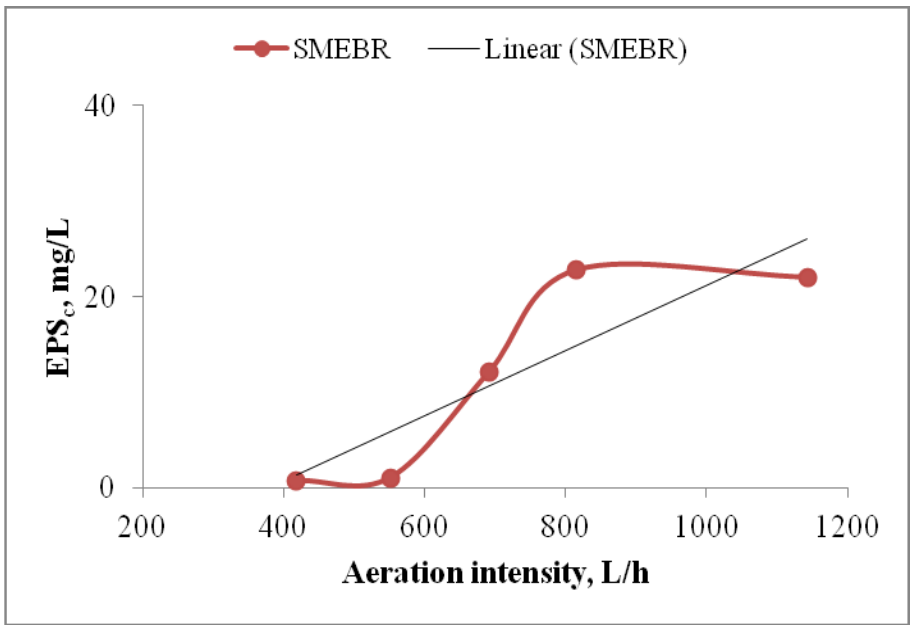

Fig. 4.4: EPS_c variation at different aeration intensities.

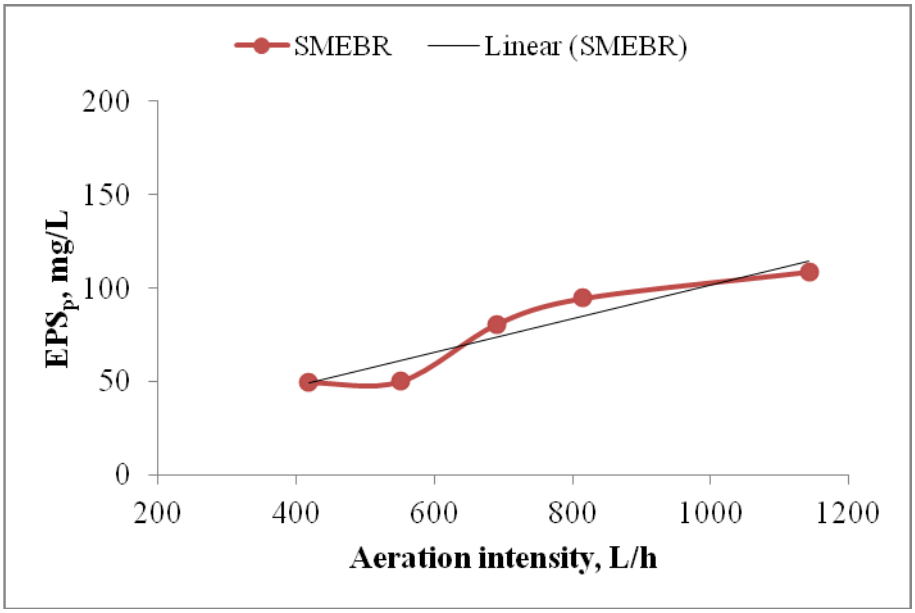

Fig. 4.5: EPS_p variation at different aeration intensities.

4.2.3 Relationship between aeration intensity and zeta potential

Zeta potential reflects the surface charge of sludge particles or flocs. Several studies suggested that EPS concentration had a significant effect on the surface charge of sludge flocs. It was also reported that the release of such polymeric substances to the sludge flocs lead to more negative surface charge through which proteins were major contributors to such an increase (Wilén et al., 2003). This could be attributed to the fact that some functional groups (carboxylic, sulfate, and phosphate) of EPS were ionized (Sutherland, 2001). Fig. 4.6 showed the variation of zeta potential with aeration.

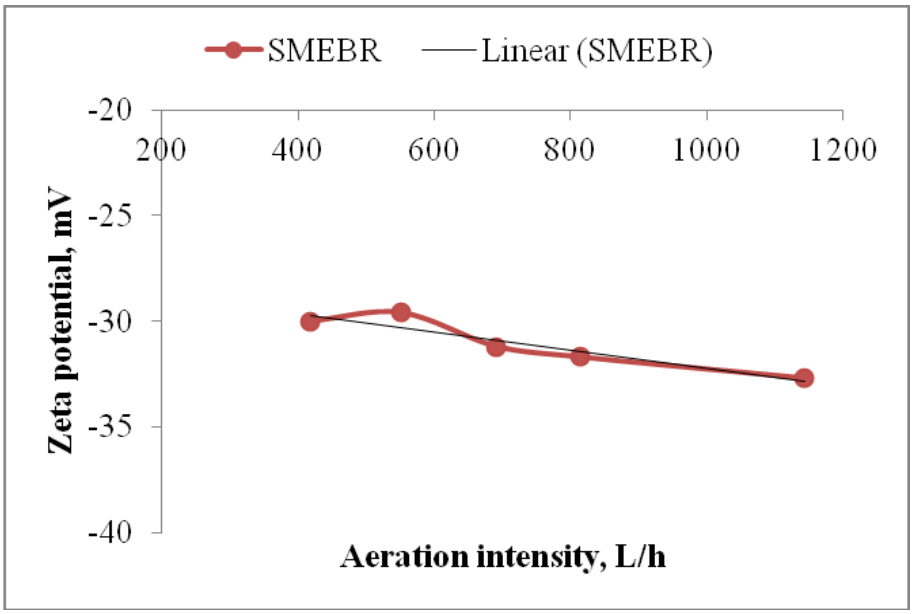

Fig. 4.6: Zeta potential variation at different aeration intensities.

It could be summarized that as the aeration intensity increased beyond 552 L/h, more EPS were released to the sludge suspension leading to an increase in the magnitude of zeta potential and therefore less bioflocculation. From the above results, it could be summarized that an aeration intensity of 552 L/h achieved better results than the rest of the

higher aeration intensities. Statistical analysis performed reached the same conclusion which stated that zeta potential had been significantly influenced by the aeration intensity (P = 0.00067).

4.2.4 Relationship between aeration intensity and filterability

Filterability test was used to identify sludge dewatering. Soluble microbial products and colloids were considered as major foulants, especially their role in pore blocking mechanism (Drews et al., 2006). Fig. 4.7 showed the variation of filtration time required to filter 50 mL of sludge suspension with aeration. It was observed that at aeration intensity of 552 L/h, the best filterability or sludge dewatering was achieved. Further aeration caused flocs breakage and therefore lots of polymeric materials especially soluble EPS were released to the sludge suspension and caused a reduction in filtration time. This was due to the presence of small particles in sludge suspension. In addition, it was noticed that beyond 552 L/h both membrane fouling index and specific cake resistance have increased significantly (from $\alpha = 0.044 \times 10^{14}$ to 0.144×10^{14} m/kg and from MFI = 0.0029×10^{6} to 0.01×10^{6} L/s^2) as shown in Figs 4.9 and 4.10 indicating that higher aeration intensity enhanced the release of small and fine particles in the sludge suspension. The specific cake resistance was calculated from the plot of elapsed time (t) versus volume (V), and the slope of the filtration curve giving membrane fouling index (MFI) values represented the fouling potential (eq. 2.4). From the above results, it could be summarized that an aeration intensity of 552 L/h achieved better results than the rest of the higher aeration intensities. Statistical analysis performed reached the same conclusion which stated that filterability had been significantly influenced by the aeration intensity ($P_{Filterability}$ = 0.02618, P_{MFI} = 0.00072, P_{α} = 0.00072).

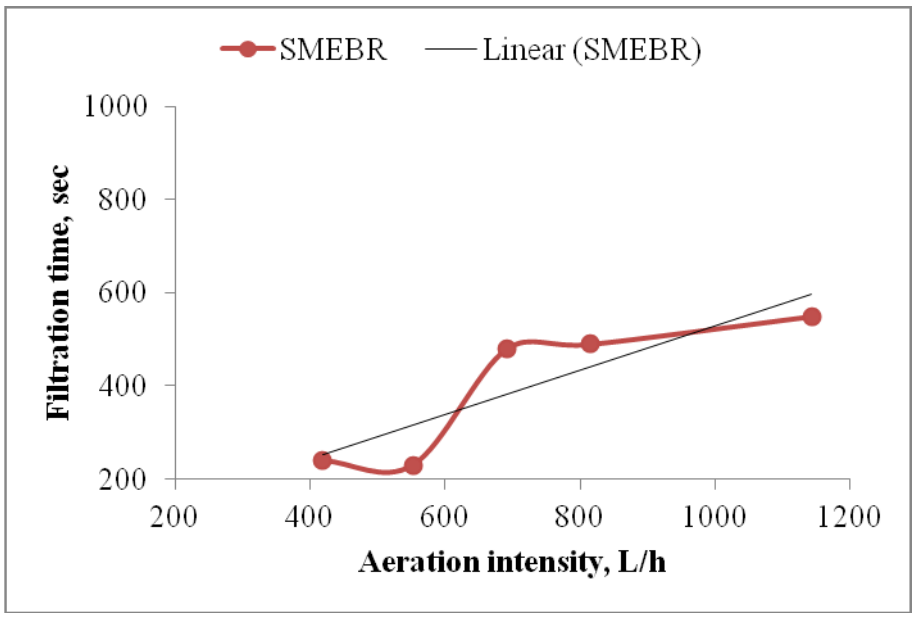

Fig. 4.7: Time to filter 50 mL sample - variation at different aeration intensities.

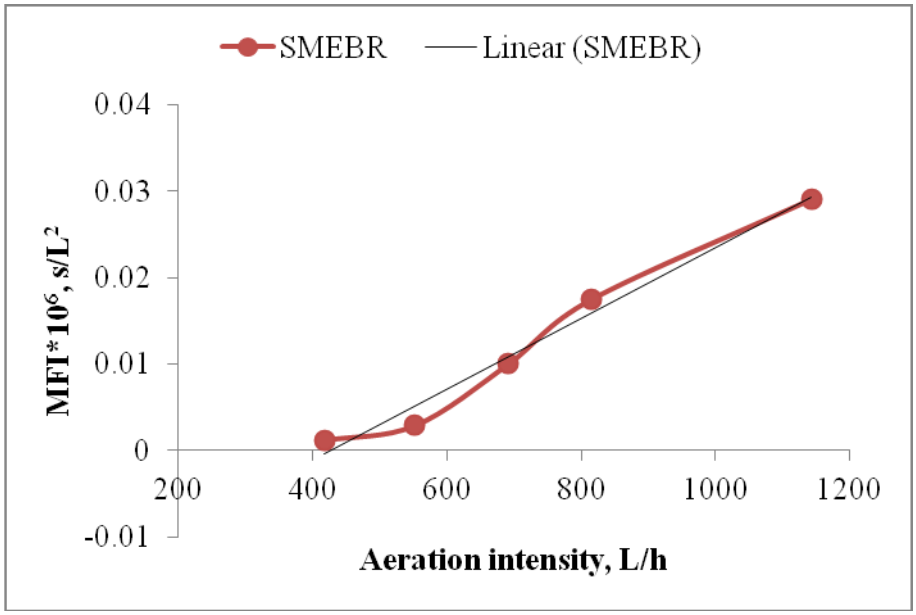

Fig. 4.8: Membrane fouling index (MFI) variation at different aeration intensities.

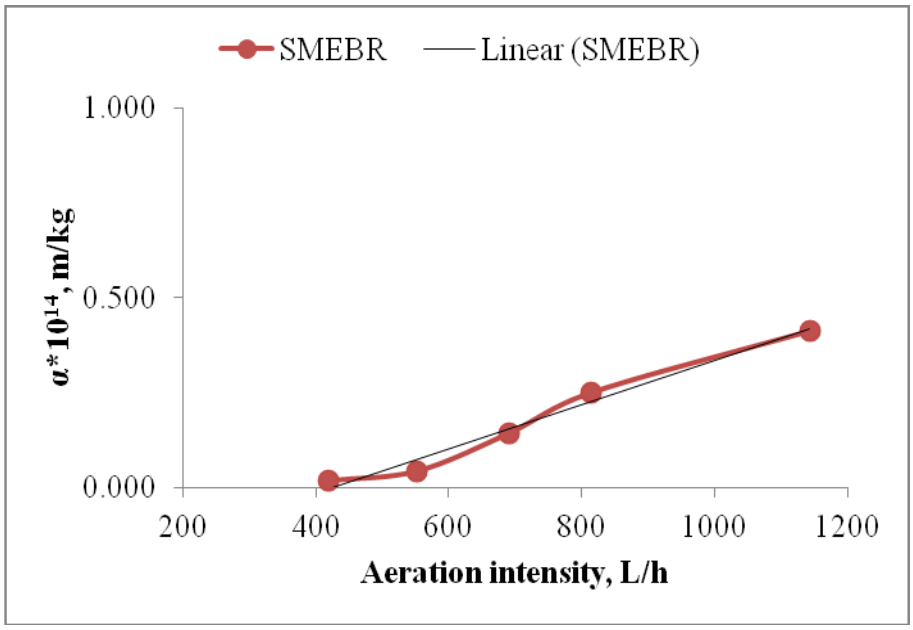

Fig. 4.9: Specific cake resistance variation at different aeration intensities.

4.2.5 Relationship between aeration intensity and oxygen uptake rate (OUR)

Oxygen uptake rate (OUR) was an important parameter used to control biological processes through which microorganisms and their behaviors were frequently monitored. Oxygen uptake rate measurements could provide more information concerning treatment plant performance, wastewater characteristics, degradability of special concentrated streams as well as parameters needed for mathematical models, in order to predict possible optimizations of a treatment plant (Hagman et al., 2008). Fig. 4.10 showed the variation of OUR with aeration. It could be noticed that OUR has increased until aeration intensity was 552 L/h where it decreased. Stability in OUR was observed at higher aeration intensities. Statistical analysis performed reached the conclusion that OUR had been significantly influenced by the aeration intensity ($P = 0.0009$).

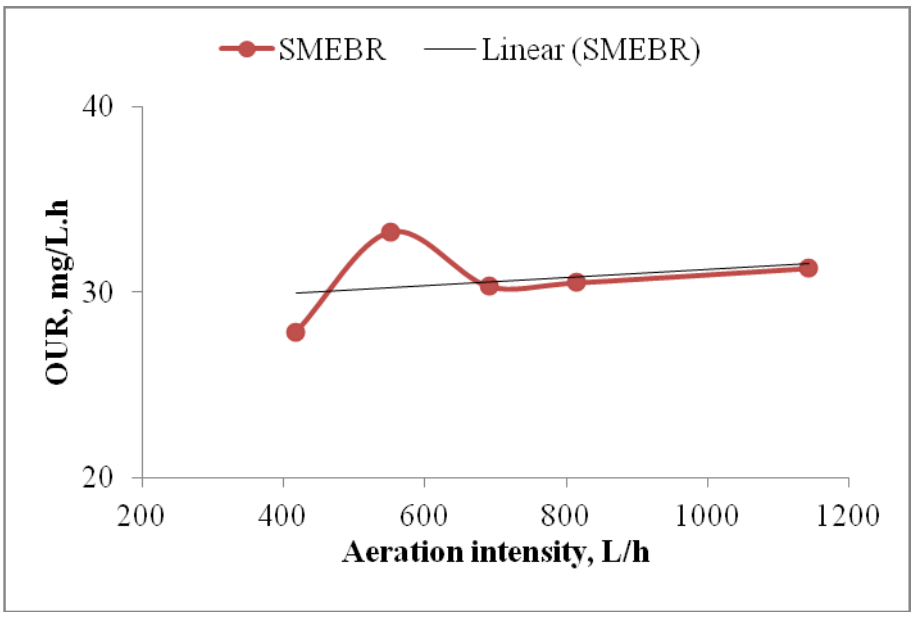

Fig. 4.10: Oxygen uptake rate variation at different aeration intensities.

Table 4.5: P-values showing correlations between aeration intensity and sludge properties

Parameter	P-value	Degree of significance
PSD	0.00097	highly significant
Zeta potential	0.00067	highly significant
EPS_c	0.00073	highly significant
EPS_p	0.00079	highly significant
MFI	0.00072	highly significant
Specific cake resistance	0.00072	highly significant
Filtration time	0.02618	Significant
OUR	0.0008	highly significant

4.3 Stage 2: Objective: Effect of current density in SMEBR

As it was explained in Chapter 2 - Section 2.3.2, the electrolytic dissolution (electrooxidation) of the aluminum anode produces cationic monomeric species such as Al^{3+} and $Al(OH)_2^+$ at acidic conditions. At suitable pH values, they were first transformed to $Al(OH)_3$ and finally polymerized to $Al_n(OH)_{3n}$ (reactions 2.5 to 2.7) (Mollah et al., 2004). Other compounds could be formed in the system depending on the pH of the aqueous media. Examples were: $Al(OH)^{2+}$, $Al_2(OH)_2^{4+}$ and $Al(OH)_4^-$. Water oxidation produced oxygen gas at the anode where water reduction produced hydrogen gas at the cathode. The size of the gas bubbles was a current density dependent.

Four experiments were carried out to investigate the relationship between the current density and membrane fouling, effluent quality, and sludge properties. At a fixed sludge retention time (SRT) of 20 d with controlled HRT of 9 h and organic loading of 1.3 kg COD/m^3.d, SMEBR was operated at four current densities: 5, 10, 15, and 27 A/m^2 for 14 days each. Two bioreactors (MBR and SMEBR) with an effective volume of 15 L each were operated in parallel. The intermittent electrical mode in SMEBR of 5 min ON: 10 min OFF was controlled using a timer.

4.3.1 Impact of current density on removal efficiency

4.3.1-1 COD removal

Fig. 4.11 showed the variation of chemical oxygen demand (COD) removal efficiency over operation time. It could be observed that after five days of operation, COD removal was 96%, 93%, 96%, and 89% at 5, 10, 15, and 27 A/m^2 current densities, respectively. After eight days of operation, COD removal was 97%, 97%, 95%, and 89% at 5, 10, 15, and 27 A/m^2 current

densities, respectively. Furthermore, after two weeks of operation, COD removal was 96%, 97%, 98%, and 90% at 5, 10, 15, and 27 A/m^2 current densities, respectively. It could be concluded that COD removal was not affected by the change in current density, however, it reported less efficiency at higher current density (i.e. at 27 A/m^2) due to the death of some microorganisms at high electrical pulse or due to the higher dose of aluminum ions which had adverse impact via increasing the positive charge on the negatively charged sludge particles (Luo et al., 2011). Thus, bridging of particles during flocculation was assumed to be very difficult and therefore low removal efficiency was observed at 27 A/m^2. On the other hand, MBR reported high COD removal as well ranging between 91 to 92%. Yet, it was less than those accomplished in SMEBR.

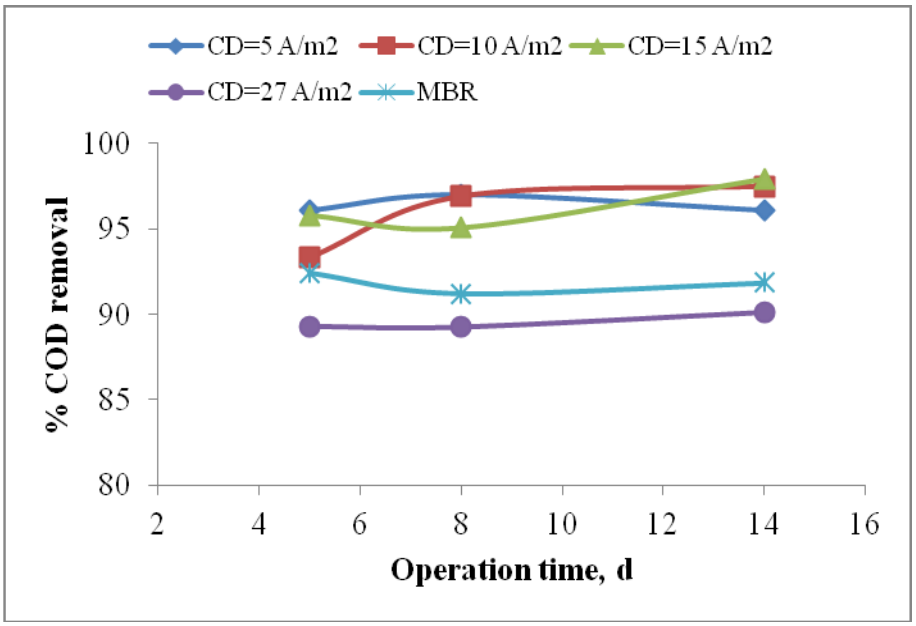

Fig. 4.11: COD removal at different current densities.

4.3.1-2 Phosphorus removal

Fig. 4.12 showed the variation of orthophosphate (as PO_4^{3-}-P) removal efficiency over operation time. It could be observed that after five days of operation, phosphorus removal was 66%, 74%, 83%, and 87% at 5, 10, 15, and 27 A/m^2 current densities, respectively. After eight days of operation, P removal was 78%, 74%, 84%, and 64% at 5, 10, 15, and 27 A/m^2 current densities, respectively. Furthermore, after two weeks of operation, phosphorus removal was 75%, 100%, 82%, and 70% at 5, 10, 15, and 27 A/m^2 current densities, respectively. It could be concluded that phosphorus removal was significantly affected by the change in current density; however, it reported some fluctuations in efficiency at higher current density (i.e. at 27 A/m^2). Several studies reported the influence of current density on the removal efficiency (Mahesh et al., 2006; Phalakornkule et al., 2010). As the current density increased, more active ions (Al^{3+}) due to the electrooxidation of the aluminum anode were generated, along with an increase in the rate of bubbles generation. Contrary to Adhoum and Monser (2004), further increase in the current density would not enhance the removal of the pollutants. In this study, the reduction in phosphorus removal could be attributed to the fact that the size of the gas bubbles increased at high current density allowing more phosphorus to be attached to the gas bubbles. This would result in less collision between phosphorus compounds and the active aluminum ions, which would reduce the attachment of phosphorus to sludge flocs. Less removal rates could also be due to the reduction in the microbial activity at high electrical pulse through which some kind of microorganisms died in the sludge suspension. In contrast, MBR reported low phosphorus removal around 53% which was dramatically less than those achieved in SMEBR.

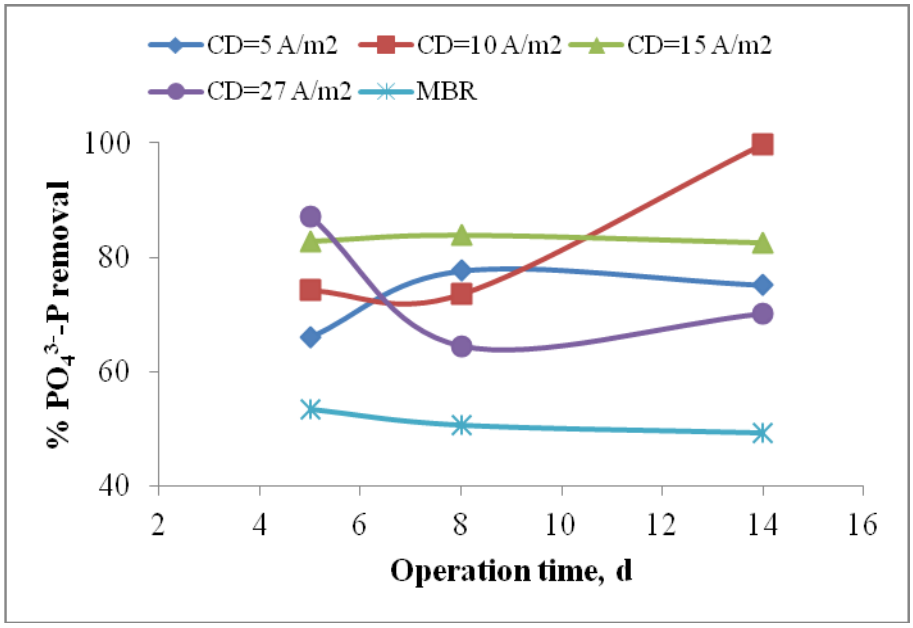

Fig. 4.12: Phosphorus removal at different current densities.

4.3.1-3 Ammonia and total nitrogen removal

Fig. 4.13 showed the variation of ammonia (as NH_3^+-N) removal efficiency over operation time. It could be observed that after five days of operation, NH_3^+ removal was 73%, 73%, 77%, and 61% at 5, 10, 15, and 27 A/m^2 current densities, respectively. After eight days of operation, NH_3^+ removal was 80%, 87%, 77%, and 63% at 5, 10, 15, and 27 A/m^2 current densities, respectively. Furthermore, after two weeks of operation, NH_3^+ removal was 80%, 87%, 86%, and 63% at 5, 10, 15, and 27 A/m^2 current densities, respectively. It could be concluded that NH_3^+ removal was significantly affected by the change in current density except at higher current density (i.e. at 27 A/m^2) where the increase in removal efficiency was not very significant. In addition, the removal efficiency at 27 A/m^2 was less compared to the rest of the current densities. This could be explained by the fact that some of the microorganisms died during the operation at high electrical pulse causing an increase in the amount of ammonia in the effluent, and therefore achieving less removal efficiency. It could

be also due the increase in the overall charge (as demonstrated in COD removal). MBR reported 72% NH_3^+ removal efficiency. Average concentrations of nitrates (as NO_3^--N) in the treated effluents were 35, 21, 17, 19, and 40 mg/L at 5, 10, 15, 27 A/m^2 and MBR, respectively.

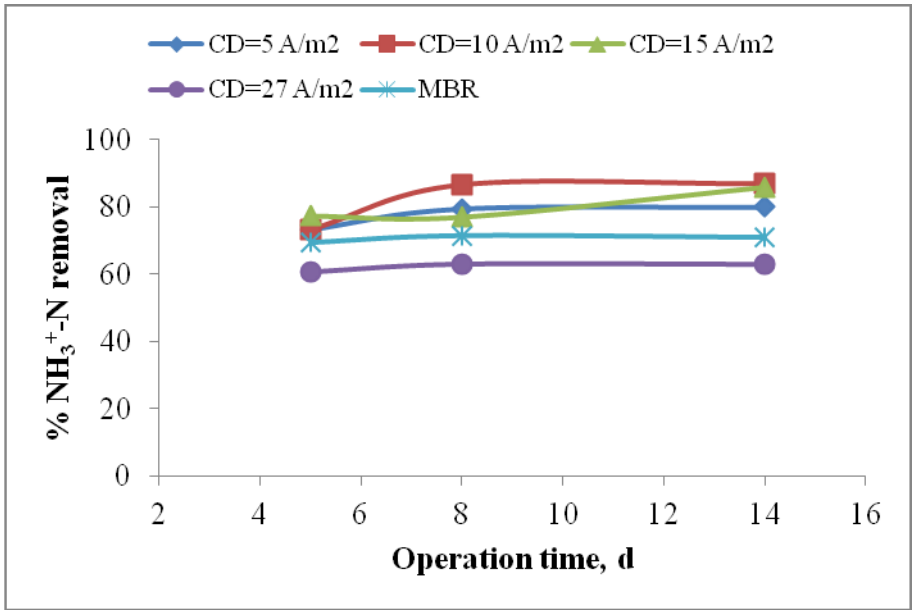

Fig. 4.13: Ammonia removal at different current densities.

Fig. 4.14 showed the variation of total nitrogen (TN) removal efficiency over operation time. It could be noted that low removal efficiencies were achieved in all reactors under different current densities. However, a significant increase was reported after two weeks of operation at higher current densities (i.e. at 15 and 27 A/m^2). Similarly, low and insignificant results were accomplished in MBR. Total nitrogen contained several organic compounds where some of them were slowly biodegradable. They contribute to the oxidation of ammonia but not the change in the concentration of TN, and thus were oxidized less rapidly than other organic compounds during the electrooxidation (Szpyrkowicz et al., 2005).

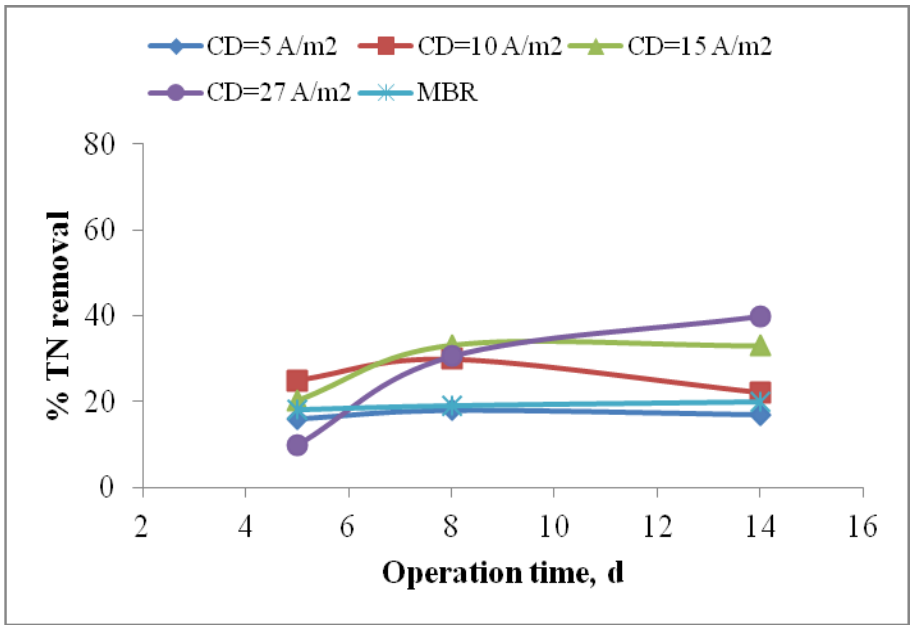

Fig. 4.14: Total nitrogen removal at different current densities.

4.3.2 Impact of current density on membrane fouling

The change of transmembrane pressure (TMP) with time in SMEBRs and MBR was monitored (Fig. 4.15) to investigate membrane fouling behavior at constant flux of 16.7 L/m^2.h. It could be observed that SMEBRs operated under 15 and 27 A/m^2 reported no fouling after two weeks of operation. At 10 A/m^2, no fouling was also observed, yet a gradual increase in TMP was reported expecting future membrane fouling. On the other hand, as the current density decreased (i.e. 5 A/m^2), fouling started to be more remarkable and the membrane fouled after 12 days where it reached to 63.4 kPa. The membrane in MBR had fouled after 11 days of operation. Fouling at low current density and in MBR occurred as the viscosity started to increase by 5 and 2.5% in MBR and SMEBR operated at 5 A/m^2, resulting in less shear rate generated by the coarse bubbles aeration, and hence more colloids might have deposited on the membrane surfaces (Lin and Shien, 2001). Besides, SMEBR system operated at 5 A/m^2 did not have sufficient Al^{3+} ions originating from the anode

electrodissolution, and thus these ions were not able to break the repulsion forces between the negatively charged particles present in the sludge suspension, and therefore the rate of coagulation was less than the rest of the reactors operating at higher current densities. Considering the membrane fouling rate calculated from the slope of TMP versus operation time (days) (Basu and Huck, 2005; Ye et al., 2005), it was noted that the rate of average membrane fouling increased in the order of 1.05 kPa/d, 0.21 kPa/d and 0.097 kPa/d, kPa/d at 10, 15 and 27 A/m^2, respectively. The rate of fouling at 5 A/m^2 was calculated after the first nine days as well as for the period from 10 to 12 d when SMEBR experienced fouling. Results reported 0.695 and 15 kPa/d, respectively. Similarly, the rate of fouling in MBR was calculated after the first eight days as well as for the period from 9 to 11 d when MBR experienced fouling. Results reported 1.33 and 26.05 kPa/d, respectively. Therefore, it could be concluded that by applying adequate current density to the system, higher rates of coagulation (due to the electrodissolution of the anode) could be achieved and consequently membrane fouling as well as frequency of membranes cleaning were significantly reduced and thus longer membranes lifetime. These findings were in accordance with previous studies where different polymeric coagulants such as $Al_2(SO_4)_3$, $FeCl_3$, PAC (polymeric aluminum chloride) and PFS (polymeric ferric sulfate) were added to the submerged MBR and resulted in significant decrease in fouling rate (Wu et al., 2006) through restraining the formation of gel layer, decelerating the development of foulants and removing stable foulants from the membrane surface. Song et al. (2008) had also investigated the impact of adding inorganic coagulants such as alum to MBR. They observed that the fouling rate in MBR was significantly reduced when they added 30 mg/L of alum. Other studies, on the other hand, had explained the rapid increase in TMP due to the pore blocking with soluble microbial

products and polymeric substances (Cho and Fane, 2002). Membrane cleaning was performed as was described in Chapter 3 - Section 3.4.

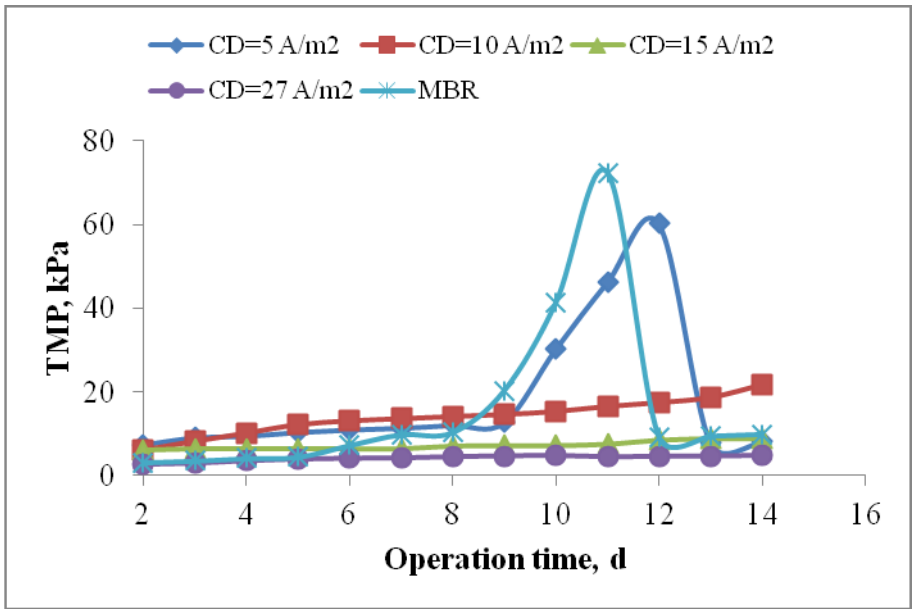

Fig. 4.15: TMP variation at different current densities.

4.3.3 Impact of current density on sludge characteristics

4.3.3-1 Relationship between current density and mean particle size diameter

Fig. 4.16 showed the variation of flocs mean particle size diamater (PSD) over time at different current densities. It could be observed that the reduction in floc size was 29.9%, 34%, 50.6%, and 60.8% at 5, 10, 15, and 27 A/m^2 current densities, respectively. This could be explained by the electroosmosis phenomenon which took place within SMEBR. The electric double layer was formed as the negative charged particles of the sludge were surrounded by a layer of the positive ions. When an electric field was applied in the solution, the positive counterions were attracted by the cathode. As they would move, they would repel water molecules resulting in a total transport of water out of the sludge particles (Yu et al.,

2011). Electroosmosis phenomenon (due to electrokinetics) enhanced the extraction of bound water from sludge flocs, minimized their attachment to the surface of the membrane, and hence resulting in less membrane fouling as demonstrated earlier in Fig. 4.15. These results were not in line with Luo et al. (2011) and Zhe et al. (2009) who observed an increase in the flocs size while adding different coagulants indicating that SMEBR is a different system than the conventional MBR, and thus a different behavior was expected. Alternatively, the change in the mean particle size diameter in MBR was insignificant indicating a very slow coagulation rate.

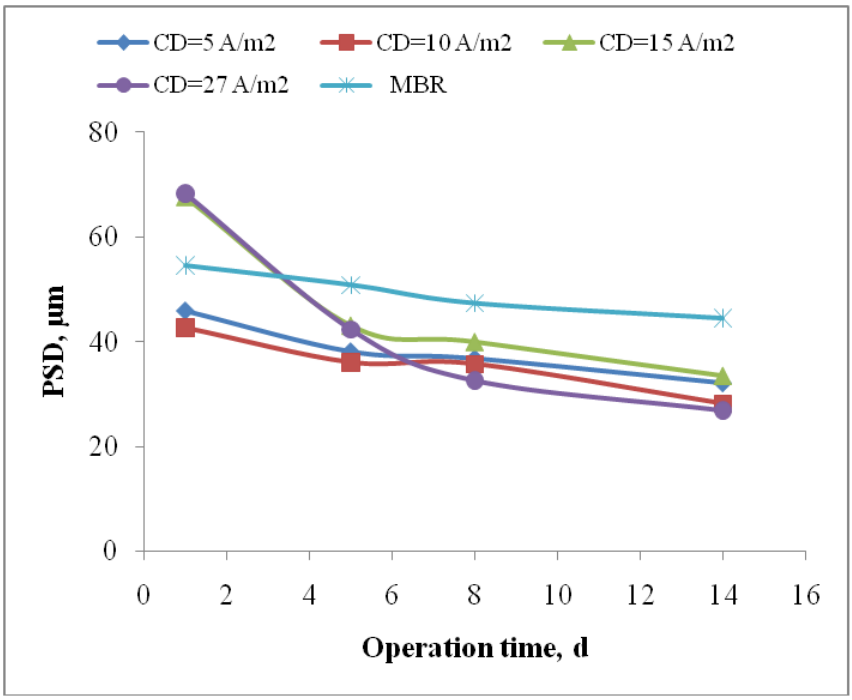

Fig. 4.16: Mean particle size diameter variation at different current densities.

4.3.3-2 Relationship between current density and mixed liquor suspended solids (MLSS)

Fig. 4.17 showed the variation of mixed liqour suspended soilds (MLSS) over time at different current densities. It could be observed that the total suspended solids increased with

current density. They increased from 5060 to 7520 mg/L, from 5560 to 10240 mg/L, and from 7000 to 14360 mg/L at 10, 15, and 27 A/m^2 current densities, respectively. There was no significant increase in MLSS neither at 5 A/m^2 or in MBR. The significant increase in MLSS was due to the chemical sludge or inorganics produced due to the electrodissolution of aluminum anode.

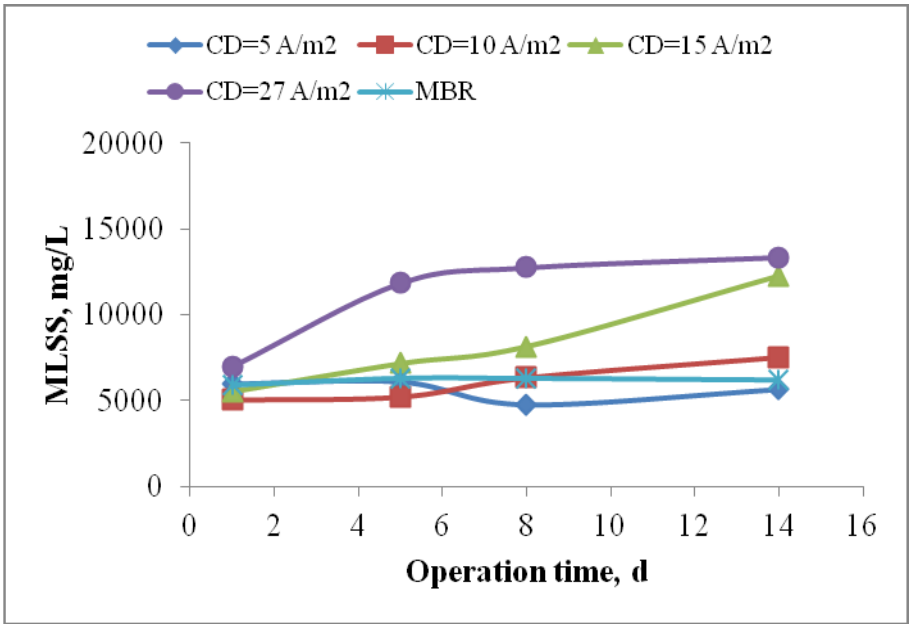

Fig. 4.17: MLSS variation at different current densities.

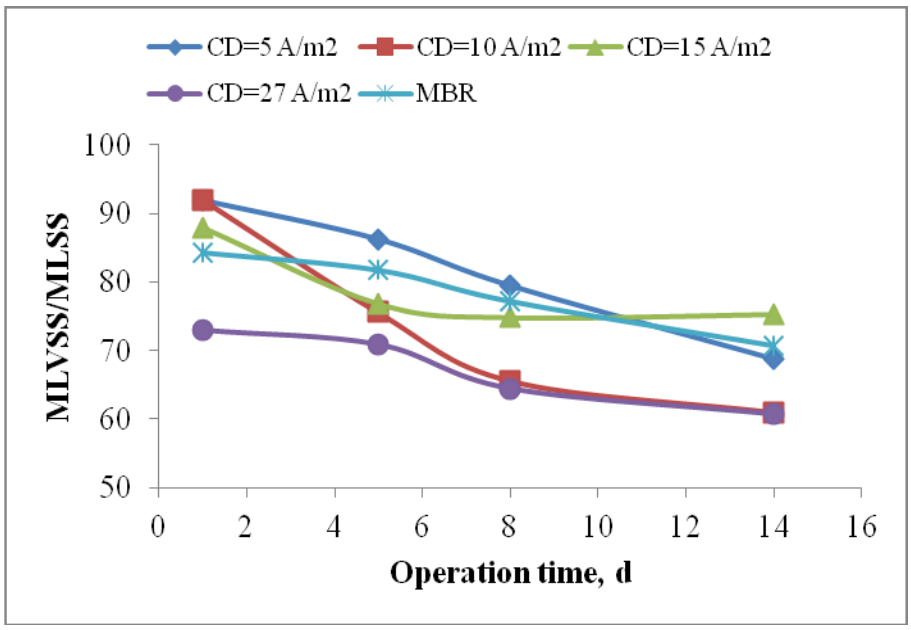

Fig. 4.18: MLVSS/MLSS ratio variation at different current densities.

More aluminum ions, generated at high current density, were dissolved into the solution, which resulted in an increase in the overall total suspended solids. Fig. 4.18 showed the variation of volatile suspended solids (MLVSS) to MLSS ratio observed at different current densities. It showed that there was a reduction in MLVSS/MLSS ratio over time at all conditions, which was explained by the generations of inorganics (mainly aluminum complexes mainly oxides and hydroxides) in the solution.

4.3.3-3 Relationship between current density and colloids

Fig. 4.19 showed the variation of colloidal particles over time at different current densities. Colloids were represented as colloidal COD (COD_c) after extracting soluble COD (COD_s) from the sludge supernatent. According to the resutls, it could be concluded that as the current density increased, more colloidal particles were removed from wastewater. The negative colloids were nuetralized by the positive aluminum ions generated in the solution, and therefore removed from the wastewater. The removal of colloids from wastewater had

positive impact on membrane fouling through overcoming pore blocking or pore clogging (Fig. 4.15). Several studies reported that colloids significantly contributed to membrane fouling, and thus removing them would have positive impact on fouling (Wisniewski et al., 2000; Rosenberger et al., 2006). The removal was significant at 10, 15 and 27 A/m^2, respectively whereas at 5 A/m^2, the generation of aluminum ions into the sludge suspension was not sufficient to remove the colloids as low removal rate was reported. MBR had also achieved good removal of colloids as coagulants were added to the raw wastewater when discharged to the WWTP at l'Assomption, thus contributing to the charge neutralization of the negative colloids.

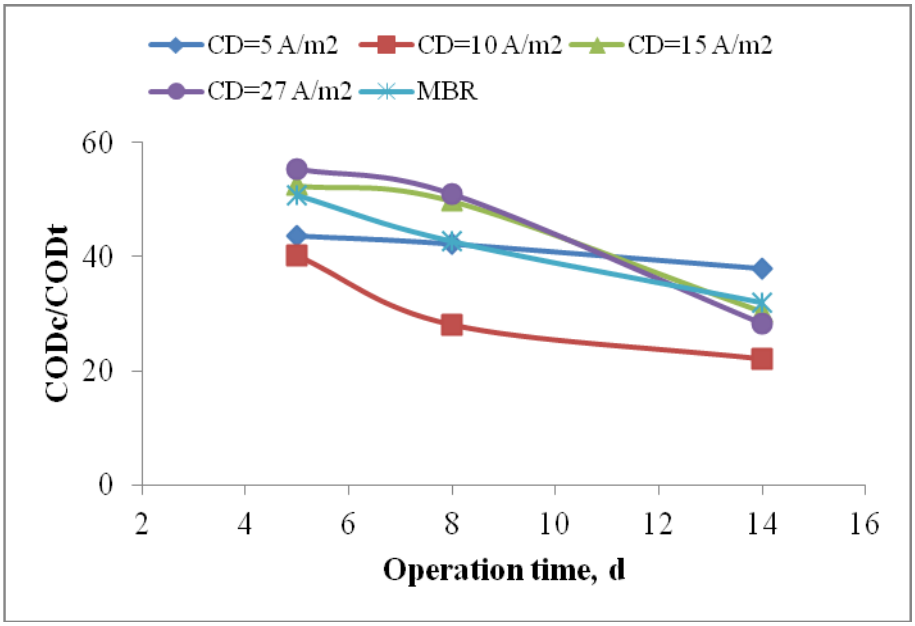

Fig. 4.19: Colloidal fractions variation at different current densities.

4.3.3-4 Relationship between current density, zeta potential, viscosity, and soluble extracellular polymeric substances (soluble EPS)

It was reported that soluble extracellular polymeric substances, i.e. soluble EPS had a significant influence on sludge viscosity (Chang et al., 2001), and zeta potential (Wilén et al., 2003). It was suggested that as the soluble EPS released into the solution, the sludge viscosity increased, along with the magnitude of zeta potential. Figs 4.20 to 4.23 showed that the change in current density had slight effects on sludge viscosity and zeta potential. Similarly, soluble EPS (as soluble carbohydrates EPS_c and soluble proteins EPS_p) were found in lower concentrations than in MBR, leading to the conclusion that soluble EPS were removed at higher extends under electrokinetics through which the aluminum cations generated from the electrooxidation of the anode neutralized the negatively charged (Wilén et al., 2003) EPS, and thus were removed from the sludge suspension. Several studies reported that soluble EPS were considered as major foulants, where the increase in EPS would lead to further deposition on the membrane surface (Flemming and Wingender, 2003; Kim et al., 2006). Therefore, electrokinetics in SMEBR had significantly contributed in removing the soluble EPS and thus resolved membrane fouling and the costly cleaning processes (Fig. 4.15). It could be also observed that the coagulation rate in SMEBR was significantly higher than MBR as the magnitude of zeta potential (as average values) were -28.3, -25.1, -26.2, -24.7, and -33.1 mV at 5, 10, 15, 27 A/m^2 and MBR, respectively. The positive aluminum ions were absorbed by the negatively charged particles in the sludge suspension; creating electrostatic attraction forces and better coagulation. Similar conclusions with respect to the role of coagulants were reached by Patience et al. (2003) and Luo et al. (2011).

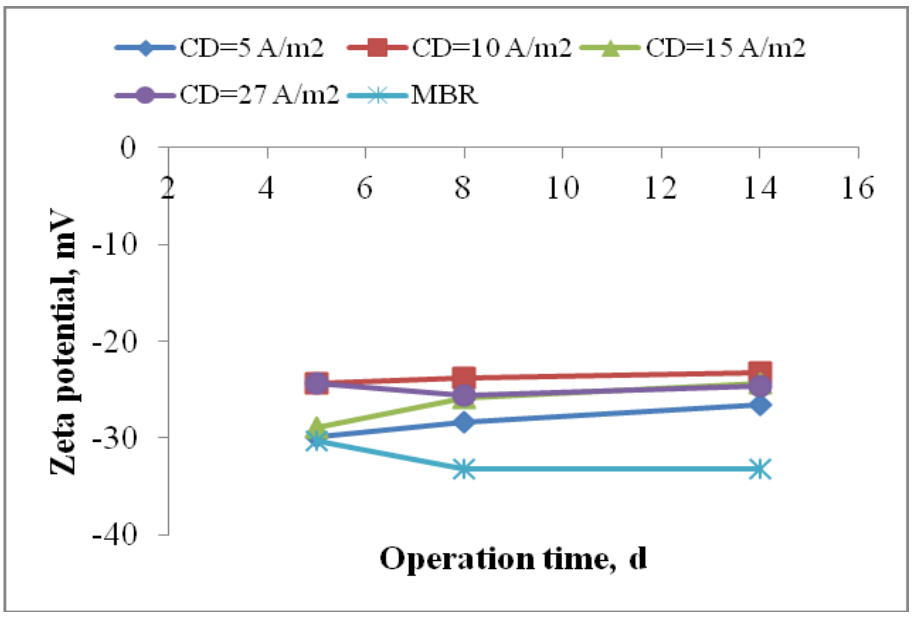

Fig. 4.20: Zeta potential variation at different current densities.

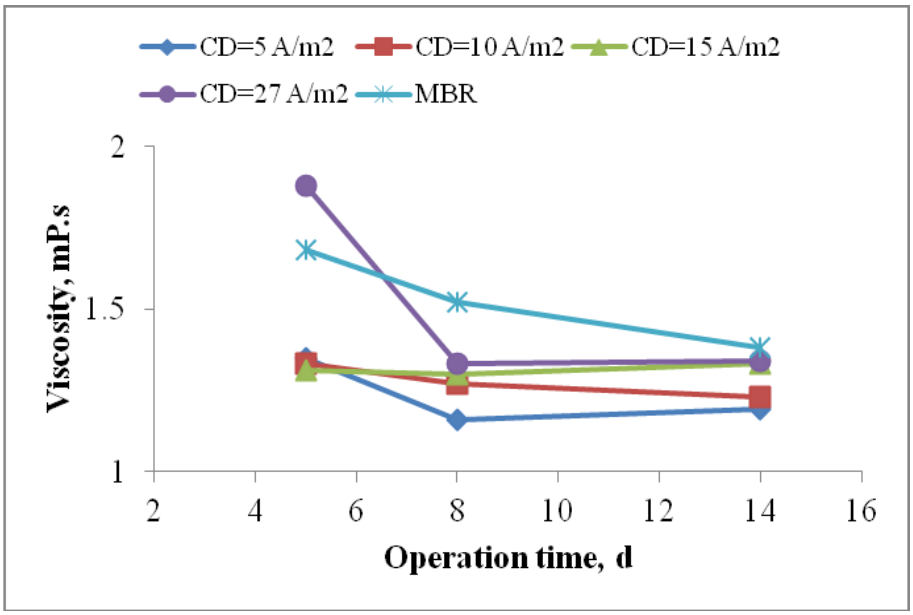

Fig. 4.21: Sludge viscosity variation at different current densities.

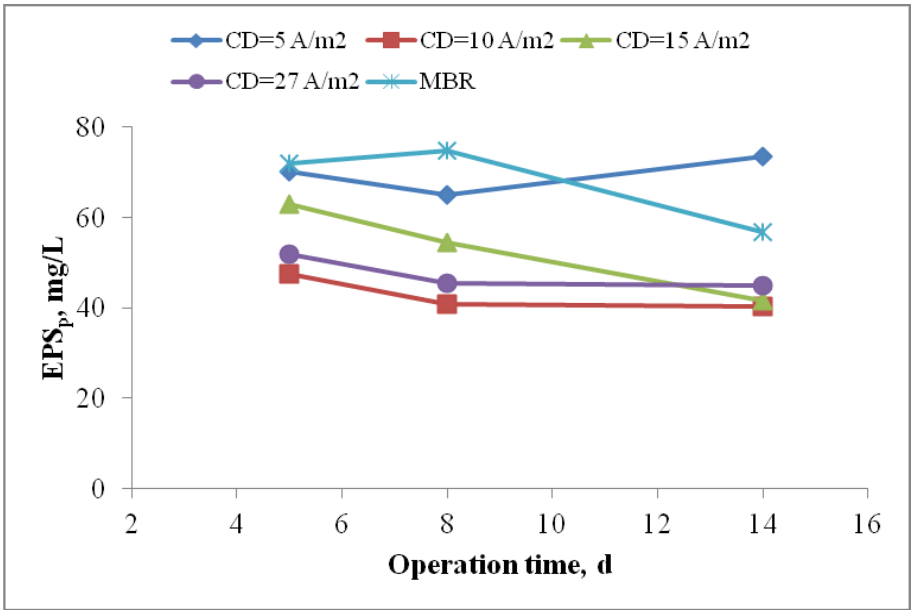

Fig. 4.22: EPS_p variation at different current densities.

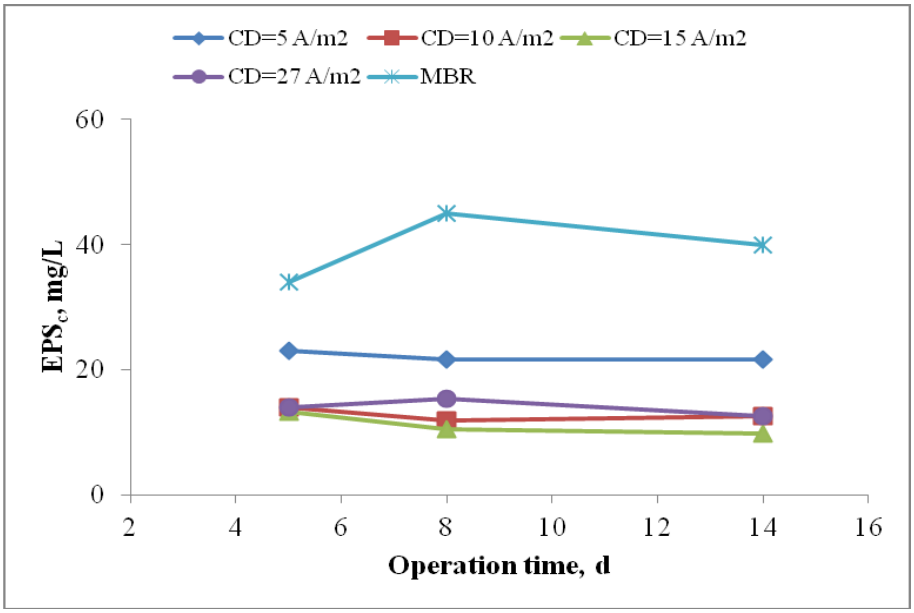

Fig. 4.23: EPS_c variation at different current densities.

4.3.3-5 Relationship between current density, oxygen uptake rate (OUR), and oxidation-reduction potential (ORP)

Oxygen uptake rate (OUR) measurements provided essential information regarding the performance of treatment plants and wastewater characteristics which played a key role in the optimizations of a treatment plant (Hagman et al., 2008). Fig. 4.24 showed the variation of OUR over time under different current densities as well as under membrane filtration process (MBR). From the results, a slight reduction in OUR was observed in the first week of operation due to the increase in mixed liquor. However, stability in behavior was observed afterwards. This could be explained by the fact that microorganisms in SMEBR required an adaptation period to the wastewater and the operating conditions. Another important observation was that OUR was significantly affected by the electrical field, more importantly, the microbial activity increased with current density.

Oxidation-reduction potential (ORP) was another parameter used to deterimne the performance of wastewater treatment systems. ORP has different ranges; below -200 mV for anaerobic conditions, from -200 to +200 mV for anoxic conditions, and higher than +200 mV for aerobic conditions (Holman and Warehem, 2000). Moreover, activated sludge process occurred under aerobic conditions, methanogenesis took place in anaerobic conditions; nitrification and denitrification took place under anoxic and aerobic conditions (Inniss, 2005). Fig. 4.25 showed the variation of ORP over time under different current densities. It could be noted that all recorded results were positive hence all runs were carried out under aerobic conditions. However, a reduction in the first six days was noticed, and then stability took place. These results and OUR results followed the same trend.

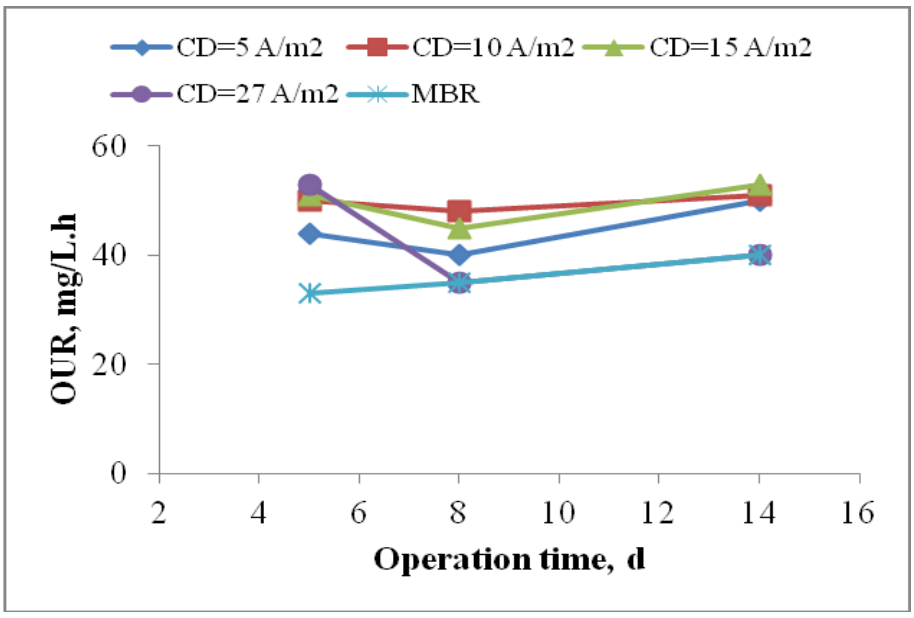

Fig. 4.24: Oxygen uptake rate variation at different current densities.

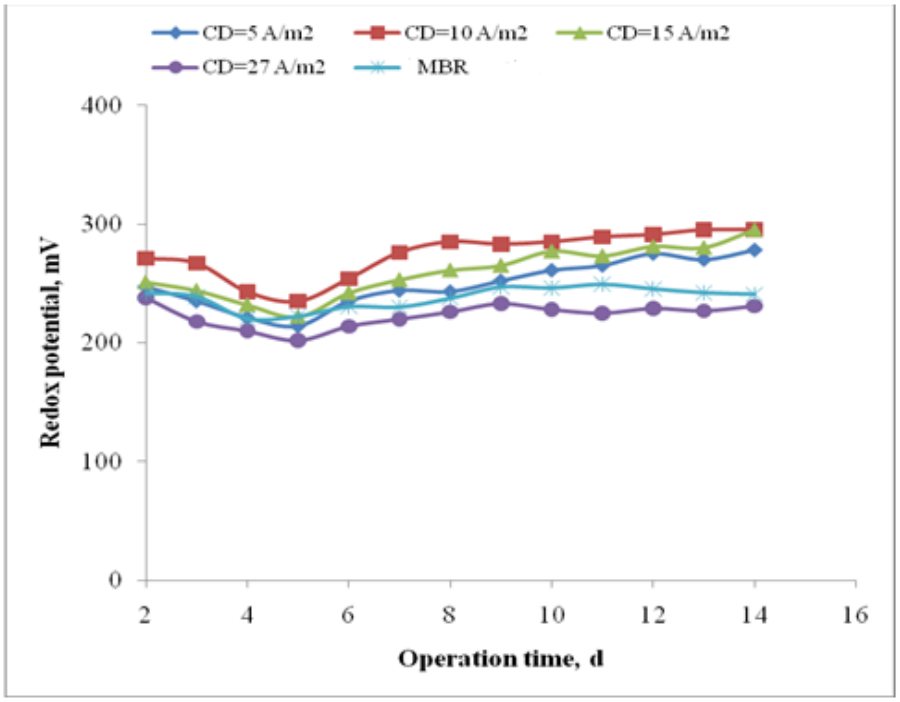

Fig. 4.25: Oxidation-reduction potential variation at different current densities.

4.3.3-6 Relationship between current density, filterability and settleability

Filterability test was used to identify sludge dewatering. Fig. 4.26 showed the variation of filtration time required to filter 50 mL of sludge suspension under different current densities. It was observed that as the current density increased, better results were accomplished. For instance, after two weeks of operation, filtration times were 63, 31, 25, 14, and 465 seconds at 5, 10, 15, 27 A/m^2 and MBR, respectively. It could be said that the sludge filterability was significantly enhanced by electrokinetics through which electroosmosis took place resulting in smaller flocs (yet with less bound water) as demonstrated in Fig. 4.16. The filterability results were in agreement with Wu et al. (2011) and Zhang et al. (2004) who improved sludge filterability when adding polymeric coagulants such as $Al_2(SO_4)_3$ and $FeCl_3$.

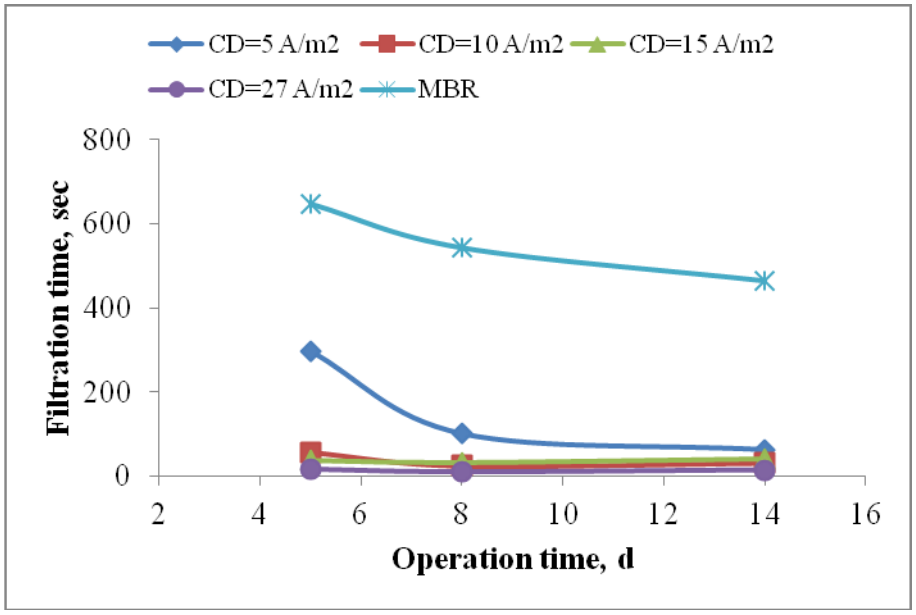

Fig. 4.26: Time to filter 50 mL sample - variation at different current densities.

Sludge volume index (SVI) was often used to characterise the settleability of a specific sludge. It was the volume in milliliters occupied by 1 g of a suspension after 30 min settling. Fig. 4.27 showed the SVI at different current densities and MBR. It could be

summarized that the sludge in SMEBR had better settleability than MBR where SVI reached 164.98 mL/g. This could be explained by the presence of filamentous bacteria which presented at SVI > 150 causing sludge bulking (Parker et al., 2001). On the other hand, at higher current densities, denser flocs were generated and better settleabilities were achieved as 65.8 and 60.6 mL/g were reported at 15 and 27 A/m^2, respectively. Similar findings were reported by Luo et al. (2011) when they added PAM (generic name of several polymers containing acrylamide as the major constituent) in sequencing batch reactors. They concluded that the addition of PAM significantly contributed to the reduction of SVI where better settleabilities were reported.

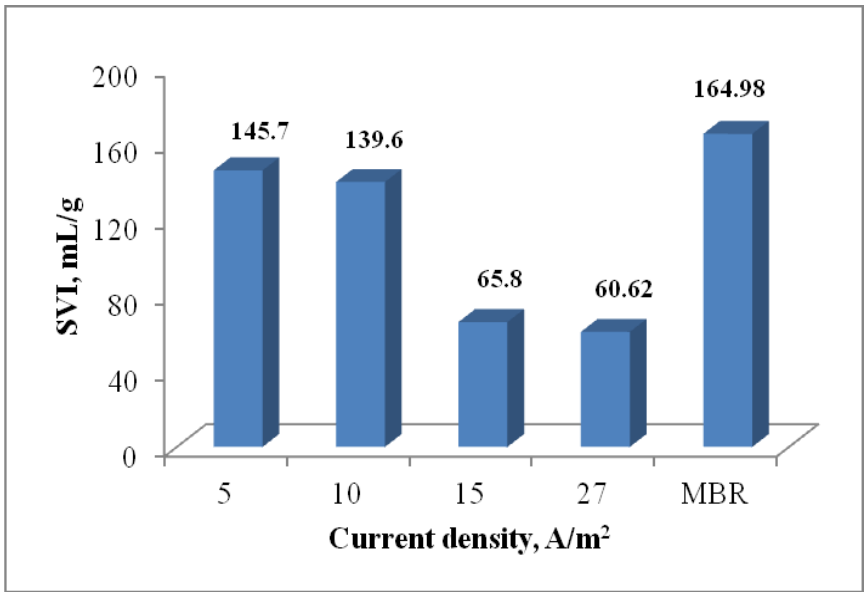

Fig. 4.27: Sludge volume index at different current densities.

Specific cake resistance (α) results shown in Fig. 4.28 indicated that less cake layer was formed on the membrane surface of SMEBR system, and thus less fouling. It was observed that specific cake resistance decreased over time and reached to 0.9351 x10^{14}, 0.1763 x10^{14},

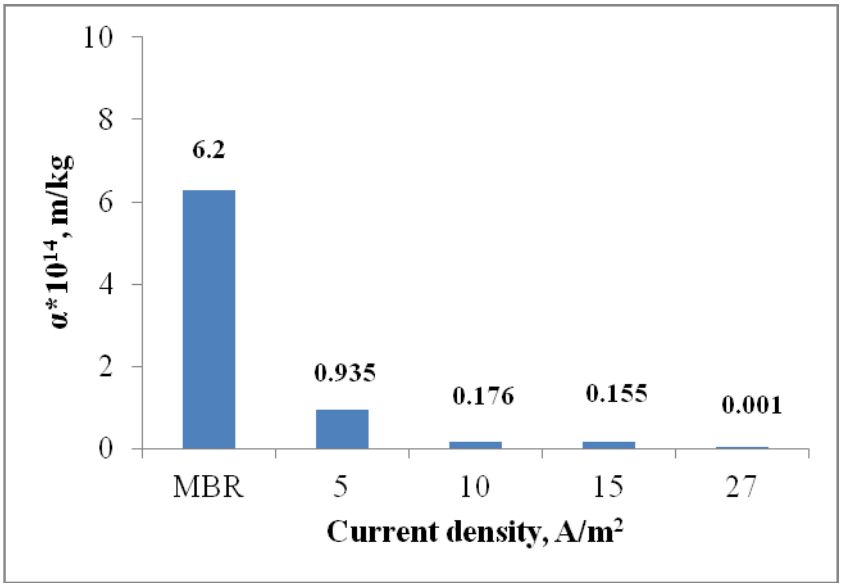

Fig. 4.28: Specific cake resistance variation at different current densities.

0.1549 x10^{14} and 0.0015 x10^{14} m/kg at 5, 10, 15 and 27 A/m^2 current densities, respectively after two weeks of operation. Song et al. (2008) reported that the specific cake resistance decreased with the increasing coagulant concentration. Those results agreed with the membrane fouling index (MFI) results where MFI decreased as the current density increased as shown in Fig. 4.29. They were 0.0217x10^6, 0.0072x10^6, 0.0053x10^6, and 0.0001x10^6 L/s^2 at 5, 10, 15, and 27 A/m^2 current densities, respectively after two weeks of operation. Specific cake resistance and membrane fouling index in MBR were significantly higher compared to other SMEBR reactors operated under electrokinetics as 6.28x10^{14} m/kg and 0.2147x10^6 L/s^2, respectively were reported after two weeks of operation. It could be said that electrokinetics minimized the formation of the cake layer, enhanced sludge filterability (Fig. 4.26) and reduced fouling potential (Fig. 4.15).

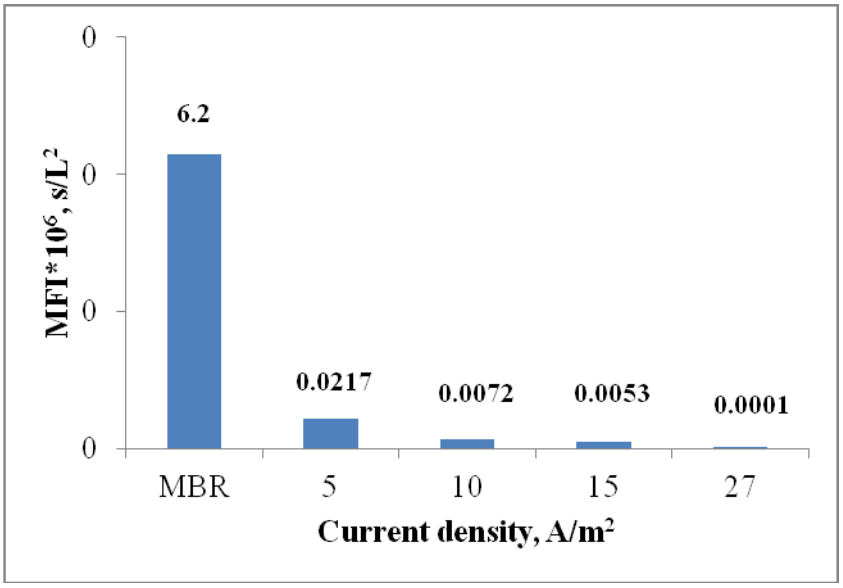

Fig. 4.29: Membrane fouling index variation at different current densities.

4.3.4 Monitored parameters

During all runs, several parameters were monitored in order to investigate the performance of the treatment systems used in this study.

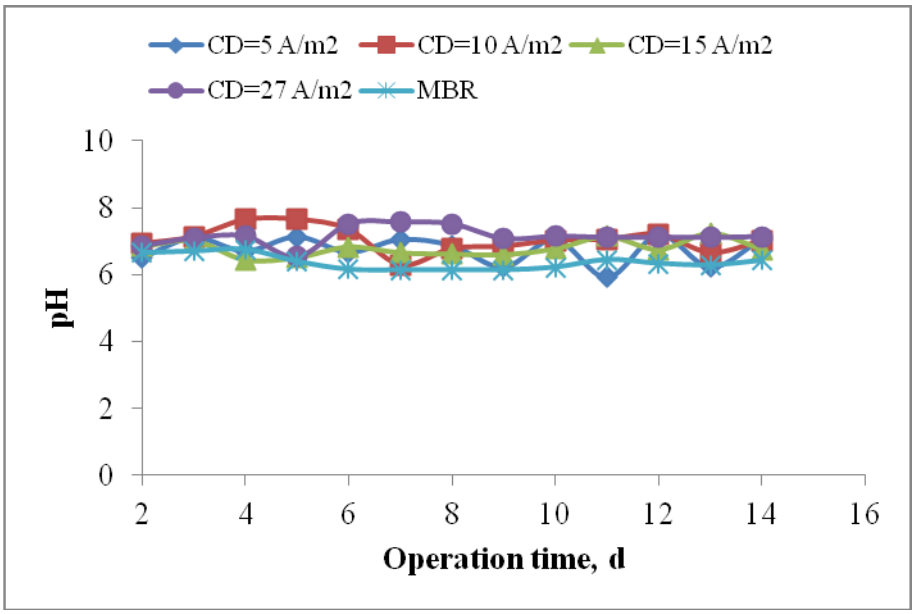

Fig. 4.30: pH variation at different current densities in SMEBR.

Examples were: pH, Temperature (^{o}C), sludge conductivity (σ, µS/cm), and applied voltage (in V/cm). Fig. 4.30 showed the variation of pH with time. It was noticed that an increase in pH was observed as the current density increased. This was due to the loss of hydrogen gas at the cathode which caused hydroxide ions accumulation. In addition, Fig. 4.31 showed the variation of temperature with time. It was observed that as the current density increased, more heat was applied to the reactor, and thus the temperature of the sludge suspension had increased. Fig. 4.32 showed the variation of sludge conductivity with time. The higher the current density was, the more ions were generated from the electrooxidation of the anode, and therefore the lower the sludge conductivity. The decrease in conductivity indicated the reduction in the concentration of ions in the solution (Perng et al., 2007). Moreover, the higher the sludge conductivity, the better the characteristics of the wastewater, and hence the lower applied voltage, as shown in Fig. 4.33.

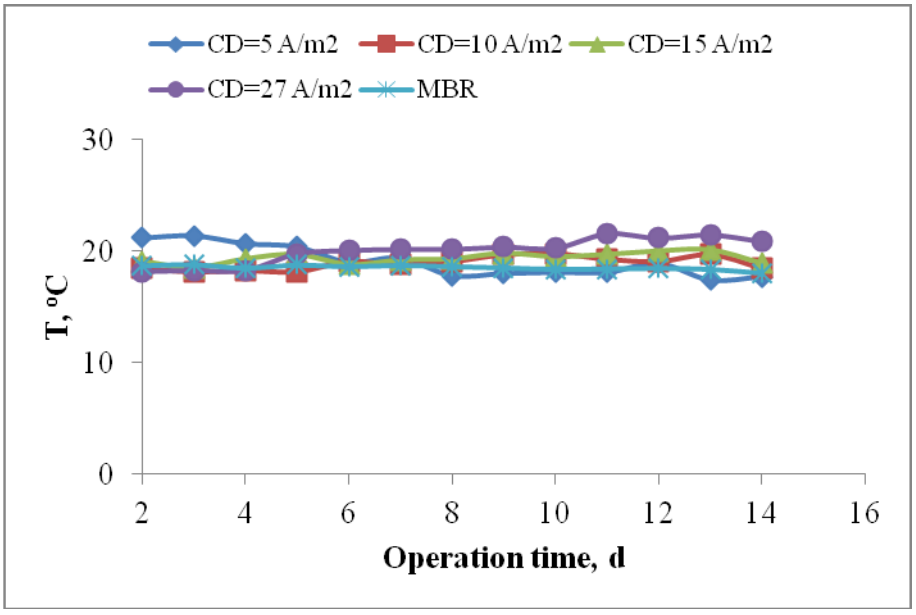

Fig. 4.31: Temperature variation at different current densities in SMEBR.

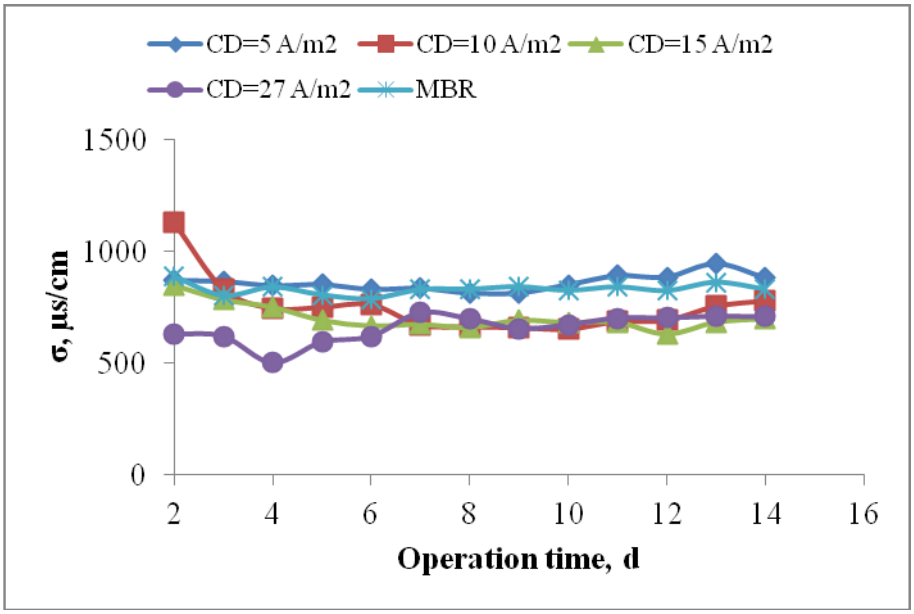

Fig. 4.32: Sludge conductivity variation at different current densities in SMEBR.

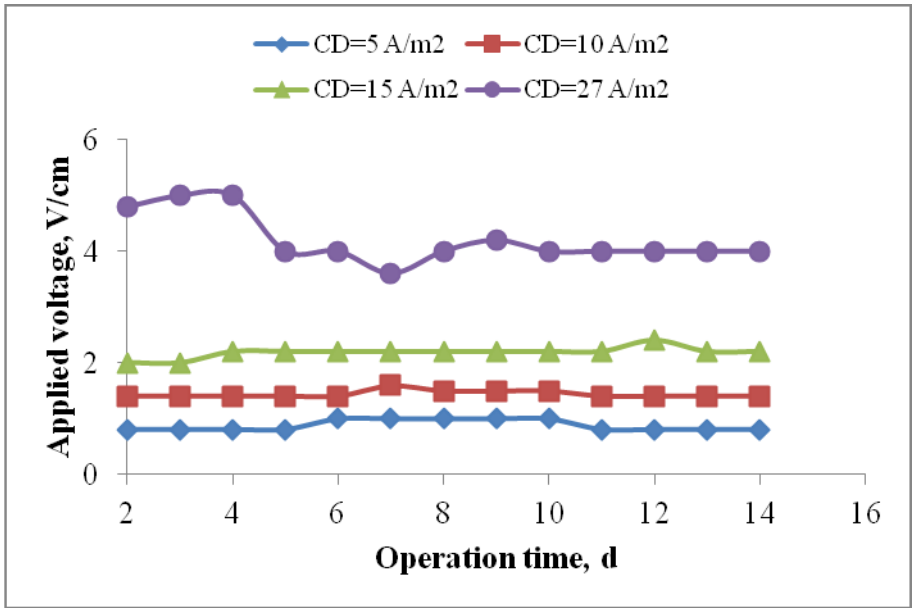

Fig. 4.33: Applied voltage variation at different current densities in SMEBR.

4.3.5 Sludge production and generation of inorganic solids at different current densities

Total suspended solids (MLSS) in SMEBR had increased as a function of the applied current density (Fig. 4.17). Sludge production accounted for the heterotrophic biomass growth, cell debris from endogenous decay, nitrifying bacteria biomass, non-biodegradable volatile suspended solids (MLVSS), and the inorganic solids in the influent wastewater (Metcalf and Eddy, 2003-eq. 4.1).

$$P_{x,\,TSS} = A + B + C + D + E = \frac{Q(Y)(S_0 - S)}{1+(k_d)SRT} + \frac{f_d(k_d)Q(Y)(S_0 - S)SRT}{1+(k_d)SRT} + \frac{QY_n(NO_x)}{1+(k_{dn})SRT} + Q\,(nbVSS) + Q\,(TSS_o - VSS_o) \qquad (4.1)$$

Where, A, B, C, D, and E represent the heterotrophic biomass, cell debris, nitrifying biomass, non-biodegradable VSS in influent, and the inert TSS in the influent, respectively.

The total MLSS in SMEBR is the sum of the organics, and the inorganics (fixed suspended solids, i.e. MLFSS) present in the bioreactor. The contribution of the inorganics produced due to electrokinetics was investigated in order to optimize the design current density required for SMEBR operation since sludge production was considered as a dramatic problem facing membrane bioreactors. Six batch bioreactors having 1 L of effective liquid each were used in this experiment. Five bioreactors operated under five current densities (5, 10, 12, 15, and 27 A/m^2) along with a control reactor (i.e. without electrodes). MLSS fractionations such as MLVSS and MLFSS were determined in a daily basis for 10 days. The difference between MLFSS in the control and MLFSS in the SMEBR resulted in determining the MLFSS due to electrokinetics. Fig. 4.35 showed the increase in the suspended solids (in kg/m^3 wastewater) in terms of the increase in the fixed suspended solids or the inorganics generated in SMEBR due to electrokinetics.

It could be concluded that the sludge production increased with current density. Therefore, depending on the desired objectives of the treatment process, an operating current density is recommended. The solid increase due to electrokinetics was described by equation 4.2:

$$\xi^* = 0.0064\ CD + 0.0342 \qquad (4.2)$$

Where, ξ^* is the solid increase in kg/m^3, CD is the current density in A/m^2.

Consequently, an additional term (ζ^* Q) was added to equation 4.1 as shown in equation 4.3:

$$P_{x,\,TSS} = \frac{Q(Y)(S_0 - S)}{1 + (k_d)SRT} + \frac{f_d(k_d)Q(Y)(S_0 - S)SRT}{1 + (k_d)SRT} + \frac{QY_n(NO_x)}{1 + (k_{dn})SRT} + Q\ (nbVSS) +$$

$$Q\ (TSS_o - VSS_o) + \zeta^*\ Q \qquad (4.3)$$

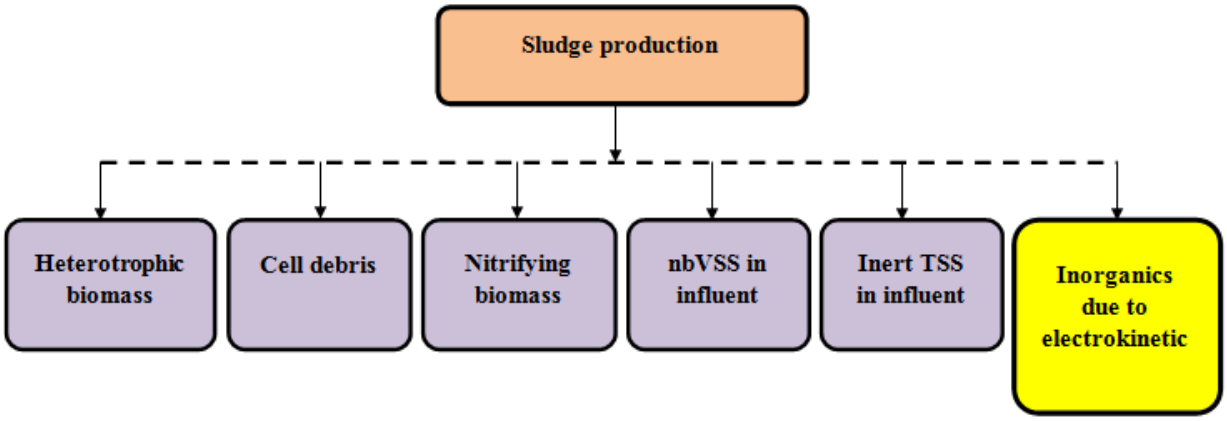

Fig. 4.34: Sludge production in SMEBR system.

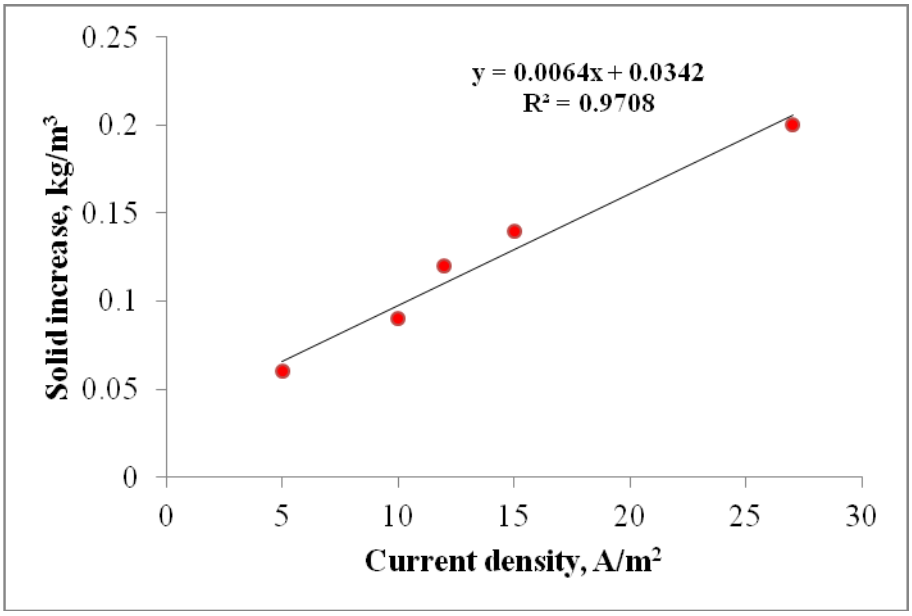

Fig. 4.35: Daily solid increase in SMEBR due to electrokinetics at different current densities.

From Stage 2, it could be concluded that SMEBR showed superiority in performance over MBR, and therefore several operating conditions were investigated (in Stages 3 and 4) in SMEBR to ensure excellent performance in the treatment of wastewater.

4.4 Stage 3: <u>Objective:</u> Impact of hydraulic retention time (HRT) in SMEBR

Stage 2 concluded that SMEBR is an efficient technology for wastewater treatment provided that it operates under adequate current density (Hasan et al., 2011). Thus determining the volume of the effective liquid in the reactor (related to the volume of SMEBR) was necessary to assess the design process. Experiments were carried out in SMEBR system to investigate the impact of HRT on membrane fouling, removal efficiency, and sludge properties. At a fixed SRT of 20 d with controlled current density of 15 A/m^2 and varying organic loading, SMEBR having an effective volume of 15 L was operated at different HRTs (i.e. different

fluxes) of 6, 9, and 15 h for 8 days each. The distance between electrodes was less than 10 cm and electrodes were connected to the DC power supply. The intermittent electrical mode of 5 min ON: 10 min OFF was controlled using a timer.

4.4.1 Impact of HRT on removal efficiency

4.4.1-1 COD removal

Fig. 4.36 showed the variation of chemical oxygen demand (COD) removal efficiency over operation time. It was observed that after four days of operation, COD removal was 94%, 95%, and 96%, at 6, 9, and 15 h, respectively. After six days of operation, COD removal was 95%, 96%, and 94% at 6, 9, and 15 h, respectively. Furthermore, after eight days of operation, COD removal was 95%, 95%, and 95% at 6, 9, and 15 h, respectively. It could be concluded that COD removal was not affected by the change in HRT.

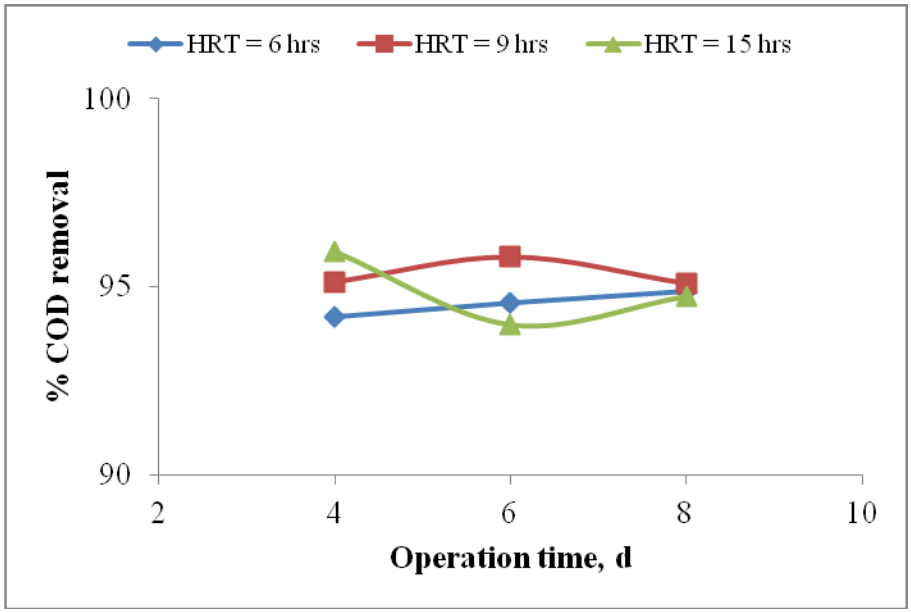

Fig. 4.36: COD removal at different HRT in SMEBR.

These results were in agreement with previous studies conducted in MBR and concluded that HRT had no impact on COD removal (Ngo et al., 2008; Sombatsompop, 2007).

4.4.1-2 Phosphorus removal

Fig. 4.37 showed the variation of orthophosphate (as PO_4^{3-}-P) removal efficiency over operation time. It was noticed that after four days of operation, phosphorus removal was 86%, 84%, and 99%, at 6, 9, and 15 h, respectively. After six days of operation, phosphorus removal was 86%, 83%, and 93% at 6, 9, and 15 h, respectively. Furthermore, after eight days of operation, phosphorus removal was 86%, 84%, and 98% at 6, 9, and 15 h, respectively.

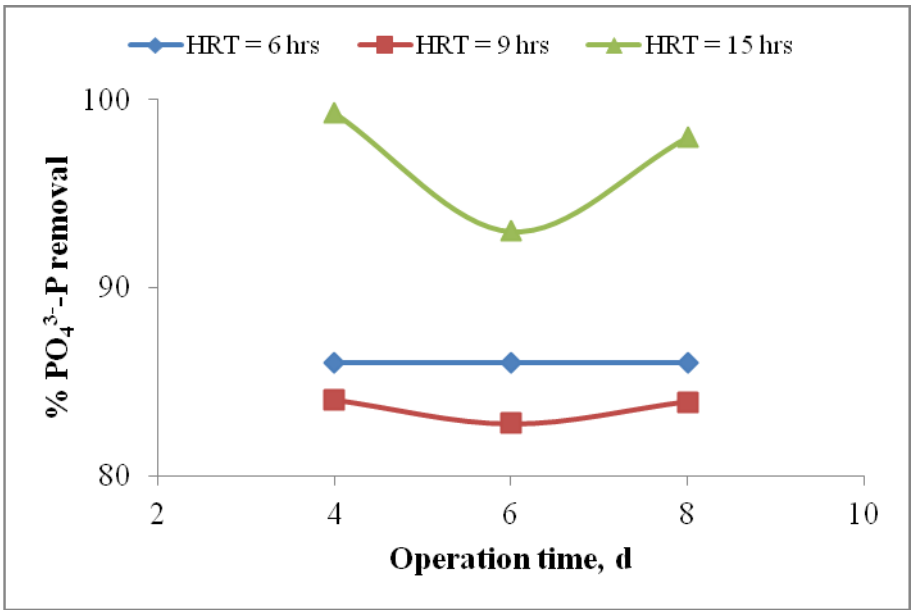

Fig. 4.37: Phosphorus removal at different HRT in SMEBR.

It could be concluded that HRT had impact on phosphorus removal and better results were achieved at 15 h where the wastewater was exposed longer to biological process and electrokinetics. As a result, more phosphorus complexes would be generated; precipitated

in the solution and deposited on the surface of electrodes (fate of phosphorus is discussed in Subsection 5.2.6).

4.4.1-3 Ammonia and total nitrogen removal

Fig. 4.38 showed the variation of ammonia (as NH_3^+-N) removal efficiency over operation time. It could be observed that after four days of operation, NH_3^+ removal was 37%, 76%, and 88%, at 6, 9, and 15 h, respectively. After six days of operation, NH_3^+ removal was 32%, 77%, and 99% at 6, 9, and 15 h, respectively. Furthermore, after eight days of operation, NH_3^+ removal was 34%, 76%, and 93% at 6, 9, and 15 h, respectively. It could be concluded that NH_3^+ removal was significantly affected by the change in HRT. As previously demonstrated in the removal of phosphorus, ammonia at high HRT had the chance to stay longer in the reactor thus higher rates of oxidation occurred. Consequently, as the ammonia was oxidized, more nitrates were generated. In aerobic conditions, autotrophic nitrifiers converted ammonia into nitrite or nitrate (Jeong and Chung, 2006). Average concentrations of nitrates (as NO_3^--N) in the treated effluents were 37, 17, and 16 mg/L at 6, 9, and 15 h, respectively. It could be concluded that the increase in NO_3^--N was significantly affected by the change in HRT where at high HRT, both biological oxidation as well as electrooxidation enhanced the conversion of ammonia to nitrates and better nitrification was achieved resulting in lower concentrations of nitrates present in the treated effluent.

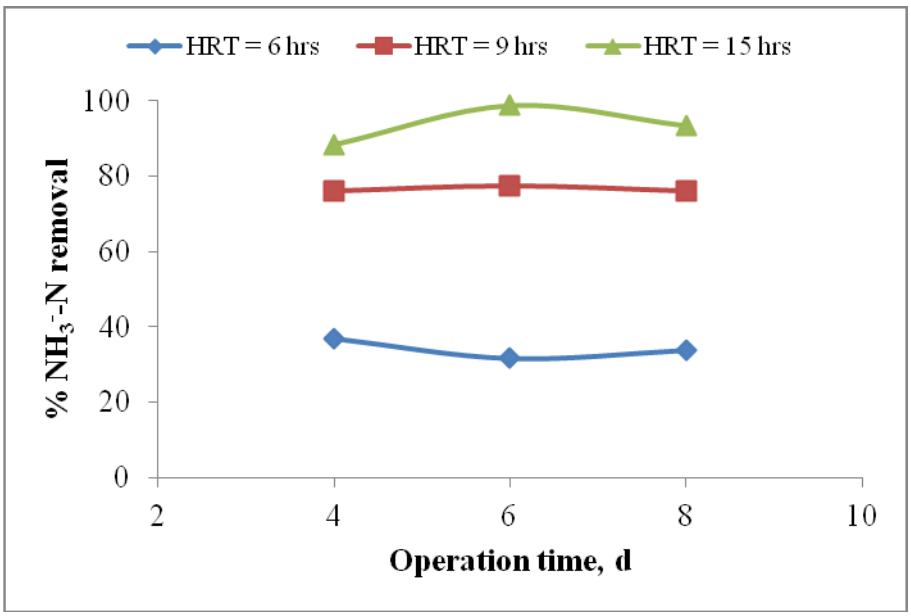

Fig. 4.38: Ammonia removal at different HRT in SMEBR.

Fig. 4.39 showed the variation of total nitrogen (TN) removal efficiency over operation time. It was noted that after four days of operation, TN removal was 19%, 21%, and 39%, at 6, 9, and 15 h, respectively. After six days of operation, TN removal was 18%, 36%, and 58% at 6, 9, and 15 h, respectively. Furthermore, after eight days of operation, TN removal was 18%, 38%, and 54% at 6, 9, and 15 h, respectively. It could be concluded that TN removal was significantly affected by the change in HRT. Better removal efficiency was accomplished at high HRT. The biodegradation of the organic compounds is a very slow process, and many nitrogen organics are slowly biodegraded. Hence, by increasing HRT (i.e. allowing a longer period of contact between the wastewater and biological-electrokinetics processes); several nitrogen compounds were degraded and more nitrates were reduced at the cathode. Thus, nitrogen compounds were removed and better water quality was achieved.

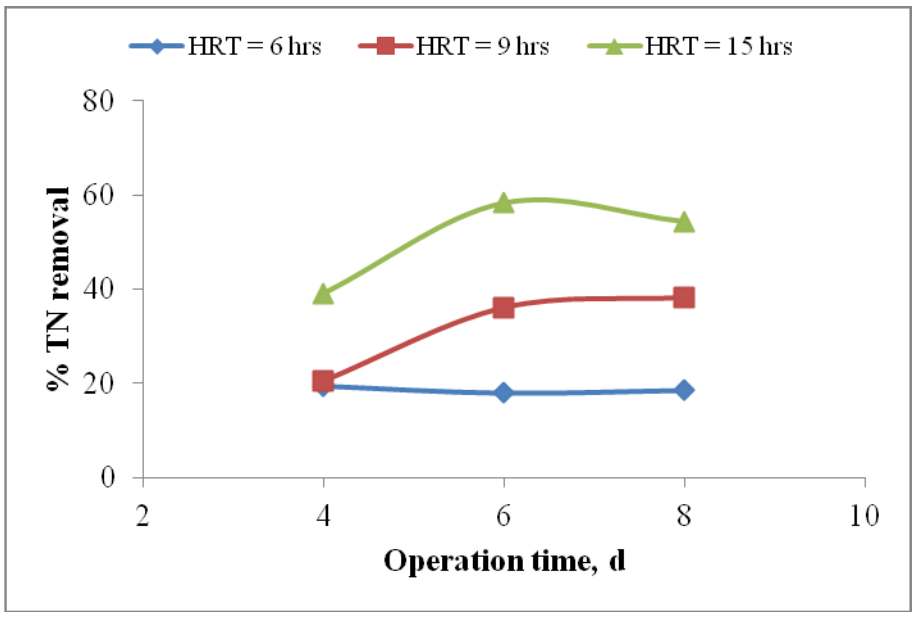

Fig. 4.39: Total nitrogen removal at different HRT in SMEBR.

4.4.2 Impact of HRT on sludge properties

4.4.2-1 Relationship between HRT and mean particle size diameter

Fig. 4.40 showed the variation of the mean particle size diamater (PSD) over time at different HRT. As was expected, the reduction in floc size was 7.8%, 41%, and 41.6% at 6, 9, and 15 h, respectively. Therefore, as HRT increased, the phenomenon of electroosmosis occurred in significant rates permitting the extraction of bound water from the sludge flocs, and hence shrinking in their sizes.

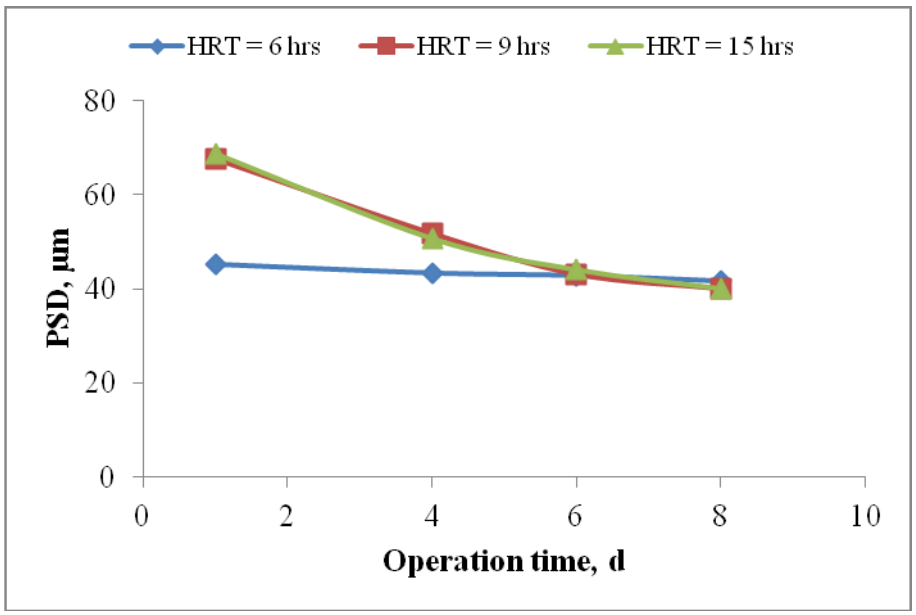

Fig. 4.40: Mean particle size diameter variation at diffirent HRT in SMEBR.

4.4.2-2 Relationship between HRT and mixed liquor suspended solids (MLSS)

Fig. 4.41 showed the variation of mixed liqour suspended soilds (MLSS) over time at different HRT. It could be observed that more total suspended solids were generated at high HRT. They increased from 5560 to 8160 mg/L, and from 5010 to 11100 mg/L at 9, and 15 h, respectively, while no significant increase in MLSS was reported at 6 h. It could be postulated that electrokinetics contributed to the increase in MLSS as HRT increased. In addition, the increase in solids could be attributed to the fact that as the reactors operated under fixed SRT; i.e. equal amounts of sludge were wasted per day, more solids would accumulate at high HRT in the reactor resulting in increase in total MLSS.

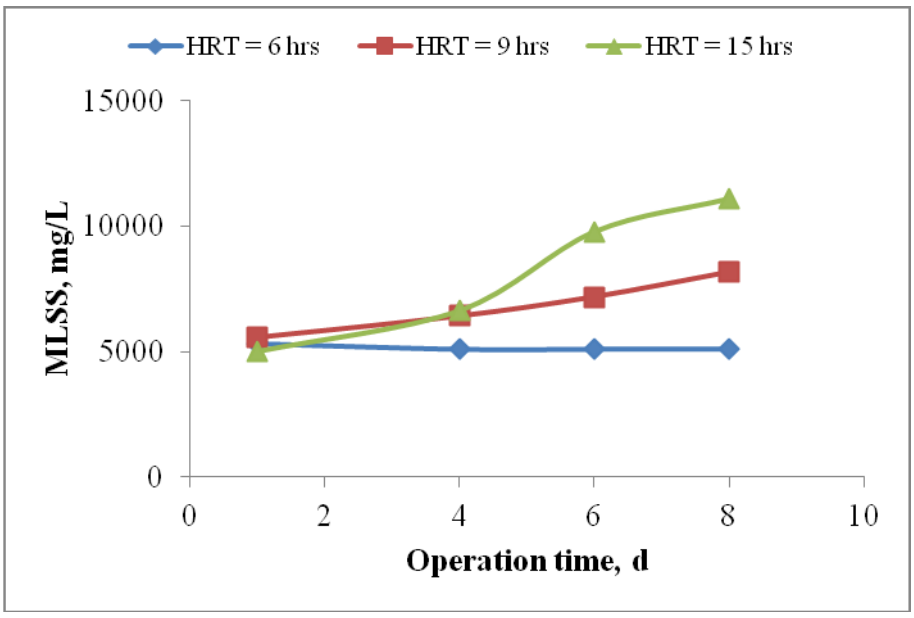

Fig. 4.41: MLSS variation at different HRT in SMEBR.

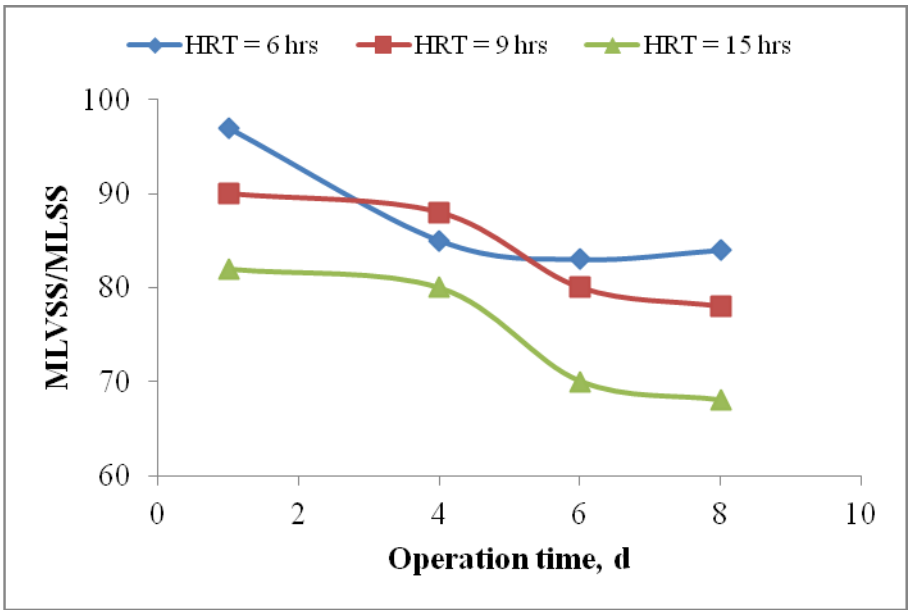

Fig. 4.42: MLVSS/MLSS ratio variation at different HRT in SMEBR.

Fig. 4.42 showed the variation of volatile suspended solids (MLVSS) to MLSS ratio observed at HRT. It showed that there was a reduction in MLVSS/MLSS ratio over time

at all conditions, which explained the generation of the inorganics, due to electrokinetics, in the bulk solution.

4.4.2-3 Relationship between HRT, filterability and settelability

Sludge dewatering was determined by the filterability test. Fig. 4.43 showed the variation of filtration time required to filter 50 mL of sludge suspension under different HRT. It was observed that better results were observed as HRT decreased. It could be said that the sludge filterability was significantly enhanced by electrokinetics. Moreover, the sludge in SMEBR had better settleability at low HRT. For example, the sludge volume index (SVI) was 65.7, 65.8, and 123.1 mL/g at 6, 9, and 15 h, respectively. This could be explained by the absence of filamentous bacteria where they form at SVI > 150 causing sludge bulking (Parker et al., 2001).

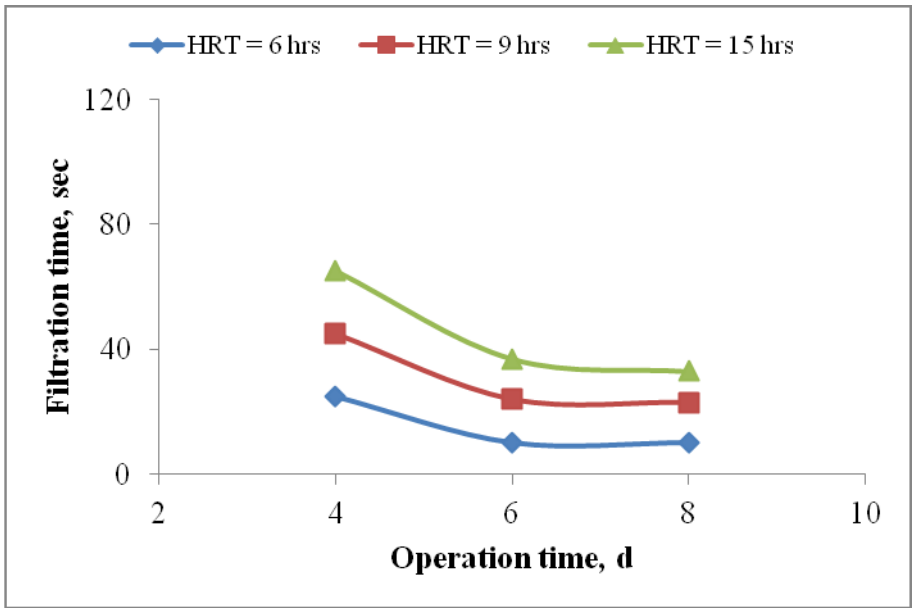

Fig. 4.43: Time to filter 50 mL sample - variation at different HRT in SMEBR.

4.4.3 Impact of HRT on membrane fouling

The change of transmembrane pressure (TMP) with time in all reactors, shown in Fig. 4.44, was monitored to investigate membrane fouling behavior at constant fluxes of 25, 16.7, and 10 L/m^2.h. SMEBR operated under 6 h had fouled very often since the operating flux was close to the critical flux which was measured in Section 4.1. That is why the results at HRT of 6 h were not shown.

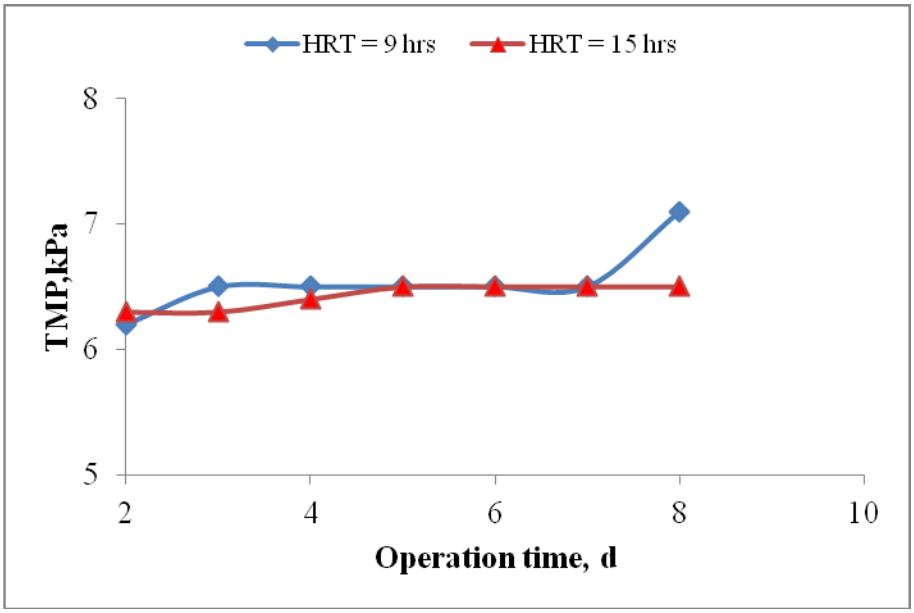

Fig. 4.44: TMP variation at different HRT in SMEBR.

On the other hand, fouling was insignificant at high HRT (9 and 15 h). Considering the membrane fouling rate calculated from the slope of TMP versus operation time (days) (Basu and Huck, 2005, Ye et al., 2005), it was noted that the rate of average membrane fouling decreased in the order of 0.0964 kPa/d, and 0.0393 kPa/d at 9, and 15 h, respectively. As the operating flux decreased below the critical flux of the membrane, transmembrane pressure would significantly decrease, and therefore less membrane fouling. Therefore, it could be concluded that by applying electrokinetics to the MBR system; i.e.

SMEBR, membrane fouling as well as frequency of membranes cleaning were significantly reduced and thus longer membranes lifetime. Membrane cleaning was performed as was explained in Chapter 3 - Section 3.4.

4.5 Stage 4: Objective: Impact of the variation of the volume of the electrical zone in SMBER

According to the results obtained from Stage 2 (shown in Section 4.3), SMEBR showed superiority in performance and produced better results than the conventional MBR. SMEBR was divided into different zones (Fig. 3.1), and therefore investigating the impact of changing the volume of the electrical zone with respect to the volume of the effective liquid in SMEBR was necessary to assess the design of SMEBR system. Therefore, in Stage 4; the ratio of the volume of the electrical zone (V^*) with respect to the volume of the effective liquid (V); i.e. V^*/V was decreased from 47% to 24% by increasing the SMEBR inside diameter, while keeping constant reactor height. Experiments were carried out to investigate the influence of such a variation on membrane fouling, removal efficiency, and sludge properties. At a fixed SRT of 20 d with controlled current density of 15 A/m^2 and varying HRT of 9 (at 47%) and 18 h (at 24%), SMEBRs having volumes of 15 and 30 L were operated at two volume ratios (V^*/V) of 47%, and 24% for 8 days each. The distance between electrodes was less than 10 cm and electrodes were connected to the power supply. The intermittent electrical mode of 5 min ON: 10 min OFF was controlled using a timer.

4.5.1 Impact of volume variation on removal efficiency

4.5.1-1 COD removal

Fig. 4.45 showed the variation of chemical oxygen demand (COD) removal efficiency over operation time. It could be observed that after four days of operation, COD removal was 95% and 98% at 47%, and 24%, respectively. After six days of operation, COD removal was 96% and 98% at 47%, and 24%, respectively. Furthermore, after eight days of operation, COD removal was 95% and 100% at 47%, and 24%, respectively. It could be concluded that COD removal was affected by the change in volume ratio and better results were achieved at higher extends when V^*/V ratio had decreased allowing the wastewater to stay longer time under biological oxidation. Up to 100% removal could be accomplished in SMEBR system.

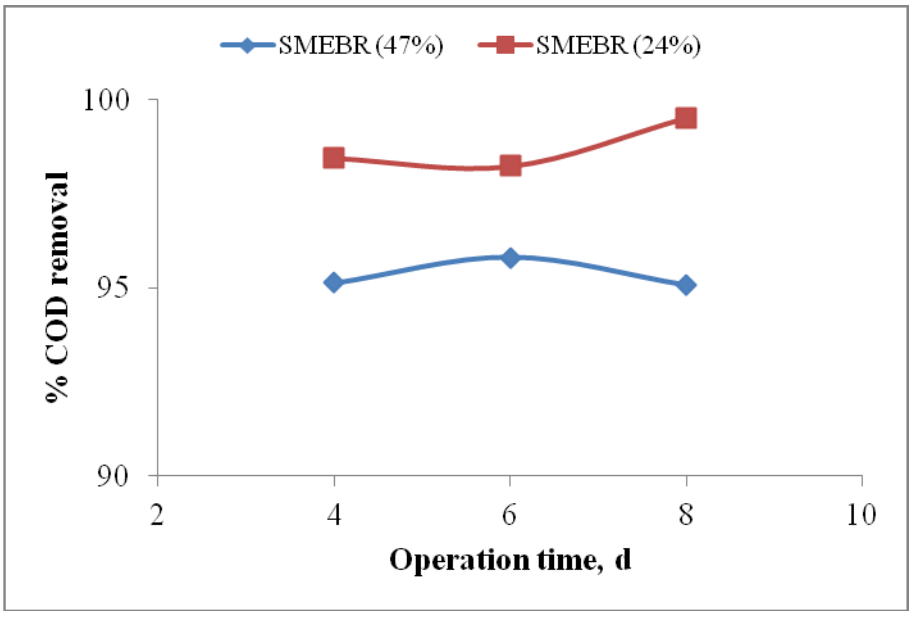

Fig. 4.45: COD removal at different electrical zone volume to total effective liquid volume ratios (V^*/V) of 47% and 24% in SMEBR.

4.5.1-2 Phosphorus removal

Fig. 4.46 showed the variation of orthophosphate (as PO_4^{3-}-P) removal efficiency over operation time. It was observed that after four days of operation, P removal was 84% and 100% at 47%, and 24%, respectively. After six days of operation, P removal was 83% and 91% at 47%, and 24%, respectively. Furthermore, after eight days of operation, P removal was 84% and 92% at 47%, and 24%, respectively. It could be therefore concluded that P removal was significantly affected by the change in volume and achieved better results at 24% (up to 100%).

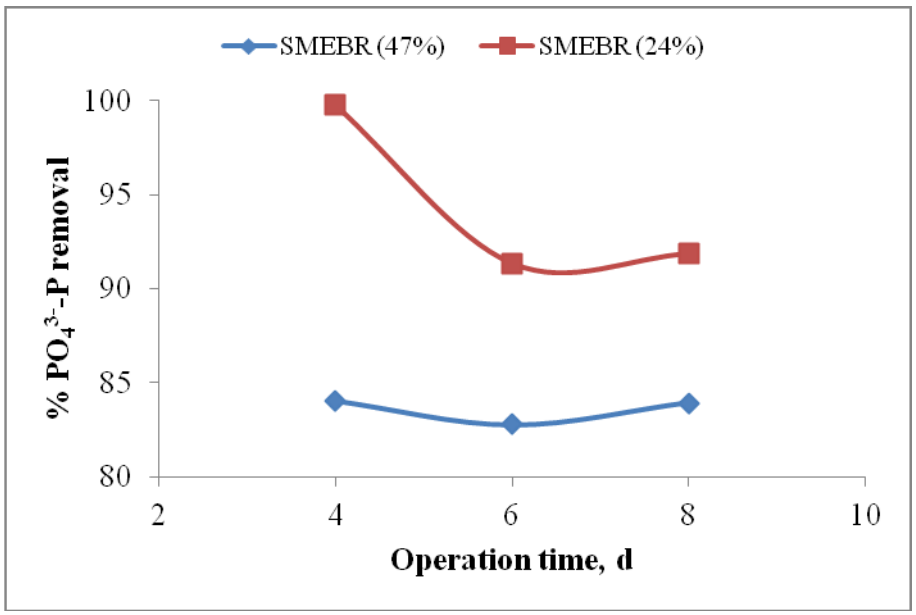

Fig. 4.46: Phosphorus removal at different electrical zone volume to total effective liquid volume ratios (V^*/V) of 47% and 24% in SMEBR.

This could be explained by the fact that by decreasing the volume ratio and keeping into consideration the locations of the air diffusers towards the centre of the reactor; an anoxic zone was created in the reactor (i.e. non complete mixed reactor with a pre-

denitrification step) which therefore enhanced the release of phosphorus compounds before entering the aerobic zones.

4.5.1-3 Ammonia and total nitrogen removal

Fig. 4.47 showed the variation of ammonia (as NH_3^+-N) removal efficiency over operation time. It could be observed that after four days of operation, NH_3^+ removal was 76% and 92% at 47%, and 24%, respectively. After six days of operation, NH_3^+ removal was 83% and 77% at 47%, and 24%, respectively. Furthermore, after eight days of operation, NH_3^+ removal was 76% and 89% at 47%, and 24%, respectively. It could be concluded that NH_3^+ removal was significantly affected by the change in volume and achieved better results at 24% (up to 92%) as the wastewater remained longer time (18 h) and was exposed to higher rates of biological oxidation. These conclusions were in line with the NH_3^+ removal obtained at higher HRT (Fig. 4.38). Similar findings were reported by Kim et al. (2008) when a pre-denitrification process was introduced which consisted of an anoxic reactor, an aerobic reactor, and a settler tank. Another mechanism of ammonia and total nitrogen removal at the 24% configuration could be related to the presence of hydrogen and oxygen gases in the system (due to electrokinetics); and their impacts on the nitrification-denitrification process. For these processes to take place, oxygen was required for the oxidation of ammonium and was used as an electron acceptor by the autotrophic nitrifying bacteria (eq. 4.4), whereas an electron donor (hydrogen gas) was needed for the denitrification to occur (eq. 4.5). Cowman (2004) reported high removal rates of total nitrogen and ammonia (97.1%) when oxygen gas was supplied into the aerobic (nitrifying) zone whilst hydrogen gas was be supplied to the anoxic (denitrifying) zone. Celmer et al. (2006) also evaluated the hydrogen-driven denitrification using the fiber membrane biofilm reactor (MBfR); and concluded that

controlling the process rates as well as the biofilm parameters were possible via applying limited amounts of hydrogen gas as an electron donor.

$$NH_4^+ + 2O_2 \rightarrow NO_3^- + 2H^+ + H_2O \quad (4.4)$$

$$NO_3^- + 2.5H_2 \rightarrow \frac{1}{2} N_2 + OH^- + 2H_2O \quad (4.5)$$

Average concentrations of nitrates (as NO_3^--N) in the treated effluents were 17, and 13 mg/L at 47%, and 24%, respectively. It could be concluded that the conversion of ammonia to NO_3^--N was better at 24% due to the anoxic zone which was created in SMEBR as demonstrated above in phosphorus and ammonia removal.

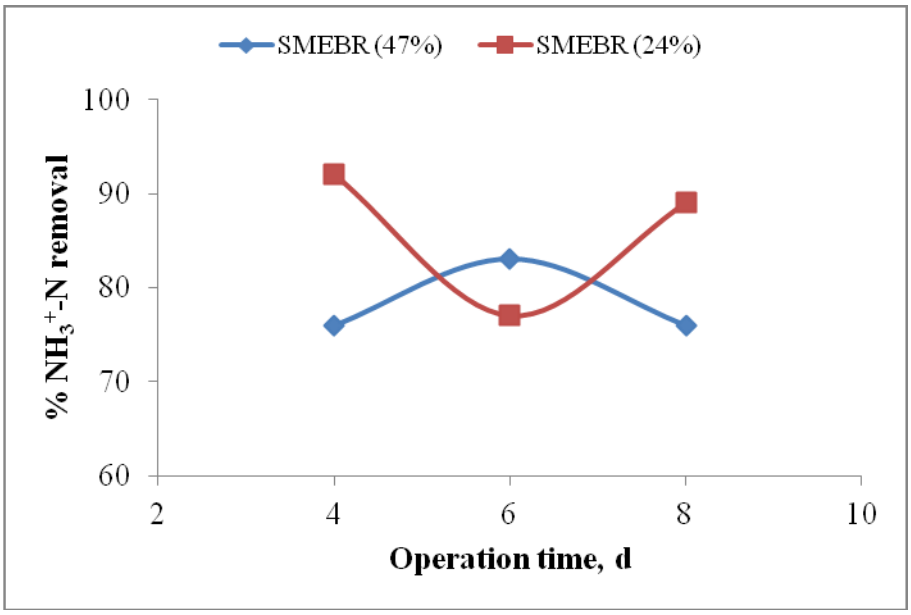

Fig. 4.47: Ammonia removal at different electrical zone volume to total effective liquid volume ratios (V^*/V) of 47% and 24% in SMEBR.

Fig. 4.48 showed the variation of total nitrogen (TN) removal efficiency over operation time. It could be observed that after four days of operation, TN removal was 21% and 66% at 47%, and 24%, respectively. After six days of operation, TN removal was 36% and 71% at 47%, and 24%, respectively. Furthermore, after eight days of operation, TN

removal was 38% and 78% at 47%, and 24%, respectively. It could be concluded that TN removal was significantly affected by the change in volume due to the anoxic zone which enhanced the nutrient removal.

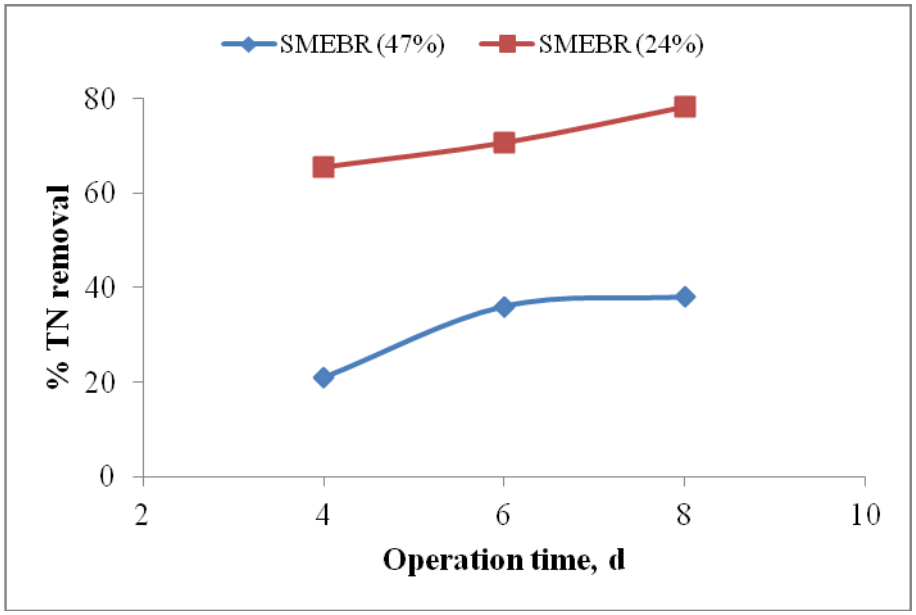

Fig. 4.48: Total nitrogen removal at different electrical zone volume to total effective liquid volume ratios (V^*/V) of 47% and 24% in SMEBR.

4.5.2 Impact of volume variation on sludge properties

4.5.2-1 Impact of volume variation on mean particle size diameter

Fig. 4.49 showed the variation of flocs mean particle size diamater (PSD) over time at different volume ratios. It could be observed that the reduction in floc size was 41% and 7% at 47%, and 24% respectively. However, after six days of operation, stability in mean particle size diameter was observed. Consequently, electroosmosis phenomenon might have occurred at lower rates in 24% than 47% as the retention time was significantly higher in 24% and thus, lower exposure time to electrokinetics.

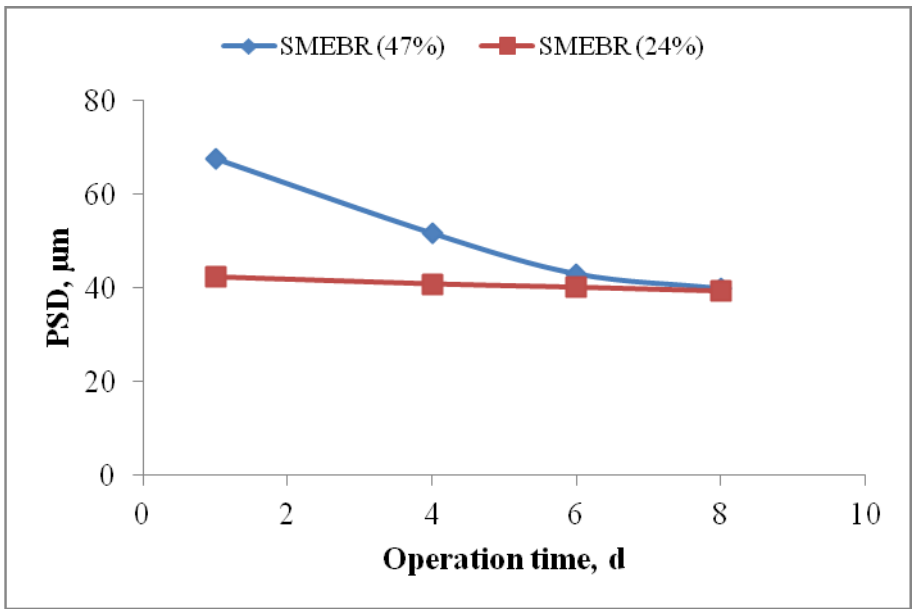

Fig. 4.49: Mean particle size diameter variation at different electrical zone volume to total effective liquid volume ratios (V^*/V) of 47% and 24% in SMEBR.

4.5.2-2 Impact of volume variation on mixed liquor suspended solids (MLSS)

Fig. 4.50 showed the variation of mixed liqour suspended soilds (MLSS) over time at different volume ratios. It could be observed that there was no remarkable difference in the biomass in both reactors and the slight change in the MLSS was therefore attributed to HRT (Fig. 4.41). Fig. 4.51 showed the variation of volatile suspended solids (MLVSS) to MLSS ratio observed at different volume ratios. It showed that there was a reduction in MLVSS/MLSS ratio over time at all conditions, which explained the generations of inorganics, due to electrokinetics in the reactors.

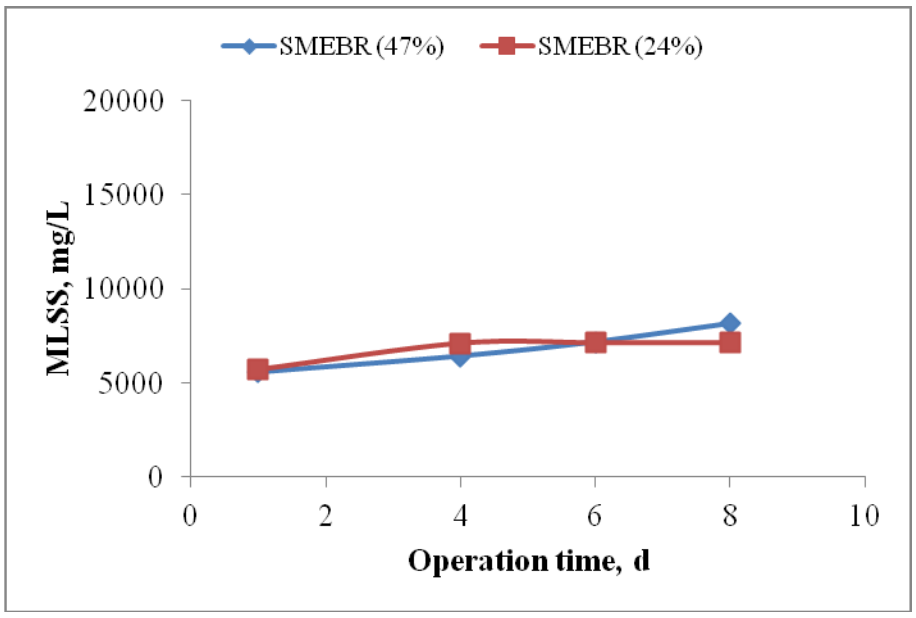

Fig. 4.50: MLSS variation at different electrical zone volume to total effective liquid volume ratios (V^*/V) of 47% and 24% in SMEBR.

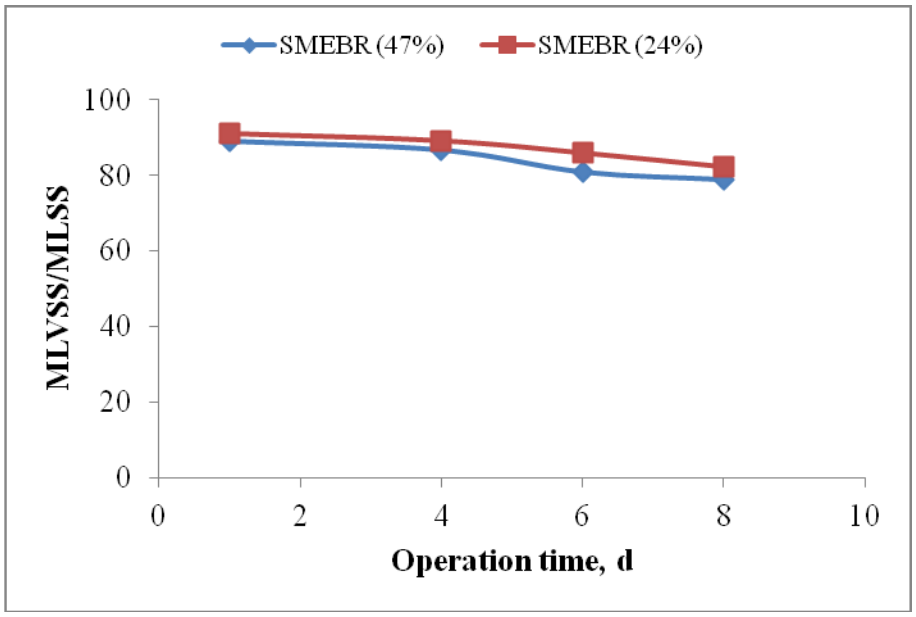

Fig. 4.51: MLVSS/MLSS ratio variation at different electrical zone volume to total effective liquid volume ratios (V^*/V) of 47% and 24% in SMEBR.

4.5.2-3 Impact of volume variation on zeta potential and soluble extracellular polymeric substances (soluble EPS)

As demonstrated in Section 4.3.2-4, the soluble extracellular polymeric substances (mainly soluble EPS_c and soluble EPS_p) had significant influence on zeta potential (Wilén et al., 2003). The more soluble EPS were released into the solution, the higher the magnitude of zeta potential.

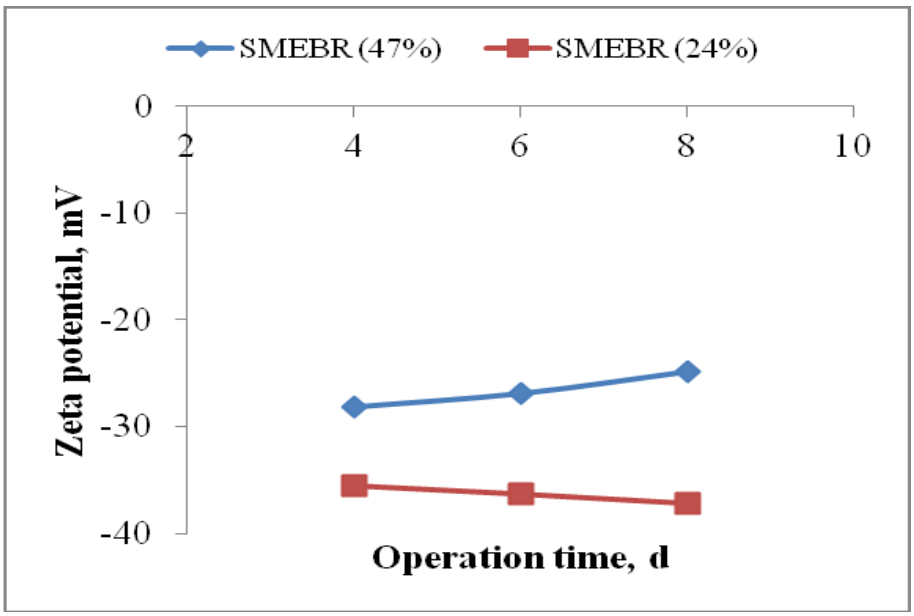

Fig. 4.52: Zeta potential variation at different electrical zone volume to total effective liquid volume ratios (V^*/V) of 47% and 24% in SMEBR.

This could be shown in Figs 4.52 to 4.54. It could be noticed that at 24%, more soluble EPS were present in the solution causing higher magnitude of zeta potential of -37.20 mV compared to zeta potential of -25.80 mV at 47% after eight days of operation, and as a result, less bioflocculation was observed at 24%. It could be said that the electrocoagulation process was slower in 24% than 47% as the retention time in the electrical zone was much less than the retention time in the biological treatment zone (due to the presence of the anoxic

zone in the 24% configuration), and hence less contact time between the negatively charged particles and the positive ions generated from the electrooxidation process.

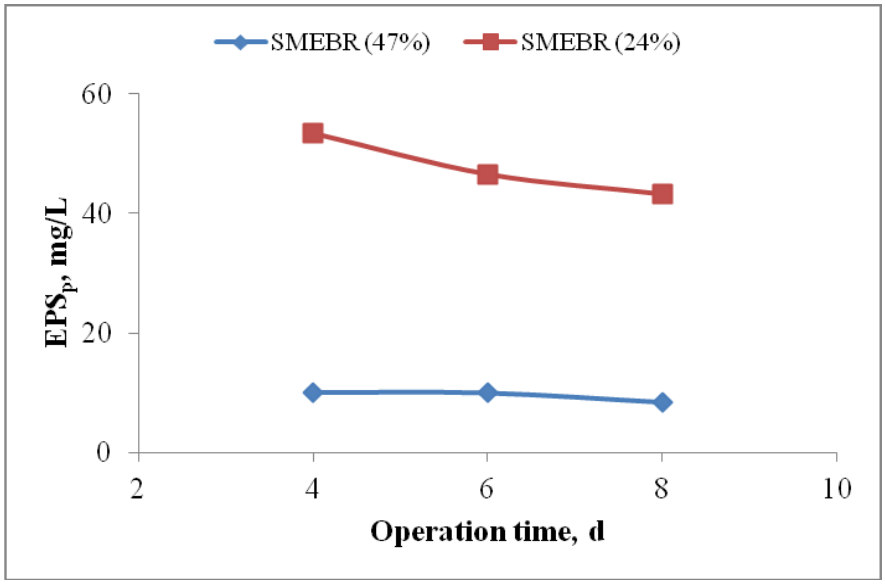

Fig. 4.53: EPS_p variation at different electrical zone volume to total effective liquid volume ratios (V^*/V) of 47% and 24% in SMEBR.

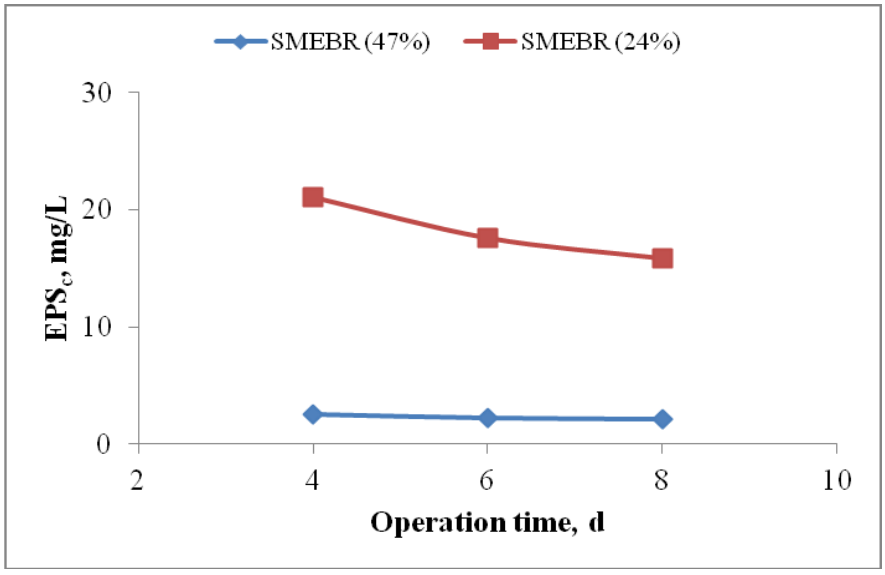

Fig. 4.54: EPS_c variation at different electrical zone volume to total effective liquid volume ratios (V^*/V) of 47% and 24% in SMEBR.

4.5.2-4 Impact of volume variation on filterability and sludge settleability

The filterability test was used to identify sludge dewatering. Fig. 4.55 showed the variation of filtration time required to filter 50 mL of sludge suspension under different volume ratios. It was observed that as volume to volume ratio increased, better results were accomplished. For instance, after eight days of operations; 26, and 47 seconds were required to filter 50 mL of sludge suspension at 47, and 24% volume ratio, respectively. It could be said that filterability was significantly influenced by the change of volume ratio and better results were obtained at 47%.

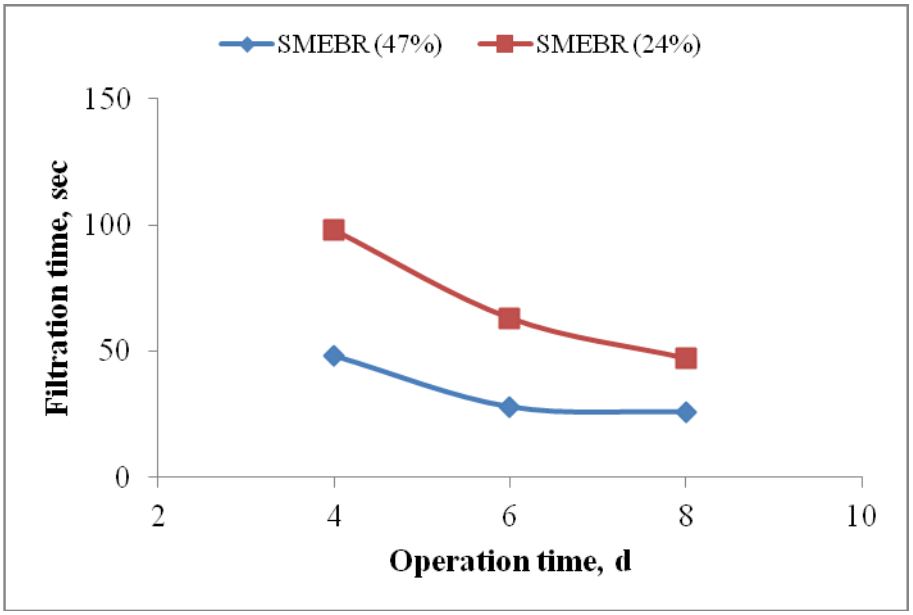

Fig. 4.55: Time to filter 50 mL sample - variation at different electrical zone volume to total effective liquid volume ratios (V^*/V) of 47% and 24% in SMEBR.

These results confirmed the significance of electroosmosis phenomenon where smaller flocs with less bound water were produced in SMEBR (Fig. 4.49), and therefore better filterability. Settleability of a specific sludge was characterised by the sludge volume index (SVI). It was the volume in milliliters occupied by 1 g of a suspension after 30 min

settling. Reported SVI were 65.8 and 121.5 mL/g at 47%, and 24 %, respectively. From the results, it could be summarized that the sludge at 47% had better settleability and no bulky sludge was produced in both configurations due to the absence of the filamentous bacteria which would exist at SVI > 150 (Parker et al., 2001).

4.5.3 Relationship between variation of volume and membrane fouling

The change of transmembrane pressure (TMP) with time in all reactors (Fig. 4.56) was monitored to investigate the membrane fouling behavior at constant flux of 16.7 $L/m^2.h$. It could be observed that TMP was increased faster at 24% than 47%. Previous studies illustrated the contribution of EPS_p to membrane fouling (Bourgeous et al., 2001). Accordingly, the higher amount of soluble EPS present in the reactors (Figs 4.53 and 4.54) resulted in higher TMP values at 24%. In addition, by decreasing the volume ratio as well as locating the air diffuseres towards the center of the reactor; the depostion of the organics and inorganic materials on the aluminum anode might have increased; and thus had adverse impact on the effeciency of electrokinetic process in SMEBR when compared to 47% where flocs fomartion was more significant (Fig. 4.52).

Considering the membrane fouling rate calculated from the slope of TMP versus operation time (days) (Basu and Huck, 2005, Ye et al., 2005), it was noted that the rate of average membrane fouling increased in the order of 0.0964 kPa/d and 0.1893 kPa/d at 47% and 24%, respectively. Therefore, it could be concluded that by decreasing the volume ratio in the reactor, the rate of membrane fouling as well as the frequency of membranes cleaning could be significantly increased.

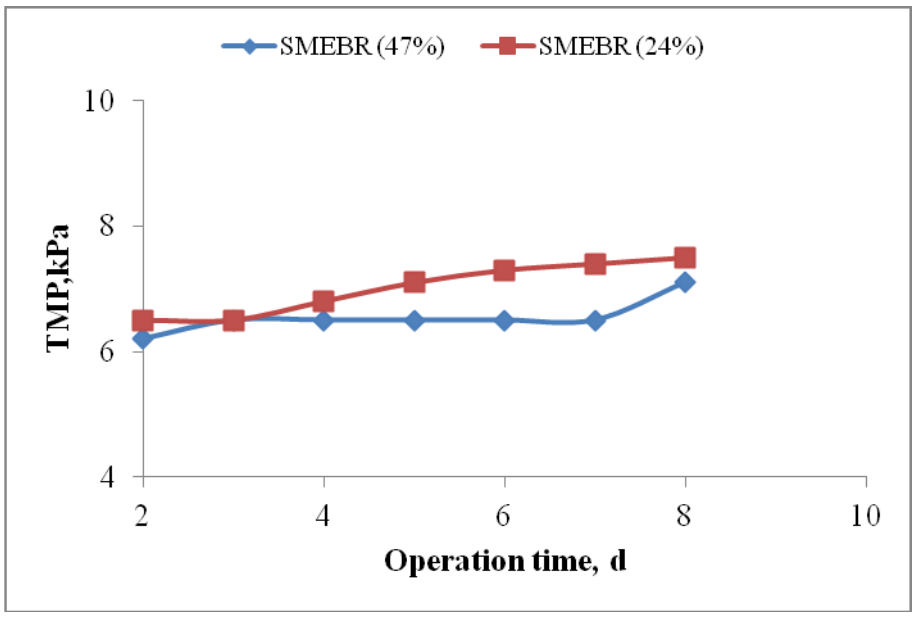

Fig. 4.56: TMP variation at different electrical zone volume to total effective liquid volume ratios (V^*/V) of 47% and 24% in SMEBR.

4.6 General conclusions from Phase 1

From the laboratory study conducted in Phase 1, it could be concluded that the operating ranges of the technological design parameters of SMEBR were:

- **Current density:** operation in the range of 10-15 A/m^2 is recommended.
- **Exposure time:** 5 min ON: 10 min OFF.
- **HRT:** operation in the range of 9-15 HRT is recommended taking into account the membrane design flux and electrical conditions.
- **V^*/V ratio:** operation in the range of 24% to 47% is recommended.
- **Aeration intensity (per 15 L volume of SMEBR-biological and membrane scouring):** up to 552 L/h.

The above data assisted the designing process of SMEBR in pilot scale (Phase 2 – Chapter 5). To evaluate the performance of SMEBR system, a laboratory scale experiment was also carried out under steady state conditions (Phase 3 – Chapter 6).

Chapter 5: Results and Discussion of Pilot Scale Experiments - Phase 2

The objective of Phase 2 was to design, install and investigate the performance of a new hybrid, compact wastewater treatment system which would yield an excellent effluent quality and could be reused in several applications. To accomplish the desired objectives, Phase 2 consisted of 3 Stages: design and installation of pilot SMEBR - Stage 1, operation of SMEBR in the municipal wastewater treatment plant in the City of l'Assomption along with testing conventional MBR pilot system - Stage 2, and investigation the relationship between the transmembrane pressure (TMP) and the sludge characteristics in SMEBR and MBR as well as the interaction among the sludge properties - Stage 3. The design protocol for full scale applications was also provided (Chapter 6).

SMEBR is a complex system due to the simultaneous interaction of biological treatment, membrane filtration, and electrokinetics in one SMEBR unit (Fig. 1.1). The work done in Phase 1 contributed significantly in Phase 2; where the operational ranges of the technological parameters such as HRT, aeration intensity, V^*/V ratio, current density and electrical exposure time were recommended as illustrated in Chapter 4. Statistical analyses (Phase 2 - Stage 3) were used to interpret and verify the results obtained from the experimental tests.

5.1 Stage 1: <u>Objective:</u> Design and installation of SMEBR and MBR pilot facilities

5.1.1 Stage 1a: <u>Objective:</u> Design of SMEBR pilot system

The design of SMEBR pilot system followed the Preliminary design scale-up approach illustrated in Fig. 3.5. A hollow fiber microfiltration membrane (Microza, Asahi Kasei Chem. Corp., Japan - MUNC 600-A) was placed in the center of the reactor. The membrane has an

effective membrane area of 12.5 m^2, pore size of 0.1 µm, and the module was equipped with a built-in bottom air diffuser for scouring. The membrane dimensions were 0.167 m dia.x1.131 m height (Table 3.2). Two cylindrical perforated electrodes having heights of 1.2 m (aluminum anode) were placed inside the SMEBR and connected to a low DC voltage gradient. An electrical field was provided in intermittent supply of 5 min ON: 10 min OFF. Accordingly, the pilot unit of the submerged membrane electro-bioreactor (SMEBR) consisted of a PVC-cylinder having dimensions of 1.6 m high and 0.46 m in diameter (effective volume of 235 L). Compressed air was introduced through several fine bubble air diffusers placed at the bottom of the reactor. Pressure regulator and air flow meter were used to adjust the air pressure and flow rate, respectively. The SMEBR operated under continuous flow of raw wastewater pumped directly from the main channel at a constant flow rate of 550 L/d, after screening, and without any pre-treatment. Based on the results of Phase 1 and the literature review done in Chapter 2, the solids residence time (SRT) and hydraulic residence time (HRT) were 10 d and 11 h, respectively. The raw wastewater was subject to daily and seasonal variation (Table 5.1).

Table 5.1: Average characteristics of influent wastewater pumped into SMEBR and MBR pilot systems (WWTP at l'Assomption)

Parameter	SMEBR	MBR
COD, mg/L	316 ± 145.9	371 ± 230.4
PO_4^{3-}-P, mg/L	4.13 ± 1.84	3.87 ± 1.3
NH_3^{+}-N, mg/L	42.9 ± 11.2	41.4 ± 10.4
NO_3^{-}-N, mg/L	0.41 ± 0.11	0.66 ± 0.64
TSS, mg/L	120 ± 9.6	118 ± 10.1

Fig. 5.1 showed the process flow diagram (PFD) - the piping and instrumentation diagram (PID) of SMEBR pilot facility. All piping and instrumentations were also provided in details. The design operating conditions were selected according to the results obtained from the laboratory scale study done in Phase 1 and following the design methodology (Fig. 3.5).

Design operating conditions:

- **Total applied current** = 9.5 A (current density = 12 A/m^2)
- **Hydraulic retention time (HRT)** = 11 h
- **Effective volume of liquid in SMEBR** = 0.235 m^3
- **Wastewater input flow rate** = 0.550 m^3/d
- **Organic loading** = 0.53 kg COD/m^3.d
- **Sludge retention time (SRT)** = 10 d → sludge wasted per day = 0.0235 m^3
- **Initial MLSS** = 2400 g/m^3
- **F/M** = 0.28 - 0.4 1/d
- **Aeration requirements: (determined from laboratory experiments in Phase 1-Stage 1b)**
    - Membrane scouring aeration rate = 0.08 m^3/m^2.h
    - Tank mixing (4 fine bubble air diffusers) = 0.8 $m^3$of air/ h

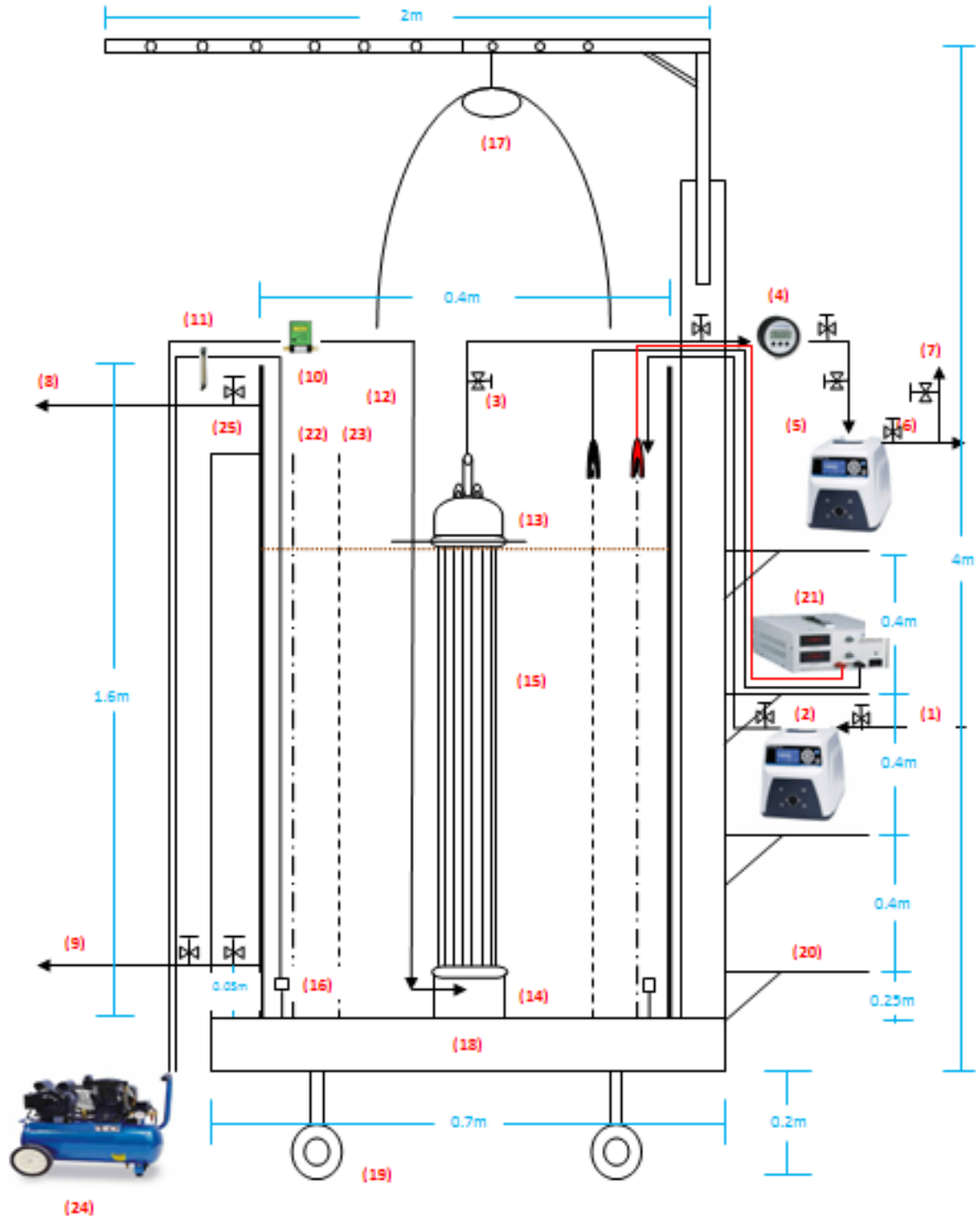

Fig. 5.1: SMEBR pilot unit process and instrumentation diagram (PFD - PID).

5.1.2 Stage 1b: Objective: Installation of SMEBR pilot system

SMEBR pilot facility – basic equipment and requirements

Basic equipment:

1. Raw influent wastewater transfer line (1/2" dia.): from raw wastewater storage tank to SMEBR process tank equipped with 2 isolation valves: one upstream and one downstream of the transfer pump.
2. Raw influent wastewater transfer pump (MasterFlex pump, Cole-Parmer).
3. Treated wastewater membrane suction line (1/2" dia.): from membrane top to suction pump and to drain. Equipped with 5 isolation valves: one at the top of membrane, four other upstream and downstream of suction gauge and effluent suction pump.
4. Suction line pressure gauge.
5. Treated wastewater membrane suction pump (MasterFlex pump, Cole-Parmer).
6. SMEBR process vessel (0.46 m dia. x 1.6 m high).
7. Sampling line (1/2" dia.) with one isolating valve.
8. Overflow line (1" dia.) from SMEBR at 1.5 m height to drain: equipped with one isolating valve.
9. Waste line (1/2" dia.): positioned at 0.05 m from tank bottom to drain with one isolating valve.
10. Air supply line (1/4" dia. and 1/2" dia.): from air compressor to flow meter and 4 diffusers located at bottom of SMEBR.
11. Air supply line (1/4" dia. and 1/2" dia.) from air compressor to flow meter to bottom side of membrane aeration adapter.
12. Air supply hose.

13. Membrane head: SS reducer, gasket, clamp and a plastic band for air hose attachment (part of membrane supply).
14. Membrane aeration adapter (part of membrane supply).
15. Membrane module.
16. Fine bubble air diffusers (4).
17. Lift and pulley system (3.5 m high x 1.2 m reach) to provide access to membrane for cleaning.
18. Mobile platform/skid to accommodate SMEBR unit. Two other smaller skids to accommodate 2 cleaning solution tanks. All 3 tanks are positioned in a triangular fashion for membrane and electrodes removal/installation.
19. Front/swivel wheels welded to platform to accommodate 500 kg load.
20. Four (4) shelves.
21. Power supply.
22. Aluminum anode.
23. Steel cathode.
24. Air compressor with twin manifold outlets (1/4" dia.).
25. Isolating valves (1/2" opening).

Requirements:

The following were required for the installation of the pilot facility:

- Space requirement for all tanks and equipment: 4 m long x 1.5 m wide footprint. Ceiling 4 m high.
- Total of 4 tanks used for the pilot facility as follows:
  - The main SMEBR process tank having dimensions of 0.46 m x 1.6 m.

- Raw wastewater storage tank: 0.8 m^3 working capacity, with two (2) isolating valves (1/2" dia.) located at 0.05 m and 0.22 m, respectively from tank bottom (Fig. 5.2).
- Two (2) tanks with same dimensions of 0.4 m x 1.5 m used for membrane cleaning (physically and chemically). One valve (1/2" dia.) located at 0.05 m from bottom of each tank for drainage purposes (Fig. 5.2).

- DC power supply for connecting all electrical equipment. Three (3) electrical wall outlets were needed to ensure the safety and the continuous operation of all equipment. 110 V AC/10 A outlets were required.

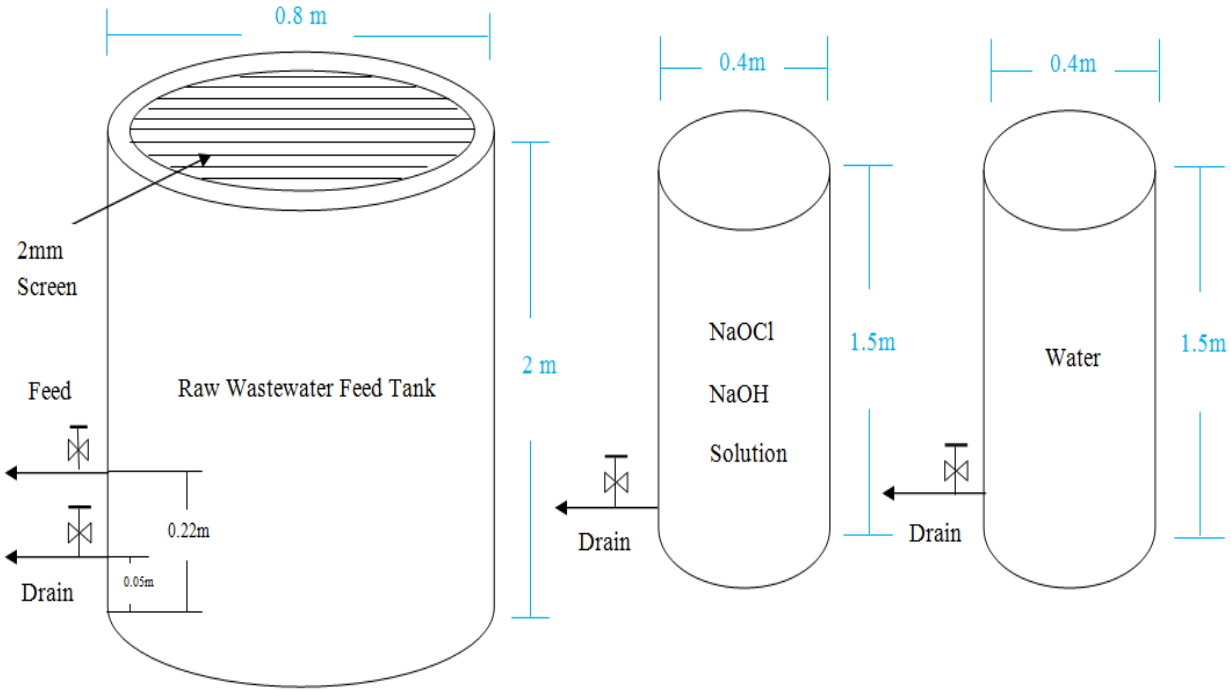

Fig. 5.2 Feed and cleaning tanks prepared in pilot SMEBR operation.

5.2 Stage 2: Objective: Performance of SMEBR and MBR pilot facilities

The objective of Stage 2 was to investigate the performance of the new hybrid SMEBR system in a pilot scale. A comparative study to the conventional membrane bioreactor (MBR) was performed. SMEBR and MBR were operated under the same operating conditions, and fed with the same raw wastewater which was subject to daily and seasonal variations shown earlier in Table 5.1. The results of SMEBR and MBR pilot systems were tabulated in Appendix C – Figs C-1 to C-6.

5.2.1 Effluent water quality

Figs 5.3 to 5.6 presented the effluent quality of SMEBR and MBR pilot facilities over 7 weeks of operation with respect to COD, P, and NH_3 removal. Some fluctuations in the data in SMEBR and MBR were observed in the first thirty days while stability in the removal effeciencies was evident after 3 SRT. Regarding COD removal, after six days of operation 91.3% and 80.4% were observed in SMEBR and MBR, respectively. Reaching 3 SRT, SMEBR was able to remove COD by 92% which was significantly higher than those accomplished by MBR (86.6%, low COD level in the influent in the last 4 days) indicating that removal of COD was affected by the electrical field which influenced both microorganisms and wastewater matrix. The concentrations of COD in SMEBR effluent were in the range of 4 to 37 mg/L, whilst in MBR effluent were much higher and in the range of 17 to 63 mg/L.

Accordingly, it could be speculated that the treated wastewater leaving the biological treatment zone (i.e. between the reactor wall and the outer electrode), and entering the electrical zone (i.e. between the electrodes); was exposed to electrokinetic phenomena

(including oxidation – eq. 2.5) which produced more bioavailable substrate and resulted in higher COD removal in SMEBR compared to MBR.

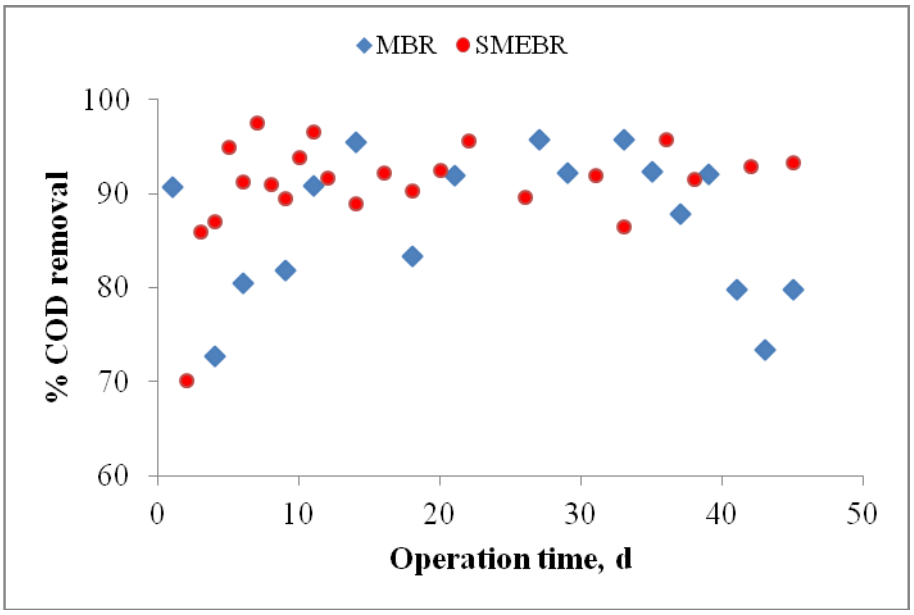

Fig. 5.3: COD removal in the pilot scale SMEBR and MBR.

Therefore, the charge loading (Al^{3+}) generated in the solution was enough to destabilize and remove the colloids via charge nuetralisation (Ni'am et al., 2007; Daneshvar et al., 2006; Saleem et al., 2011), as well as via cathodic reaction where hydrogen gas bubbles were formed (Dermentzis et al., 2011). It could be said that SMEBR, operated under an adequate current density, enhanced the growth of other microorganisms and nitrifires existing in the reactor. The mixed liqour volatile suspended solids (MLVSS) in SMEBR was 1.7 times higher than MLVSS in MBR – Fig. 5.4 .

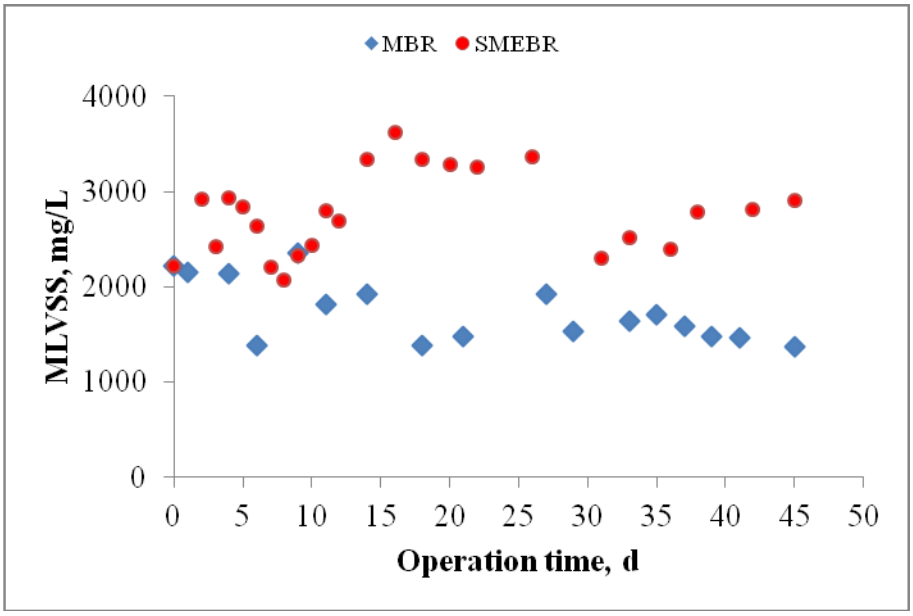

Fi.g 5.4: Mixed liquor volatile suspended solids (MLVSS) variation in the pilot scale SMEBR and MBR.

More than 99% removal of PO_4^{3-}-P was reported in SMEBR over 7 weeks of operation time while an average of 59% was observed in MBR (Fig. 5.5). The phosphorus removal in MBR could be attributed to the reaction between the different ions present in the influent wastewater (eg. aluminum) with the released phosphorus in the sludge suspension. The concentrations of PO_4^{3-}-P in SMEBR effluent were in the range of 0.01-0.3 mg/L, whilst PO_4^{3-}-P concentrations in MBR effluent were in the range of 0.7-2.5 mg/L. It was expected that electrokinetics enhanced phosphorus removal (eq. 5.1). Some of the non bioavailable inorganic fractions of phosphorus (as orthophosphate) remained in the wastewater after leaving the biological zone. They were easily uptaken in SMEBR due to the significant contribution of elektrokinetic phenomenon. Phosphorus removal due to electrocoagulation illustrates the process of the chemical reaction and coagulation - settling through which the metal ions released from the electrooxidation and the organic pollutants react in the presence

of DC voltage. Therefore, phosphate could be completely removed from the wastewater by SMEBR in conjuntion with the precipitation of $AlPO_4$ (eq. 5.1), and $Al(OH)_3$ (eq. 2.6). In addition, at high pH (8-8.5), phosphate as apatite and hydroxyapatite (Grubb et al., 2000) could be also precipitated in the presence of calcium ions (eq. 5.2).

$$Al^{3+} + H_nPO_4^{3-n} \leftrightarrow AlPO_4 + nH^+ \quad (5.1)$$

$$10Ca^{2+} + 6PO_4^{3-} + 2OH^- \leftrightarrow Ca_{10}(PO_4)_6(OH)_2 \quad (5.2)$$

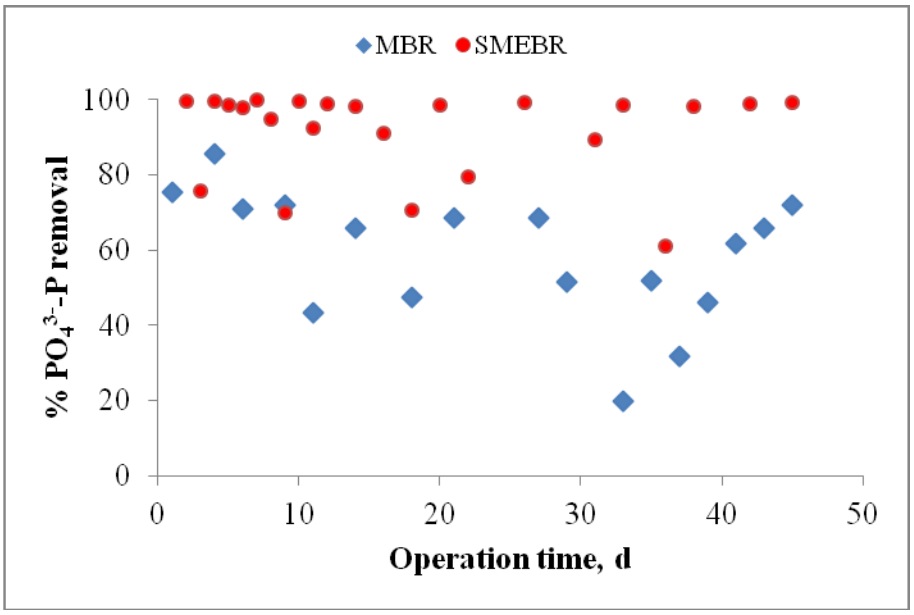

Fig. 5.5: Phosphorus removal in the pilot scale SMEBR and MBR.

Furthermore, the complete removal of phosphates in SMEBR could be also attributed to the fact that some phosphorus were deposited on the surface of the electrodes. Two samples of the deposited material from the anode (250.6 mg) and the cathode (115.3 mg) were analyzed for total phosphorus. Samples were digested by nitric acid and heated at 100°C for one hour. The results confirmed our hypothesis and showed that higher deposition was noticed on the surface of the cathode when compared to the anode as 113.15 and 4.43 mg

PO_4^{3-}-P/m^2 were reported, respectively (detailed discussion about fate of phosphorus in Subsection 5.2.6).

Monitoring of ammonia (as NH_3^+-N) removal showed that SMEBR experienced an adaptation period which affected its ability of removing ammonia from the wastewater. After that, SMEBR responded effectively and reported a significant ammonia removal at more than 99% (Fig. 5.6). MBR acheived an increase in ammonia removal during the operation period, and it accomplished 97% removal rates at steady state. The concentrations of NH_3^+-N in effluents were below acceptable level: 0.3-0.9 mg/L for SMEBR and 0.5-0.9 mg/L for MBR.

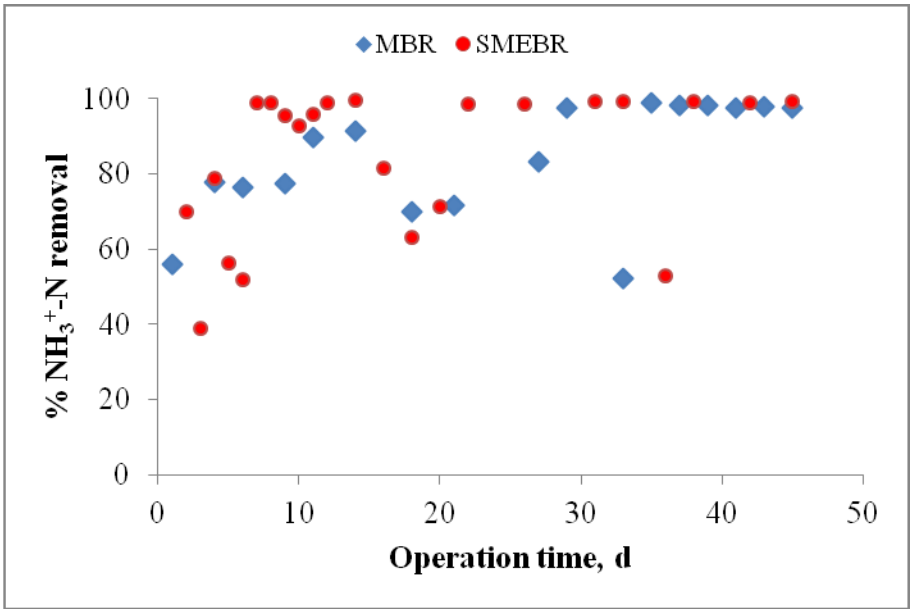

Fig. 5.6: Ammonia removal in the pilot scale SMEBR and MBR.

A difference of 2% in the removal effeciencies between SMEBR and MBR could be attributed to the electrokinetics. Ammonia degradation might occur during the direct anodic oxidation (Cabeza et al., 2007; Li et al., 2010). Indirect oxidation also took place

where ammonia was destroyed in the bulk solution due to the role of the strong oxidants, such as hydrogen peroxide, chlorine and hypochlorite generated by the electrochemical reactions (Cabeza et al., 2007). Chlorine, in the presence of chloride, was generated at the anode surface (eq. 5.3) and dependent on the applied current density and the hydrodynamic conditions. Chlorine was then diffused into the bulk to form hypochlorus acid and hypochlorite ions (eqs 5.4 and 5.5) depending on the pH (Li et al., 2010).

Anode:

$$2Cl^- \rightarrow Cl_2 + 2e^- \quad (5.3)$$

Bulk:

$$Cl_2 + H_2O \rightarrow HOCl + H^+ + Cl^- \quad (5.4)$$

$$HOCl \rightarrow H^+ + OCl^- \quad (5.5)$$

The formation of chlorine at the anode was coupled to its homogeneous reaction with ammonium ions:

$$2NH_4^+ + HClO \rightarrow N_2 + 2H_2O + 6H^+ + 2Cl^- \quad (5.6)$$

It was reported that ammonia could be also removed or stripped via increasing the pH (between 8 and 9) along with diffused areation, i.e. ammonia stripping (Ilhan et al., 2008). SMEBR experinced an increase in pH around 8.5, due to the domination of cathode activities. Hence, it could be speculated that some ammonia stripping could have taken place in SMEBR. Furthermore, it was speculated that microbial activities were also enhanced by the presence of the electrical field as it was demonstrated in case of COD removal.

The results of SMEBR pilot system confirmed the work done in Phase 1 and reported similar results when comapred to the laboratory scale SMEBR system (Chapter 4) indicating that SMEBR was properly designed at pilot scale.

5.2.2 Membrane fouling

The transmembrane pressure (TMP) was directly related to membrane fouling. The rate of fouling (i.e. *d(TMP)/dt*) was measured in SMEBR and MBR from the slope of TMP versus operation time (Basu and Huck, 2005; Ye et al., 2005). SMEBR showed consistent performance independent of variable conditions and reported no fouling over 7 weeks of operation, which made it an efficient method of overcoming the costly frequent membrane cleaning (Fig. 5.7). At the end of the pilot tests, the rates of fouling (*d(TMP)/dt*) in SMEBR and MBR over 7 weeks of operation were found to be 0.018 and 0.371 kPa/d, respectively where TMP in MBR was 8 times higher (17.2 kPa). A significant increase in TMP in MBR in the period between 10 and 15 days was also noticed. This could be attributed to the low temperature recorded in that period (around 11.6^{o}C), which adversely affected the filtration process along with higher density of sludge and differences in biological processes. It could be postulated that the characteristics of the mixed liquor have changed and more EPS, particularly proteins were released in the solution, and hence increased the fouling rate (Fig 5.7). These results were in agreement with previous studies who reported higher fouling at low temperature (Wilén et al., 2000; Jiang et al., 2005, van den Brink et al., 2011). In this study, sludge viscosity in MBR had increased by 9% indicating that the sludge became viscous at low temperature. Thus, less shear rate was generated by the coarse bubbles aeration, and more colloids might have deposited on the membrane surface (Lin and Shien, 2001).

In addition, membrane fouling index (MFI) and specific cake resistance in SMEBR had decreased from 0.016×10^{6} to 0.003×10^{6} L/s^{2} and from 0.83×10^{14} to 0.15×10^{14} m/kg after 7 weeks of operation. It could be concluded that the formation of the cake layer on

the membrane surface in SMEBR was significantly reduced by 82%. It was reported that the addition of chemical alum coagulant, powdered activated carbon with a high porosity, and carriers (Yang et al., 2006) was effective in reducing the specific cake resistance, and therefore minimizing membrane fouling.

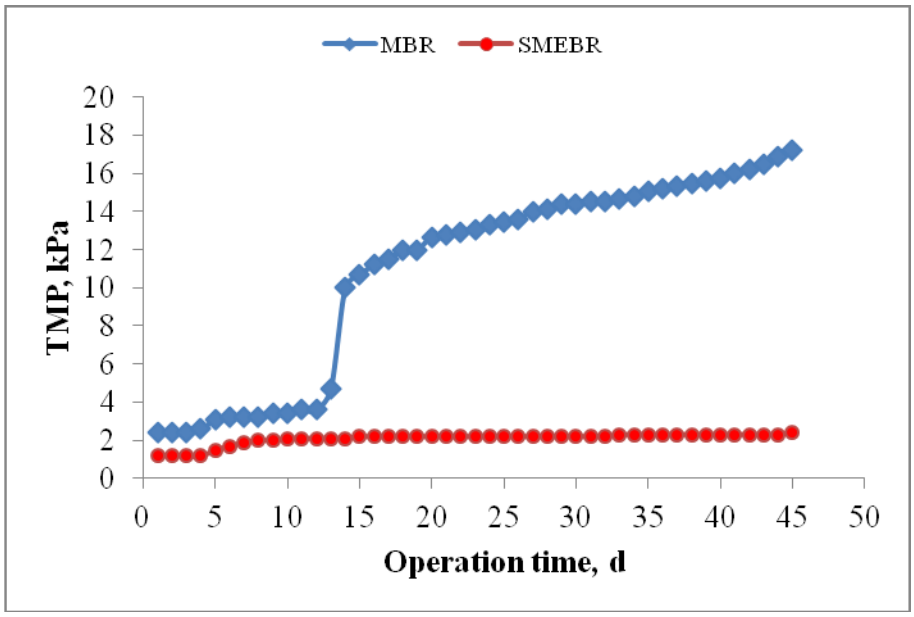

Fig. 5.7: Transmebrane pressure (TMP) variation in the pilot scale SMEBR and MBR.

Well designed laboratory and pilot SMEBR systems showed consistency in overcoming membrane fouling and the costly cleaning processes.

5.2.3 Sludge properties

5.2.3-1 Variation of mean particle size diameter

The results (Fig. 5.8) showed an increase in the mean particle size diameter (PSD) of the sludge flocs in MBR from 69 to 116 µm over the entire operation time. Contrary, SMEBR experienced an opposite phenomenon where the mean particle size diameter of the sludge flocs had decreased over time from 69 to 17.5 µm (75% reduction). This could be explained

according to the electroosmosis phenomenon occurred in SMEBR, through which the bound water was removed from the sludge flocs and hence reducing their size. Similar phenomenon was speculated to take place according to the results obtained from Phase 1 (Chapter 4). These findings were in line with the results of the membrane fouling (Fig. 5.7).

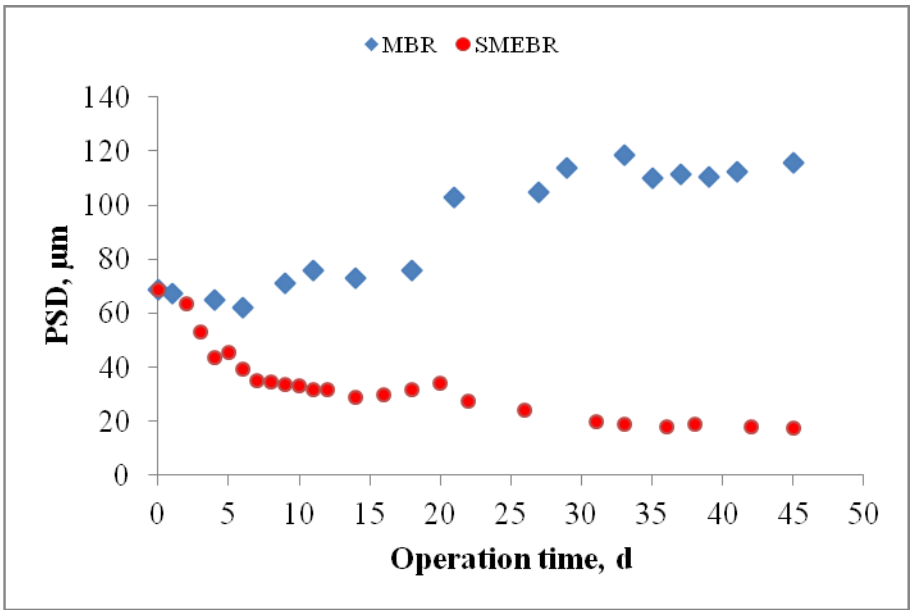

Fig. 5.8: Mean particle size diameter (PSD) variation in the pilot scale SMEBR and MBR.

5.2.3-2 Variation of mixed liquor suspended solids (MLSS)

Mixed liquor suspended solids (MLSS) had significantly increased (from 2400 to 5000 mg/L) in SMEBR compared to the increase observed in MBR (Fig. 5.9). This could be attributed to the inorganics and the chemical sludge produced due to the presence of electrokinetics in the system. This situation led to the reduction in the MLVSS/MLSS (Fig. 5.10). MBR experienced no significant increase in MLVSS due to operation under low SRT.

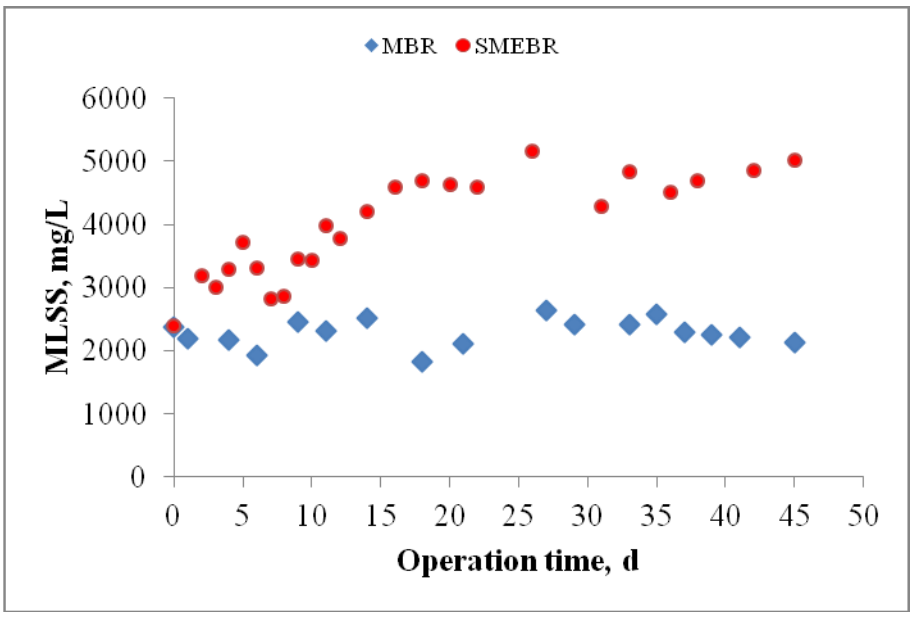

Fig. 5.9: MLSS variation in the pilot scale SMEBR and MBR.

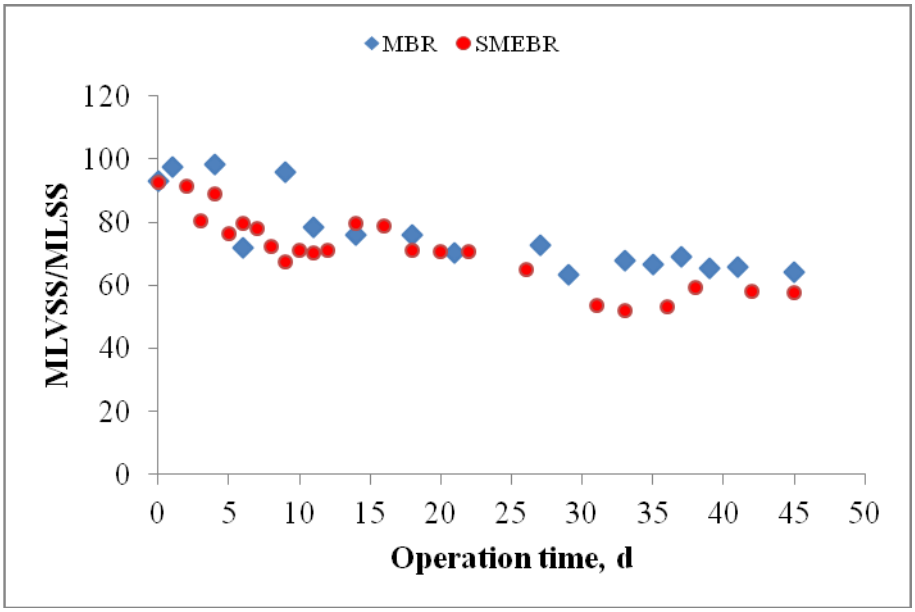

Fig. 5.10: MLVSS/MLSS variation in the pilot scale SMEBR and MBR.

5.2.3-3 Variation of soluble extracellular polymeric substances (soluble EPS)

It was observed that SMEBR was able to remove soluble EPS to larger extent than MBR (Fig. 5.11). Some 63% removal of soluble EPS_c was reported in SMEBR, whereas 21% removal of soluble EPS_c was noticed in MBR. These conclusions were in agreement with previous studies, which showed the influence of soluble EPS_c on membrane fouling. It was reported that membrane fouling had a linear correlation with soluble EPS_c concentration (Lesjean et al., 2005; Rosenberger et al., 2006). However, Drews et al. (2008) had not observed any linear correlation between soluble EPS_c and membrane fouling.

On the other hand, the average of the soluble EPS_p concentrations in SMEBR and MBR were 38.4 mg/L and 52.8 mg/L, respectively through which soluble EPS_p showed significant influence on membrane fouling. Similar findings were reported by other studies (Chang and Lee, 1998; Flemming and Wingender, 2003; Kim et al., 2006). Soluble EPS carried negative charges (Shin et al., 2001), where proteins were considered as major contributors to such an increase in the negative charges in the solution (Wilén et al., 2003). The presence of Al^{3+} ions (eq. 2.5) originating from the anode electrooxidation destabilized the soluble EPS, and thus neutralized the negative charges. It could be concluded that the electric field had significant impact on EPS_p and EPS_c. The increase in the concentration of EPS_p over time could be related to the concentration of proteins in the influent wastewater.

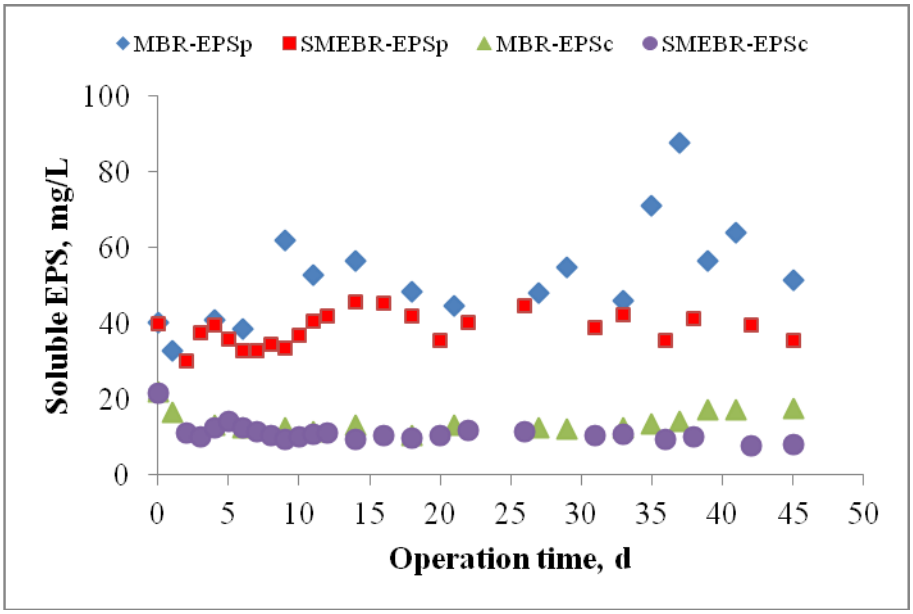

Fig. 5.11: Soluble EPS variation in the pilot scale SMEBR and MBR.

5.2.3-4 Variation of zeta potential

The results of zeta potential (Fig. 5.12) indicated that SMEBR enhanced flocs formation resulted from the electrokinetics phenomenon interacted with biological process as well as membrane filtration. The coagulation in MBR was at slower rate according to the slow changes in the magnitude of zeta potential (average -26.9 mV). However, the magnitude of zeta potential reduction (from -26.2 to -14.2 mV) in SMEBR indicated an enhancement of the agglomoration of the sludge flocs due to the presence of sufficient aluminum ions in the solution. DLVO theory (named after Derjaguin and Landau, Verwey and Overbeek) described the force between charged surfaces in a liquid medium, and combined the effects of van der Waals attraction and electrostatic repulsion. The aluminum ions generated from the anodic electrooxidation (eq. 2.5) destabilized the negatively charged colloids and according to DLVO theory changed net energy permitting van der Waals attraction forces to dominate, and hence the sludge flocs to coagulate. In addition and according to Smoluchowski's (eq. 5.7)

(Sze et al., 2003), the electrophoretic mobility of the particles was proportional to the electrophoretic velocity which was dependent on the strength of electric field. Particles moved relatively faster when they carried bigger charge.

$$v = \frac{\varepsilon_r \varepsilon_o (ZP) E}{\mu} \tag{5.7}$$

Where, v is the particle velocity, ε_r is the media dielectric constant, ε_o is the permittivity of free space, ZP is zeta potential, E is the applied electric field, and μ is the medium viscosity.

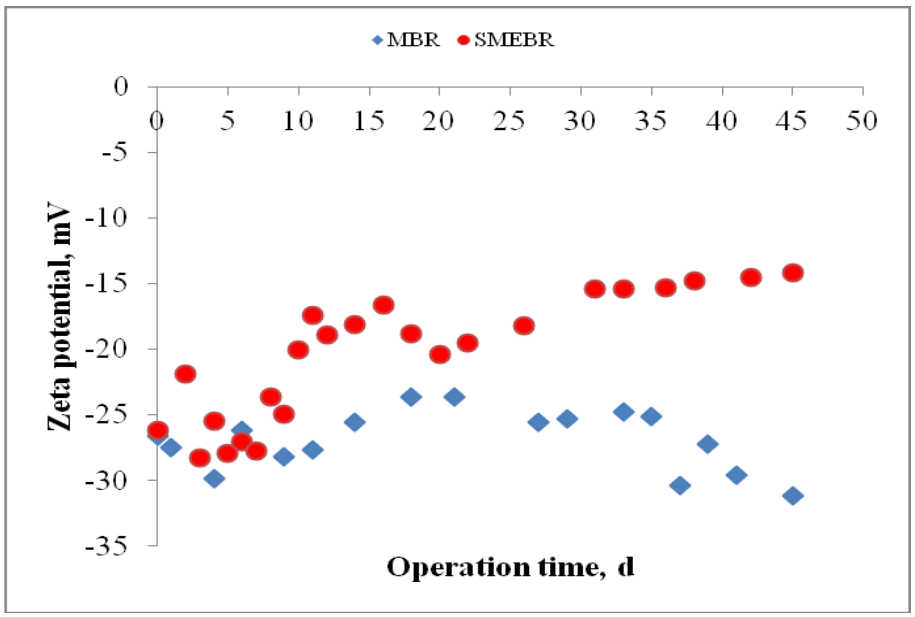

Fig. 5.12: Zeta potential variation in the pilot scale SMEBR and MBR.

5.2.3-5 Sludge volume index (SVI) and filterability

The sludge volume index (SVI) which represented the settleability of the sludge reached 119 mL/g in SMEBR, while 142 mL/g was found in MBR. It could be concluded that electrokinetics improved the settleability of the sludge by producing denser flocs with good settling properties as previously demonstrated in Phase 1 - Chapter 4. Considering that SVI

higher than 150 mL/g was associated with the growth of the filamentous microorganisms (Parker et al., 2001) and resulting in high effluent suspended solids and poor treatment performance, sludge in SMEBR showed much better properties.

Filterability test was used to measure sludge dewatering. It was noted that the dewaterability of the sludge had improved over the entire operation time. Time necessary to filter 100 mL of the sludge sample had decreased significantly (by 78%). It could be said that filterability in SMEBR was significantly enhanced due to the generation of the electroosmosis phenomenon. These results agreed with previous studies testing electrocoagulation cells and reported that the flocs generated due to electrocoagulation contained less bound water, had more shear resistance, and enhanced filterability (Mollah et al., 2004; Kurt et al., 2008).

The relationship between sludge filterability and flocs size was also investigated as the floc size had impact on the total particle surface area and the porosity formed from these particles, as a result had significant impact on the sludge dewaterability (Radaideh et al., 2010). Previous studies concluded that as the floc size decreased, the cake moisture content increased and the rate of filtration decreased. Yet, SMEBR results were not in agreement with Karr and Keinath (1978), Novak et al. (1988) and Radaideh et al. (2010); and showed a different behavior through which the sludge filterability was significantly enhanced when the size of the flocs had decreased.

5.2.4 Lifetime of aluminum anode and fate of aluminum in SMEBR

5.2.4-1 Lifetime of aluminum anode

Prior to SMEBR operation, aluminum anode was initially weighted. After 45 days of operation, it was cleaned in order to remove the insoluble inorganics deposited on the surface

of the electrode. The electrode was soaked 3 times in the CLR solution and rinsed with cold water. Air was also used to wash away any residuals. After drying, the final weight of the electrode was recorded. The loss in the electrode's material and electrode lifetime were therefore calculated using equations 5.8 and 5.9, respectively.

$$L_{Al} = (W_i - W_f) \quad (5.8)$$

$$t_e = (W_i * t_d)/(L_{Al}) \quad (5.9)$$

Where L_{Al}: aluminum loss (kg), W_i: aluminum electrode initial weight (kg), W_f: aluminum electrode final weight (kg), t_d: duration of experiment (d), t_e: electrode lifetime (d).

Thus, an average aluminum loss was 23 g/d and calculated electrode lifetime in similar operation conditions might be over 5 months (t_e). It was observed that SMEBR operated under adequate current density, and thus minimized electrodes consumption. The regeneration of a fouled electrode could be done by physical (water and air), and/or chemical cleaning.

5.2.4-2 Generation of aluminum ions

The relationship between the theoretical amount of aluminum generated in the reactor (eq. 2.5) to the exposure time and applied current could be expressed using Faraday's law (Mollah et al., 2004) - eq. 5.10.

$$\text{Theoretical } Al^{3+} \text{ ions generated} = \frac{ItM_w}{zF_aV} \quad (5.10)$$

Where I: applied current (A), t: electrolysis exposure time (s), F_a: Faraday's constant (C/mol), z: number of electron transfer, M_w: aluminum molecular weight (g/mol), V: volume of treated wastewater (m^3).

Thus,

Theoretical Al^{3+} ions generated = [(9.5 A) (480 min) (60 s/1 min) (26.98 g/mol)]/[(3) (96487 C/mol) (0.550 m^3) (10^3 g/kg)] = 0.051 kg Al/m^3 = 46 g Al/m^3

5.2.4-3 Fate of aluminum

The aluminum concentration was tested at different locations; influent, effluent, sludge supernatant, biomass, and electrodes (anode and cathode). It was found that aluminum entered SMEBR at a high concentration of 1.68 mg/l (or 924 mg/d as mass flow rate), and left at 0.36 mg/l (or 171 mg/d as mass flow rate) leading to 79% removal. Aluminum concentration in the sludge supernatant was 0.4 mg/l; same as in the treated effluent (i.e. SMEBR behaves similar to CSTR - continuous stirred tank reactor). The concentration of aluminum in wasted sludge; i.e. solid waste was measured (8 mg Al/l or 0.2 g Al/d as mass flow rate). Most importantly, the concentration of aluminum was measured in 0.1153 g and 0.2506 g samples of cathode and anode, respectively. Results showed 1401.3 mg Al/m^2 were deposited on the surface of the cathode whilst 402.7 mg Al/m^2 were observed on the surface of the anode. These results might indicate that the some of $AlPO_4$ were adsorbed at higher extends on the surface of the cathode where more phosphorus was also found (illustrated earlier in phosphorus removal – Fig. 5.5, Section 5.2.1).

These findings concluded that SMEBR is considered as a “self-purification” unit through which most of the aluminum ions produced due to electrokinetics were retained in the reactor, and they were not discharged with the effluent.

5.2.5 Fate of metals in SMEBR

The fate of metals in SMEBR system was investigated. Subsequently, samples: a) in the influent at the last phase of pilot tests, b) in effluent coming out of membrane module, c) of

the depositions on both electrodes), d) and in the wasted sludge were collected and analyzed for major metals (Al, P, Ca, Fe, Cu, Zn, Cd, Co, Sr, Pb, Ni, Hg, Mn, As, K and Cr).

5.2.5-1 Metals in influent and treated effluent

Samples from influent and treated effluent streams were collected at the last stage of SMEBR pilot test. They were digested with 4% nitric acid (HNO_3) for 24 h, and then an Atomic Absorption Spectrometer (Perkin Elmer, Analyst 100) was used to analyze major metals (Ni, Pb, Cd, Cu, Fe, Ca, Mg and Zn) present in both samples. All readings were repeated three times for each sample and average values were reported in Table 1. The results showed that SMEBR without any additional unit was able to remove undesirable metals from wastewater (Table 5.2). High removal rates of Pb (100%), Ni (98.1%), Cu (100%), and Cd (94.6%) were reported at this range of pH (8-9) with very low concentrations in the treated effluent (0.0, 0.24, 0.0 and 0.04 mg/L for Pb, Ni, Cu, and Cd, respectively), while the removal rates of Mg, Zn, and Fe were 87.5%, 80.4%, and 85%, respectively. SMEBR produced a very high quality effluent where the concentrations of Ca, Mg, Zn, and Fe in the treated effluent were significantly low (0.0, 0.009, 0.09, and 0.27 mg/L, respectively).

Table 5.2: Average concentrations of metals in influent and SMEBR treated effluent streams

Contaminant	Influent, mg/L	Effluent, mg/L	Removal efficiency %
Pb	0.009	0.0	100
Cu	0.05	0.0	100
Ni	12.5	0.24	98.1
Cd	0.75	0.04	94.6
Mg	0.072	0.009	87.5
Zn	0.46	0.09	80.4
Fe	1.8	0.27	85
Ca	5.9	0.0	100

Metals such as calcium, nickel, cadmium, copper, chromium and zinc are non-biodegradable and very toxic constituents when they present in wastewater treated effluents. Therefore, many researchers have suggested several treatment processes to remove metals from wastewater such as biosorption (Senthikumar et al., 2010), ion exchange (Inglezakis et al., 2003), chemical precipitation (Kurniawan et al., 2006), electrodialysis (Marder et al., 2004), and electrocoagulation (Dermentzis et al., 2011).

The pH in SMEBR system did not change noticeably (around 8-9) as the generated OH^- ions at the cathode were consumed by the aluminum ions generated at the anode, consequently forming the desired $Al(OH)_3$ flocs. The removal of metals was associated with the solution pH, and previous studies reported the impact of the solution pH on the removal efficiency (Maleki et al., 2009; Hemambika et al., 2011). Shama et al. (2010) reported that the removal of metal ions was pH dependent as the adsorption capacity increases with increasing the pH value of the solution, and at a particular pH the order of increasing the removal percentage was $Cu^{2+} < Cr^{3+} < Cd^{2+} < Zn^{2+} < Pb^{2+} < Fe^{3+}$. At low pH, poor removal rates were reported as the hydrogen ions were dominants over the metal hydrolysis products, whereas at high pH hydroxide ions would compete with organic compounds for metal adsorption sites and the precipitation of the metal hydroxides. These findings were in line with Dermentzis et al. (2011) who investigated the removal of metals using electrocoagulation, and reported low removal rates of Ni^{2+}, Zn^{2+}, Cu^{2+} at low pH (less than 2), while more than 97% removal efficiencies were reported in the pH range of 4-9.

The removal of metals in SMEBR could be also attributed to the large number of the negatively charged functional groups in EPS matrix (Liu et al., 2001; Sheng et al., 2005; Bhaskar and Bhosle, 2006) which could form multiple complexes with many metals and as a

result had a significant impact on geochemical behavior, bioavailability and toxicity of heavy metal ions (Selck et al., 1999).

5.2.5-2 Fate of metals in wasted sludge (biosolids)

Metals in treated sludge (biosolids) were also measured in order to see if the sludge produced by SMEBR system can be used as a fertilizer or it should undergo further treatment processes before discharging to the surrounding environment. At the last day of the SMEBR pilot testing, a sample from the sludge waste was collected and dried at 105^{o}C for 24 h to extract water from sludge. Then, the solid sample was ground to fine powder which was later injected in the NITON XRF analyzer to detect all metals present in the sludge waste. The sludge analysis was repeated two times and average values in mg/kg dry weight were reported in Table 5.3.

It could be observed that the sludge produced by SMEBR system contained some of the micronutrients metals within acceptable levels necessary to plants and animals according to Quebec regulations. These included Zn (1013 mg/kg), Cu (191.4 mg/kg), Co (33.5 mg/kg), and Ni (4.9 mg/kg). On the hand, other toxic metals in the influent did not precipitate with the sludge (eg. Pb, Cr, As, K, Cd, Mo, Se, and Sc). The formation of aluminum hydroxide $Al(OH)_3$ flocs within SMEBR system would have the tendency to act as biosorbents and therefore would enhance the absorption of the metal ions. Additionally, the production of hydrogen gas within SMEBR system (due to electrokinetics) could have enhanced the reduction of several metals to other sequestered products (Nerenberg, 2005). For example, Selenate (SeO_4^{2-}), which occurred naturally in certain mineral deposits, could be reduced to less mobile selenide (Se^{2-}) or elemental selenium (Se).

While some metal compounds are essential to animals and humans, others are known to be toxic and the environmental impact of many of them had to be elucidated. For example, sewage sludge contained high concentrations of potentially toxic elements such as Zn, Ni, Cd, and Cu would cause serious problems when sludge was applied to an agricultural land (Sanders et al., 1986; Sanchez-Monedore et al., 2004; Madyiwa et al., 2002). Excessive accumulation in soils over the long term might result in toxicity to plants, animals and humans. However, copper, cobalt, molybdenum and zinc (and possibly nickel and selenium) were plant micronutrients, and their presence might be useful in compost and required by animals and humans (Webber and Singh, 1995).

Table 5.3: Average concentrations of metals in wasted sludge (biosolids)

Element	Concentration in mg/kg in dry waste sludge
Fe	2345
Ca	23200
P	450
Cu	191.4
Zn	1013
Pb	0
Hg	11.1
Cr	0
Mn	160.6
As	0
Ni	4.9
Sr	107.2
K	0
Cd	0
Co	33.5
Sc	0
Mo	0
Se	0

Guidelines for the beneficial use of fertilizing residuals, as direct application to land or offered for sale as fertilizers, in Québec are shown in Table 5.4. Two categories were classified as C1 and C2. For a compost to meet the unrestricted use category, it must meet the guidelines of Category C1 for all contaminants. If the compost failed one criterion of the guideline for C1 but would meet the criteria for the Category C2 use, then it was classified as a Category C2 product.

Table 5.4: Concentrations of trace elements in Compost in Québec – Category C (Guide sur la valorisation des matières résiduelles fertilisantes, 2008)

Contaminant	**Category C1:** *Maximum concentration within product (mg/kg dry weight)*	**Category C2:** *Maximum concentration within product (mg/kg dry weight)*
Essential to plants and animals		
Arsenic (As)	13	41
Cobalt (Co)	34	150
Chromium (Cr)	210	1060
Copper (Cu)	400	1000
Molybdenum (Mo)	5	20
Nickel (Ni)	62	180
Selenium (Se)	2	14
Zinc (Zn)	700	1850
Strict contaminants		
Cadmium (Cd)	3	10
Mercury (Hg)	0.8	4
Lead (Pb)	150	300

Several methods were used to remove metals from the contaminated sludge, however, were not completely sufficient. Examples were: the chemical extraction process through the addition of inorganic acids (H_2SO_4, HCl, and HNO_3), organic acids (citric and oxalic), chelating agents (EDTA and NTA). The removal mechanism was achieved by precipitation followed by settling or by ion exchange system. The addition of those acids would decrease the pH in order to achieve the desired removal rates, yet it was not satisfactory as the maximum removal rates of Cd, Cr, Fe, Ni and Zn were about 70% (Jenkins and Scheybeler, 1981). Another common approach to deal with metal contaminants was metal stabilization using lime amendments (Wong, 1999); however, lime treatment was not a permanent solution as the metals could potentially resolubilize if the pH decreased significantly. Electrokinetics, on the other hand, is a new approach to treat contaminated sludge from metals (Elektorowicz and Oleszkiewicz, 2009; Elektorowicz et al., 2007). Habel (2010) reported mean removal levels of over 54 %, 30 %, and 24 % for metals such as Zn, Cd, and Pb, respectively, within a period of 3 d when applying electrokinetics to contaminated sludge.

Consequently, when SMEBR system is compared to other available methods, it could be summarized that the interaction between biological process, membrane filtration and electrokinetics in SMEBR system had significant impact; being capable of removing different metals at desired rates. All levels of investigated metals were below the guidelines outlined in Table 5.4; yet for mercury, and therefore the sludge produced during the treatment process using SMEBR system could be used as fertilizers and applied to agricultural lands after reducing the level of mercury in it using phytoremediation for instance.

5.2.5-3 Metals in electrode deposits

Samples of deposits on the surface of the anode and the cathode were analyzed for the chemical constituents using NITON XRF analyzer (Table 5.5). At the end of the pilot test, samples of deposits on both electrodes were collected from different locations separately. Concentrations of metals were assumed similar over the entire surface of each electrode. Thus, samples from different parts of each electrode were mixed where the new sample (mixed) was ground to a fine powder and finally injected into NITON XRF analyzer.

Table 5.5: Average concentrations of chemical constituents of electrodes deposits

Element	Concentration in mg/kg at anode	Concentration in mg/kg at cathode
Fe	251.9	355.1
Ca	868.2	236300
Al	1065.5	2432.8
P	11.72	197.4
Cu	76	315.1
Zn	117.3	370.8
Pb	14.8	10.7
Hg	5.5	56.2
Cr	51.1	166
Mn	0	418
As	7.6	7
Ni	131.7	109.5
Sr	0	1022
K	0	12400
Cd	9.7	24.7
Co	0	268.6
Sc	0	1943
Mo	7.8	6.9
Se	6.7	30.8

The results of analysis (Table 5.5) showed much higher deposition (eg. more than 270 times in case of Ca) of metals on the cathode, with exception of Co, Sr, Mn, K, which were entirely deposited on cathode surface. Results showed that metals such as Ca (868.2 mg/kg), Ni (131.7 mg/kg), and Zn (117.3 mg/kg) were the main constituents found on the surface of the anode while Cr (51.1 mg/kg), Pb (14.8 mg/kg) and Cd (9.7 mg/kg) were reported in very low concentrations. On the other hand, metals such as Ca (236300 mg/kg), Mn (418 mg/kg), Sr (1022 mg/kg), K (12400 mg/kg), Co (268.6 mg/kg), Sc (1943 mg/kg), Ni (109.5 mg/kg), Cu (315.1 mg/kg), Zn (379.8 mg/kg), Cr (166 mg/kg), and Cd (24.7 mg/kg) were reported at higher fractions on the surface of the cathode indicating that most of these metal hydroxides were precipitated and deposited on the surface of the cathode and thus removed from the treated wastewater.

When DC voltage was applied, the transportation of polar molecules towards the electrodes was expected through electromigration phenomenon. Table 5.5 showed that the cationic forms were prevalent in DC field. Furthermore, metal complexes found adequate conditions to precipitate in reducing conditions (presence of OH^- and H_2 gas) produced by the stainless steel cathode. Therefore, the hydroxide ions produced under electrical field would react with metals and insoluble metal hydroxides such as $Ni(OH)_2$, $Zn(OH)_2$, $Pb(OH)_2$, $Cd(OH)_2$, and $Cr(OH)_3$ might have precipitated or deposited on the surface of the electrodes. These metals hydroxides were insoluble in water with very low solubility products (K_{sp}) at 25^{o}C of $2x10^{-15}$, $1.2x10^{-17}$, $1.2x10^{-5}$, $2.5x10^{-14}$, and $2x10^{-16}$, respectively.

Chromium, on the other hand, might be present in the solution as hexavalent Cr^{6+} and hence the removal mechanism could somehow be different and based on the reduction of Cr^{6+} to Cr^{3+} at the cathode, followed by the reaction with OH^- ions at alkaline conditions (eqs

5.11 and 5.12). The $Cr(OH)_3$ precipitate would form and deposit on the surface of the electrodes.

$$Cr_2O_7^{2-} + 6e^- + 7H_2O \rightarrow 2Cr^{3+} + 14OH^- \quad (5.11)$$

$$CrO_4^{2-} + 4H_2O + 3e^- \rightarrow Cr(OH)_3 + 5OH^- \quad (5.12)$$

In addition, the results of Cu, Zn, Pb, Cd, Hg, and Ni (Table 5.5) showed presence of these metals on both electrodes (anode and cathode) with tendency to deposit on the surface of the cathode. Thus, these metals could be partially removed via direct electroreduction at the cathode or by electroless deposition at the anode (see eq. 5.13 for Zn as an example).

$$3Zn^{2+} + 2Al \rightarrow 3Zn + 2Al^{3+} \quad (5.13)$$

It was reported that the electroless deposition occurred mainly at the anode where, due to electrodissolution, the aluminum surface was more active than that of the cathode (Emamjomeh and Sivakumar, 2009).Yet in this study more metals were deposited on the surface of the cathode rather than on the surface of the anode.

Other complexes might have also formed in the presence of phosphorus. Examples are $Zn_3(PO_4)_2$, $Pb_3(PO_4)_2$, and $Ni_3(PO_4)_2$.. Organometallic compounds would have possibly generated according to the detected elements (Table 4). Examples are: organonickel compound $Ni(CO)_4$ where in the presence of hydroxides, clusters such as $[Ni_5(CO)_{12}]^{2-}$ and $[Ni_6(CO)_{12}]^{2-}$ are formed. Other cationic and anionic metal carbonyls might exist in the deposits such as $[Mn(CO)_6]^+$, $[Fe(CO)_6]^{2+}$, and $[Fe(CO)_4]^{2-}$.

Inorganic fouling in MBR was investigated and several studied reported that the presence of metal ions such as calcium would increase scaling problems, decrease the

permeate flux and thus enhance membrane fouling (You et al., 2006). The results of this study revealed that the presence of the stainless steel cathode in SMEBR system hindered the movement of the inorganic hydroxides or any other compounds towards the surface of the membrane and thus might also prevent fouling. These conclusions were in agreement with the membrane fouling results (Fig. 5.7) through which SMEBR showed no fouling over the entire period.

5.2.6 Fate of phosphorus in SMEBR

The complete removal of phosphorus in SMEBR, besides biologically by the living microorganisms, could be attributed to electrokinetics. It was shown earlier that phosphorus was found in significant amount on the electrodes deposits, mainly on the surface of the cathode (197.4 mg/kg). Consequently, it was speculated that phosphorus might have formed different chemical complexes at the surface of the cathode. Divalent cations were generally known to improve the microbial flocculation due to formation of bridges with extracellular polymeric substances. It was reported that calcium had an important role in the formation of bioflocs (Mashhad, 2010; Song et al., 2008). Since calcium was the most divalent cation present in the analyzed samples of the deposits formed on the surface of the electrodes; the author suggested that many chemical compounds could be generated.

Accordingly, it could be deduced that phosphorus might have created strong bonds with other cations such as magnesium, ammonium and potassium to form several complexes such as calcium phosphate (eq. 5.14), struvite (magnesium, ammonium and phosphate), and K-struvite (magnesium, potassium and phosphate). Crystallization (i.e. controlled precipitation of desired substances in crystal forms (Giesen, 1999)) of phosphorus was essential so as to enhance the recovery of phosphorus from such complexes, and

therefore creating new sources of phosphate, moving phosphorus towards sustainability, as well as reducing the sludge production and the associated disposal cost (Jeanmaire and Evans, 2001; Forrest et al., 2008). Efforts were gathered to supply phosphate fertilizers of the desired quantity and quality to farmland areas where agriculture fertilizers and animal feed used 85% of the world's phosphate supply while detergents used 12%.

$$Ca_3(PO_4)_2 \longleftrightarrow 3Ca^{2+} + 2PO_4^{3-} \qquad (5.14)$$

It was reported that calcium phosphate, struvite, and K-struvite were insoluble in alkaline pH (Borgerding, 1972; Nelson et al., 2003). Calcium and phosphate were found in SMEBR system (Table 4) and therefore many forms of calcium phosphates such as dicalcium phosphate $CaHPO_4.2H_2O$, tricalcium phosphate $Ca_3(PO_4)_2$, octocalcium phosphate $Ca_4H(PO_4)_3.2.5H_2O$, Monetite $CaHPO_4$, Brushite $CaHPO_4.2H_2O$, and hydroxyapatite $Ca_5(PO_4)_3OH$ (Nancollas, 1984) could have been generated and deposited on the surface of the electrodes, particularly, on the surface of the cathode. It was reported that the formation of calcium phosphate salts depended on the solution composition and pH (Valsami-Jones, 2001). It was reported that any calcium phosphate precipitated would probably transform into the thermodynamically more stable hydroxyapatite (Kibalczyc, 1989) which was considered as the prevalent form of calcium phosphate in the environment and in the bio-minerals (Skinner, 2000).

In addition, dicalcium phosphate, tricalcium phosphate, octocalcium phosphate, Monetite and Brushite might be the precursor phase where they would precipitate and eventually recrystallize to form hydroxyapatite (Kibalczyc, 1989; Nancollas, 1984). For example, tricalcium phosphate was a precursor resulting in the formation of hydroxyapatite when pH was greater than 7 (Bosky and Posner, 1973). A three stage formation of

hydroxyapatite starting with the formation of tricalcium phosphate followed by octocalcium phosphate had also been suggested. Kibalczyc et al. (1990) noticed that the formation of hydroxyapatite was a resultant of the transformation of tricalcium phosphate to another at pH range of 7 to 9. Calcium phosphate salts might form in SMEBR system as it created alkaline conditions (pH between 8 and 9), and could be recycled into industrial processes or undergone further processing to be used as fertilizers (Alamdari and Rohani, 2007).

Phosphate might have also reacted also with magnesium and ammonium forming magnesium-ammonium phosphate "struvite-$MgNH_4PO_4.6H_2O$" (Schulze-Rettmer, 1991), a precipitates which could be directly used as fertilizers (de-Bashan and Bashan, 2004). It crystallized according to equation 5.15.

$$Mg^{2+} + NH_4^+ + HPO_4^{2-} + OH^- + 6H_2O \rightarrow MgNH_4PO_4.6H_2O + H_2O \qquad (5.15)$$

K-struvite ($MgKPO_4.6H_2O$) was similar to struvite with small structural changes and thus could be another source of phosphorus recovery (Mathew and Schroeder, 1979). Struvite and K-struvite were slightly soluble in water, where the solubility product of struvite is between 10^{-10} and $10^{-13.3}$ (Burns and Finlayson, 1982; Taylor et al., 1963), while the solubility product of K-struvite was $2.4x10^{-11}$ (Taylor et al., 1963).

Other possible reactions could take place and contribute to the complete removal of phosphorus. It could be postulated that phosphorus might have reacted with other metals present in the deposits (see Table 5.5) and formed other complexes such as lazulite $MgAl_2(PO_4)_2(OH)_2$, grandallite $CaAl_3(PO_4)_2(OH).5H_2O$, scorzalite $Fe^{2+}_{0.75}Mg_{0.25}Al_2(PO_4)_2(OH)_2$, bearthite $Ca_2Al(PO_4)_2(OH)$, variscite $AlPO_4.2H_2O$, brazilianite $NaAl_3(PO_4)_2(OH)_4$, and wavellite $Al_3(PO_4)(OH)_3.5H_2O$ (Frossard et al., 1996). Pearson's Crystal Data software was used to predict the possible combinations which might rise from

the existence of specific chemical constituents in the deposits. Examples were $Al_4Ca_4[H_2O]_{12}Mg[OH]_4[PO_4]_6$ and $Al_{0.18}Ca_2Fe_{4.26}[H_2O]_2Mg_{0.96}Mn_{0.6}Na[PO_4]_6$.

The foregoing results agreed with the results of membrane fouling (Fig. 5.7). Struvite, for example, was considered as a major foulant in anaerobic MBR through forming a white precipitate on the surface of the membrane and thus increasing the rate of fouling (Choo and Lee, 1996). Yet, SMEBR showed tendency towards generating and forming such inorganic compound on the surface of the cathode which again acted as an efficient barrier preventing the flow of any organics or inorganic complexes towards the membrane pores.

It could be concluded that the removal mechanisms of several metals could be attributed to the precipitation of the metal hydroxides, absorption to sludge flocs, or deposited on the surface of the electrodes, mainly on the surface of the cathode.

5.2.7 General conclusions from the operation of pilot SMEBR

SMEBR obtained excellent water quality in term of COD and nutrients removal, as well as enhanced sludge settleability and filterability (Fig. 5.13). Membrane fouling was significantly eliminated during the operation. In spite that SMEBR generated metal ions into the bulk solution; aluminum did not leave with the treated effluent, and was present in small amounts in the wasted sludge. Most of the aluminum was retained on the surface of the electrodes. The electrodes did not require any physical or chemical cleaning during the operation and it was predicted that the aluminum anode would last for five months whereas the stainless steel cathode would last much longer (one year at minimum prediction). Detailed design and technological parameters were determined and showed adequate microbial activity, preventing inhibitory conditions in the electrical field.

(a) (b) (c)

Fig. 5.13: (a) Raw (influent) wastewater, (b) SMEBR treated effluent, (c) SMEBR treated sludge.

5.3 Stage 3: <u>Objective:</u> Impact of activated sludge properties on transmembrane pressure (TMP) in SMEBR and MBR

Stage 2 demonstrated the significant difference in membrane fouling between SMEBR and MBR pilot systems through which the lack of membrane fouling in SMEBR system was a significant accomplishment. Therefore, the specific objective of Stage 3 was to investigate the difference in performance between SMEBR and MBR at a pilot scale with regard to the physical, chemical and biological changes of the sludge properties while DC electrical field was implemented. This comparative study was based on a statistical analysis illustrated in Chapter 3 - Section 3.3. It was used to investigate the impact of the sludge properties on membrane fouling (indicated by the change in TMP) in SMEBR and MBR. The transmembrane pressure (TMP) was selected as a fouling indicator. Since SMEBR is a complex system and interactions among the sludge properties have not been yet fully

understood, a statistical approach was implemented to assess the impact of sludge properties on TMP as well as reciprocal interactions among the physical-chemical and biological properties of sludge in SMEBR and submerged MBR. It was found that many physical, chemical, and biological sludge parameters contributed to the membrane fouling, more importantly, to change in the transmembrane pressure (TMP). Table 5.6 showed the results obtained from statistical analyses of these parameters for SMEBR and MBR.

Table 5.6: Pearson`s correlation coefficient (r_p) for linear correlations between TMP and sludge properties in SMEBR (bold) and MBR

	TMP kPa	PSD µm	MLSS mg/L	EPS_c mg/L	EPS_p mg/L	Visc. mPa.s	Zeta Potential mV	σ_{sludge} µS/cm	σ_{in} µS/cm	T °C
TMP, kPa	1									
PSD, µm	**-0.9205** 0.9182	1								
MLSS, mg/L	**0.7757** 0.1940	**-0.7844** 0.3215	1							
EPS_c, mg/L	**-0.6118** 0.3051	**0.6895** 0.3550	**-0.5312** -0.0516	1						
EPS_p, mg/L	**0.3448** 0.4856	**-0.3362** 0.4630	**0.4961** 0.3776	**0.0160** 0.0967	1					
Visc., mPa.s	**-0.6629** -0.4726	**0.5290** -0.3933	**-0.4427** -0.0173	**0.4400** 0.1243	**-0.0202** -0.3530	1				
Zeta Potential, mV	**0.7931** 0.0796	**-0.7611** -0.0225	**0.8246** 0.0409	**-0.5130** -0.5903	**0.4811** -0.2948	**-0.5239** 0.1285	1			
σ_{sludge}, µS/cm	**-0.4250** -0.3349	**0.4347** -0.4361	**-0.2879** -0.1049	**0.5124** -0.2530	**0.0785** -0.0927	**0.4008** 0.0813	**-0.3538** -0.0802	1		
σ_{in}, µS/cm	**-0.1231** -0.1111	**0.0848** -0.1392	**-0.2175** 0.1795	**0.2531** 0.1485	**-0.1864** 0.0883	**0.2224** -0.0444	**-0.2230** -0.1978	**0.7363** 0.7460	1	
T, °C	**-0.6172** 0.3489	**0.7145** 0.3222	**-0.7495** 0.3233	**0.5488** -0.1990	**-0.3095** -0.1034	**0.3279** -0.2557	**-0.7621** 0.4443	**0.4958** -0.2131	**0.3375** -0.2607	1

Note: Results generated from SMEBR are shown in bold

5.3.1 Impact of mean particle size diameter (PSD) on membrane fouling

The TMP in SMEBR was found to correlate strongly, inversely, to the PSD (r_p = -0.9205) (Fig. 5.14, Table 5.6). As the particle size decreased the TMP increased, which could be attributed to the deposition of the small colloids on the membrane surface (Itonaga et al., 2004). Table 5.2 showed that the mean PSD had a more significant contribution to membrane fouling than the rest of the sludge properties, namely MLSS: r_p = 0.7757, Zeta Potential: r_p = 0.7931, viscosity: r_p = -0.6628, EPS_c: r_p = -0.6118.

In the case of conventional MBR configuration a strong direct correlation to the mean PSD was observed (r_p = 0.9182), indicating that as the sludge particles coagulated (forming bigger particles which as a result migrate away from the membrane surface); the permeate flux increased, yet TMP slightly increased. Results from statistical analysis agreed with experimental results shown earlier in Fig. 5.7.

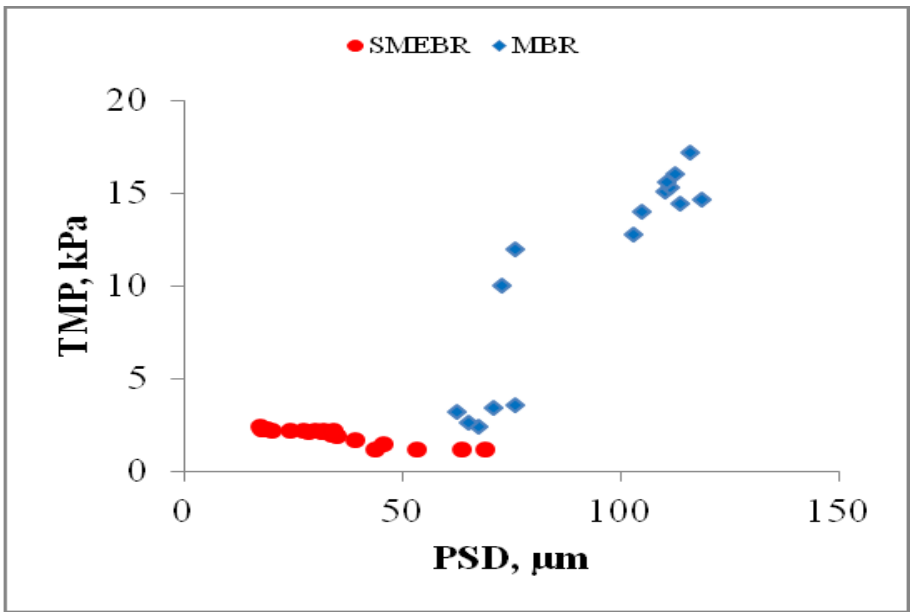

Fig. 5.14: Effect of mean particle size diameter on TMP.

5.3.2 Impact of soluble EPS on membrane fouling

As it was illustrated in Chapter 2, extracellular polymeric substances (EPS) were secreted by microorganisms and accumulate on cell surfaces (Tsuneda et al., 2003; Liu and Fang, 2002), and consist of carbohydrates, proteins, nucleic acids, humic substances, and ionisable functional groups such as carboxylic, phosphoric amino and hydroxyl groups (Tsuneda et al., 2003; Guibaud et al., 2008). Table 5.6 showed that TMP was influenced by the soluble carbohydrates (EPS_c) and soluble proteins (EPS_p). In this study, SMEBR showed a moderate inverse correlation between TMP and EPS_c (r_p = -0.6118) and a very weak direct correlation to EPS_p (r_p = 0.3448). This would infer that EPS_p contributed to membrane fouling more than EPS_c.

EPS_p (r_p = 0.4856) in MBR had more significant impact on membrane fouling than EPS_c (r_p = 0.3051). This conclusion agreed with several studies, which have reported that the composition of EPS, in particular, proteins (EPS_p) and carbohydrates (EPS_c) contributed to membrane fouling (Nagaoka et al., 1998, Flemming and Wingender, 2003;, Kim et al., 2006), and conversely, disagreed with other studies which have ignored the influence of soluble EPS on membrane fouling (Lee et al., 2003; Cho and Fang, 2002).

5.3.3 Impact of zeta potential (ZP) and sludge viscosity (SV) on membrane fouling

Zeta potential (ZP) measurements reflected the surface charge of sludge particles and flocs. Zeta potential in SMEBR had significantly affected the TMP (Fig. 5.15, Table 5.6). TMP in SMEBR had a direct strong correlation with ZP as the particles in the sludge coagulated their ZP decreased and therefore TMP decreased (r_p = 0.7931).

MBR experienced a different behavior where zeta potential had no correlation with TMP meaning that the coagulation process in MBR was slower. This could also be inferred from weak correlations between zeta potential and other sludge properties such as MLSS (r_p = 0.0409), temperature (r_p = 0.4443), and PSD (r_p = -0.0225). Results from statistical analysis agreed with experimental results shown earlier in Fig. 5.12.

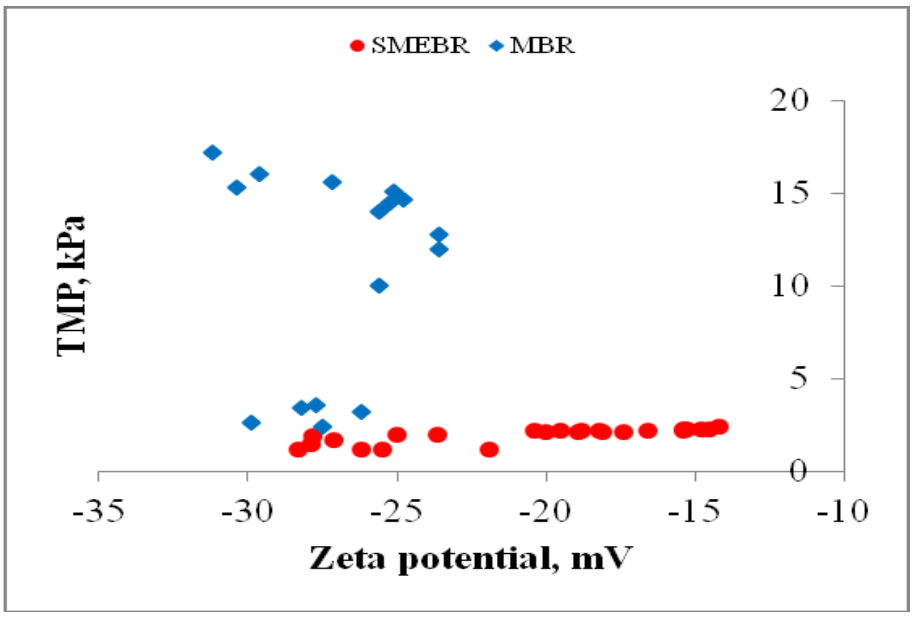

Fig. 5.15: Effect of zeta potential on TMP.

According to Smoluchowski (eq. 5.7), zeta potential was directly proportional to the particle's (electrophoretic) velocity and medium viscosity, while on the other hand ZP and the electric field were inversely proportional. In this study, the samples used to measure ZP were taken from the sludge supernatant at different locations, mostly in front of the membrane in SMEBR and MBR. Viscosity of the sludge did not change and therefore could be negligible. ZP was measured by tracking the motion of the particles in a DC voltage field which was referred to the electrophoretic mobility. The electrophoretic mobility was proportional to the electrophoretic velocity which was dependent on the strength of electric

field or voltage gradient. Generally speaking, the bigger the charge the particles carried, the faster they moved. More importantly, the voltage gradient in SMEBR (operated at constant current density) was also dependent on the incoming raw wastewater conductivity (σ_{in}). It was observed that the higher the conductivity, the less the voltage gradient which made SMEBR to be strongly conductivity-dependent. Consequently, a direct relationship between zeta potential and the electric field was observed.

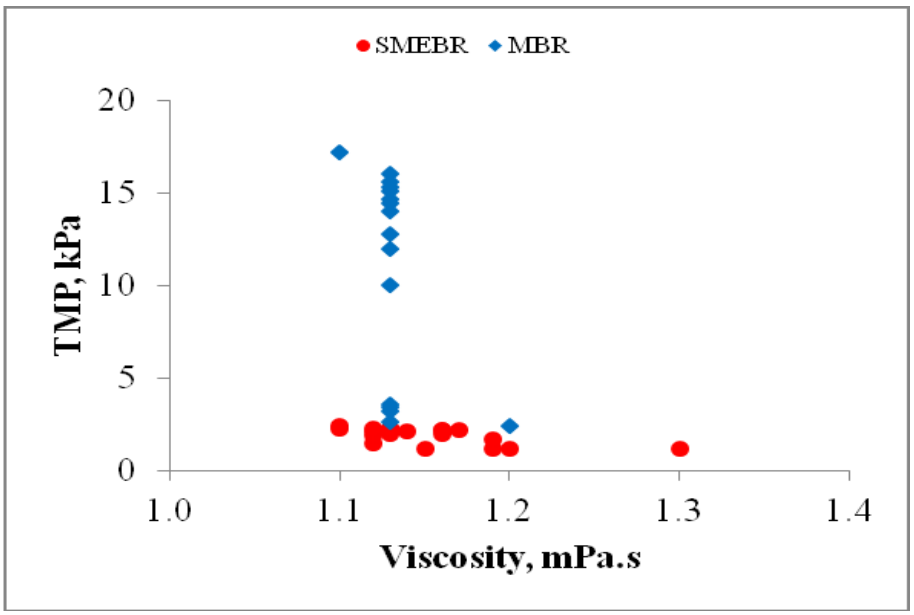

Fig. 5.16: Effect of sludge viscosity on TMP.

On the other hand, the coagulation process in MBR was achieved at a slower rate than SMEBR. It could be concluded that due to electrokinetics SMEBR enhanced flocs formation and improved coagulation. This could also be noted from the strong correlations (r_p = -0.7611) between ZP and PSD in SMEBR and weak correlation between ZP and PSD in MBR (r_p =, -0.0225).

An inverse strong correlation was obtained between TMP and sludge viscosity in SMEBR (r_p = -0.6628) whilst an inverse moderate correlation was obtained between TMP and sludge viscosity in MBR (r_p = -0.4726) as shown in Fig. 5.16 and Table 5.6. Thus, as the sludge viscosity increased, the permeate flux decreased which would lead to TMP increase. It was assumed that EPS_c in SMEBR has increased the sludge viscosity as a moderate direct correlation was obtained (r_p = 0.4400), yet, it showed no correlation to sludge viscosity in MBR (r_p = 0.1243). SMEBR findings confirmed several studies (Monteiro, 1997), which identified the sludge rheological properties to be related to solid concentration and sludge nature (particle size, surface charge, degree of hydration, and cohesion of flocs of agglomerated particles in colloidal suspension). Results from this study were also in accordance with other works (Chang et al., 2001; Günder , 2001), which reported that soluble microbial products, extracellular polymer and filamentous microorganisms had a significant influence on sludge viscosity.

5.3.4 Impact of mixed liquor suspended solids (MLSS) on membrane fouling

SMEBR did not experience any membrane fouling despite the increase in MLSS, contrary to MBR where the transmembrane pressure had increased as shown earlier in Figs 5.7 and 5.9. This study (Fig. 5.17, Table 5.6) showed that TMP had a strong direct correlation to the sludge MLSS (r_p = 0.7757). The increase in MLSS was related to the generation of monomeric and polymeric aluminum complexes in the sludge suspension during electrokinetics process. SMEBR results agreed with several studies which reported the influence of MLSS in MBR on membrane fouling (Chang and Kim, 2005). Consequently, changes in the hydrodynamic and the shear stress at the filtration cake surface would occur (Stephenson et al., 2000). It was reported that the cake resistance had decreased with MLSS

concentration. It was also found that the specific cake resistance increased as the MLSS concentration decreased. It was previously reported for MBR (Meng et al., 2006) that the increase in MLSS may lead to more sludge particles, colloids, and macromolecular matter which resulted in an increased membrane fouling.

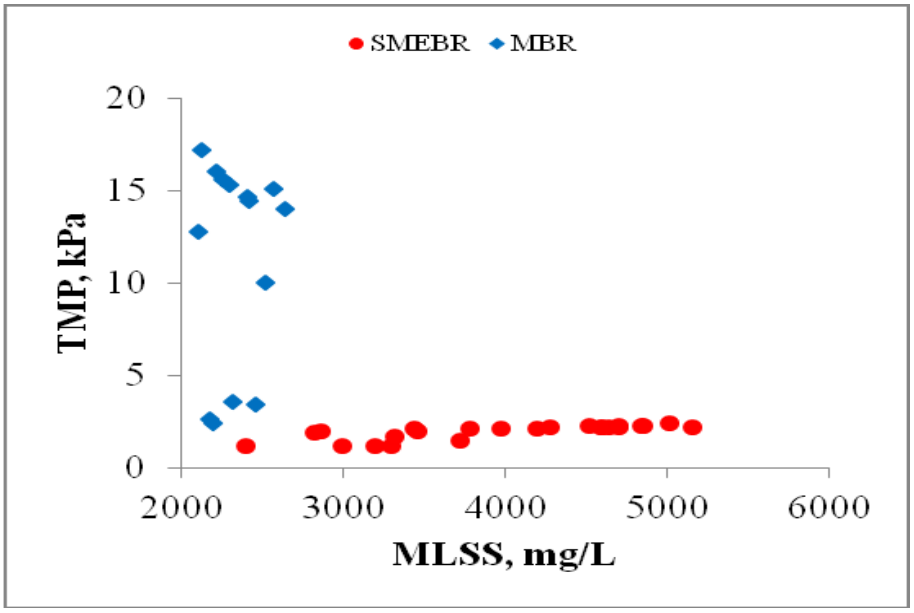

Fig. 5.17: Effect of MLSS on TMP.

In this study the MBR showed that TMP had a weak direct correlation to MLSS (r_p = 0.1940), which could be attributed to the fact that MLSS in MBR did not increase as the bioreactor operated under low SRT.

5.3.5 Relationship between SMEBR parameters

Statistical analyses permitted to conclude that PSD had strong correlations with many sludge properties (Table 5.6). PSD had a strong correlation with ZP, MLSS, and temperature (r_p = -0.7611, r_p = -0.7844, r_p = 0.7145, respectively), a moderate correlation with EPS_c and sludge viscosity (r_p = 0.6895, r_p = 0.5290, respectively), and a weak correlation with sludge

conductivity (r_p = 0.4347). The decrease in the magnitude of zeta potential (ZP) resulted from the electrocoagulation occurring in SMEBR (r_p = -0.7611). In addition, the PSD had a very strong inverse correlation with MLSS meaning that as the MLSS increased, PSD would decrease in size and get smaller (r_p = -0.7844). This could be explained by the electroosmosis phenomenon which took place within SMEBR. As a result, smaller flocs were produced enhancing sludge filterability and preventing membrane fouling.

Furthermore, PSD in SMEBR and MBR showed dependency on soluble EPS (EPS_p: r_p = -0.3362, 0.4630 in SMEBR and MBR, respectively; and EPS_c: r_p = 0.6895, 0.3550 in SMEBR and MBR, respectively) which disagreed with a previous report (Yigit et al., 2008) which did not find any correlations between the particle size and soluble EPS.

Statistical analyses showed that the decrease in the magnitude of ZP was observed in SMEBR as the carbohydrates (EPS_c) increased in the solution (moderate inverse correlation r_p = -0.5129). This confirmed the previous conclusion that EPS_c enhanced floc formation as the correlation between PSD and EPS_c (r_p = 0.6895) was fairly strong. A direct moderate correlation between ZP and the proteins (EPS_p) was also observed (r_p = 0.4811) which means that the presence of EPS_p in the solution could enhance the addition of the negative charges into the solution (Yigit et al., 2008). Yet, SMEBR appeared to be an efficient method of removing EPS_p especially during the first day where EPS_p was reduced by 25%. By applying a DC voltage, the negatively charged EPS_p was destabilized and thus neutralized by the positive metal ions generated due to the electrolytic oxidation of the aluminum anode. The observation in SMEBR agreed with a previous study (Wilén et al., 2003) which concluded that the release of such polymeric substances to the sludge flocs in MBR lead to higher negative surface charge through which proteins (EPS_p) were major

contributors to such an increase. This could be attributed to the fact that some functional groups (carboxylic, sulfate, and phosphate) of EPS were ionized (Sutherland, 2001). These results were in line with the conclusions drawn from Phase 1 (laboratory scale) and Phase 2 - Stage 2 (pilot scale). Alternatively, MBR tests showed that ZP had inverse relationships with carbohydrates (r_p = -0.5903) and proteins (r_p = -0.2948).

A strong direct correlation between ZP and MLSS was obtained (r_p = 0.8246). The increase in MLSS in SMEBR was caused by the generation of inorganics in the colloidal suspension due to anode dissolution and electrocoagulation process. Furthermore, the sludge conductivity (σ_{sludge}) in the reactor was an essential parameter as it was related to the applied voltage in the reactor. The higher the conductivity of wastewater, the less voltage (energy) was required by SMEBR to operate. SMEBR appeared to be strongly dependent on sludge conductivity which was directly related to the conductivity of the raw wastewater (σ_{in}) (r_p = 0.7363).

Besides, the concentration of carbohydrates in the sludge supernatant was influenced by the sludge temperature (r_p = 0.5488). Similar observations were reported (Stephenson et al., 2000). ZP was noted to be also influenced by temperature (r_p = -0.7621), i.e. as the temperature increased, the magnitude of zeta potential decreased, and thus flocs were electrically coagulated (r_p = 0.7145) which contributed to decreased membrane fouling.

5.4 Significant parameters affecting TMP in SMEBR and MBR

The statistical analyses (Table 5.6) showed that sludge properties such as PSD, zeta potential (ZP), sludge viscosity (SV) and MLSS influenced the change in TMP in SMEBR, whereas in MBR, TMP was described by slightly different “the most significant” sludge properties such

as sludge viscosity (SV), mean particle size diameter (PSD), and soluble EPS in tems of proteins (EPS_p). Table 5.7 showed the sludge properties significantly affecting TMP (significant when P-values were less than 0.05, shown in bold) in SMEBR and MBR. The mean particle size diameter (PSD) and viscosity in SMEBR while PSD in MBR appeared to have the most significant impact on membrane fouling, which confirmed previous analysis (Table 5.2).

Table 5.7: P-values of sludge properties generated from multiple regression analysis for SMEBR and MBR.

	SMEBR	**MBR**
PSD, µm	**$4.59x10^{-05}$**	**$2.29x10^{-05}$**
Zeta potential, mV	0.354	-
Viscosity, mPa.s	**0.021**	0.3317
MLSS, mg/L	0.751	-
EPS_p, mg/L	-	0.6923

Chapter 6: Results and Discussion of the Scale-up Verification – Phase 3

6.1 Introduction: SMEBR model calculations and design scale-up protocol

Scale-up could be defined as the reproduction of optimal laboratory conditions to either pilot or full scale operation. Nevertheless, this could be a limiting definition since there was no standard way to follow; yet actual production processes were due to successful decisions and sometimes of several mistakes (Donati and Paludetto, 1997). Laboratory and pilot studies were used to determine various parameters and operational conditions to be used in the process design, for example: process kinetics, amount of sludge production, oxygen requirements for biological needs and membrane scouring (in the case of a MBR), horsepower requirements, nutrients requirements, temperature effects and foaming problems (Eckenfelder et al., 1972).

Since SMEBR is a novel and complex process (due to the interaction between three processes in one reactor, Elektorowicz et al., 2009); scale-up methodology had not yet been defined in the literature. Based on the results from the laboratory tests conducted in Phase 1 (Chapter 4), and the preliminary design scale-up protocol proposed in Chapter 3 (see Fig. 3.5); the dimensions of the SMEBR pilot system, operating conditions, and the inputs of the electrical parameters were assessed. The proposed design scale-up protocol (shown in Fig. 6.1) was verified and validated through a series of computational analyses (detailed calculations were provided in Appendix D). A comparison between the results obtained from the preliminary design scale-up (experimental) and the proposed scale-up (theoretical) protocols was summarized in Table 6.1 at the end of this Section.

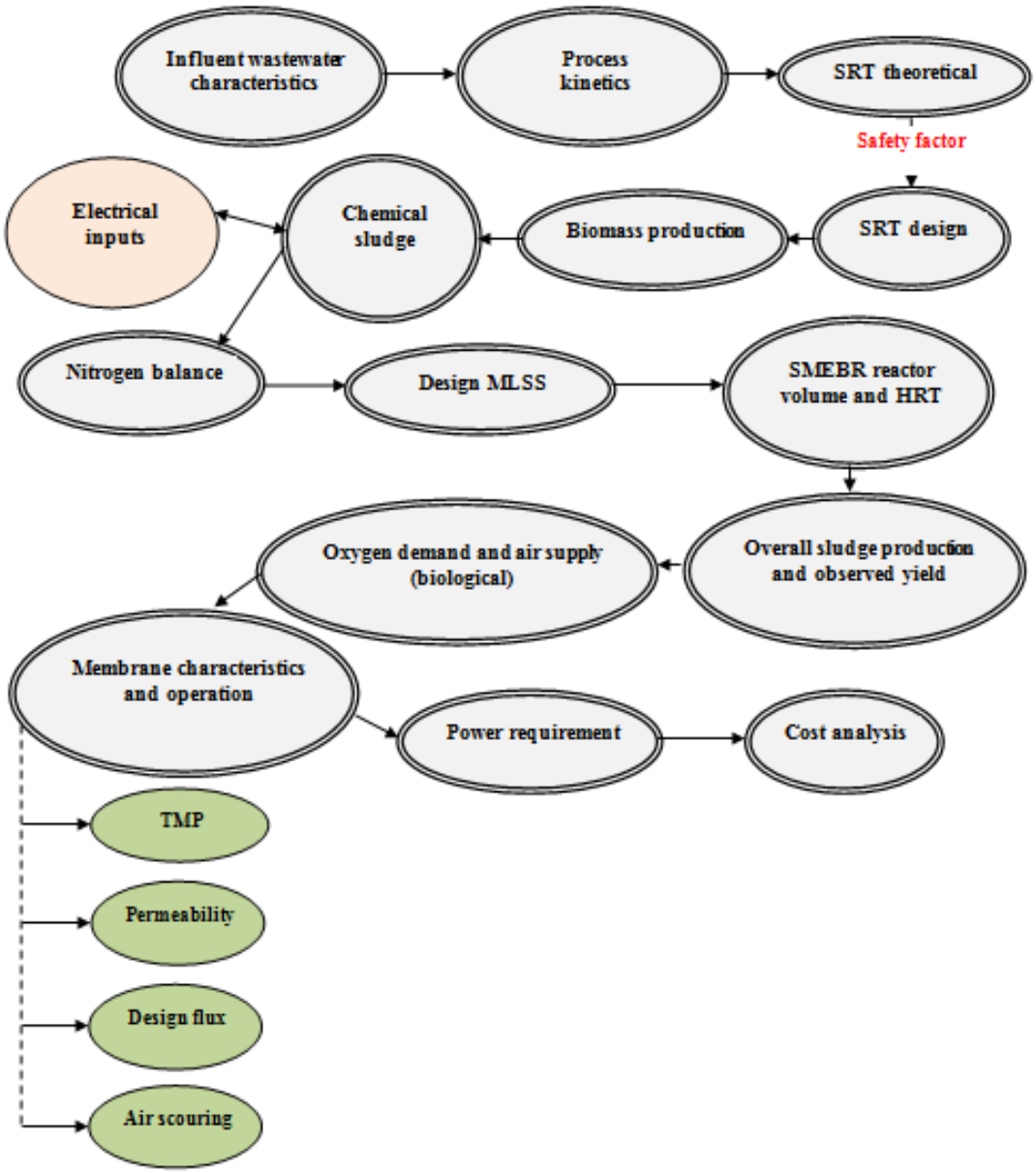

Fig. 6.1 SMEBR scale-up designing protocol (theoretical approach based on computational analyses).

6.2 Comparison between preliminary (experimental) and proposed design (theoretical) scale-up protocols - concluding remarks

Table 6.1 summarized the results of the preliminary (experimental) and proposed design (theoretical) scale-up protocols. It could be observed that SMEBR behaved slightly different in reality as was expected. The interaction between the three processes influenced some parameters during the operation. For instance, when fixing the rate of sludge to be wasted per day, the fraction of VSS at steady state stabilized at 56%, whilst it should not exceed 47.8% according to the computational approaches. It could be speculated that the intermittent supply of electricity at low or adequate current density (i.e. non-toxic adequate level) had positive impacts on some kinds of the existing microorganisms in SMEBR. The results illustrated in Chapter 5 (see Fig. 5.4) showed an increase in MLVSS (2620 g/m^3 as an average value at steady state) in SMEBR compared with MLVSS (1540 g/m^3 as an average value at steady state) in MBR (1.7 times higher).

Table 6.1: Results of experimental and theoretical design scale-up protocols

Parameter	Preliminary (experimental)	Proposed (theoretical)
HRT, h	11	13.5
SRT, d	10	10
VSS/TSS	56%	47.8%
$V_{Effective\ liquid}$, L	235	267
F/M, 1/d	0.19	0.15
L_{org}, $kg/m^3.d$	0.51	0.43
$P_{x,\ TSS}$, kg TSS/d	0.1201	0.166

It could be concluded that the computational analyses (shown in Appendix D) based on the proposed methodology shown in Fig. 6.1 could be considered as a protocol to

design and scale-up SMEBR for full scale applications. Ranges of design parameters should be taken into considerations as: a) HRT = 9-15 h, b) current density = 10-15 A/m^2, c) electrical mode: 5 min ON: 10 min OFF, e) V^*/V ratio = 24%-47%, f) distance between electrodes is less than 10 cm.

6.3 Analysis of SMEBR laboratory and pilot tests treating raw wastewater

In order to validate and verify the aforementioned design scale-up protocol, a laboratory scale experiment was carried out in conjunction with the pilot scale test. Both SMEBRs operated under the same conditions (obtained from Phase 1) and fed with the same raw wastewater. The results showed that the scaled-up pilot SMEBR and the laboratory scale SMEBR behaved similarly with slight differences. For example, after 3 SRT (i.e. steady state conditions) both bioreactors achieved similar results with respect to COD, phosphorus, and ammonia removal rates (Figs 6.2 to 6.4).

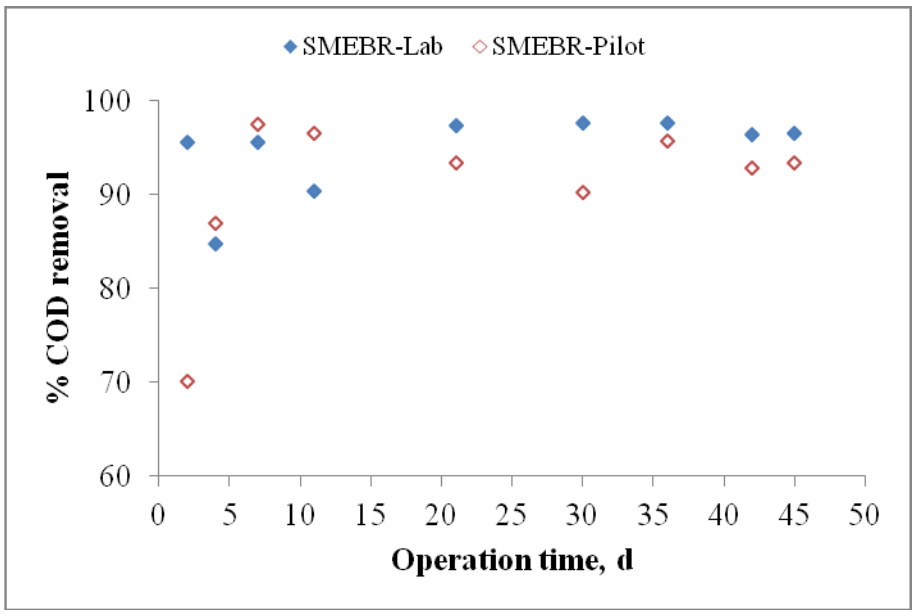

Fig. 6.2: COD removal efficiency in laboratory and pilot SMEBRs.

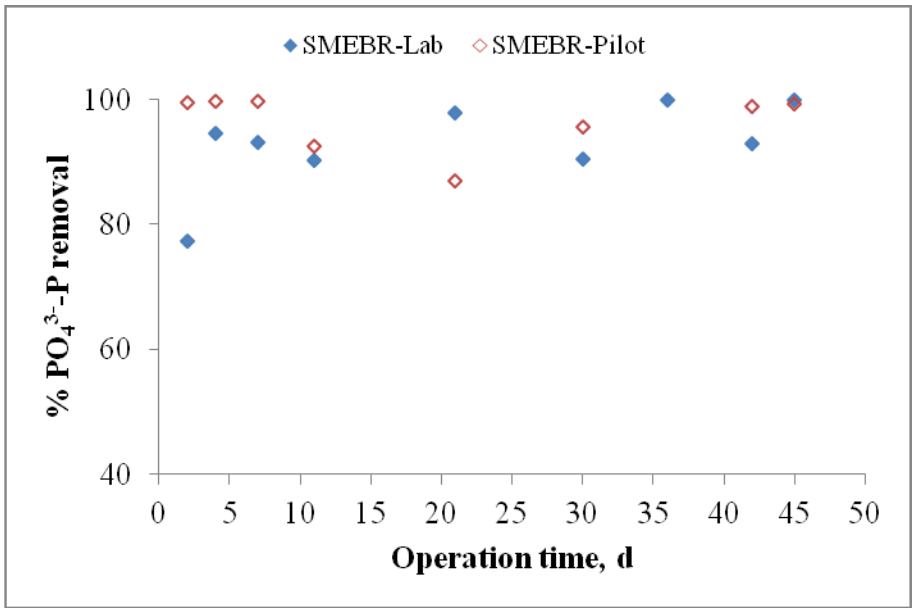

Fig. 6.3: Phosphorus removal efficiency in laboratory and pilot SMEBRs.

It could be concluded that the removal of pollutants such as COD, ammonia, and phosphorus was not scale dependent, and similar results would be achieved in full scale.

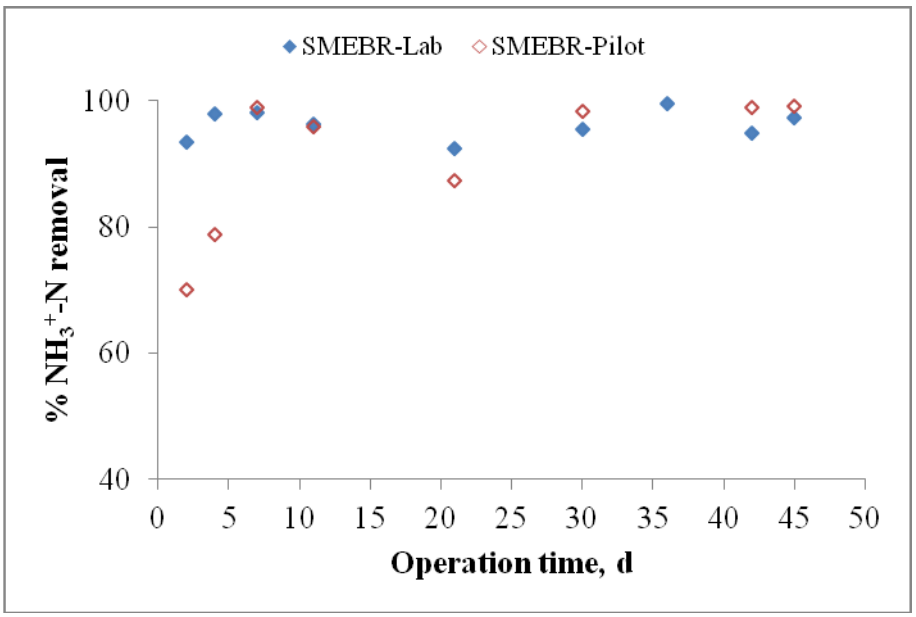

Fig. 6.4: Ammonia removal efficiency in laboratory and pilot SMEBRs.

Coagulation process in the bioreactors was fairly similar as shown in the results of zeta potential (Fig. 6.5). It was concluded that the electrooxidation of the aluminum anode in both bioreactors assessed in breaking the repulsive forces between the negatively charged sludge colloids, and permitting the van der Waals forces to predominate and therefore flocs to aggregate as demonstrated in Phases 1 and 2. Generally, electrokinetics in SMEBR enhanced the coagulation process and similar results were expected in full scale.

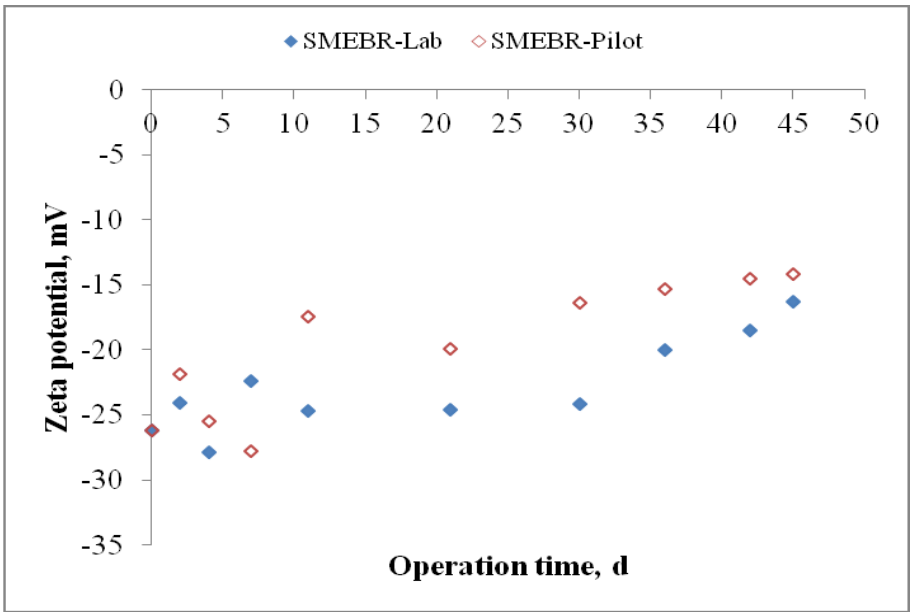

Fig. 6.5: Zeta potential variation in laboratory and pilot SMEBRs.

Sludge filterability was enhanced significantly in both bioreactors as the mean particle size diameter (PSD) of the sludge flocs had decreased in similar rates allowing the generation of electroosmosis phenomena in SMEBR and hence reducing their size (Fig. 6.6). Sludge settleability was also improved and denser flocs were produced as the sludge volume indices (SVIs) were 112 and 119 mL/g in laboratory and pilot scales SMEBRs, respectively. Therefore, it could be concluded that sludge filterability and settleability were not scale dependent, and similar results would be accomplished in full scale.

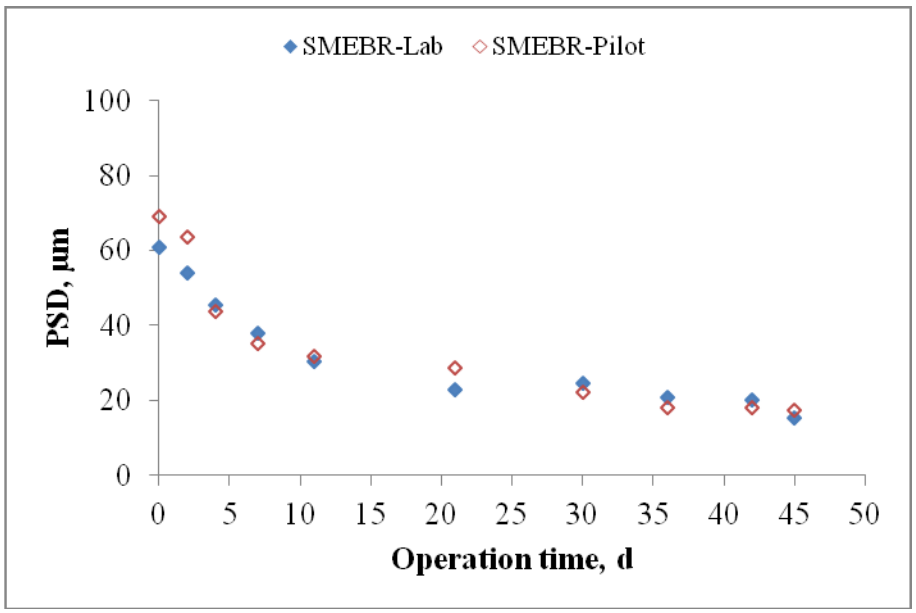

Fig. 6.6: Mean particle size diameter variation in laboratory and pilot SMEBRs.

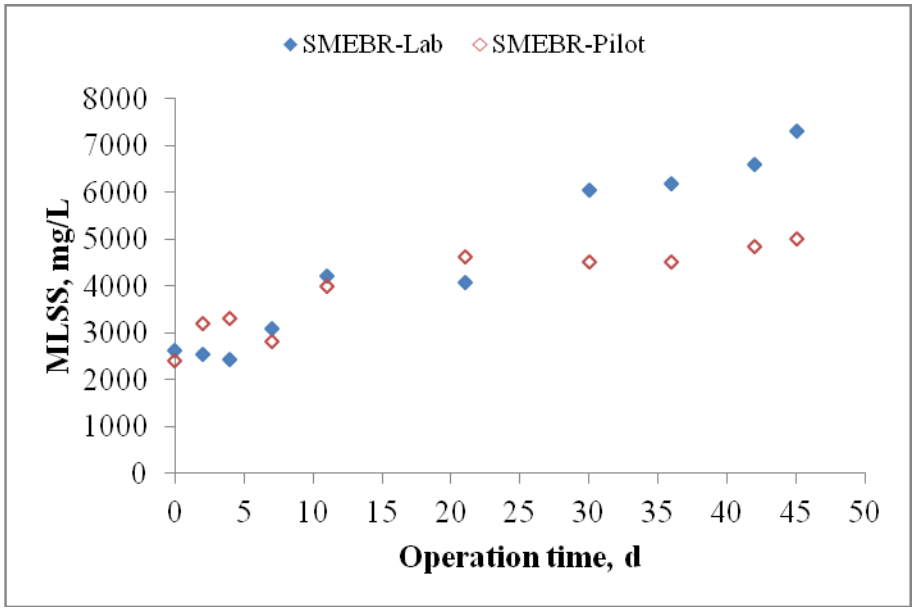

Fig. 6.7: Total suspended solids variation in laboratory and pilot SMEBRs.

The change in the biomass, i.e. the total suspended solids (MLSS) in SMEBR pilot facility was not significant over 7 weeks of operation, while it had increased significantly in the laboratory scale SMEBR system (Fig. 6.7). This could be explained by the

deposition of some solid particles, mainly the generated inorganic aluminum compounds (due to electrokinetics) on the surfaces of the electrodes in SMEBR pilot system as they did not leave with the treated effluent (shown earlier in Chapter 5, Section 5.2.4). As a result, the anodic rate of corrosion was manipulated in pilot SMEBR system allowing less sludge production.

6.4 Power requirements and cost analysis

The specific energy demand of submerged membrane electro-bioreactors was mainly due to the aeration intensity (i.e. liquid pumping has low contribution to the energy demand), and the electrical power generated due to the electrical system present in SMEBR. The power and the specific energy consumption due to aeration (biological and membrane scouring: 0.042 and 0.0407in kWh/m^3, respectively) were calculated according to eqs D.23 and D.24 (Simon, 2006). Detailed calculations were summarized in Appendix D. The specific energy consumption per m^3 of wastewater treated due to electrical system was calculated as shown in Table D.3.

Fig. 6.8 showed the distribution of the specific energy consumption per m^3 of wastewater over 7 weeks of operation. Specific energy consumption was related to the applied voltage which was also in direct proportion with the conductivity of the raw wastewater. It could be noticed that the specific energy consumption of SMEBR system could be lowered to 1 kWh/m^3 as it was strongly dependent on the conductivity of the treated wastewater. In addition, the specific energy could be also reduced to less than 1 kWh/m^3 taking into considerations the operating conditions mainly the exposure time to electrical field.

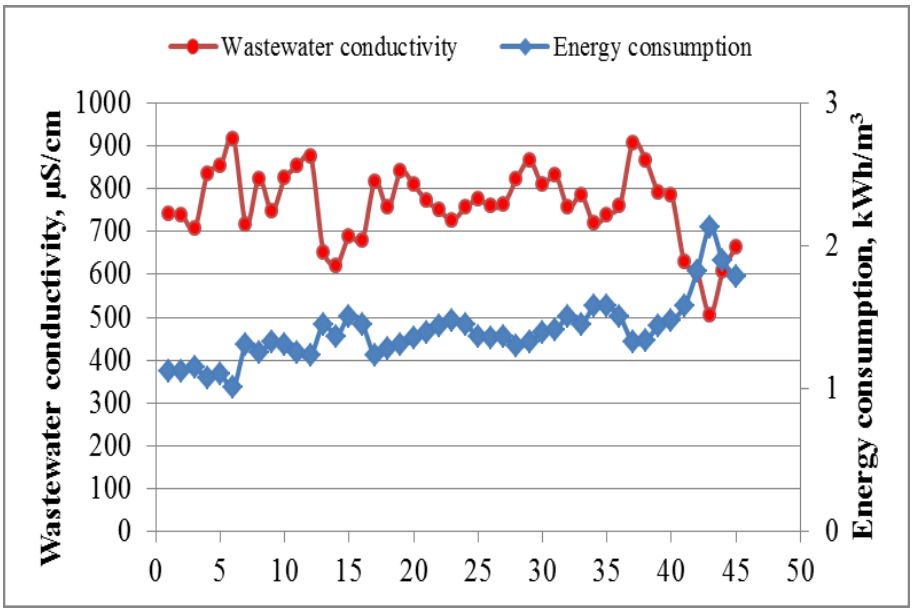

Fig. 6.8: Distribution of specific energy consumption in SMEBR pilot system due to electrokinetics over 7 weeks.

Therefore,

- ✓ **Total energy/unit permeate = (0.042 + 0.0407 + 1) = 1.09 kWh/m^3**

Table 6.2 showed different energy requirements for different wastewater treatment methods such as conventional activated sludge, MBR and electrocoagulation (EC). It could be concluded that SMEBR system had reasonable consumption of energy and would compete against the rest of the treatment methods. More importantly, SMEBR had reduced the footprint as it eliminated many other treatment operational units such as primary treatment and sludge processing (as demonstrated earlier in the sludge dewaterbility results). Therefore, the energy requirements for those operational units would be eliminated when SMEBR system is applied in full scale applications of wastewater treatment.

Table 6.2: Comparison between energy requirements in different wastewater treatment technologies

Treatment method	Energy requirements, kWh/m^3	Reference
Immersed MBR	0.6 - 1.1	Evans and Laughton (1994)
Immersed MBR	< 0.14	Visvanathan et al. (1997)
Immersed MBR	0.7 - 0.8	Krause and Cornel (2006)
Immersed MBR	4	Jefferson et al. (1998)
Immersed MBR	6 - 8	Zhan et al. (2003)
Immersed MBR	4.88 - 6.06	Gil et al. (2010)
Conventional activated sludge process	0.38 - 0.48	Evans and Laughton (1994)
EC with 31 aluminum plates electrodes, 1.5 cm gap and operating at 6 A/dm^2	7.58	Chu and Shi (2010)
EC with six iron plates electrodes, 5 mm gap	0.85 - 1.11	Irdemez et al. (2006)
EC with stainless steel electrodes	8	Arslan-Alaton et al. (2008)
Full scale MBR	2 - 3.6	Bolzonella et al. (2010)
Pilot scale SMEBR	**< 1**	**This study** **Hasan et al. (2011)**

The cost estimation of SMEBR was calculated based on the specific energy demand due to biomass aeration, membrane aeration, as well as the specific energy required to create the electrical field between the electrodes. It did not take into account the cost of the materials (electrodes), liquid pumping, labors, maintenance, and membrane lifetime as they have lesser contributions to the total cost (Judd, 2006). Sludge disposal costs were also excluded since costs related to this process were process dependent such as sludge thickening which had a huge impact on disposal costs. Additionally, the cost of sludge treatment and disposal was assumed to be small compared with power costs (Judd, 2006). The following was an estimate of the total energy cost.

- **Power cost** in the City of Montreal (Québec, Canada) for high power customers = CAD $0.048/kWh (Hydro- Québec, 2010).

Therefore,

- ✓ **Total energy cost = (1.09 kWh/m^3) (CAD $0.048/kWh) = CAD $0.052/m^3**

As stated earlier, the total energy cost of SMEBR system could be reduced to less than CAD $0.052/m^3 depending on the characteristics of the wastewater (mainly ionic strength and conductivity) as well as the operating conditions such as aeration intensity, HRT, and intermittent supply of electricity (i.e. less exposure time, Ibeid et al., 2010b).

Chapter 7: Conclusions

In conclusion, the pilot SMEBR system operated successfully despite the daily and seasonal variations in the characteristics of the raw wastewater. SMEBR pilot system showed superiority in performance over conventional MBR and produced excellent quality effluent. Membrane fouling was significantly reduced during the operation of SMEBR compared to MBR unit. The electric field in SMEBR generated coagulation through the destabilization of the charged particles in the colloidal suspension. SMEBR as tested was a very compact system and included three unit operations in one hybrid reactor. No primary treatment was necessary and thus required a very small footprint.

7.1 Conclusions obtained from Phase 1

Twenty eight laboratory scale experiments were conducted so as to screen out and determine the best operating conditions which were used in the design and the operation of the SMEBR pilot facility.

.**Variation of aeration intensity**

- Critical flux and aeration intensity were found to be in direct proportion.
- Aeration intensity per SMEBR unit should be kept below 552 to L/h so as to prevent:
    - Breakage of flocs.
    - The increase in the amount of EPS released into the solution.
    - The increase of membrane fouling index and specific cake resistance from $\alpha = 0.044 \times 10^{14}$ to 0.144×10^{14} m/kg and from MFI = 0.0029×10^{6} to 0.01×10^{6} L/s^2.

- The increase in the magnitude of zeta potential which would slow the rate of bioflocculation.
- The increase in sludge suspension viscosity from 1.69 to1.76 mPa.s (by 10%).

- Statistical analysis using ANOVA showed that aeration intensity had significant influence (expressed by P-values) on sludge characteristics such as PSD, soluble EPS, zeta potential, sludge viscosity and specific cake resistance.

Variation of current density

- COD removal was not affected by the change in current density, however, it reported less efficiency at higher current density (i.e. at 27 A/m^2). Average COD removal was 96%, 96%, 96%, and 90% at 5, 10, 15, and 27 A/m^2, respectively. On the other hand, average COD removal in MBR was 92%.

- Phosphorus removal was significantly affected by the change in current density; however, it reported instable results at higher current density (i.e. at 27 A/m^2). Average phosphorus was 73%, 82%, 83%, and 84% at 5, 10, 15, and 27 A/m^2, respectively. In contrast, average phosphorus removal in MBR was 53%.

- Ammonia removal was significantly affected by the change in current density; yet, it reported less removal at higher current density (i.e. at 27 A/m^2). Average ammonia removal was 78%, 82%, 80%, and 62% at 5, 10, 15, and 27 A/m^2, respectively. On the contrary, average ammonia removal in MBR was 72%. Low removal efficiencies of total nitrogen were achieved in all reactors under different current densities as well as in MBR.

- The reduction in floc size diameter was directly porportional to the current density. 29.9%, 34%, 50.6%, and 60.8% were reported at 5, 10, 15, and 27 A/m^2, respectively.
- As the current density increased, MLSS was increased due to the generation of chemical sludge resulting from the anodic electrooxidation.
- As the current density increased, more colloidal particles were removed from wastewater.
- Change in current density had no significant effects on either sludge viscosity or Zeta Potential.
- Soluble EPS were removed at higher fractions under electrokinetics process compared to MBR.
- Filterability was significantly enhanced by applying electricity, and the formation of the cake layer was minimized leading to less fouling potential.
- Sludge in SMEBR had better settleability than in MBR.
- Membrane fouling as well as frequency of membranes cleaning were significantly reduced in SMEBR when compared to MBR (1.05 kPa/d, 0.21 kPa/d and 0.097 kPa/d, at 10, 15 and 27 A/m^2, respectively). The rate of fouling at 5 A/m^2 was calculated after the first nine days as well as for the period from 10 to 12 d when SMEBR experienced fouling. Results reported 0.695 and 15 kPa/d, respectively. Similarly, the rate of fouling in MBR was calculated after the first eight days as well as for the period from 9 to 11 d when MBR experienced fouling. Results reported 1.33 and 26.05 kPa/d, respectively.

- Inorganic solids generated due to electrokinetics in SMEBR were directly proportional to current density.

Variation of HRT

- COD removal efficiency was not affected by the change in HRT: average of 95% was achieved in all HRTs.
- Phosphorus removal was more significant at 15 h. Average removal efficiencies were 86%, 84% and 97% at 6, 9 and 15 h, respectively.
- Ammonia removal was highly significant at 15 h. Average removal efficiencies were 34%, 76% and 94% at 6, 9 and 15 h, respectively. Similarly, total nitrogen removal was very significant at 15 h. Average removal efficiencies were 19%, 32% and 51% at 6, 9 and 15 h, respectively.
- Amount of reduction in floc size was 7.8%, 41%, and 41.6% at 6, 9 and 15 h, respectively.
- Total suspended solids (MLSS) were increasingly generated at high HRT. They increased from 5560 to 8160 mg/L, and from 5010 to 11100 mg/L at 9, and 15 hours, respectively.
- Better sludge filterability and settleability were obtained at low HRT (6 h). The sludge volume index (SVI) was 65.7, 65.8, and 123.1 mL/g at 6, 9, and 15 hours, respectively.
- The rate of membrane fouling decreased with HRT. 0.0964 kPa/d, and 0.0393 kPa/d were reported at 9, and 15 h, respectively. SMEBR operated under 6 h fouled very often since the operating flux was close to the critical flux.

Variation of electrical zone volume

- Both designs (47% and 24%) achieved high COD removal efficiency: Average removal efficiencies were 95% and 99%, respectively.
- Phosphorus removal in 24% was higher than 47%: average of 84% and 94%, respectively.
- Ammonia removal in 24% was higher than 47%: average of 78% and 86%, respectively. Total nitrogen removal in 24% was higher than 47%: average of 32% and 72%, respectively. This lead to the fact that by increasing the outer zone (between the anode and the reactor wall), an anoxic zone was created which improved the nutrients removal.
- Reduction in floc size diameter and volume to volume ratio were in inverse proportion. 41% and 7% were reported at 47% and 24%, respectively.
- No significant difference in the biomass (MLSS) in both reactors.
- More soluble EPS were present in the solution at 24% causing higher magnitude of zeta potential of -37.20 mV when compared to -25.80 mV at 47%.
- No significant change on sludge viscosity was reported.
- Sludge at 47% had better settleability. SVI were 65.8 and 121.5 mL/g at 47% and 24%, respectively.
- As the volume to volume ratio decreased, the rate of membrane fouling had increased. 0.0964 kPa/d and 0.1893 kPa/d were reported at 47 and 24%, respectively.

7.2 Conclusions obtained from Phase 2

Performance of SMEBR and MBR pilot systems

- SMEBR pilot system produced excellent quality effluent due to the removal efficiency of 92% COD, 99% P, and 99% NH_3^+ which was higher than those of MBR pilot unit (86.6%, 59%, and 97% for COD, P and NH_3^+, respectively).

- SMEBR pilot tests did not report any increase in the transmembrane pressure, and thus appeared to be an adequate technology for avoiding membrane fouling. Membrane fouling in SMEBR was decreased by 8 times and the rate of fouling in SMEBR and MBR over 7 weeks of operation were 0.018 and 0.371 kPa/d, respectively.

- SMEBR showed a different response to sludge properties than MBR and resulted in a decrease in the mean particle size of sludge flocs by 75%. The magnitude of zeta potential in SMEBR had decreased significantly by 46%; conversely, a slow rate of coagulation was reported in MBR. Results showed that the mixed liqour volatile suspended solids (MLVSS) in SMEBR was 1.7 times higher than in MBR. Accordingly, SMEBR operated under adequate current density which had positive impacts on the living microorganisms. Soluble EPS_c were removed 3 times higher under electrokinetics process in SMEBR than in MBR. SMEBR had improved the sludge settleability by 30% two times more than MBR. Furthermore, sludge dewaterability (filterability) in SMEBR had enhanced by 78%.

- Although SMEBR generated metal ions into the bulk solution, aluminum did not leave with the treated effluent, and was present in small amounts in the wasted sludge. Most of the aluminum was retained on the surface of the electrodes. The electrodes did not

require any physical or chemical cleaning during the operation and it was predicted they would last for five months.

- SMEBR without any additional unit was able to remove undesirable metals from wastewater. High removal rates of Pb (100%), Ni (98.1%), Cu (100%), and Cd (94.6%) were reported with very low concentrations in the treated effluent (0.0, 0.24, 0.0 and 0.04 mg/L for Pb, Ni, Cu, and Cd, respectively). The removal rates of Mg, Zn, and Fe were 87.5%, 80.4%, and 85%, respectively.
- The sludge produced during the treatment process using SMEBR system could be used as fertilizers and applied to agricultural lands.
- Higher deposition of metals was found on the surface of the cathode than on the surface of the anode, where several complexes might be generated and used as agricultural fertilizers.
- SMEBR was a compact unit which included three operational units in one hybrid reactor, without primary treatment and thus required small footprint. SMEBR could be also placed on a mobile unit and used in different applications such as military basis and mining.

Impact of sludge properties on transmembrane pressure (TMP)

- TMP had strong correlations to the mean particle size diameter (PSD) in SMEBR and MBR, respectively which appeared to be the most sludge parameter affecting the membrane fouling. PSD also showed dependency on soluble EPS (i.e. soluble carbohydrates (EPS_c) and soluble proteins (EPS_p)).

- The composition of soluble EPS in SMEBR, in particular, proteins (EPS_p) contributed to membrane fouling through which the release of proteins had adverse impacts on zeta potential; and consequently membrane fouling. In contrary, EPS_c, enhanced flocs formation according to the inverse correlation between EPS_c and zeta potential. The electric field in SMEBR improved the coagulation process when compared to MBR through the destabilization of the charged particles in the colloidal suspension.
- TMP had strong and weak correlations to the sludge MLSS in SMEBR and MBR, respectively.
- TMP had strong and moderate correlations to the sludge viscosity in SMEBR and MBR, respectively which appeared to be influenced by the release of the soluble EPS.
- It was also concluded that the TMP in SMEBR was a function of PSD, sludge viscosity, zeta potential, and MLSS, whilst TMP in MBR was a function of PSD, EPS_p, and sludge viscosity.

7.3 Conclusions obtained from Phase 3

- Validation of the design scale-up protocol was confirmed through parallel experiments between the laboratory scale and the pilot scale SMEBRs. Observations showed similar behaviors with regard to COD, phosphorus, ammonia, mean particle size diameter, zeta potential, sludge filterability and settleability.
- Total specific energy and total energy cost of SMEBR pilot system were 1.09 kWh/m^3 and CAD \$0.052/m^3, respectively.

Chapter 8: Research Contributions and Recommendations for Future Work

8.1 Research contributions

The SMEBR hybrid unit operated based on the interactive biological, membrane filtration, and electrochemical processes. The most important contribution to the knowledge in this field was the balanced design of three processes in one operation unit, which had never been done before in pilot scale. Furthermore, the study of membrane fouling response to electro-kinetically degraded wastewater by-products, and energy saving solutions represented a major contribution to the current body of understanding. Detailed contributions were:

- Providing technological design parameters such as bioreactor dimensions, hydraulic retention time, solids retention time, adequate current density, aeration intensity and location of air diffusers required to operate a successful SMEBR system.
- Determining the chemical or inorganic sludge production due to electrokinetics in SMEBR system operated at different current densities.
- Assessing the performance of SMEBR system with respect to water quality, membrane fouling and the changes in the physical, chemical, and biological sludge properties through performing comparative study to the conventional membrane bioreactor (MBR) operated under the same operating conditions.
- Validation of the technological design parameters through designing and operating complete mixed SMEBR and MBR pilot systems supplied with continuous flows of raw wastewater. These facilities were located in the municipal wastewater treatment plant in the City of l`Assomption (Quebec, Canada). Several goals were achieved:

    - Obtaining superior water quality and eliminating the presence of nutrients such as phosphorus and ammonia in the treated effluent.
    - Providing mechanisms of organics and nutrients removal in SMEBR.
    - Minimizing membrane fouling and the frequency of membrane cleaning through applying an adequate current density in SMEBR system.
    - Avoiding the damage of the membrane materials in the presence of electrical field.
    - Improving flocs coagulation and enhancing sludge filterability and settleability.
    - Preventing inhibitory conditions for microorganisms in electrical field.
- Providing computational approach to design SMEBR system to full scale applications.
- Validating the compatibility between laboratory scale and pilot scale designs with respect to water quality and sludge properties.
- Applying statistical approach to verify the experimental results obtained from the pilot tests and compare the impact of sludge properties on membrane fouling (indicated by the transmembrane pressure, i.e. TMP) in SMEBR and MBR pilot systems.
- Generation of statistical mathematical models correlating the change in TMP with respect to the most significant sludge properties affecting membrane fouling.
- Finding the relationships among the sludge properties in SMEBR (exposed to adequate current density) and MBR pilot systems.

- Assessing the electrodes lifetime and proving that SMEBR is a "self-purification" system where most of the generated aluminum ions (due to anode electrooxidation) were retained on the surfaces of the electrodes, thus preventing them from leaving neither with the effluent nor with the wasted sludge. Investigating the fate of aluminum and phosphorus in SMEBR system.
- Providing electrodes chemical cleaning protocol.
- Providing the major chemical constituents and metals existed in the deposits observed on the surface of the electrodes as well as in the waste sludge.
- Investigating the fate of different metals in the influent and the treated effluent leaving SMEBR system.
- Providing methods of cost analysis and power requirements for SMEBR pilot system which can be used in full scale applications.

8.2 Recommendations for future work

- Test SMEBR pilot facility at different operating conditions to expand its applications.
- Conduct a full scale study to verify the pilot scale results.
- Perform SMEBR batch experiments to determine the process biokinetics for autotrophic and heterotrophic microorganisms.
- Consider the microbial activity and perform microscopic analysis to identify the different kinds of microorganisms present in SMEBR system.
- Model SMEBR system using wastewater treatment modeling and simulation software.

References

Abbassi B., Dullstein S., and Rabiger N. (1999). Minimization of excess sludge production by increase of oxygen concentration in activated sludge flocs; experimental and theoretical approach. *Water Research*, 34, 139-146.

Abdel-Ghani N.T. and El-Chaghaby, G.A. (2007). Influence of operating conditions on the removal of Cu, Zn, Cd and Pb ions from wastewater by adsorption. *International Journal of Environmental Science and Technology*, 4 (4), 451-456.

Abuzaid N.S., Bukhari A.A., and Al-Hamouz Z.M. (1998). Removal of bentonite causing turbidity by electrocoagulation. *Journal of Environmental Science and Health*, Part A 33 (7), 1341-1358.

Adhoum N. and Monser L. (2004). Decolourization and removal of phenolic compounds from olive mill wastewater by electrocoagulation, *Chemical Engineering Processing*, 43, 1281-1287.

Adhoum N., Monser L., Bellakhal N., and Belgaied, J.E. (2004). Treatment of electroplating wastewater containing $Cu^{2+,}$ Zn^{2+} and Cr (IV) by electrocoagulation. *Journal of Hazardous Materials*, 112 (3), 207-213.

Akpor O.B., Momba M.N.B., Okonkwo J.O., and Coetzee M.A. (2008). Nutrient removal from activated sludge mixed liquor by wastewater protozoa in a laboratory scale batch reactor. *International Journal of Environmental Science and Technology*, 5 (4), 463-470.

Alamdari A. and Rohani S. (2007). Phosphate recovery from municipal wastewater through crystallization of calcium phosphate. The Pacific Journal of Science and Technology, 8 (1), 27-31.

Al-Malack M., Bukhari A.A., and Abuzain N.S. (2004). Crossflow microfiltration of electrocoagulated kaolin suspension: fouling mechanism. *Journal of Membrane Science*, 243 (1-2), 143-153.

Apaydin Ö., Kurt U., Gonullu M.T. (2009). An investigation on the treatment of tannery wastewater by electrocoagulation. *Global Nest Journal*, 11 (4), 546-555.

APHA, AWWWA, WPCF (1998). Standard method for the examination of water and wastewater, 20th Edition, Washington DC.

Aptel P. and Buckley C.A. (1996). Water treatment: membrane processes, chapter 2, New York, McGraw-Hill, Inc.

Arslan-Alaton I., Gursoy B.H., Akyol A., Kobya M., and Bayramoglu M. (2008). Modeling and optimization of acid dye manufacturing wastewater treatment with Fenton's reagent: Comparison with electrocoagulation treatment results and effects on activated sludge inhibition. *Water Science and Technol*ogy, *62*, 209-216.

Asano T., Burton F., Leverenz H., Tsuchinashi R., and Tchobanoglous G. (2006). Water Reuse: Issues, Technologies and Applications. Metcalf and Eddy/AECOM. ISBN: 978-0-07-145927-3. 1st edition.

Bai R. and Leow H.F. (2002). Microfiltartion of activated sludge wastewater-the effect of system operation parameters. *Separation Purification Technology*, 29 (2), 189-198.

Balasubramamian N. and Madhavan K. (2001). *Chemical Engineering Technology*, 24 (5), 519-521.

Bani-Melehm K. and Elektorowicz M. (2011). Performance of the Submerged Membrane Electro-Bioreactor (SMEBR) with Iron Electrodes for Wastewater Treatment and Fouling Reduction. *Journal of Membrane Science,* 379, 434-439.

Bani-Melhem K. (2008). Development of a novel submerged membrane electro-bioreactor for wastewater treatment, Ph.D. thesis, Concordia University. Montreal, Canada.

Bani-Melhem K. and Elektorowicz M. (2010). Development of a novel submerged membrane electro-bioreactor (SMEBR): Performance for fouling reduction. *Environmental Science and Technology*, 44, 3298-3304.

Basu O.D. and Huck P.M. (2005). Impact of support media in an integrated biofilter submerged membrane system. *Water Research*, 39 (17), 4220-4228.

Bektas N., Akbulut H., Inan H., and Dimoglo A. (2004). Removal of phosphate from aqueous solutions by electrocoagulation. *Journal of Hazardous Materials*, 106 (2-3), 101-105.

Bhaskar P.V. and Bhosle N.B. (2006). Bacterial extracellular polymeric substances (EPS): A carrier of heavy metals in the marine food-chain. *Environment International*, 32 (2), 191-198.

Boerlage S-F.E., Kennedy M.D., Aniye M.P., Abogrean E., Tarawneh Z.S., and Schippers, J.C. (2003). The MFI-UF as a water quality test and monitor. *Journal of Membrane Science*, 211 (2), 271-289.

Bolzonella D., Fatone F., Pavan P., and Cecchi F. (2010). Application of a membrane bioreactor for winery wastewater treatment. *Water Science and Technology*, 62 (12), 2754-2759.

Borgerding J. (1972). Phosphate deposits in digestion systems. *Journal Wastewater Pollution Control Federation*, 44(5), 813-819.

Bosky A.L. and Posner A.S. (1973). Conversion of amorphous calcium phosphate to microcrystalline hydroxyapatite. A pH dependent, solution mediated, solid-solid concersion. The Journal of Physical Chemistry, 7, 2313-2317.

Bouhabia E.H., Aim R.B., and Buisson H. (2001). Fouling characterisation in membrane bioreactors. *Separation Purification Technology*, 22-23, 123-132.

Bourgeous K.N., Darby J.L., and Tchobanoglous G. (2001). Ultrafiltration of wastewater: effects of particles, mode of operation, and backwash effectiveness. *Water Research*, 35 (1), 77-90.

Burns J.R. and Finlayson B. (1982). Solubility product of magnesium ammonium phosphate hexahydrate at various temperatures. *Journal of Urology*, 128, 426-428.

Cabassud C., Masse A., Espinosa-Bouchot M., and Sperandio M. (2004). Submerged membrane bioreactor: interactions between membrane filtration and biological activity. *Water Environment-Membrane Technology Conference,* Seoul, Korea.

Cabeza A., Utriaga M.J., and Rivero I.O. (2007). Ammonium removal from landfill leachate by anodix oxidation. *Journal of Hazardous Materials*, 144, 715-719.

Can O.T., Kobya M., Demirbas E., and Bayramoglu M., (2006). Treatment of the textile wastewater by combined electrocoagulation. *Chemosphere*, 62 (2), 181-187.

Canadian Council of Ministers of the Environment (CCME). Municipal wastewater effluent development committee. December, 2006.

Celmer D, Oleszkiewicz J., Cicek N., and Husain H. (2008). Hydrogen limitation-a method for controlling the performance of membrane biofilm reactor for autotrophic denitrification of wastewater. *Water Science and Technology*, 54 (9), 165-172.

Cenkin V.E. and Belevstev A.N. (1985). Electrochemical treatment of industrial wastewater effluents. *Water Treatment Journal*, 25 (7), 243–247.

Chang I.S, Clech P.C., Jefferson B., and Judd S. (2002). Membrane fouling in membrane bioreactors for wastewater. *Journal of Environmental Engineering*, 128 (11) 1018-1029.

Chang I.S. and Kim, S.N. (2005). Wastewater treatment using membrane filtration-effect of biosolids concentration on cake resistance. *Process Biochemistry*, 40 (3-4), 1307-1314.

Chang I.S. and Lee C.H. (1998). Membrane filtration characteristics in membrane-coupled activated sludge system - the effect of physiological states of activated sludge on membrane fouling. *Desalination*, 120, 221-233.

Chang I.S., Bag S.O., and Lee C.H. (2001). Effects of membrane fouling on solute rejection during membrane filtration of activated sludge. *Process Biochemistry*, 36 (8-9), 855-860.

Chen G., Chen X., and Yue P.L. (2000). Electrocoagulation and electroflotation of restaurant wastewater. *Journal of Environmental Engineering*, 126 (9), 858-863.

Chen J.P., Yang C.Z., Zhou J.H.,Wang X.Y. (2007). Study of the influence of the electric field on membrane flux of a new type of membrane bioreactor. *Journal of Chemical Engineering*, 128, 177–180.

Chen X., Chen G., and Yue P. L. (2000). Separation of pollutants from restaurant wastewater by electrocoagulation. *Separation Purification Technology*, 19, 65-76.

Cheryan M. (1998). Ultrafiltration and Microfiltration Handbook, Switzerland, Technomic publication, Inc., 31-69.

Cho B.D. and Fane A.G. (2002). Fouling transients in nominally sub-critical flux operation of a membrane bioreactor. *Journal of Membrane Science*, 209 (2), 391-403.

Cho J., Song K.G., and Ahn K.H. (2009). Contribution of microfiltration on phosphorus removal in the sequencing anoxic/anaerobic membrane bioreactor. *Bioprocess and Biosystems Engineering*, 32 (5), 593-602.

Choi,Y.H., Kweona J.H., Kim D.I., and Lee S. (2009). Evaluation of various pretreatment for particle and inorganic fouling control on performance of SWRO. *Desalination*, 247 (1-3), 137-147.

Chu J. and Shi X. (2010). Study on the application of electro coagulation for wastewater treatment from an electroplating plant. School of Environment, Jiangsu University, Zhenjiang, China.

Chua H.C., Arnot T.C., and Howell, J.A. (2002). Controlling fouling in membrane bioreactors operated with a variable throughput. *Desalination*, 149 (1-3), 225-229.

Churchouse S. (2002). Membrane bioreactors: going from laboratory to large scale-problems to clear solutions, in: *Proceeding in Membranes and the Environment*, University of Oxford.

Cicek N., Franco J.P., Suidan M.T., Urbain V., and Manem J. (1999). Characterization and comparison of a membrane bioreactor and a conventional activated sludge system in the treatment of wastewater containing high-molecular-weight compounds. *Water Environment Research*, 71, 64-70.

Cicek N., Winnen H., Suidan M., Wren B., Urbain V., and Manem J. (1998). Effectiveness of the membrane bioreactor in the biodegradation of high molecular weight compounds. *Water Research*, 32 (5), 1553-1563.

Cornel P. and Krause S. (2006), Membrane bioreactors in industrial wastewater treatment - European experiences, examples and trends, *Water Science and Technology*, 53 (3), 37-44.

Côté P., Buisson H., Pound C., and Arakaki G. (1997). Immersed membrane activated sludge for the reuse of municipal wastewater. *Desalination*, 113, 189-196.

Cowman J. (2004). Total nitrogen removal in a completely mixed membrane biofilm reactor for nitrification and denitrification. Northwestern University, Chicago, USA.

Cui Z-G., Li S-Y., Xia J-L., Xue T., and Huang X. (2009). Enhanced phosphorus removal in membrane bioreactor combined with electrocoagulation. *China water and wastewater*, 7, 1-4.

Daneshvar N., Oladegaragoze A., and Djafarzadeh N. (2006). Decolorization of basic dye solutions by electrocoagulation: an investigation of the effect of operational parameters. *Journal of Hazardous Materials*, B129, 116-122.

De-Bashan L.E. and Bashan Y. (2004). Recent advances in removing phosphorus from wastewater and its future use as fertilizer (1997–2003). Water Research, 38 (19), 4222-4246.

Den W. and Huang C. (2006). Parameter optimization and design aspect for electrocoagulation of silica nano-particles in wafer polishing wastewater. *Water Science and Technology*, 53 (6), 187-194.

Dermentzis K., Christoforidis A., and Valsamidou E. (2011). Removal of nickel, copper, zinc and chromium from synthetic and industrial wastewater by electrocoagulation. *International Journal of Environmental Sciences*, 1 (5). ISSN 0976-4402.

Dermentzis K., Christoforidis A., and Valsamidou E. (2011). Removal of nickel, copper, zinc and chromium from synthetic and industrial wastewater by electrocoagulation. *International Journal of Environmental Sciences*, 1 (5), 697-710.

Diaz C.B., Pardave M.P., Romo M.R., and Martinez S. (2003). Chemical and electrochemical considerations on the removal process of hexavalent chromium from aqueous media. *Journal of Applied Electrochemistry*, 33, 61-71.

Dizge N., Koseoglu-Imer D.Y., Karagunduz A. and Keskinler B. (2011). Effects of cationic polyelectrolyte on filterability and fouling reduction of submerged membrane bioreactor (MBR). *Journal of Membrane Science*, 377 (1-2), 175-181.

Donati G. and Paludetto R. (1997). Scale up of Chemical Reactors. *Catalysis Today*, (34) 483-533.

Drews A., Vocks M., Bracklow U., Iversen V., and Kraume M. (2008). Does fouling in MBR depend on SMP?. *Desalination*, 231, 141-149.

Drews A., Vocks M., Iversen V., Lesjean B., and Kraume M. (2006). Influence of unsteady membrane bioreactor operation on EPS formation and filtration resistance. *Desalination*, 192, 1-9.

Drews A. Vocks M., Bracklow U., Iversen V., and Kraume M. (2008). Does fouling in MBR depend on SMP?. *Desalination*, 231, 141-149.

Dubois M., Gilles K.A., Hamilton J.K., Rebers P.A., and Smith F. (1956). Colorimetric method for determination of sugar and related substances. Analytical Chemistry, 28, 350-356.

Dytczak M., Londry K.L., and Oleszkiewicz J. (2008). Activated sludge operational regime has significant impact on the type of nitrifying community and its nitrification rates. *Water Research*, 42, 2320-2328.

Eckenfelder W., Goodman B., and Englande A. (1972). Scale-up of biological wastewater treatment reactors. *Advances in Biochemical Engineering Biotechnology*, 2, 145-180..

Elektorowicz M,, Abdoli H., and Oleszkiewicz J.A. (2007), Assessment of electrokinetic metal removal from biosolids. *EREM 2007 6th Symposium on Electrokinetic Remediation*, Vigo, Spain, 12-15 June, 2007.

Elektorowicz M. and Oleszkiewicz J.A. (2009). Method of treating sludge material using Electrokinetics. EKDIM, US Patent 12/571,482.

Elektorowicz M., Bani-Melhem K., and Oleszkiewicz J. (2009). Submerged membrane electro-bioreactor - SMEBR, US Patent 12/553,680.

Elektorowicz M., Hasan S., and Oleszkiewicz J. (2011). Pilot Studies of a Novel Submerged Membrane Electro-Bioreactor (SMEBR). *Proceedings WEFTEC* 2011, New Orleans.

Elimelech M., Greory J., and Jia X. (1995). Prticle deposition and aggregation - measurement, modeling and simulation. ElSevier.

Emamjomeh M. M. and Sivakumar M. (2009). Denitrification using a monopolar electrocoagulation/flotation (ECF) process. *Journal of Environmental Management,* 91, 516-522.

Evans B. and Laughton P. (1994). Emerging trends in electrical usage at Canadian (Ontario) municipal wastewater treatment facilities and strategies for improving energy efficiency. *Water Science and Technology*, 30 (4), 17-23.

Fan F. and Zhou H. (2007). Interrelated effects of aeration and mixed liquor fractions on membrane fouling for submerged membrane bioreactor processes in wastewater treatment. *Environmental Science and Technology*, 41 (7), 2523-2528.

Fane A.G., Chang S., and Chardon E. (2002). Submerged hollow fibre membrane module-design options and operational considerations. *Desalination*, 146 (1-3), 231-236.

Ferrero G. (2011). Development of an air-scour control system for membrane bioreactors, Ph.D. thesis, University of Girona, Girona, Catalonia, Spain.

Field R.W., Wu D., Howell J.A., and Gupta B.B. (1995). Critical flux concept for microfiltration fouling. *Journal of Membrane Science*, 100, 259-272.

Flemming H.C. and Wingender J. (2001). Relevance of microbial extracellular polymeric substances (EPSs)-part I: structural and ecological aspects. *Water Science and Technology*, 43 (6), 1-8.

Flemming H.C. and Wingender J. (2003). The crucial role of extracellular polymeric substances in biofilms. In: Wuertz, S., Bishop, P.L., Wilderer, P.A. (Eds.), Biofilms in wastewater treatment: an interdisciplinary approach. *IWA Publishing, London*, 178-210.

Forrest A.L., Fattah K.P., Mavinic D.S., and Koch F.A. (2008). Optimizing struvite production for phosphate recovery in WWTP. Journal of Environmental Engineering, 134 (5), 395-402.

Frossard E., López-Hernández D., and Brossard M. (1996). Can isotopic exchange kinetics give valuable information of the rate of mineralization of organic phosphorus in soils?. Soil Biology and Biochemistry, 28, 857-864.

Gao P., Chen X., Shen F., and Chen G., (2005). Removal of chromium (VI) from wastewater by combined electrocoagulation-electroflotation without a filter. *Separation Purification Technology*, 43 (2), 117-23.

Giesen A. (1999). Crystallization process enables environmental friendly phosphate removal at low costs. *Environmental Technology*, 20 (7), 769-775.

Gil J.A., Túa L., Rueda A., Montaño B., Rodríguez M., and Prats D. (2010). Monitoring and analysis of the energy cost of an MBR. *Desalination*, 250, 997-1001.

Greenwood R. (2003). Review of the measurement of zeta potentials in concentrated aqueous suspensions using electroacoustics. *Advances in Colloid and Interface Science*, 106, 55-81 Elsevier, New York.

Grubb D.G., Guimaraes M.S., and Valencia R. (2000). Phosphate immobilization using an acidic type F fly ash. *Journal of Hazardous Materials*, 76, 217-236.

Günder B. (2001). The membrane coupled activated sludge process in municipal wastewater treatment. United States of America Technomic publishing Co., Inc. 140-147.

Gui P., Huang X., Chen,Y., and Qian, Y. (2002). Effect of operational parameters on sludge accumulation on membrane surfaces in a submerged membrane bioreactor. *Desalination*, 151 (2), 185-194.

Guibaud G., Bordas F., Saaid A., D ' abzac F., and Van Hullebusch E. (2008). Effect of pH on cadmium and lead binding by extracellular polymeric substances (EPS) extracted from environmental bacterial strains. *Colloids and Surfaces*, B 63 (1), 48-54.

Guide sur la valorisation des matières résiduelles fertilisantes. Critères de référence et normes réglementaires. Édition 2008.

Habel A.. (2010). Electrokinetic management of biosolids for the inactivation of helminth ova. Master's thesis. Concordia University. Montreal, Canada.

Hagman M., Heander E., and Jansen J.L.C. (2008). Advanced oxidation of refractory organics in leachate potential methods and evaluation of biodegradability of the remaining substrate. *Environmental Technology*, 29 (9), 941-946.

Harada H., Momonoi K., Yamazaki S., and Takizawa S. (1994). Application of anaerobic-UF membrane reactor for treatment of a wastewater containing high strength particulate organics. *Water Science and Technology*, 30 (12), 307-319.

Hasan S., Elektorowicz M., and Oleszkiewicz J. (2011). Novel submerged membrane electro-bioreactor (SMEBR) tested in l'Assomption, QC. *46th Central Canadian Symposium on Water Quality Research*, Burlington, 21-23 February, 2011.

Hasan S., Elektorowicz M., Oleszkiewicz J., and Ibeid S. (2011). Impact of current density on water quality and membrane fouling in submerged membrane electro-bioreactor (SMEBR). *26th Eastern Canadian Symposium on Water Quality Research*, Quebec, 07 - October, 2011.

Hemambika B., Johncy Rani M., and Rajesh Kannan V. (2011). Biosorption of heavy metals by immobilized and dead fungal cells: A comparative assessment. *Journal of Ecology and the Natural Environment*, 3 (5), 168-175.

Hernandez Rojas M.E., Van Kaam R., Schetrite S. and Albasi C. (2005). Role and variations of supernatant compounds in submerged membrane bioreactor fouling. *Desalination*, 179, 95-107.

Hiemenz P.C. and Rajagopalan R. (1997). Principles of Colloid and Surface Chemistry, 3rd edition, Marcel Dekker, Inc., New York.

Holler S. and Trösch W. (2001). Treatment of urban wastewater in a membrane bioreactor at high organic loading rates. *Journal of Biotechnology*, 92 (2), 95-101.

Holman J.B. and Warehem D.G. (2000). ORP as a monitoring tool in a low dissolved oxygen wastewater treatment process. *Journal of Environmental Engineering*, 129 (1), American Society of Civil Engineers, 52-58.

Holt P.K., Barton G.W., and Mitchell C.A. (1999). Electrocoagulation as a wastewater treatment. *The Third Annual Australian Environmental Engineering Research Event*. Victoria.

Holt P.K., Barton G.W., and Mitchell C.A. (2004). Deciphering the science behind electrocoagulation to remove suspended clay particles from water. *Journal of Water Science and Technology*, 50 (12), 177-184.

Holt P.K., Barton G.W., and Mitchell C.A. (2005). The future for electrocoagulation as a localized water treatment technology. Chemosphere, 59, 355-367.

Hong S.K. and Elimelech M. (1997). Chemical and physical aspects of natural organic matter (NOM) fouling of nanofiltration membranes. *Journal of Membrane Science*, 132 (2), 159-181.

Howell J.A. (1995). Sub-critical flux operation of microfiltration. *Journal of Membrane Science*, 107, 165-171.

Hribljan M.J. (2007). WEF Webcast "large MBR design and residuals handling".

Huang X., Liu R., and Qian Y. (2000). Behaviour of soluble microbial products in a membrane bioreactor. *Process Biochemistry*, 36, 401-406.

Hulser P., Kruger U.A., and Beck F. (1996). The cathodic corrosion of aluminum during the electrodeposition of paint: electrochemical measurements. *Corrosion Science*, 38 (1), 47-57.

Hunter R.J. (1981). Zeta Potential in colloid science. *Academic Press*, London.

Hwang E.J., Sun D.D., and Tay J.H. (2002). Operational factors of submerged inorganic membrane bioreactor for organic wastewater treatment: sludge concentration and aeration rate. *Water Science and Technology*, 36 (11), 9-18.

Hwang J.H. and Oleszkiewicz J.A. (2007). Effect of cold-temperature shock on nitrification. *Water Environment Research*, 79 (9), 964-968.

Ibanez J.G., Takimoto M.M., and Vasquez R.C. (1995). Laboratory experiments on electrochemical remediation of the environment: electrocoagulation of oily wastewater, *Journal of Chemical Education*, 72 (11), 1050-1052.

Ibeid S., Elektorowicz M., and Oleszkiewicz J. (2010a). Modification of activated sludge characteristics due to applying direct current (DC) field. *Proceedings IWA Water World Congress*, Montreal, 20-27 September, 2010.

Ibeid S., Elektorowicz M., and Oleszkiewicz J. (2010b). Impact of electro-coagulation on the fate of soluble microbial products (SMP) in submerged membrane electro-bioreactor (SMEBR). *Proceedings CSCE Specialty Conference on Environmental Engineering*, Winnipeg, 9-12 June, 2010.

Ibeid S., Elektorowicz M., Oleszkiewicz J., and Hasan S. (2011). Novel approach for the reduction of membrane fouling. *46th Central Canadian Symposium on Water Quality Research*, Burlington, 21-23, February, 2011.

Ilhan F., Kurt U., Apaydin O., Gonullu M.T. (2008). Treatment of leachate by electrocoagulation using aluminum and iron electrodes. *Journal of Hazardous Materials*, 154, 381-389.

Inan H., Dimoglo A., Simisek H., and Karpuzcu M. (2004). Olive oil mill wastewater treatment by means of electrocoagulation. *Separation Purification Technology*, 36, 23-31.

Inglezakis V.J., Loizidou M.D., and Grigoropoulou H.P. (2003). Ion exchange of Pb^{2+}, Cu^{2+}, Fe^{3+} and Cr^{3+} on natural clinoptilolite: selectivity determination and influence on activity on metal uptake. *Journal of Colloid and Interface Science,* 261, 49-54.

Irdemez S., Yildiz Y.S., and Tosunoglu V. (2006). Optimization of phosphate removal from wastewater by electrocoagulation with aluminum plate electrodes. *Separation and Purification Technology*, 52, 394-401.

Irdemez, S., Demircioglu, N. and Sevki Yildiz, Y. (2006). The effects of pH on phosphate removal from wastewater by electrocoagulation with iron plate electrodes. *Journal of Hazardous Materials*, B137 (2), 1231-1235.

Itonaga T., Kimura K., and Watanabe Y. (2004), Influence of suspension viscosity and colloidal particles on permeability of membrane used in membrane bioreactor (MBR). *Water Science and Technology*, 50, 301-309.

Jahn A. and Nielsen P.H. (1998). Cell biomass and exopolymer composition in sewer biofilms. *Water Science and Technology*, 37 (1), 17-24.

Jeanmaire N., and Evans T. (2001). Technico-economic feasibility of P-recovery from municipal wastewaters. *Environmental Technology*, 22 (11), 1355-1361.

Jefferson B., Laine A., Brindle K., and Judd S., and Stephenson T. (1998). *Proceedings of Water Environment 98: maintaining the flow*, London, 26 March, 1998.

Jenkins R.L. and Scheybeler B.J. (1981). Metals removal and recovery from municipal sludge. *Journal of the Water Pollution Control Federation*, 5, 25-31.

Jeong Y.S. and Chung J.S. (2006). Biodegradation of thiocyanate in biofilm reactor using fluidized-carriers. *Process Biochemistry*, 41, 701-707.

Jiang T., Kennedy M.D., Guinzbourg B.F., Vanrolleghem P.A., and Schippers J.C. (2005). Optimising the operation of a MBR pilot plant by quantitative analysis of the membrane fouling mechanism. *Water Science and Technology*, 51 (6), 19-25.

Jin B., Wilén B.M., and Lant P. (2004). Impacts of morphological, physical and chemical properties of activated flocs on dewaterability of activated sludge. *Journal of Chemical Engineering*, 98, 115-126.

Judd S. (2006). The MBR book: principles and applications of membrane bioreactors in water and wastewater treatment. 1st edition, Elsevier.

Judd S. (2011). The MBR book: principles and applications of membrane bioreactors in water and wastewater treatment. 2nd edition, Elsevier.

Karr P.R., Keinath T.M. (1978). Influence of particle size on sludge dewaterability. *Journal of the Water Pollution Control Federation*, 50, 1911-1930.

Kermani M., Bina B., Movahedian H., Mehdi Amin M., and Nikaeen M. (2009). Biological phosphorus and nitrogen removal from wastewater using moving bed biofilm process. *Iranian Journal of Biotechnology*, 7 (1), 19-27.

Kibalczyc W. (1989). Study of calcium phosphate precipitation at 378C. *Crystal Research and Technol*ogy, 24, 773-780.

Kibalczyc W., Christoffersen J., Christoffersen M.R. Zielenkiewicz A. and Zielenkiewicz W. (1990). The effect of magnesium-ions on the precipitation of calcium phosphates. *Journal of Crystal Growth,* 106, 355-366.

Kim H.Y., Yeon K.M., Lee C.H., Lee S.H., and Swaminathan T. (2006). Biofilm structure and extracellular polymeric substances in low and high dissolved oxygen membrane bioreactors. *Separation Science and Technology*, 41 (7), 1213-1230.

Kim K.J., Chen V., and Fane A.G. (1993). Ultrafiltration of colloidal silver particles : flux, rejection and fouling. *Colloid and Interface Science*, 155, 347-359.

Kim Y.M., Park D., Jeon C.O., Lee D.S., Park J.M.(2008). Effect of HRT on the biological pre-denitrification process for the simultaneous removal of toxic pollutants from cokes wastewater. *Bioresource Technology*, 99, 8824-8832.

Kobya M., Hiz H., Senturk E., Aydiner C., and Demirbas E. (2006). Treatment of potato chips manufacturing wastewater by electrocoagulation. *Desalination*, 190, 201-211.

Koparal A.S. and Ogutveren U.B. (2002). Removal of nitrate from water by electroreduction and electrocoagulation. *Journal of Hazardous Materials*, 89, 83-94.

Kristine C.F. (2005). The application of a membrane bioreactor for wastewater treatment on a northern Manitoban aboriginal community. Master thesis. University of Manitoba. Manitoba, Canada.

Kumar P.R., Chaudhari S., Khilar K.C., and Mahajan S.P. (2004). Removal of arsenic from water by electrocoagulation. *Chemosphere*, 55 (9), 1245-1252.

Kurniawan A., Chan G.Y.S., Lo W.H., and Babel S. (2006). Physicochemical treatment techniques for wastewater laden with heavy metals. *Chemical Engineering Journal*, 118, 83-98.

Kurt U., Gonullu M.T., Ilhan F., and Varinca K. (2008). Treatment of domestic wastewater by electrocoagulation in a cell with Fe-Fe electrodes. *Environmental Engineering Science*, 25 (2), 135-161.

Kuzmenko D., Arkhangelsky E., Belfer S., Freger V., and Gitis V. (2005). Chemical cleaning of ultrafiltration membranes fouled by BSA. *Desalination*, 179 (1-3), 323-333.

Kwannate M.S. (2007). Membrane fouling studies in suspended and attached growth membrane bioreactor systems. Asian Institute of Technology. School of Environment, Resources, and Development, Thailand.

Lai C.L. and Lin S.H. (2003). Electrocoagulation of chemical mechanical polishing (CMP) wastewater from semiconductor fabrication. *Journal of Chemical Engineering*, 95, 205-211.

Laridi R., Auclair J.C., and Benmoussa H. (2005). Laboratory and pilot-scale phosphate and ammonium removal by controlled struvite precipitation following coagulation and flocculation of swine wastewater. *Environmental Technology*, 26, 525-536.

Laspidou C.S. and Rittmann B.E. (2002). A unified theory for extracellular polymeric substances, soluble microbial products, and active and inert biomass. *Water Research*, 36 (11), 2711-2720.

Le-Clech P., Chen V., and Fane T.A.G. (2006). Fouling in membrane bioreactors used for wastewater treatment-A review. *Journal of Membrane Science*, 284 (1-2), 17-53.

Le-Clech P., Jefferson B., Chang I.S., and Judd S.J. (2003). Critical flux determination by the flux-step method in a submerged membrane bioreactor. *Journal of Membrane Science*, 227, 81-93.

Lee M. and Kim J. (2009). Membrane autopsy to investigate CaCO3 scale formation in pilot-scale, submerged membrane bioreactor treating calcium-rich wastewater. *Journal of Chemical Technology and Biotechnology*, 84 (9), 1397-1404.

Lee N., Amy G., and Lozier J. (2005). Understanding natural organic matter fouling in low-pressure membrane filtration. *Desalination*, 178 (1-3), 85-93.

Lee W., Kang S., and Shin H. (2003). Sludge characteristics and their contribution to microfiltration in submerged membrane bioreactors. *Journal of Membrane Science*, 216 (1-2), 217-227.

Lesjean B. (2009). Salient outcomes of the European R&D projects on MBR technology, In: *Final MBR-Network Workshop*, Berlin, 31 March-April 1, 2009.

Lesjean B., Rosenberger S., Laabs C., Jekel M., Gnirss R., and Amy G. (2005). Correlation between membrane fouling and soluble/colloidal organic substances in membrane bioreactors for municipal wastewater treatment. *Water Science and Technology*, 51 (6-7), 1-8.

Li W., Zhou Q., and Hua T. (2010). Removal of organic matter from landfill leachate by advanced oxidation processes: A review. *International Journal of Chemical Engineering*, Hindawi Publishing Corporation. Volume 2010, Article ID 270532, 10 pages.

Liao B.Q., Bagley D.M., Kraemer H.E., Leppard G.G., and Liss S.N. (2004). A review of biofouling and its control in membrane separation bioreactors. *Water Environment Research*, 76 (5), 425-436.

Lin C.F. and Shien Y. (2001). Sludge dewatering using centrifuge with thermal/polymer conditioning. *Water Science and Technology*, 44 (10), 321-325.

Lin C.J., Lo S.L., Kuo C.Y., and Wu C.H. (2005). Pilot-scale electrocoagulation with bipolar aluminum electrodes for onsite domestic greywater reuse. *Journal of Environmental Engineering*, 131 (3), 491-495.

Liu H. and Fang H.H.P. (2002). Extraction of extracellular polymeric substances (EPS) of sludge. *Journal of Biotechnology*, 95 (3), 249-256.

Liu H., Chen L., Cai L., and Hong D. (2010). Effects of nitrogen and phosphorus removal in sequencing batch membrane bioreactor with different modes. *International Conference on Mechanic Automation and Control Engineering (MACE)*, Wuhan, 26-28 June, 2010.

Liu R., Huang X., Sun Y.F., and Qian Y. (2003). Hydrodynamic effect on sludge accumulation over membrane surfaces in a submerged membrane bioreactor. *Process Biochemistry*, 39 (2), 157-163.

Liu R., Huang X., Wang C., Chen L., and Qian Y. (2000). Study on hydraulic characteristics in a submerged membrane bioreactor process. *Process Biochemistry*, 36 (3), 249-254.

Liu Y., Lam M.C., and Fang H.H.P. (2001). Adsorption of heavy metals by EPS of activated sludge. *Water Science and Technology*, 43 (6), 59-66.

Lowry O.H., Resebrough N.J., Farr A.L., and Randall R. (1951). Protein measurement with the folin phenol reagent. *Journal of Biological Chemistry*, 193, 265-275.

Luo Y.L., Yang Z.H., Xu Z.Y., Zhou L.J., Zeng G.M., Huang J., Xiao Y., and Wang L.K. (2011). Effect of trace amounts of polyacrylamide (PAM) on long-term performance of activated sludge. *Journal of Hazardous Materials*, 189, 69-75.

Madaeni S.S., Fane A.G., and Wiley D.E. (1999). Factors influencing critical flux in membrane filtration of activated sludge. *Journal of Chemical Technology and Biotechnology*, 74, 539-543.

Madyiwa S., Chimbari M., Nyamangara J., and Bangira C. (2002). Cumulative effects of sewage sludge and effluent mixture application on soil properties of sandy soil under a mixture of star and kikuyu grasses in Zimbabwe. *Physics and Chemistry of the Earth*, 27, 747-753.

Mahesh S., Prasad B., Mall I.D., and Mishra I.M. (2006). Electrochemical degradation of pulp and paper mill wastewater. Part 1. COD and color removal. *Industrial and Engineering Chemistry Research*, 45, 2830-2839.

Maleki A., Ali Zazouli M., Izanloo H., and Rezaee R. (2009). Composting plant leachate treatment by coagulation-flocculation process. *American-Eurasian Journal of Agricultural and Environmental Science*, 5 (5), 638-643.

Mallevialle J., Odendaal P.E., and Wiesner M.R., (1996). Water treatment membrane processes, McGraw-Hill.

Manem J. and Sanderson R. (1996). Membrane bioreactors in water treatment processes, chapter17. AWWARF/Lyonnaise des Eaux/WRC, McGraw Hill.

Marder L., Bernardes A.M., and Ferreira J.Z. (2004). Cadmium electroplating wastewater treatment using a laboratoryscale electrodialysis system. *Separation and Purification Technology*, 37, 247-255.

Mashhad N.S. (2010). Investigation of activated sludge properties under different electrical field and in the presence of calcium. Master's thesis. Concordia University. Montreal, Canada.

Mathew M. and Schroeder L.W. (1979). Crystal structure of a struvite analogue, $MgKPO_4.6H_2O$. *Act Crystallographica*, B35, 11-13.

Matteson M.J., Dobson R.L., Glenn R.W., and Kukunoor N.S. (1995). Electrocoagulation and separation of aqueous suspensions of ultrafine particles. *Colloids and Surfaces*, A 104, 101-109.

Mavrov V., Stamenov S., Todorova E., Chmiel H., and Erwe T. (2006). New hybrid electrocoagulation membrane process for removing selenium from industrial wastewater. *Desalination*, 201 (1-3), 290-296.

Meng F., Chae S., Drews A., Kraume M, Shin H., and Yang F. (2009). Recent advances in membrane bioreactors (MBR): membrane fouling and membrane material. *Water Research*, 43 (6), 1489-1512.

Meng F., Shi B., Yang F., and Zhang, H. (2007). Effect of hydraulic retention time on membrane fouling and biomass characteristics in submerged membrane bioreactors. *Bioprocess and Biosystems Engineering*, 30 (5), 359-367.

Meng F., Zhang H., Yang F., Zhang S., Li Y., and Zhang X. (2006). Identification of activated sludge properties affecting membrane fouling in submerged membrane bioreactors. *Separation Purification Technology*, *51*, 95-103.

Metcalf and Eddy (2003). Wastewater engineering: treatment and reuse (4^{th} international edition). McGraw-Hill, New York.

MinGu K. and Nakhla G. (2010). Comparative Performance of A^2/O and a Novel Membrane-Bioreactor-Based Process for Biological Nitrogen and Phosphorus Removal. *Water Environment Research*, 82 (1), 69-76.

Mollah M.Y.A., Morkovsky P., Gomes J.A.G., Kesmez M., Parga J., and Cocke D.L. (2004). Fundamentals, present and future perspectives of electrocoagulation. *Journal of Hazardous Materials*, 114 (1-3), 199-210.

Monteiro P.S. (1997). The influence of the anaerobic digestion process on the sewage sludge rheological behaviour. *Water Science and Technology*, 36 (11), 61-67.

Mueller J.A., Boyle W.C., and Popel H.J. (2002). Aeration: principles and practice in: Eckenfelder WW, Malina JR and Patterson JW (Eds.) water quality management library, CRC Press, Boca Raton.

Mulder M. (1996). Basic principle of membrane technology, 2nd edition, Nertherland, Kluwer Academic Publisher.

Muller E.B., Stouthamer A.H., van Verserveld H.W., and Eikelboom D.H. (1995). Aerobic domestic waste water treatment in a pilot plant with complete sludge retention by cross-flow filtration. *Water Research*, 29 (40), 1179-1189.

Nagaoka H. and Kudo C. (2002). Effect of loading rate and intermittent aeration cycle on nitrogen removal in membrane separation activated sludge process. *Water Science and Technology*, 46 (8), 119-126.

Nagaoka H., Ueda S., and Miya A. (1996). Influence of extracellular polymers on the membrane separation activated sludge process. *Water Science and Technology*, 34, 165-172.

Nagaoka H., Yamanishi S., and Miya A. (1998). Modeling of biofouling by extracellular polymers in a membrane separation activated sludge. *Water Science and Technology*, 38, 497-504.

Nancollas G.H. (1984). Phosphate minerals. Springer-Verlag, London.

Nelson N.O., Mikkelsen R.L., and Hesterberg D.L. (2003). Struvite precipitation in anaerobic swine lagoon liquid: Effect of pH and Mg:P ratio and determination of rate constant. *Bioresource Technology*, 89, 229-236.

Nerenberg R. (2005). Membrane biofilm reactors for water and wastewater treatment. *Borchardt Conference: A Seminar on Advances in Water and Wastewater Treatment,* February 23-25, Ann Arbor, MI.

Ng H.Y. and Hermanowicz S. (2005). Membrane bioreactor operation at short solids retention times: performance and biomass characteristics. *Water Research*, 39 (6), 981-992.

Ngo H.H., Guo W., and Xing W. (2008). Evaluation of a novel sponge-submerged membrane bioreactor (SSMBR) for sustainable water reclamation. *Bioresource Technology*, 99 (7), 2429-2435.

Ni'am M.F., Othman F., Sohaili J, and Fauzia Z. (2007). Electrocoagulation technique in enhancing COD and suspended solids removal to improve wastewater quality. *Water Science and Technology*, 56 (7), 47-53.

Nielsen P.H. and Jahn A. (1999). Microbial extracellular polymeric substances: characterization, structure, and function. Germany. *Springer*, 49-69.

Nikolaev N.V., Kozlovskii A.S., and Utkin I.I. (1982). Treating natural waters in small water systems by filtration with electrocoagulation. *Soviet Journal of Water Chemistry and Technology*, 4 (3), 244-247.

Novak J.T., Goodman G.L., Pariroo A., and Huang J.C.h. (1988). The blinding of sludges during filtration. *Journal of the Water Pollution Control Federation*, 60, 206-214.

Novikova S.P., Shkorbatova T.L., and Sokol E.Y. (1982). Purification of effluents from the production of synthetic detergents by electrocoagulation. *Soviet Journal of Water Chemistry and Technology*, 4 (4), 353-357.

Nystrom M., Kaipia L., and Luque S. (1995). Fouling and retention of nanofiltration membranes. *Journal of Membrane Science*, 98 (3), 249-262.

of total chromium from aqueous solution using Sargassum polycystum. *Environmental Progress and Sustainable Energy*, DOI: 10.1002/ep.10416.

Ognier S., Wisniewski C., and Grasmick A. (2002). Influence of macromolecule adsorption during filtration of a membrane bioreactor mixed liquor suspension. *Journal of Membrane Science*, 209 (1), 27-37.

Owen G., Bandi M., Howell J.A., and Churchuose S.J. (1995). Economic assessment of membrane processes for water and wastewater treatment. *Journal of Membrane Science*, 102, 77-91.

Panayotiva M. and Fritsch J. (1996). Treatment of wastewater from the lead-zinc ore processing industry. *Journal of Environmental Science and Health*, A 31 (9), 2155-2165.

Parga j.R., Cocke D.L., Valenzuela J.L., Gomes J.A., Kesmez M., Irwin G., Moreno H., and Weir M. (2005). Arsenic removal via electrocoagulation from heavy metal contaminated

groundwater in La Comarca Lagunera Me´xico. *Journal of Hazardous Materials*, 124, 247-254.

Parker D.S., Kaufman W.J., and Jenkins D. (1972). Floc breakup in turbulent flocculation processes. *Journal of the Sanitary Engineering Division: proceedings of the American Society of Civil Engineers*, 98, 79-99.

Parker D.S., Kinnear D.J., and Wahlberg E.J. (2001). Review of folklore in the design and operation of secondary clarifiers. *Journal of Environmental Engineering*, 127 (6), 476-484.

Patience M., Addai-Menash J., and Ralston J. (2003). Investigation of the effect of polymer type on flocculation, rheology and dewatering behavior of kaolinite dispersions, *International Journal of Mineral Processing*, 71, 247-268.

Pendashteh A.R., Fakhru'l-Razi A., Madaeni S.S., Abdullah L.C., Day Z.Z.A., and Biak R.A. (2011). Membrane foulants characterization in a membrane bioreactor (MBR) treating hypersaline oily wastewater. *Chemical Engineering Journal*, 168 (1), 140-150.

Phalakornkule C., Mangmeemak J., Intrachod K., and Nuntakumjorn B. (2010). Pretreatment of palm oil mill effluent by electrocoagulation and coagulation. *Science Asia*, 36, 142-149.

Pouet M.F. and Grasmick A. (1995). Urban wastewater treatment by electrocoagulation and flotation. *Water Science and Technology*, 31 (3-4), 275-283.

Radaideh J.A., Ammary B.Y., and Al-Zboon K.K. (2010). Dewaterability of sludge digested in extended aeration plants using conventional sand drying beds. *African Journal of Biotechnology*, 9 (29), 4578-4583.

Rittmann B.E., Bae W., Namkung E., and Lu C.J. (1987). A critical evaluation of microbial product formation in biological processes. *Water Science and Technology*, 19 (3-4), 517-528.

Roorda J.H. and van der Graaf J.H.J.M. (2001). New parameter for monitoring fouling during ultrafiltration of WWTP effluent. *Water Science and Technology*, 43 (10), 241-248.

Rosenberger S. and Kraume M. (2003). Parameters influencing filterability of activated sludge in membrane bioreactors. *Proceeding, AWWA Membrane Technology*, Atlanta 2-5 March 2003.

Rosenberger S., Kubin K., and Kraume, M. (2002). Rheology of activated sludge in membrane bioreactors. *Engineering in Life Sciences*, 2 (9), 269-275.

Rosenberger S., Laabs C., Lesjean B., Gnirss R., Amy G., Jekel M., and Schrotter J.C. (2006). Impact of colloidal and soluble organic material on membrane performance in membrane bioreactors for municipal wastewater treatment. *Water Research*, 40, 710-720.

Rosenberger S., Schreiner A., Wiesmann U., and Kraume M. (2001). Impact of different sludge ages on the performance of membrane bioreactors. *In: Proceedings IWA Berlin World Water Congress*, 15-19 October 2001.

Saleem M., Bukhari A.A., and Akram M.N. (2011). Electrocoagulation for the treatment of wastewater for reuse in irrigation and plantation. *Journal of Basic and Applied Sciences*, 7 (1), 11-20.

Sanchez-Monedore M.A., Mondini C., Nobili M., Leita L., and Roig A. (2004). Land application of biosolids: soil response to different stabilization degree of treated organic matter, *Waste Management*, 24, 325-332.

Sanders J.R., Trevor Mc.MA., and Christensen B.T. (1986). Extractability and bioavailability of Zn, Ni, Cd, and Cu in three Danish soils sampled 5 years after application of sewage sludge. *Journal of the Science of Food and Agriculture*, 37, 1155-1164.

Schafer A.I., Pihlajamaki A., Fane A.G., Waite T.D., and Nystrom M. (2004). Natural organic matter removal by nanofiltration: effects of solution chemistry on retention of low molar mass acids versus bulk organic matter. *Journal of Membrane Science*, 242 (1-2), 73-85.

Schulze-Rettmer R. (1991). The simultaneous chemical precipitation of ammonium and phosphate in the form of magnesium-ammonium-phosphate. *Water Science and Technology,* 23, 659-667.

Selck H., Decho A.W., and Forbes V.E. (1999). Effect of chronic metal exposure and sediment organic matter on digestive absorption efficiency of cadmium by the deposit-feeding polychaete Capitella species I. *Environmental Toxicology and Chemistry*, 18 (6), 1289-97.

Senthikumar R., Vijaraghavan K., Jegan J., and Velan M. (2010) Batch and column removal

Seo G.T., Lee T.S., Moon B.H., Choi K.S., and Lee H.D. (1997). Membrane separation activated sludge for residual organic removal in oil wastewater. *Water Science and Technology*, 36 (12), 275-282.

Sears K., Oleszkiewicz J.A., and P. Lagasse P. (2003). Nitrification in pure oxygen activated sludge systems. *Journal of Environmental Engineering*, 129 (2), 130-135.

Shama S.A., Moustafa M.E., and Gad M.A. (2010). Removal of heavy metals Fe^{3+}, Cu^{2+}, Zn^{2+}, Pb^{2+}, Cr^{3+} and Cd^{2+} from aqueous solutions by using eichhornia crassipes.*Portugaliae Electrochimica Acta , 28(2), 125-133.*

Sheng G.P., Yu H.Q., and Yue Z.B. (2005). Production of extracellular polymeric substances from Rhodopseudomonas acidophila in the presence of toxic substances. *Applied Microbiology and Biotechnology*, 69 (2), 216-222.

Shin H.S., Kang S.T., Nam S.Y. (2001). Effect of carbohydrate and protein in the EPS on sludge settling characteristics. *Water Science and Technology*, 43 (6), 193-196.

Simon J. (2006). The MBR Book, Elsevier, Jordan Hill, Oxford, UK, 1st edition.

Skinner H.C.W. (2000). Minerals and human health. *Environmental Mineralogy,* 2, 383-412, (D.J. Vaughan and R.A. Wogelius, editors). European Mineralogical Union.

Soltanali S. and Shams H.Z. (2008). Modeling of air stripping from volatile organic compounds in biological treatment processes. *International Journal of Environmental Science and Technology*, 5 (3), 353-360.

Sombatsompop K. (2007). Membrane fouling studies in suspended and attached growth membrane bioreactor systems (Doctoral dissertation, Asian Institute of Technology, 2007), Bangkok: Asian institute of Technology.

Song K.G., Kim Y., and Ahn K.H. (2008). Effect of coagulant addition on membrane fouling and nutrient removal in a submerged membrane bioreactor. *Desalination*, 221 (1-3), 467-474.

Soriano G.A., Erb M., Garel C., and Audic J.M. (2003). A comparative piot-scale study of the performance of conventional activated sludge and membrane bioreactors under limiting operating conditions. *Water Environmental Research*, 75 (3), 225-231.

Stephenson T., Judd S.J., Jefferson B., and Brindle K., (2000). Membrane bioreactors for wastewater treatment. *IWA publishing*, London.

Sun Y., Wang Y., and Huang X. (2007). Relationship between sludge settleability and membrane fouling in a membrane bioreactor. *Frontiers of Environmental Science and Engineering in China*, 1 (2), 221-225.

Sutherland I.W. (2001). The biofilm matrix - an immobilized but dynamic microbial environment. *Trends in Microbiology*, 9 (5), 222-227.

Sze A., Erickson D., Ren L., and Li D. (2003). Zeta-Potential measurement using the Smoluchowski equation and the slope of the current-time relationship in electroosmotic flow. *Journal of Colloid and Interface Science*, *261*, 402-410.

Szpyrkowicza L., Kaulb S.N., Netib R.N., and Satyanarayan S. (2005). Influence of anode material on electrochemical oxidation for the treatment of tannery wastewater. *Water Research*, 39, 1601-1613.

Tarnacki K., Lyko S., Wintgens T., and Natau F. (2005). Impact of extracellular polymeric substances on the filterability of activated sludge in membrane bioreactors for landfill leachate treatment. *Desalination*, 179, 181-190.

Taylor A.W., Fraizer A.W., and Gurney E.L. (1963). Solubility products of magnesium ammonium and magnesium potassium phosphates. *Journal of the Chemical Societ*y, 59, 1580-1584.

Taylor J.S. and Jacobs Ed.P. (1996). Water treatment: membrane processes, chapter 9. New York, McGraw-Hill, Inc.

Trivedi H.K. (2004). Flat-plate microfiltration membrane bioreactor designed for ultimate nutrient removal (UNRTM). *Proceedings WEFTEC* 2004, New Orleans.

Trouve E., Urbain V. and Manem J. (1994). Treatment of municipal wastewater by a membrane bioreactor: reusults of a semi-industrial pilot-scale study. *Water Science and Technology*, 30 (4), 151-157.

Trussell R.S., Merlo R.P., Hermanowicz S. W., and Jenkins D. (2006). The effect of organic loading on process performance and membrane fouling in a submerged membrane bioreactor treating municipal wastewater. *Water Research*, 40 (14), 2675-2683.

Tsuneda S., Aikawa H., Hayashi H., Yuasa A., and Hirata A. (2003). Extracellular polymeric substances responsible for bacterial adhesion onto solid surface. *FEMS microbiology Letters*, 223 (2), 287-292.

Ueda T., Hata K., and Kikuoka Y. (1996). Treatment of domestic sewage from rural settlements by a membrane bioreactor. *Water Science and Technology*, 34 (9), 189-196.

Valsami-Jones E. (2001). Mineralogical controls on phosphorus recovery from wastewaters. *Mineralogical Magazine, 65 (5), 611-620.*

van den Brink P., Zwijnenburg A., Temmink H., van Loosdrecht M. (2011). Effect of temperature shocks on membrane fouling in membrane bioreactors. *ICOM 2011*, July 23-29, Amsterdam, 2011.

Van de Graaf A.A., Mulder A., de Bruijn P., Jetten M.S.M., Robertson L.A., and Kuenen J.G. (1996). Autotrophic growth of anaerobic ammonium oxidizing micro-organisms in a fluidised bed reactor. *Microbiology*, 142, 2187-2196.

Vik E.A., Carlson D.A., Eikun A.S., and Gjessing E.T. (1984). Electrocoagulation of potable water. *Water Research*, 18 (11), 1355-1360.

Visvanathan C., Yang B.S., Muttamara S., and Maythanukhraw R. (1997). Application of air backflushing technique in membrane bioreactor. *Water Science and Technology*, 36 (12), 259-266.

Visvanathan C., Yang B.S., Muttamara S., and Maythanukhraw R. (1997). Application of air backflushing technique in membrane bioreactor. *Water Science and Technology*, 36 (12), 259-266.

Wang P., Wang Z., Wu Z., and Mai S. (2011). Fouling behaviors of two membranes in a submerged membrane bioreactor for municipal wastewater treatment. *Journal of Membrane Science*, 382 (1-2), 60-69.

Wastewater Engineering Treatment and Reuse, Metcalf and Eddy, revised by George Tchobanoglous, Franklin L. Burton and H. David Stensel, (2003), McGraw-Hill, New York, 4th edition.

Webber M. and Singh S.S. (1995) Contamination of agricultural soils. In D.F. Acton and L.J. Gregorich (Eds.). The health of our soils: toward sustainable agriculture in Canada. (Chap. 9). Centre for land and biological resources research, research branch, agriculture and Agri-Food Canada.

Wei V., Oleszkiewicz J.A., and Elektorowicz M. (2009). Nutrient removal in an electrically enhanced membrane bioreactor. *Water Science and Technology*, 60 (31), 59-3164.

Wei V., Oleszkiewicz J.A., and Elektorowicz M. (2010). Membrane fouling reduction in an electrically enhanced membrane bioreactor. *Proceedings IWA Regional Conference and Exhibition on Membrane Technology and Water Reuse* (IWA-MTWR-2010) in Istanbul-Turkey, October 18-22, 2010.

Wicaksana F., Fane A.G., and Chen V. (2006). Fibre movement induced by bubbling using submerged hollow fibre membranes. *Journal of Membrane Science,* 271, 186-195.

Wilén B.M, Keiding K., and Nielsen P.H. (2000). Anaerobic deflocculation and aerobic reflocculation of activated sludge. *Water Research*, 34 (16), 3933-3942.

Wilén B.M., Jin B., and Lant P. (2003). Relationship between flocculation of activated sludge and composition of extracellular polymeric substances. *Water Science and Technology*, 47 (12), 95-103.

Wisniewski C., Grasmick A., and Cruz A.L. (2000). Critical particle size in membrane bioreactors case of denitrifying bacterial suspension. *Journal of Membrane Science*, 178 (1-2), 141-150.

Wolny L., Wolski P., and Zawieja I. (2008). Rheological parameters of dewatered sewage sludge after conditioning. *Desalination*, 222, 382-387.

Wong K.Y.K. (2002). Ultrasound as a sole or synergistic disinfectant in drinking water, PhD thesis, Worcester Polytechnic Institute.

Wong J.W.C. (1999). Effects of lime amendment on availability of heavy metals and maturation in sewage sludge composting. *Environmental Pollution, 106* (1), 83-89.

Wu J., Chen F., Huang X., Geng W., and Wen X. (2006). Using inorganic coagulants to control membrane fouling in a submerged membrane bioreactor. *Desalination*, 197, 124-136.

Yamamoto K. and Win K.M. (1991). Tannery wastewater treatment using sequencing batch membrane reactor. *Water Science and Technology*, 23, 1639-1648.

Yang Q., Chen J., and Zhang F. (2006). Membrane fouling control in a submerged membrane bioreactor with porous, flexible suspended carriers. *Desalination*, 189, 292-302.

Ye Y., Le Clech P., Chen V., and Fane A.G. (2005). Evolution of fouling during crossflow filtration of model EPS solutions. *Journal of Membrane Science*, 264, 190-199.

Yigit N.O., Harman I., Civelekoglu G., Koseoglu H., Cicek N., and Kitis M. (2008). Membrane fouling in a pilot-scale submerged membrane bioreactor operated under various conditions. *Desalination*, 231, 124-132.

Yongbo L., Yang Y., and Shuai W. (2011). The study of phosphorus removal by electrocoagulation with iron anodes. *Advanced Materials Research*, 183-185, 417-421.

You H.S., Huang C.P., Pan J.R., and Chang S.C. (2006). Behavior of Membrane scaling during crossflow filtration in the anaerobic MBR system. *Separation Science and Technology*, 41 (7), 1265-1278.

Zeta Potential of colloids in water and wastewater. (1985). *American Society for Testing and Materials* (ASTM Standard D 4187-82).

Zhan S., van Houten R., Eikelboom D.H., Doddema H., Jiang Z., Fan Y., and Wang J. (2003). Sewage treatment by a low energy membrane bioreactor, *Bioresource Technology*, 90, 185-192.

Zhang B. and Yamamoto K. (1996). Seasonal change of microbial population and activities in a building wastewater reuse system using a membrane separation activated sludge process. *Water Science and Technology*, 34, 295-302.

Zhang J., Zhou J., Liu Y., and Fane A.G. (2010**).** A comparison of membrane fouling under constant and variable organic loadings in submerge membrane bioreactors. *Water Research*, 44 (18), 5407-5413.

Zhang Y., Bu D., Liu G.C., Luo X., and Gu P. (2004). Study on retarding membrane fouling by ferric salts dosing in membrane bioreactors. WEMT2004, *IWA Specialty Conference*, 2004.

Zhang Z. and Huang X. (2011). Study on enhanced biological phosphorus removal using membrane bioreactor at different sludge retention times. *International Journal of Environment and Pollution*, 45 (1-3), 15-24.

Zhe Z., Tao L., Jiajuan L., Dongsheng W., and Chonghua Y. (2009). Characterization of kaolin flocs formed by polyacrylamide as flocculation aids. *International Journal of Mineral Processing*, 91, 94-99.

http://www.hydroquebec.com

Golder Associates Inc., Lakewood, CO USA. (2009). www.golder.com

Malvern Instruments Ltd., United Kingdom. (2005). www.malvern.com

Appendices

Appendix A

Critical flux at different aeration intensities in MBR and SMEBR using stepwise method

<u>Membrane critical flux vs. aeration intensity-MBR:</u>

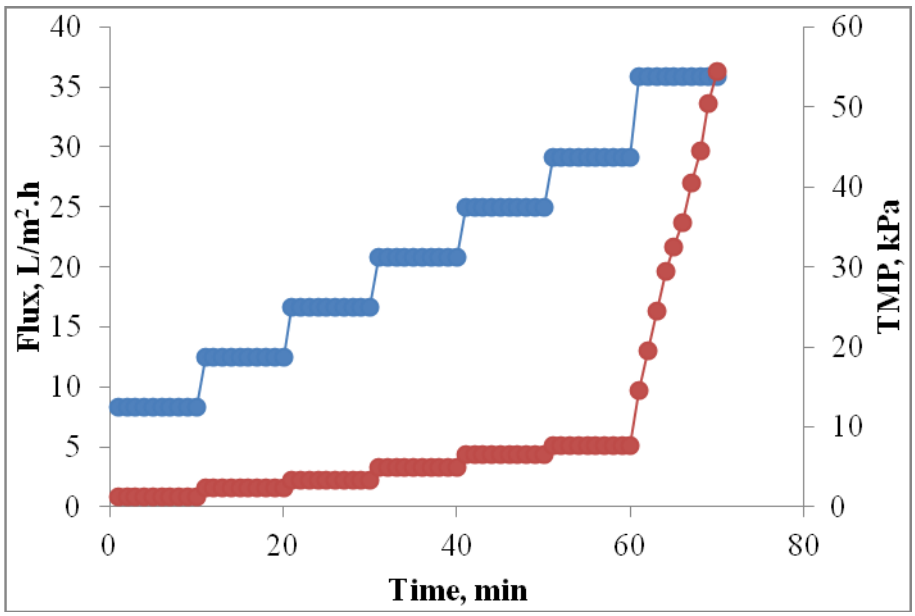

Fig. A-1: Determination of critical flux at 418 L/h in MBR.

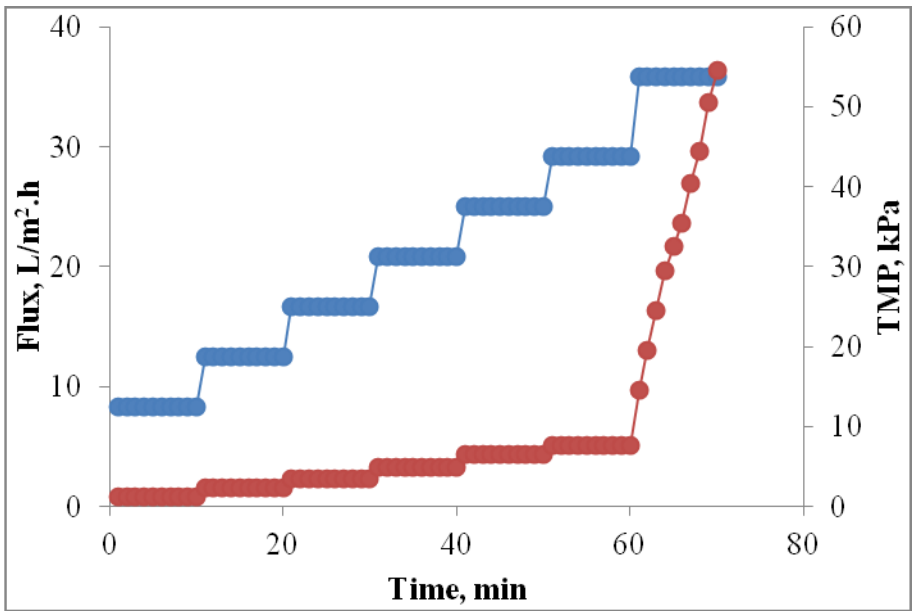

Fig. A-2: Determination of critical flux at 552 L/h in MBR.

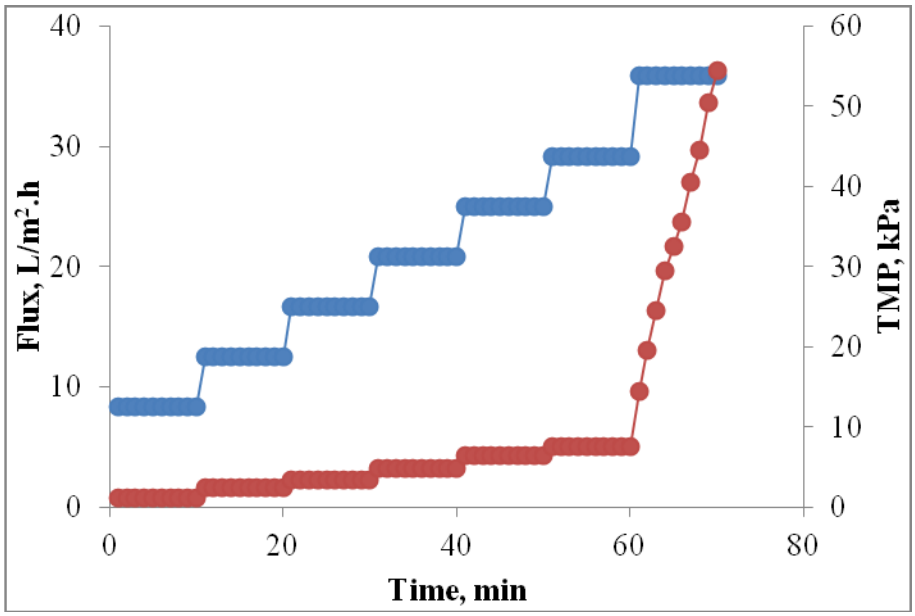

Fig. A-3: Determination of critical flux at 691 L/h in MBR.

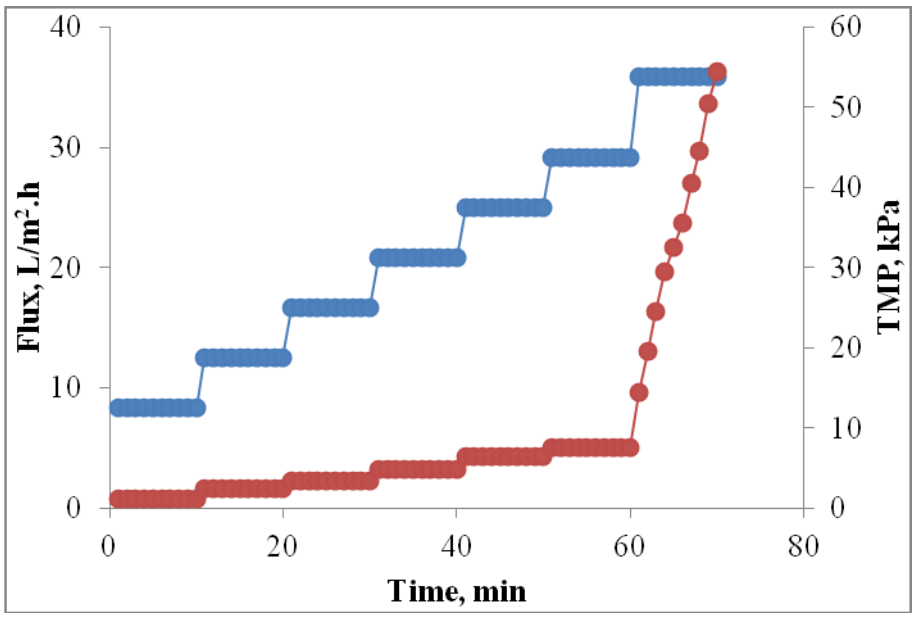

Fig. A-4: Determination of critical flux at 815 L/h in MBR.

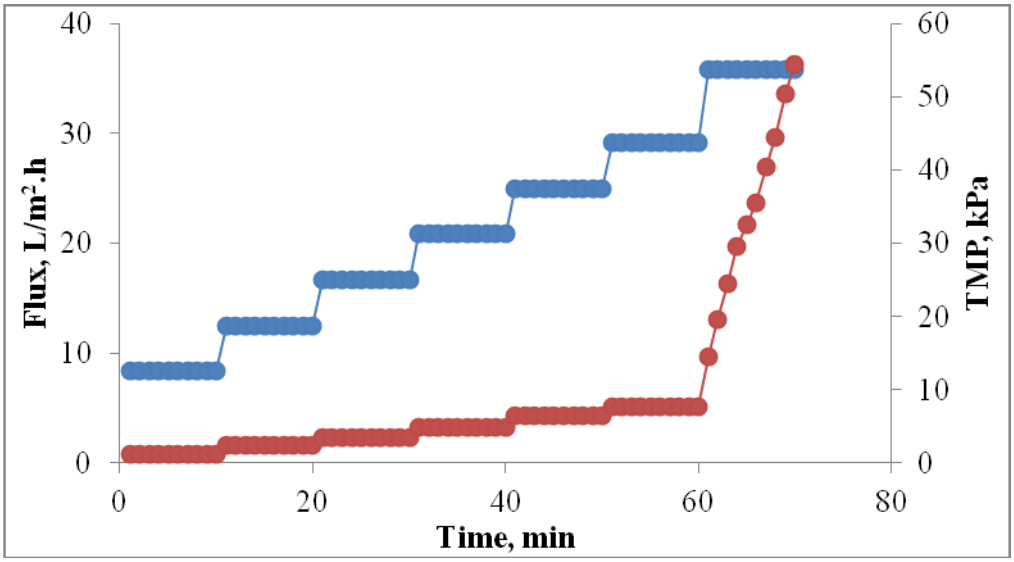

Fig. A-5: Determination of critical flux at 1143 L/h in MBR.

Membrane critical flux vs. aeration intensity-SMEBR:

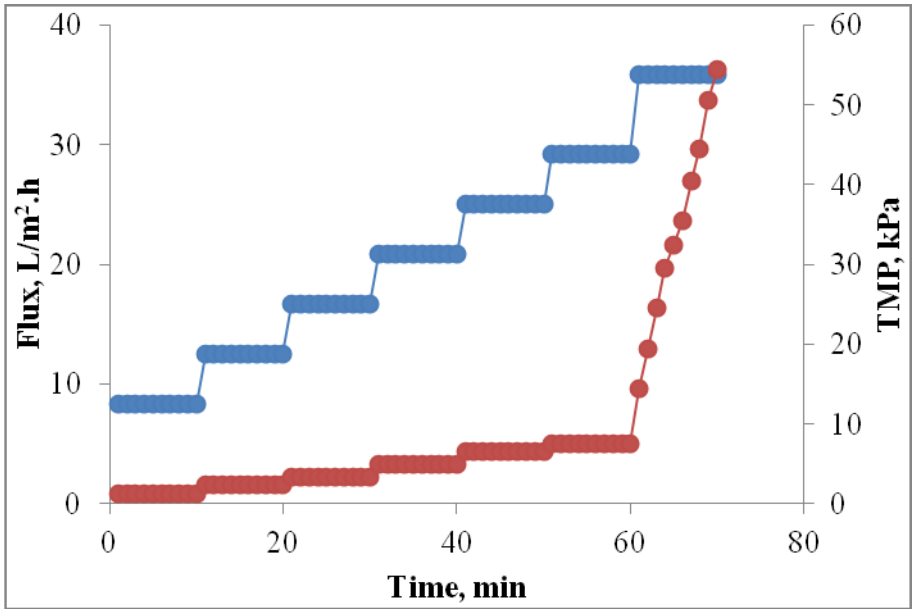

Fig. A-6: Determination of critical flux at 418 L/h in SMEBR.

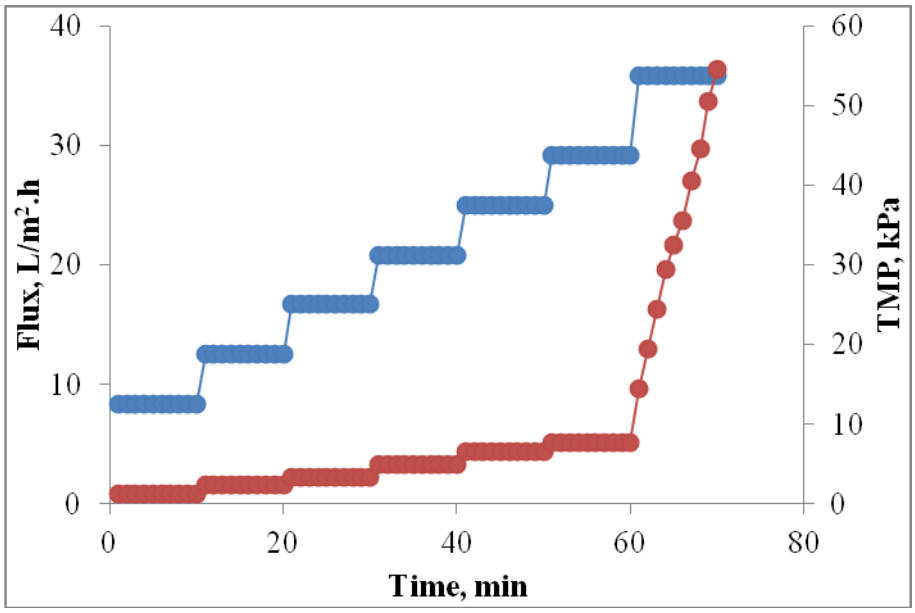

Fig. A-7: Determination of critical flux at 552 L/h in SMEBR.

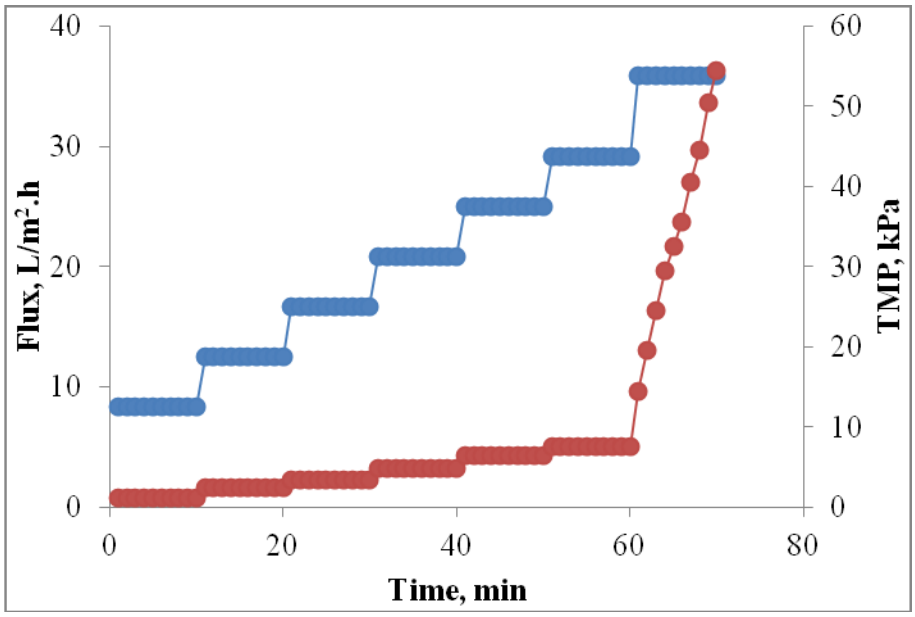

Fig. A-8: Determination of critical flux at 691 L/h in SMEBR.

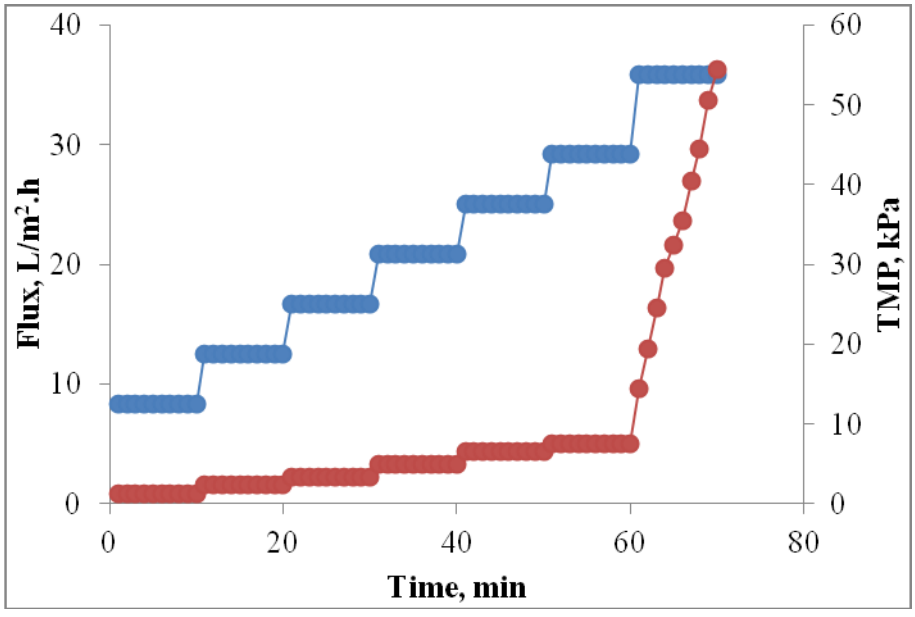

Fig. A-9: Determination of critical flux at 815 L/h in SMEBR.

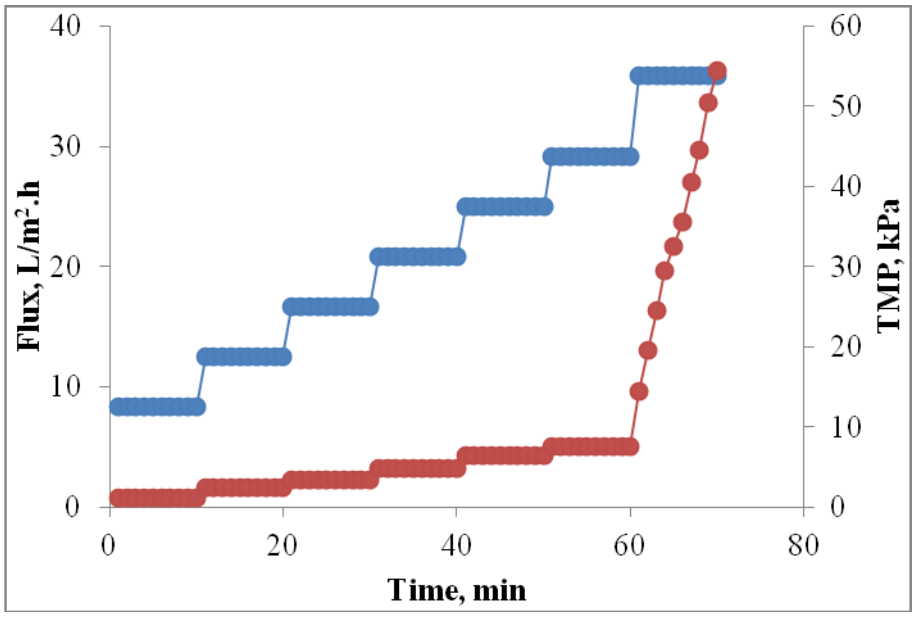

Fig. A-10: Determination of critical flux at 1143 L/h in SMEBR.

Appendix B

Experimental data

Table B-1: Sludge properties in the pilot SMEBR

Time, d	MLSS, mg/L	MLVSS, mg/L	MLVSS/MLSS	EPS_c, mg/L	EPS_p, mg/L	Zeta Potential, mV	Viscosity, mPa.s	PSD, µm
0	2400	2220	92.5	21.6	40.1	-26.2	1.2	69.0
2	3200	2920	91.3	11.3	30.0	-21.9	1.2	63.5
3	3000	2420	80.7	10.2	37.5	-28.3	1.2	53.1
4	3300	2940	89.1	12.6	39.5	-25.5	1.3	43.7
5	3720	2840	76.3	14.3	35.8	-27.9	1.1	45.7
6	3320	2640	79.5	12.4	32.8	-27.1	1.2	39.3
7	2820	2200	78.0	11.4	32.8	-27.8	1.1	35.0
8	2860	2070	72.4	10.5	34.4	-23.7	1.1	34.8
9	3460	2330	67.3	9.3	33.4	-25.0	1.2	33.7
10	3440	2440	70.9	10.1	37.0	-20.0	1.1	33.0
11	3980	2800	70.4	10.8	40.8	-17.4	1.1	31.8
12	3780	2690	71.2	11.1	42.1	-18.9	1.1	31.5
14	4200	3340	79.5	9.4	45.6	-18.1	1.1	28.7
16	4590	3620	78.9	10.4	45.5	-16.6	1.2	29.8
18	4700	3340	71.1	9.7	41.9	-18.8	1.1	31.9
20	4640	3280	70.7	10.4	35.6	-20.4	1.2	34.2
22	4600	3260	70.9	11.8	40.3	-19.5	1.2	27.5
26	5160	3360	65.1	11.5	44.6	-18.2	1.1	24.3
31	4280	2300	53.7	10.5	38.8	-15.4	1.1	20.1
33	4840	2520	52.1	10.9	42.3	-15.4	1.1	19.0
36	4520	2400	53.1	9.5	35.4	-15.3	1.1	18.0
38	4700	2780	59.1	10.2	41.3	-14.8	1.1	18.9
42	4850	2810	57.9	7.9	39.6	-14.5	1.1	18.2
45	5010	2900	57.9	8.1	35.4	-14.2	1.1	17.5

Table B-2: Removal efficiencies in the pilot SMEBR

Time, d	COD_{in}, mg/L	$COD_{eff.}$, mg/L	% Removal	NH_3^+-$N_{inf.}$, mg/L	NH_3^+-$N_{eff.}$, mg/L	% Removal	PO_4^{3-}-$P_{inf.}$, mg/L	PO_4^{3-}-$P_{eff.}$, mg/L	% Removal	NO_3^--$N_{inf.}$, mg/L	NO_3^--$N_{eff.}$, mg/L	% Increase
2	697	208	70.2	28.7	8.6	70.0	2.93	0.012	99.6	0.383	0.561	46.5
3	227	32	85.9	59.4	36.2	39.1	3.85	0.93	75.8	0.429	5.91	1277.6
4	253	33	87.0	56	11.9	78.8	6.1	0.02	99.7	0.32	8.29	2490.6
5	253	12.8	94.9	33.8	14.8	56.2	2.87	0.04	98.6	0.375	13.3	3446.7
6	419	36.6	91.3	40.2	19.4	51.74	4.17	0.086	97.9	0.412	8.74	2021.4
7	161	4.08	97.5	36	0.421	98.8	6.62	0.012	99.8	0.415	17.3	4068.7
8	211	19.1	90.9	48	0.57	98.8	4.14	0.216	94.8	0.285	20.1	6952.6
9	218	22.9	89.5	18.8	0.854	95.5	1.94	0.583	69.9	0.303	15.2	4916.5
10	321	19.9	93.8	45.5	3.37	92.6	5.44	0.022	99.6	0.521	19	3546.8
11	466	16	96.6	68.4	2.89	95.8	4.1	0.31	92.4	0.63	20.7	3185.7
12	383	31.9	91.7	50.8	0.63	98.8	3.1	0.04	98.7	0.663	22.9	3354.0
14	247	27.4	88.9	32.7	0.17	99.5	2.9	0.05	98.3	0.365	15.82	4234.2
16	345	26.9	92.2	48.3	9.02	81.3	4.4	0.39	91.1	0.581	9.64	1559.2
18	303	29.5	90.3	52.4	19.3	63.2	3.3	0.97	70.6	0.443	11.8	2563.7
20	349	26.2	92.5	40.9	11.7	71.4	2.6	0.039	98.5	0.544	13.8	2436.8
22	683	29.7	95.7	39.7	0.558	98.6	3.3	0.68	79.4	0.397	13.7	3350.9
26	258	26.7	89.7	56.2	0.788	98.6	3.36	0.029	99.1	0.258	19.4	7419.4
31	200	16.3	91.9	40.5	0.378	99.1	3.4	0.362	89.4	0.307	18.1	5795.8
33	157	21.2	86.5	31.2	0.2	99.4	2.7	0.043	98.4	0.392	14.7	3650.0
36	414	17.9	95.7	36.6	17.3	52.7	3.6	1.4	61.1	0.313	11.7	3638.0
38	157	13.3	91.5	38.5	0.37	99.0	10.7	0.186	98.3	0.299	14.7	4816.4
42	235	16.7	92.9	40.1	0.42	99.0	4.2	0.0432	99.0	0.321	15.1	4604.0
45	310	20.7	93.3	45.3	0.41	99.1	5.3	0.034	99.4	0.341	13.1	3741.6

Table B-3: Daily measurements in the SMEBR pilot system

Time, d	TMP, kPa	DO, mg/L	T, ^{o}C	pH	I, A	V, V	$\sigma_{inf.}$, µS/cm	σ_{sludge}, µS/cm
1	1.2	6.1	23.2	8.4	9.5	8.1	740	661
2	1.2	6.8	23.1	8.4	9.5	8.1	738	659
3	1.2	7.9	20.9	8.4	9.5	8.3	707	589
4	1.2	7.9	21.1	8.6	9.5	7.8	835	680
5	1.5	7.5	22.1	8.6	9.5	8	853	677
6	1.7	5.3	23.1	8.4	9.5	7.3	916	703
7	1.9	7.7	23.3	8.4	9.5	9.5	717	581
8	2	7.6	23.1	8.2	9.5	9.1	823	600
9	2	7.9	21.5	8.4	9.5	9.6	748	565
10	2.1	7.6	21.0	8.3	9.5	9.5	824	605
11	2.1	6.7	21.1	8.2	9.5	9.1	852	638
12	2.1	7.3	22.3	8.4	9.5	8.9	876	684
13	2.1	8.3	19.9	8.4	9.5	10.5	652	514
14	2.1	6.3	19.5	8.6	9.5	9.9	621	609
15	2.2	7.6	20.8	8.4	9.5	10.9	688	519
16	2.2	5.1	20.6	8.6	9.5	10.5	678	586
17	2.2	3.8	17.4	8.8	9.5	8.9	815	750
18	2.2	5.7	19.6	8.6	9.5	9.3	755	665
19	2.2	7.1	20.7	8.4	9.5	9.5	839	637
20	2.2	6.0	20.4	8.4	9.5	9.8	809	631
21	2.2	6.3	20.7	8.5	9.5	10.1	771	589
22	2.2	6.9	19.9	8.5	9.5	10.4	749	579
23	2.2	7.5	20.1	8.5	9.5	10.7	726	544
24	2.2	5.6	16.5	8.7	9.5	10.5	755	599
25	2.2	5.2	22.2	8.4	9.5	9.9	774	631
26	2.2	5.4	21.6	8.3	9.5	9.8	758	651

27	2.2	6.2	22.1	8.4	9.5	9.9	764	661
28	2.2	7.1	21.4	8.5	9.5	9.4	823	687
29	2.2	8.1	20.5	8.8	9.5	9.6	865	654
30	2.2	7.8	20.6	8.6	9.5	10.1	810	646
31	2.2	8.2	19.7	8.6	9.5	10.2	832	621
32	2.2	7.2	18.2	8.6	9.5	10.9	755	545
33	2.3	7.5	19.6	8.5	9.5	10.5	785	610
34	2.3	7.3	21.0	8.6	9.5	11.4	719	542
35	2.3	7.8	18.2	8.6	9.5	11.4	739	555
36	2.3	7.4	16.5	8.8	9.5	10.9	761	580
37	2.3	8.3	18.5	8.8	9.5	9.6	906	709
38	2.3	8.4	17.7	8.7	9.5	9.7	866	673
39	2.3	8.8	17.0	8.6	9.5	10.4	792	610
40	2.3	8.6	16.4	8.7	9.5	10.7	785	603
41	2.3	8.7	17.2	8.7	9.5	11.4	630	556
42	2.3	9.0	17.5	8.9	9.5	13.2	603	468
43	2.3	8.5	16.1	8.9	9.5	15.4	506	401
44	2.3	8.5	17.4	8.8	9.5	13.7	608	458
45	2.4	8.6	17.9	8.9	9.5	12.9	663	499
46	2.5	6.6	17.8	8.8	9.5	11.9	745	570

Table B-4: Sludge properties in the pilot MBR

Time, d	MLSS, mg/L	MLVSS, mg/L	MLVSS/MLSS	EPS_c, mg/L	EPS_p, mg/L	Zeta Potential, mV	Viscosity, mPa.s	PSD, µm
0	2380	2220	93.3	22.1	40.3	-26.6	1.2	69.0
1	2200	2150	97.7	16.5	33.0	-27.5	1.2	67.3
4	2180	2140	98.2	13.3	40.8	-29.9	1.1	65.1
6	1920	1380	71.9	12.6	38.7	-26.2	1.1	62.3
9	2460	2360	95.9	12.6	62.0	-28.2	1.1	71.0
11	2320	1820	78.4	11.5	52.9	-27.7	1.1	75.7
14	2520	1920	76.2	13.1	56.5	-25.6	1.1	72.8
18	1830	1390	76.0	10.5	48.5	-23.6	1.1	75.8
21	2110	1480	70.1	13.2	44.8	-23.6	1.1	102.8
27	2640	1920	72.7	12.4	48.1	-25.6	1.1	104.6
29	2420	1530	63.2	12.3	54.9	-25.3	1.1	113.7
33	2410	1640	68.0	12.6	46.0	-24.8	1.1	118.7
35	2570	1710	66.5	13.6	71.0	-25.1	1.1	110.1
37	2300	1590	69.1	14.2	87.7	-30.4	1.1	111.3
39	2260	1480	65.5	17.3	56.4	-27.2	1.1	110.4
41	2220	1460	65.8	17.2	64.0	-29.6	1.1	112.5
45	2130	1370	64.3	17.5	51.4	-31.2	1.1	115.8

Table B-5: Removal efficiencies in the pilot MBR

Time, d	COD_{in}, mg/L	COD_{eff}, mg/L	% Removal	NH_3^+-$N_{inf.}$, mg/L	NH^{3+}-N_{eff}, mg/L	% Removal	PO_4^{3-}-$P_{inf.}$, mg/L	PO_4^{3-}-$P_{eff.}$, mg/L	% Removal	NO_3^--N_{inf}, mg/L	NO_3^--$N_{eff.}$, mg/L	%Increase
1	265	24.81	90.6	35.9	15.8	56.0	3.05	0.75	75.4	1.1	10.2	827.3
4	220	60	72.7	39.3	8.8	77.6	5.71	0.82	85.6	0.354	11.2	3063.8
6	183	35.8	80.4	25.8	6.12	76.3	2.5	0.725	71.0	0.215	8.72	3955.8
9	171	31	81.9	37.1	8.4	77.4	3.9	1.09	72.1	0.465	9.59	1962.4
11	410	37.8	90.8	65.5	6.75	89.7	4.4	2.49	43.4	0.828	11	1228.5
14	864	39.4	95.4	32.2	2.82	91.2	6.2	2.12	65.8	0.742	12.1	1530.7
18	177	29.6	83.3	43.7	13.1	70.0	3.65	1.92	47.4	0.329	9.88	2903.0
21	562	45.5	91.9	53.7	15.3	71.5	5.22	1.64	68.6	2.63	12	356.3
27	948	40.8	95.7	42.8	7.22	83.1	5.74	1.8	68.6	1.71	15.9	829.8
29	287	22.6	92.1	37.6	1	97.3	3.29	1.59	51.7	0.373	16.3	4270.0
33	402	17.4	95.7	30.6	14.6	52.3	2.89	2.32	19.7	0.492	17	3355.3
35	428	32.7	92.4	57.3	0.56	99.0	3.56	1.72	51.7	0.518	18.4	3452.1
37	317	38.8	87.8	33	0.56	98.3	2.32	1.58	31.9	0.367	17.4	4641.1
39	389	31	92.0	42.1	0.72	98.3	3.36	1.81	46.1	0.271	18.6	6763.5
41	159	32.2	79.7	34	0.84	97.5	1.93	0.74	61.7	0.279	17.4	6136.6
43	214	57.1	73.3	42	0.91	97.8	4.1	1.4	65.9	0.32	16.8	5150.0
45	309	62.4	79.8	51	1.2	97.6	3.9	1.1	71.8	0.24	15.4	6316.7

Table B-6: Daily measurements in the MBR pilot system

Time, d	TMP, kPa	DO, mg/L	pH	$\sigma_{inf.}$, µS/cm	σ_{sludge}, µS/cm	T, ^{o}C
1	2.4	9.5	8.4	790	722	13.4
2	2.4	9.5	8.9	787	723	13.2
3	2.4	9.2	9.0	845	747	14.6
4	2.6	9.4	8.8	765	706	13.7
5	3.1	8.3	8.8	680	650	16.7
6	3.2	9.3	9.0	687	628	16
7	3.2	9.8	8.9	650	587	13.6
8	3.2	10.2	9.0	651	579	11.4
9	3.4	9.8	9.1	940	801	13.7
10	3.4	9.6	8.9	920	871	13.7
11	3.6	8.7	8.9	777	741	11.2
12	3.6	8.9	8.9	747	707	11.6
13	4.7	8.9	8.8	710	687	12.5
14	10.0	8.7	8.8	783	700	13
15	10.7	9.8	9.2	806	684	13.6
16	11.2	9.6	9.2	812	693	14.1
17	11.5	9.5	9.1	801	672	14.7
18	12.0	9.4	9.2	805	797	14.2
19	12.0	9.2	9.0	643	608	12.1
20	12.7	7.7	8.9	693	627	15.1
21	12.8	7.0	8.8	746	681	18.5
22	12.9	7.5	8.5	705	667	20.2
23	13.1	7.5	8.5	764	637	20.1
24	13.3	7.7	8.7	644	653	20.6
25	13.5	7.4	8.6	740	642	20.7
26	13.6	7.9	8.7	763	684	20.7

27	14.0	6.7	8.7	773	720	20.6
28	14.1	8.4	8.8	797	705	18.6
29	14.4	8.7	8.9	790	689	15.3
30	14.4	7.9	8.8	794	692	16.4
31	14.5	9.6	9.0	695	674	15.2
32	14.5	9.2	8.9	704	687	15.8
33	14.7	8.7	8.7	694	620	15.4
34	14.8	8.7	8.8	787	645	16.1
35	15.1	6.3	9.0	791	648	15.8
36	15.2	7.2	8.9	681	651	15.7
37	15.3	9.5	9.0	690	653	14.5
38	15.5	9.0	8.9	723	641	15.2
39	15.6	9.1	8.9	781	629	15.1
40	15.7	9.1	8.9	756	614	15.3
41	16.0	8.3	8.7	824	719	14.9
42	16.2	8.1	8.7	821	709	15.2
43	16.5	8.4	8.7	796	634	15.1
44	16.9	8.3	8.9	785	621	15.6
45	17.2	8.4	8.5	831	711	15.2

Appendix C

SMEBR pilot facility at the municipal wastewater treatment plant in l'Assomption

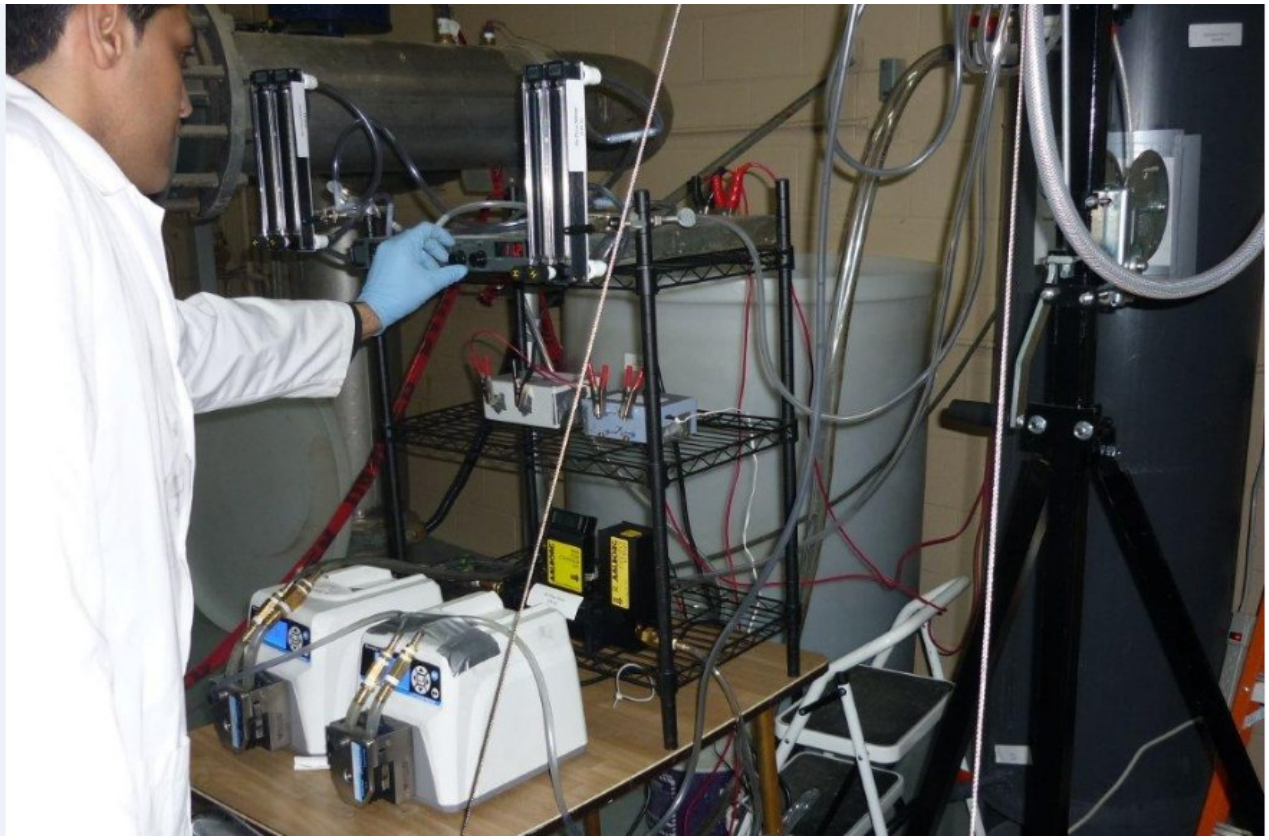

Fig. C-1: SMEBR pilot unit.

Fig. C-2: MF Microza membrane module (MUNC-600A).

Fig. C-3: Raw wastewater passing through 2 mm screens.

Appendix D

SMEBR design scale-up computational demonstration

Mathematical equations were used to validate the proposed methodology. Raw wastewater from the City of l`Assomption (Quebec, Canada) was analyzed and average values were reported as illustrated in Table D-2. Biological kinetics adopted in the design calculations were recommended values for wastewater treatment using MBR (Metcalf and Eddy, 2003; Judd, 2006).

Table D-1: Design parameters for modeling calculations of SMEBR

Parameter	**Notation**	**Unit**	**Value**
Biodegradable COD	bCOD	g/m^3	Estimated from the model calculations
Non biodegradable COD	nbCOD	g/m^3	Estimated from the model calculations
Effluent soluble COD	sCODe	g/m^3	Estimated from the model calculations
Non biodegradable VSS	nbVSS	g/m^3	Estimated from the model calculations
Biodegradable particulate COD	bpCOD	g/m^3	Estimated from the model calculations
Particulate COD	pCOD	g/m^3	Estimated from the model calculations
Soluble BOD	sBOD	g/m^3	Analysis of raw wastewater
Soluble COD	sCOD	g/m^3	Analysis of raw wastewater
Inert TSS	iTSS	g/m^3	Estimated from the model calculations
Raw wastewater	Q	m^3/d	Selected

flow rate			(0.5)
Operating temperature	T	^{o}C	Assumed (18)
Yield coefficient	Y	g VSS/g bCOD	Assumed (0.9) (Metcalf and Eddy, 2003)
Influent BOD or, bsCOD concentration	S_o	g/m^3	Analysis of raw wastewater
Concentration of growth limiting substrate in solution	S	g/m^3	Estimated from the model calculations
Half-saturation constant	K_s	g bCOD/m^3	Assumed (20) (Metcalf and Eddy, 2003)
Endogenous decay coefficient	k_d	1/d	Assumed (0.15) (Metcalf and Eddy, 2003)
Solid retention time	SRT	d	Estimated from the model calculations
Maximum specific growth rate	μ_m	g VSS/g VSS.d	Assumed (5) (Metcalf and Eddy, 2003)
Half-saturation constant (nitrification)	K_n	g NH_4-N/m^3	Assumed (0.74) (Metcalf and Eddy, 2003)
Endogenous decay coefficient (nitrification)	k_{dn}	1/d	Assumed (0.17) (Metcalf and Eddy, 2003)
Maximum specific growth rate for	$\mu_{n,m}$	g VSS/g VSS.d	Assumed (0.75)

nitrifying bacteria			(Metcalf and Eddy, 2003)
Yield coefficient (nitrification)	Y_n	g VSS/g NH_4-N	Assumed (0.12) (Metcalf and Eddy, 2003)
Fraction of cell mass remaining as cell debris	f_d	g/g	Estimated from the model calculations (Judd, 2006)
Half-saturation constant for DO	K_o	g/m^3	Assumed (0.5) (Metcalf and Eddy, 2003)
Reaction rate constant at temperature T	k_T	1/d	Assumed
Reaction rate constant at 20 ^oC	k_{20}	1/d	Assumed
Temperature activity coefficient	Θ	Unitless	Assumed (1.04 for decay and1.07 for growth) (Metcalf and Eddy, 2003)
Net waste activated sludge produced each day, measured in terms of total suspended solids	$P_{x,TSS}$	kg/d	Estimated from the model calculations
Amount of VSS produced and wasted daily	$P_{x,VSS}$	kg/d	Estimated from the model calculations
Mass of VSS in the aeration tank	$(P_{x,VSS})$ (SRT)	kg	Estimated from the model calculations
Mass of TSS in the aeration tank	$(P_{x,TSS})$ (SRT)	kg	Estimated from the model calculations
Mixed liquor	X	g/m^3	Assumed-desired

suspended solids (MLSS)			(6000)
Biomass as VSS wasted per day	$P_{x,bio}$	kg/d	Estimated from the model calculations
Concentration of NH_4-N in the influent flow that is nitrified	NH_4	g/m^3	Estimated-analysis of raw wastewater
Influent waste water TSS concentration	TSS_o	g/m^3	Analysis of raw wastewater
Influent waste water VSS concentration	VSS_o	g/m^3	Analysis of raw wastewater
Effluent ammonia concentration	N_e	g/m^3	Analysis of effluent treated wastewater
Influent TKN concentration	TKN	g/m^3	Analysis of raw wastewater
Nitrogen oxidized	NO_x	g/m^3	Estimated from the model calculations
Food to microorganisms ratio	F/M	g BOD/g VSS.d	Estimated from the model calculations
BOD volumetric organic loading	L_{org}	$kg/m^3.d$	Estimated from the model calculations
Sludge wastage per day	Q_w	m^3/d	Estimated from the model calculations
Volume	V	m^3	Estimated from the model calculations
Applied current	I	A	Estimated from the model calculations
Specific energy consumption	E	kWh/m^3	Estimated from the model calculations
Oxygen demand for BOD oxidation	R_0	kg/h	Estimated from the model calculations
standard oxygen	SOTR	kg/h	Estimated from the

transfer rate			model calculations
Aeration factor	α*	Unitless	Assumed (0.62) (Judd, 2006)
The value relating oxygen saturation in waste water compared to clean water	β	Unitless	Assumed (0.95) (Judd, 2006)
Diffuser fouling factor	F	Unitless	Assumed (0.9) (Judd, 2006)
Oxygen saturation concentration corrected for altitude and temperature	$C_{s,T,H}$	g/m^3	Assumed (12) (Metcalf and Eddy, 2003)
Operating dissolved oxygen concentration	C_L	g/m^3	Assumed (2) (Metcalf and Eddy, 2003)
Oxygen saturation concentration for pure water at 20°C	$C_{s,20}$	g/m^3	Assumed (9.08) (Metcalf and Eddy, 2003)
Air density	ρ_A	kg/m^3	Estimated
Oxygen transfer efficiency	OTE		Assumed (0.05 for fine diffusers and 0.02 for membrane) (Judd, 2006)
air flow rate through the fine bubble diffusers (biological)	$Q_{A,b}$	m^3/h	Estimated from the model calculations
Flux per membrane	J	$m^3/m^2.d$	Estimated according to manufacturer
Permeability	K	LMH/bar	Estimated according to manufacturer
Aeration rate per unit membrane	$Q_{A,m}$	m^3/h	Estimated from the model calculations
Transmembrane	TMP	kPa	Estimated from the

pressure			model calculations
Permeate flow rate	$Q_{Permeate}$	m^3/h	Estimated according to manufacturer
Inlet air pressure to membrane module	$P_{A,1}$	kPa	Estimated
Blower outlet pressure	$P_{A,2}$	kPa	Estimated
Membrane area	A_m	m^2	Estimated according to manufacturer
Membrane aeration demand per unit membrane area	SAD_m	$Nm^3/m^2.h$	Estimated from the model calculations
Membrane aeration demand per unit permeate flow	SAD_p	Unitless	Estimated from the model calculations
Ratio of specific heat capacity at constant pressure to constant volume	λ	Unitless	Assumed (1.4) (Judd, 2006)
Blower efficiency	ζ	%	Assumed (50) (Judd, 2006)
Anode surface area	A_s	m^2	Estimated from the model calculations
Inorganic or chemical solids produced per day due to electrokinetics	ζ^*	kg Al/m^3	Estimated experimentally (0.21)

Table D-2: Average characteristics of raw wastewater implemented in the computational analysis (City of l`Assomption, Quebec)

Constituent	Concentration, g/m^3
BOD_u	150
sBOD	75
COD	320
sCOD	140
TSS	155
VSS	127
TKN	62
NH_3^+-N	45
PO_4^{3-}-P	5
NO_3^--N	0.4
bCOD/BOD ratio	1.6

Wastewater characteristics needed for the design

- **Find biodegradable COD:**

✓ $bCOD = 1.6\ (BOD_u) = 1.6\ (150\ g/m^3) = 240\ g/m^3$

- **Find non biodegradable COD:**

✓ $nbCOD = COD - bCOD = (320 - 240)\ g/m^3 = 80\ g/m^3$

- **Find effluent sCODe (assume non biodegradable):**

✓ sCODe = sCOD – 1.6 sBOD = (140 g/m^3) – 1.6 (75 g/m^3) = 20 g/m^3

- **Find non biodegradable VSS:**

nbVSS = (1 – bpCOD/pCOD) VSS

bpCOD/pCOD = [1.6 (BOD_u – sBOD)]/(COD – sCOD) = [1.6 (150 – 75)]/(320 – 140) = 0.66

✓ nbVSS = (1 – 0.66) (127 g/m^3) = 43.2 g/m^3

- **Find inert TSS:**

✓ iTSS = TSS – VSS = (155 – 127) g/m^3 = 28 g/m^3

<u>Kinetics parameters for heterotrophic and autotrophic microorganisms</u>

Recommended values for heterotrophic microorganisms (Metcalf and Eddy, 2003; Judd, 2006)**:**

- Y = 0.90 gVSS/g bCOD (high value as there was no primary clarifier in the WWTP in l'Assomption)

- k_d = 0.15 g VSS/g VSS.d, Θ = 1.04

- μ_m = 5 g VSS/g VSS.d, Θ = 1.07

- K_s = 20 g/m^3

Kinetics parameters are corrected at the average operating temperature (18°C):

Thus,

✓ $\mu_{m,T} = \mu_m \Theta^{(T-20)} = 5\ (1.07)^{(18-20)} = 4.37$ g VSS/g VSS.d

✓ $k_{d,T} = k_{20} \Theta^{(T-20)} = 0.15\ (1.04)^{(18-20)} = 0.14$ g VSS/g VSS.d

✓ f_d ~ (g nbVSS/ g S_0) = 0.19 g/g (Judd, 2006)

Recommended values for autotrophic microorganisms (Metcalf and Eddy, 2003; Judd, 2006)**:**

- Y_n = 0.12 gVSS/g NH_4-N
- k_{dn} = 0.17 g VSS/g VSS.d, Θ = 1.04
- $\mu_{n,m}$ = 0.75 g VSS/g VSS.d, Θ = 1.07
- K_n = 0.74 g NH_4-N /m^3, Θ = 1.053
- K_0 = 0.50 g/m^3

Kinetics parameters were corrected at the average operating temperature (18°C):

Thus,

✓ $\mu_{n,m,T} = \mu_{n,m}\ \Theta^{(T-20)} = 0.75\ (1.07)^{(18-20)} = 0.66$ g VSS/g VSS.d

✓ $k_{dn,T} = k_{20}\ \Theta^{(T-20)} = 0.17\ (1.04)^{(18-20)} = 0.16$ g VSS/g VSS.d

✓ $K_{n,T} = K_{20}\ \Theta^{(T-20)} = 0.74\ (1.053)^{(18-20)} = 0.67$ g/m^3

✓ $\mu_n = [(\mu_{n,m}\ N)/(K_n + N)]\ [DO/(DO + K_0)] = [(0.66)\ (0.5)/(0.67 + 0.5)]\ [7/(7 + 0.5)] = 0.26$ g VSS/g VSS.d

<u>Theoretical and design SRT</u>

Theoretical SRT = $1/\mu_n = 1/0.2 = 3.85$ d (D.1)

μ_n was selected due to the fact that the nitrification rate will control the design since the nitrifying bacteria grow slower than the heterotrophic bacteria which remove organic carbon.

Design SRT = (Theoretical SRT) (SF) (D.2)

= (3.85 d) (2.5) = 9.6 d ~ 10 d

Biomass production, kg VSS/d

$$P_{x,\,bio} = \frac{Q(Y)(S_0 - S)}{1+(k_d)SRT} + \frac{f_d(k_d)Q(Y)(S_0 - S)SRT}{1+(k_d)SRT} + \frac{QY_n(NO_x)}{1+(k_{dn})SRT} \quad (D.3)$$

- **The effluent dissolved substrate concentration (S):**

$$S = \frac{K_s[1+(k_d)SRT]}{SRT(Yk - k_d) - 1} = 1.16 \text{ g bCOD/m}^3 \quad (D.4)$$

Where, $Yk = \mu_m$

Assumptions:

- Raw wastewater flow rate (Q) = 0.5 m^3/d
- NO_x = 80% (TKN) = 0.8 (62) = 49.6 g/m^3 (Metcalf and Eddy, 2003)

Plugging all data in equation D.3, the biomass production was:

✓ $P_{x,\,bio}$ = [0.0447 + 0.0119 + 0.00115] kg VSS/d = 0.0578 kg VSS/d

The amount of nitrogen oxidized to nitrate (nitrogen balance)

$NO_x = TKN - N_e - 0.12\ P_{X,bio}/Q$ (D.5)

Thus,

✓ NO_x = 62 g/m^3 – 0.5 g/m^3 – 0.12 [(0.06 kg VSS/d) (10^3 g/kg)/0.5 m^3/d)] = 47.6 g/m^3

The concentration and mass of VSS and TSS in SMEBR

$P_{x,\,VSS} = P_{x,\,bio} + Q$ (nbVSS) (D.6)

✓ $P_{x,\ VSS}$ = 0.0578 kg VSS/d + 0.5 m^3/d [(43.2 g/m^3)/(10^3 g/kg)] = 0.0578 + 0.0216 = 0.0794 kg/d

$$P_{x,\ TSS} = P_{x,\ bio}/0.82 + Q\ (nbVSS) + Q\ (TSS_0 - VSS_0) + \xi^* Q \quad (D.7)$$

Where, ξ^* = 0.12 kg Al/m^3: inorganic (chemical) solids produced per day due to electrokinetics and it was determined from laboratory experimental data shown earlier in Chapter 4 (Section 4.3.5 - eq. 4.2) assuming: a) intermittent supply of electricity 5 min ON: 10 min OFF, b) distance between electrodes was less than 10 cm, c) V*/V ratio was 45%, d) current density of 12 A/m^2.

VSS/TSS = 0.82 (from the characteristics of raw wastewater - Table D.2)

Therefore,

- $P_{x,\ TSS}$ = (0.0578/0.82 + 0.0216 + 0.014 + 0.06) kg/d = 0.166 kg/d

Design MLSS = 6000 g/m^3

- **Mass of MLSS :**

$$X_{TSS}\ (V) = P_{x,\ TSS}\ (SRT) \quad (D.8)$$

= (0.166 kg/d) (10 d) = 1.66 kg

- **Mass of MLVSS:**

$$X_{VSS}\ (V) = P_{x,\ VSS}\ (SRT) \quad (D.9)$$

= (0.0794 kg/d) (10 d) = 0.794 kg

$$\text{Fraction VSS} = \text{Mass MLVSS/Mass MLSS} \quad (D.10)$$

= (0.794 kg)/(1.66 kg) = 0.478 = 47.8%

✓ MLVSS = 0.478 (6000 g/m^3) = 2868 g/m^3

Solve for the total effective volume of liquid in SMEBR (V)

$V = [P_{x,\,TSS}\,(SRT)]/X_{TSS}$ (D.11)

$= (1.66\ kg)/[(6000\ g/m^3)\ (kg/10^3\ g)]$

Thus,

- ✓ $V = V_{Effective\ liquid} = 0.276\ m^3 = 276\ L$
- ✓ Height of liquid = 1.4 m → Tank diameter = 0.501 m
- ✓ Add 20 cm to the liquid height = (1.4 + 0.2) m = 1.6 m → $V_{Tank} \sim 0.315\ m^3 = 315\ L$

Sludge wastage

$Q_w = V/SRT$ (D.12)

$= (0.276\ m^3)/(10\ d) = 0.0276 m^3/d = 27.6\ L/d$

SMEBR hydraulic retention time (HRT)

$HRT = V/Q$ (D.13)

$= (0.276\ m^3)/(0.5\ m^3/d) = 0.552\ d = 13.2\ h$

Determine F/M ratio and COD volumetric organic loading

$$F/M = \frac{QS_0}{X_v V} \quad \text{(D.14)}$$

$= [(0.5\ m^3/d)\ (240\ g/m^3)]/[(2868\ g/m^3)\ (0.276\ m^3)] = 0.15\ g\ COD/g\ VSS.d$

$$L_{org} = \frac{QS_0}{V} \quad \text{(D.15)}$$

$= [(0.5\ m^3/d)\ (240\ g/m^3)]/[(0.276\ m^3)\ (10^3\ g/kg)] = 0.43\ kg/m^3.d$

Determine the observed yield based on TSS and VSS

Observed Yield based on TSS = $P_{x,\ TSS}$/bCOD removed (D.16)

bCOD removed = Q (S_0 – S) = (0.5 m^3/d) [(240 – 1.16) g/m^3/(10^3 g/kg)] = 0.119 kg/d

Thus,

- ✓ **Observed Yield based on TSS ($Y_{Obs,\ TSS}$)** = (0.166 kg/d)/(0.119 kg/d) = 1.39 kg TSS/kg bCOD = 1.39 g TSS/g bCOD

- ✓ **Observed Yield based on VSS ($Y_{Obs,\ VSS}$)** = (1.39 g TSS/g bCOD) (0.82 VSS/TSS) = 1.14 g VSS/g bCOD

Determine the oxygen demand required for microbial activity

R_0 = Q (S_0 - S) - 1.42 $P_{x,\ bio}$ + 4.33 Q (NO_x) (D.17)

= (0.5 m^3/d) [(240 – 1.16) g/m^3/(10^3 g/kg)] – 1.42 (0.0578 kg VSS/d) + 4.33 (0.5 m^3/d) [(47.6 g/m^3)/(10^3 g/kg)] = 0.2394 – 0.082 + 0.103 = 0.2604 kg/d = 0.0109 kg/h

Determine air supply requirement for the SMEBR

- Determine standard oxygen transfer rate:

$$\text{SOTR} = \frac{R_o C_{s,20}}{\alpha^* F(\beta C_{s,T,H} - C_L)}(1.024^{(20-T)}) \quad \text{(D.18)}$$

Where,

α* = 0.62, β = 0.95, F = 0.9

$C_{s,20}$ = 9.08 g/m^3, C_L = 2 g/m^3, $C_{s,T,H}$ = 12 g/m^3 (assumed data, Metcalf and Eddy, 2003)

Thus,

✓ **SOTR** = [(0.2604 kg/d) (9.08 g/m^3) (1.024 $^{(20-18)}$)]/[(0.62*0.9) (0.95*12 g/m^3 – 2 g/m^3)] = 0.47 kg/d = 0.02 kg/h

- Determine air flow rate through the fine bubble diffusers:

$$(Q_{A,b}) = \frac{(SOTRkg/h)}{[(OTE)(60\min/h)(kgO_2/m^3air)]} \quad \text{(D.19)}$$

Where,

- ρ_A = 1.29 kg/m^3 = 0.27 kg O^2/m^3 air
- Aeration tank depth = 1.4 m
- Fine bubble diffuser OTE for biology = 0.05 (Judd, 2006)
- OTE for biological = (0.05) (1.4 m) = 0.07%; this is dependent upon the depth of submergence and the type of diffuser

Therefore,

✓ **$Q_{A,b}$** = (0.02 kg/h)/[(0.07) (60 min/h) (0.27 kg O^2/m^3 air)] = 0.018 m^3/min = 1.08 m^3/h

✓ Temperature corrected aeration rate (**$Q'_{A,b}$**) = $Q_{A,b}$ (293 K/291 K) = 1.09 Nm^3/h = 0.000303 Nm^3/s

<u>Electrical inputs (electrodes specifications and current calculations)</u>

- V*/V ratio = 45% = (0.45) (0.276 m^3) = 0.1242 m^3 = 124.2 L
- Distance between electrodes is less than 10 cm
- Height of electrodes = 1.2 m

✓ Selected current density (CD) = 12 A/m^2 → Applied current = 9.5 A (40% aluminum anode perforation) according to equation E.20:

$$I = (CD)\ (A_s) \qquad (D.20)$$

Membrane characteristics and operating data

MUNC-600A hollow fibre microfiltration (MF) module was recommended for the design. The membrane characteristics were previously shown in Chapter 3 - Table 3.2.

Assumptions for membrane operation (Asahi Kasei Chemicals Corporation (Japan):

- Flux per membrane module (J) = 0.05 $m^3/m^2.d$
- The number of modules used for the design = 1 membrane module
- Permeability (K) = 100 LMH/bar (Judd, 2006 for Asahi Microza membranes)
- Membrane scouring aeration rate = 0.08 $m^3/m^2.h$ (determined from laboratory experiments in Phase 1 - Chapter 4)
- Area per membrane = 12.5 m^2

Membrane calculations: (Judd, 2006)

- Filtration area (A_m) = 12.5 m^2
- Aeration rate per unit membrane ($Q_{A,m}$) = (0.08 $m^3/m^2.h$) (12.5 m^2) = 1 m^3/h

✓ O_2 transferred by membrane aeration = (1 m^3/h) (0.27 kg O_2/m^3 air) = 0.27 kg/h = 6.48 kg/d

- ✓ Temperature corrected flux (J') = J/1.024 $^{(T-20)}$ = 0.05/1.024 $^{(18-20)}$ = 0.048 $Nm^3/m^2.d$ = 1.98 N LMH

- ✓ Temperature corrected mean Permeability (K') = 115 N LMH/bar

- ✓ Transmembrane pressure (TMP) = J'/K' = 1.98/115 = 0.0173 bar = 1.73 kPa

- ✓ $P_{A,1}$ = 101.325 kPa → $P_{A,2}$ = (101.325 + 1.73) kPa = 103.06 kPa

- ▪ Coarse bubble diffuser OTE for membrane = 0.02 (Judd, 2006)

- ▪ OTE for membrane = (0.02) (1.4) = 0.028%

- ✓ **$Q_{Permeate}$** = (0.05 $m^3/m^2.d$) (12.5 m^2) (1d/24h) = 0.026 m^3/h

- ✓ Temperature, pressure-corrected $Q_{Permeate}$ (**$Q'_{Permeate}$**) = (0.026 m^3/h) (293 K/291 K) (103.06 kPa/101.325 kPa) = 0.027 Nm^3/h

Membrane operation:

- ✓ Temperature, pressure-corrected aeration rate (**$Q'_{A,m}$**) = $Q_{A,m}$ (293 K/291 K) (103.06 kPa/101.325 kPa) = 1.03 Nm^3/h = 0.000284 Nm^3/s

- ✓ Membrane aeration demand per unit membrane area: (**SAD_m**) = $Q'_{A,m}/A_m$ (D.21)

  = (1.03 Nm^3/h)/(12.5 m^2) = 0.083 $Nm^3/ m^2.h$

- ✓ Membrane aeration demand per unit permeate flow (**SAD_p**) = $Q'_{A,m}/J'A_m$ (D.22)

  = (1.03 Nm^3/h)/[(12.5 m^2)(1.98 N LMH)(10^{-3})] = 41.9

Power requirements in SMEBR system

Air blower power consumption (biological):

$$\text{Power} = \left[\frac{108.748\lambda}{\zeta(\lambda-1)}\left((P_{A,2}/101.325)^{1-1/\lambda}-1\right)\right] Q'_{A,b} \quad \text{(D.23)}$$

Assumptions: $\lambda = 1.4$, $\zeta = 0.5$ (Judd, 2006)

Therefore,

- ✓ **Power** = [(108.748)(1.4)/(0.5)(0.4)](103.06 kPa/101.325 kPa)$^{0.286}$ – 1) (0.000303 Nm^3/s) = 0.00113 kW

- ✓ **Specific energy** = Power (kW)/Q'$_{permeate}$ (Nm^3/h) (D.24)

  = (0.00113 kW)/(0.027 Nm^3/h) = 0.042 kWh/m^3

Air blower power consumption (membrane):

$$\text{Power} = \left[\frac{108.748\lambda}{\zeta(\lambda-1)}\left((P_{A,2}/101.325)^{1-1/\lambda}-1\right)\right] Q'_{A,m}$$

Assumptions: $\lambda = 1.4$, $\zeta = 0.5$ (Judd, 2006)

Therefore,

- ✓ **Power** = [(108.748)(1.4)/(0.5)(0.4)](103.06 kPa/101.325 kPa)$^{0.286}$ – 1) (0.000284 Nm^3/s) = 0.0011 kW

- ✓ **Specific energy** = Power (kW)/Q'$_{permeate}$ (Nm^3/h) = (0.0011 kW)/(0.027 Nm^3/h) = 0.0407 kWh/m^3

Table D-3: Energy requirements due to electrical system in the SMEBR system

Time, d	I, A	V, V	I^2	R	$P=I^2R$, kW	$E'=I^2R$, kWh	E=P/Volume of wastewater, kWh/m^3
1	9.5	8.1	90.25	0.853	0.077	0.616	1.12
2	9.5	8.1	90.25	0.853	0.077	0.616	1.12
3	9.5	8.3	90.25	0.874	0.079	0.631	1.15
4	9.5	7.8	90.25	0.821	0.074	0.593	1.08
5	9.5	8	90.25	0.842	0.076	0.608	1.11
6	9.5	7.3	90.25	0.768	0.069	0.555	1.01
7	9.5	9.5	90.25	1.000	0.090	0.722	1.31
8	9.5	9.1	90.25	0.958	0.086	0.692	1.26
9	9.5	9.6	90.25	1.011	0.091	0.730	1.33
10	9.5	9.5	90.25	1.000	0.090	0.722	1.31
11	9.5	9.1	90.25	0.958	0.086	0.692	1.26
12	9.5	8.9	90.25	0.937	0.085	0.676	1.23
13	9.5	10.5	90.25	1.105	0.100	0.798	1.45
14	9.5	9.9	90.25	1.042	0.094	0.752	1.37
15	9.5	10.9	90.25	1.147	0.104	0.828	1.51
16	9.5	10.5	90.25	1.105	0.100	0.798	1.45
17	9.5	8.9	90.25	0.937	0.085	0.676	1.23
18	9.5	9.3	90.25	0.979	0.088	0.707	1.29
19	9.5	9.5	90.25	1.000	0.090	0.722	1.31
20	9.5	9.8	90.25	1.032	0.093	0.745	1.35
21	9.5	10.1	90.25	1.063	0.096	0.768	1.40
22	9.5	10.4	90.25	1.095	0.099	0.790	1.44
23	9.5	10.7	90.25	1.126	0.102	0.813	1.48
24	9.5	10.5	90.25	1.105	0.100	0.798	1.45
25	9.5	9.9	90.25	1.042	0.094	0.752	1.37
26	9.5	9.8	90.25	1.032	0.093	0.745	1.35
27	9.5	9.9	90.25	1.042	0.094	0.752	1.37
28	9.5	9.4	90.25	0.989	0.089	0.714	1.30
29	9.5	9.6	90.25	1.011	0.091	0.730	1.33
30	9.5	10.1	90.25	1.063	0.096	0.768	1.40
31	9.5	10.2	90.25	1.074	0.097	0.775	1.41
32	9.5	10.9	90.25	1.147	0.104	0.828	1.51
33	9.5	10.5	90.25	1.105	0.100	0.798	1.45
34	9.5	11.4	90.25	1.200	0.108	0.866	1.58
35	9.5	11.4	90.25	1.200	0.108	0.866	1.58
36	9.5	10.9	90.25	1.147	0.104	0.828	1.51
37	9.5	9.6	90.25	1.011	0.091	0.730	1.33

38	9.5	9.7	90.25	1.021	0.092	0.737	1.34
39	9.5	10.4	90.25	1.095	0.099	0.790	1.44
40	9.5	10.7	90.25	1.126	0.102	0.813	1.48
41	9.5	11.4	90.25	1.200	0.108	0.866	1.58
42	9.5	13.2	90.25	1.389	0.125	1.003	1.82
43	9.5	15.4	90.25	1.621	0.146	1.170	2.13
44	9.5	13.7	90.25	1.442	0.130	1.041	1.89
45	9.5	12.9	90.25	1.358	0.123	0.980	1.78